Mechanisms involved in leukocyte transendothelial migration: studies of the role of hydrogen peroxide and the ecto-5'-nucleotidase, CD73

A thesis submitted for the degree of
Doctor of Philosophy
June 2008

by

Jana Katrin Gesine Gruenewald

Randall Division of Cell and Molecular Biophysics
King's College London
2nd floor New Hunts House
London SE1 1UL

Department of Structural and Molecular Biology
University College London
Gower Street
London WC1E 6BT

ProQuest LLC
789 East Eisenhower Parkway
P.O. Box 1346
Ann Arbor, MI 48106-1346

Abstract

During inflammation, leukocytes are recruited from blood vessels into the site of injury or infection. A key event in this process is transendothelial migration (TEM), a multi-step process involving various adhesion molecules on both leukocytes and endothelial cells. Oxidative stress has been linked to inflammation in the development of various diseases.

To investigate the effect of oxidative stress on TEM, leukocytes were treated with hydrogen peroxide (H_2O_2). A defect in TEM was observed across human umbilical vein endothelial cells (HUVECs), but not across a porous membrane, suggesting that H_2O_2 affects the interaction between leukocytes and endothelial cells. H_2O_2-treated leukocytes exhibited higher motility and adhesion on HUVECs, whereas their adhesion on substrates such as VCAM-1 and ICAM-1 was unaltered. The number of leukocytes exhibiting protrusions on HUVECs was decreased after H_2O_2 treatment, which is likely due to the increase in nitric oxide (NO) that was detected. Incubation of THP-1 cells with a NO donor led to a decrease in TEM and reduction of protrusions. The effects of H_2O_2 on several signalling molecules implicated in cell migration were investigated and changes in the activity of the RhoGTPases RhoA, Rac1 and Cdc42 were observed.

CD73 is a 5'-ectonucleotidase expressed on endothelial cells and has been postulated to be involved in TEM. The inhibition of endothelial CD73 activity after leukocyte binding was reduced when H_2O_2-treated leukocytes were bound. Immunofluorescence staining showed local accumulation of CD73 around transmigrating leukocytes. RNAi knock-down of endothelial CD73 led to an inflammatory phenotype with elongated cells, increased surface levels of ICAM-1, VCAM-1, E- and P-selectin and increased permeability.

Together these findings suggest that ROS have multiple effects on leukocytes leading to a defect in TEM, one of which is reduced CD73 inhibition after endothelial binding.

Contents

List of figures

List of tables

Abbreviations

A	ambion
Abi	Abl interactor
ADA	adenine deaminase
ado	adenosine
ADP	adenosine diphosphate
AJ	adherens junctions
AK	adenylate kinase
AMP	adenosine monophosphate
ang II	angiotensin II
Arf	ADP-ribosylation factor
ASK1	apoptosis signali-regulating kinase 1 (or apoptosis-stimulated kinase 1)
AT	3-amino-1,2,4-triazole
ATP	adenosine triphosphate
ATX	autotaxin
BBB	blood-brain barrier
BCP	B cell progenitor
BH_4	(6R)-5,6,7,8-tetrahydrobiopterin
CaM	calmodulin
cAMP	cyclic adenosine monophosphate
CASK	Ca^{2+}/calmodulin-dependent serine protein kinase
CBP	cysteine-based phosphatase
CCL	CC-chemokine ligand
CGD	Chronic granulomatous disease
cGMP	cyclic guanosine monophosphate
CLP	common lymphoid progenitor
CMP	common myeloid progenitor
CRIB	Cdc42/Rac interactive binding
CSF	colony-stimulating factor
CTL	cytotoxic T lymphocyte
CuZnSOD	copper-zinc SOD
CXCL	CXC-chemokine ligand
DAG	diacylgylcerol
DC	dendritic cell
DH	Dbl-homology
DHR	Dock homology region
DMP	dimethyl pimelimidate
DNA	deoxyribonucleic acid

dsDNA	double stranded ribonucleic acid
DTT	dithiothreitol
ECSOD	extracellular superoxide dismutase
EDHF	endothelial-derived hyperpolarising factor
EGM-2	EBM-2 medium with growth factors
ELMO	engulfment and motility
EM	electron microscopy
eNOS	endothelial NOS
EP	erythrocyte progenitors
EPO	erythropoietin
ERK	extracellular signal-regulated kinase
ERM	ezrin-radixin-moesin
ESAM	endothelial selective adhesion molecule
ESL1	E-selectin ligand 1
FA	focal adhesions
FAD	flavin adenine dinucleotide
FBS	fetal bovine serum
FACS	fluorescence-activated cell sorting
fMLP	fMetLeuPhe
FMN	flavin mononucleotide
FN	fibronectin
GAP	GTPase-activating protein
GDF	GDI dissociation factor
GDI	guanine-nucleotide dissociation inhibitor
GEF	guanine nucleotide exchange factor
GF	growth factor
GIT1	G protein-couples receptor kinase-interactor-1
GMP	granulocyte-macrophage progenitor
GPCR	G-protein-coupled receptor
GPI	glycosylphosphatidyl inositol
Gpx	glutathione peroxidase
GSH	glutathione
HAECs	human aortic endothelial cells
HA	hyaluronic acid
HSC	haematopoietic stem cell
HUVECs	human umbilical vein endothelial cells
ICAM	intercellular adhesion molecule
IF	immunofluorescence
IFN	interferons
IkB	inhibitor of NF-κB

IKK	IκB kinase
IL	interleukin
iNOS	inducible NOS
InsP3	inositol 1,4,5-trisphosphate
IPTG	isopropyl β-D-1-thiogalactopyranoside
IRSp53	insulin receptor substrate p53
JAM	junctional adhesion molecule
JNK	c-Jun N-terminal kinase
k-d	knock-down
LB	luria broth
LBCR	lateral border recycling compartment'
LFA-1	leukocyte function-associated antigen-1
LIMK	LIM kinase
LMW-PTP	low-molecular-weight phosphatases
L-NAME	n^{ω}-nitro-L-arginine methyl ester
5-lox	5-lipoxygenase
LPA	lysophosphatidic acid
LPS	lipopolysaccharide
m	mock-transfected
Mac-1	myeloid-specific integrin-1
MadCAM	mucosal addressin adhesion molecule
MAP-2	microtubule-associated protein-2
MAPK	mitogen-activated protein kinase
MCP-1	monocyte chemotactic protein-1
MEP	megakaryocyte erythroid progenitor
MHC	major histocompatibility complex
MkP	megakaryocyte progenitors
MLC	myosin light chain
MLCK	MLC-kinase
MM6	MonoMac6
MMPs	matrix-metalloproteases
MnSOD	manganese SOD
MβCD	methyl-β-cyclodextrin
NAC	N-acetyl-L-cysteine
NADPH	nicotinamide adenine dinucleotide phosphate
neg	negative
NF-κB	nuclear factor-κB
NK	natural killer
NKP	natural killer progenitor
NMPs	nucleoside monophosphates

nNOS	neuronal NOS
NO	nitric oxide
NOS	NO synthases
OG	n-octylglucoside
PAK	p21-activated kinase
PBD	p21-binding domain
PBS	phosphate buffered saline
PECAM-1	platelet endothelial cell adhesion molecule-1
PEITC	β-phenylethyl isothiocyanate
PGI_2	prostaglandin
Pgp-1	phagocytic glycoprotein 1
PH	pleckstrin homology
PHA	phytohaemagglutinin
phox	phagocytic oxidase
PI	propidium iodide
PI(4)P5-K	phosphatidylinositide 4-phosphate 5-kinase
PI3K	phosphatidylinositide 3-kinase
PI-mix	complete Mini EDTA-free
PI-PLC	Phosphatidylinositol-specific phospholipase C
PKA	protein kinase A
PKC	protein kinase C
PKG	cGMP-dependent protein kinase, protein kinase G
PLC	phopholipase C
PMA	phorbol 12-myristate 13-acetate
PMNs	polymorphonuclear cells
PMSF	phenylmethylsulphonyl fluoride
Prx	thioredoxin peroxidases (peroxiredoxins)
PS	phosphatidylserine
PSGL1	P-selectin glycoprotein ligand 1
PtdIns(4,5)P2	phosphatidylinositol (4,5)-bisphosphate
PTK	protein tyrosine kinases
PTP	protein tyrosine phosphatases
PTP-PEST	protein tyrosine phosphatase-proline, glutamate, serine, and threonine-rich domain
Pyk2	proline-rich tyrosine kinase 2
RAGE	receptor for advanced glycation end products
RIAM	Rap-interacting adapter molecule
Rif	Rho in filopodia
RNAi	RNA interference
RNS	reactive nitrogen species

ROCK	Rho-kinase
ROS	reactive oxygen species
RT	room temperature
RTK	receptor tyrosine kinase
SCF	stem cell factor
SDS	sodium dodecyl sulphate
sGC	guanylate cyclase
shRNA	short hairpin RNAs
siC	siControl
siRNA	short interfering RNA
SNAP	s-nitroso-N-acetylpenicillamine
SOD	superoxide dismutase
ssDNA	single stranded ribonucleic acid
T_C	cytotoxic T cell
TCP	T cell progenitor
TEA	triethanolamine
TEM	transendothelial migration
T_H	T helper cell
TJ	tight junctions
TLC	thin layer chromatography
TLM	time-lapse-microscopy
TLR	Toll-like receptors
TNF	tumor necrosis factor
TNK	T cell natural killer cell progenitor
TPO	thrombopoietin
TRAF	TNF receptor associated factor
T_{reg}	regulatory T cell
Trx	thioredoxin
UCP	uncoupling proteins
UV	ultraviolet
VASP	vasodilator-stimulated phosphoprotein
VCA	verprolin-homology-connecting acidic
VCAM-1	vascular adhesion molecule-1
VEGF	vascular endothelial growth factor
VLA-4	very late antigen-4
VSMC	vascular smooth muscle cells
VVO	vesiculo-vacuolar organelles
vWF	von Willebrand factor
WASP	Wiscott-Aldrich syndrome protein
WAVE	WASP-family verprolin homology protein

WB	western blotting
WCL	whole cell lysate
wt	wild-type
ZO	zona occludens

Acknowledgements

Firstly, I would like to thank my supervisor Professor Anne Ridley for her invaluable direction and support throughout my PhD, and for always making time for me.

I would like to thank all the members of the Ridley lab who made working at the Ludwig Institute and later the Randall Division such a pleasure. Thanks for all experimental help, support and advice throughout my PhD. Special thanks to Dr Rob Cain for giving me so much of his time and to Dr Sarah Heasman for editorial suggestions.

Thanks to Ken Brady from the Centre for Ultrastructural Imaging at King's College London for carrying out the electron microscopy experiments.

Outside the lab I would like to thank my parents who have always supported me. And most importantly, I would especially like to thank Peter for his unwavering support and his enduring patience throughout my PhD. Thanks for being my rock!

Declaration

I, Jana Katrin Gesine Gruenewald, confirm that the work presented in this thesis is my own. Where information has been derived from other sources, I confirm that this has been indicated in this thesis.

Signed:

Jana Gruenewald

Date: 01.09.09

1

Introduction

1.1 The mammalian immune system

The mammalian immune system is a highly sophisticated arrangement of biological mechanisms that has evolved over millions of years in order to protect the organism from infection by a diverse range of pathogens.

The immune system can be divided into several layers of defence that range from nonspecific and quick responses to very specific responses that take time to develop. Firstly, physical barriers such as the skin and mucous membranes lining the inner surfaces of the body, e.g. the gut, prevent pathogens from entering the body. Secondly, an immediate or 'innate' immune response mediates a fast but nonspecific attempt at clearing the body of invading pathogens. Thirdly, if these measures fail to resolve the problem, the adaptive immune response, composed of a cell-mediated and antibody-mediated response, provides a very specific defence system. Both innate and adaptive immune responses are mainly mediated by leukocytes.

1.2 Cells of the immune system

Immune cells are derived from haematopoietic stem cells of the fetal liver and postnatal bone marrow in a process referred to as haematopoiesis. The classical model of haematopoiesis as depicted in Figure 1.1 has lately come under scrutiny and revised models have been proposed, for expample with a lineage tree that has a lymphoid-myeloid branching point (Graf, 2008).

1.2.1 Mononuclear cells

Mononuclear cells include monocytes in the blood and macrophages in the tissue. Human monocytes are relatively large (10 – 18 µm diameter), have a horseshoe-shaped nucleus and contain granules (Male et al., 2006). Monocytes circulate in the blood for about eight hours before they enter the tissue and differentiate into macrophages, whose main purpose is the phagocytosis of microorganisms (Kindt et al., 2006). Killing of the engulfed microorganisms involves fusion of the phagosome

Figure 1.1: Cells of the immune system
Blood cells are derived from a common progenitor, a multipotent haematopoietic stem cell (HSC). Differentiation is driven by cytokines such as several members of the interleukin (IL) family, stem cell factor (SCF), thrombopoietin (TPO), interferons (IFN), erythropoietin (EPO) and colony-stimulating factors (CSFs) (Robb, 2007). The differentiation from primitive progenitor cells to committed precursor cells and lineage committed cells produces a range of blood cells with a variety of functions. While most blood cells are part of the immune system, erythocytes are transport vehicles for oxygen and carbon dioxide. Innate immunity is mediated by monocytes, macrophages, granulocytes, natural killer (NK) cells, and platelets, while the adaptive immune response is mainly mediated by lymphocytes (Male et al., 2006). At sites of vascular injury, platelets form hemostatic plugs (or blood clots) when collagen is exposed and von Willebrand factor (vWF) is present (Michelson, 2003). Granulocytes include neutrophils, eosinophils and basophils (Kindt et al., 2006). Neutrophils and eosinophils are phagocytic cells, while basophils are non-phagocytic. Granulocytes produce and release anti-microbial substances that kill invading pathogens (Male et al., 2006). Lymphocytes comprise B and T lymphocytes (B and T cells) and NK cells (Kindt et al., 2006). B cells are important in the humoral response, where they are involved in antibody production.

NK cells are a type of cytotoxic T cell that play an important role in host defence against tumour and virus-infected cells.
Abbr.: common lymphoid progenitor (CLP); common myeloid progenitor (CMP); T cell natural killer cell progenitor (TNK); B cell progenitor (BCP); T cell progenitor (TCP); natural killer progenitor (NKP); megakaryocyte erythroid progenitor (MEP); granulocyte-macrophage progenitor (GMP); megakaryocyte progenitors (MkP); erythrocyte progenitors (EP). From (Kaushansky, 2006)

with lysosomes to from a phagolysosome. Lysosomes contain H_2O_2, oxygen-free radicals, peroxidase, lysozyme and various hydrolytic enzymes, which digest the engulfed material. Phagocytosed antigen is digested within the macrophages into peptides that associate with class II major histocompatibility complex (MHC) molecules. Complexes of peptide and MHC II are transported to the membrane and presented on the macrophage surface. This processing and presentation is important for the humoral and cell-mediated immune response.

Monocytes can be subdivided into two main groups, the classical strongly CD14 positive (CD14++) cells and the more recently described group of CD14+/CD16+ cells (Ziegler-Heitbrock, 2007). Cytokine production seems to be increased in the latter group, while both types of monocytes have similar capacities in uptake and presentation of foreign antigens.

1.2.2 Lymphocytes and adaptive immune response

Lymphocytes are the main mediators of the adaptive immune response. T lymphocytes are produced in the bone marrow and mature in the thymus, therefore the name 'T' lymphocyte (Kindt et al., 2006). T cells are further subdivided into T helper (T_H) cells, cytotoxic T cells (T_C) and regulatory T cells (T_{reg} or T suppressor cells).

T_H and T_C cells can be distinguished by the expression of the glycoproteins CD4 and CD8 which bind to MHC II and MHC I, respectively. T cells, which are $CD4^+$ generally function as T_H, whereas $CD8^+$ cells function as T_C. When activated by the appropriate MHC complex, T_H cells differentiate into effector cells that activate T_C cells, macrophages and B cells. Recognition of an antigen-MHC I complex by T_C cells induces proliferation and differentiation into a cytotoxic T lymphocyte (CTL) or into a memory cell. CTLs recognise and kill infected or foreign cells, when foreign antigen is presented with class I MHC. T_{reg} cells express CD4 and CD25 and provide self-protection by preventing other T cells from attacking self components, thereby preventing autoimmunity.

1.3 Cell migration

Cell migration is essential for many biological processes, including immune responses. The core events during cell migration are the formation of distinct actin-based membrane protrusions, such as lamellipodia and filopodia (Ladwein and Rottner, 2008). These are linked to the assembly/disassembly of actin filaments and adhesion to the underlying substrate. The turnover of actin filaments requires a multitude of molecules, that act to stimulate nucleation and elongation, block filament growth (capping), mediate crosslinking/bundling or promote depolymerisation (Fig. 1.2) (Carlier and Pantaloni, 2007; Pollard and Borisy, 2003). A large number of proteins have been implicated in migration-mediating signalling events, including members of the mitogen-activated protein kinase (MAPK) pathway, lipid kinases, in particular phosphatidylinositide 3-kinase (PI3K), phospholipases, serine/threonine and tyrosine kinases and scaffolding proteins. However, one family of proteins has emerged as key regulators of cell migration: the family of small Rho GTPases.

1.3.1 Rho GTPases

Rho GTPases constitute a distinct family within the superfamily of Ras-related small GTPases (Jaffe and Hall, 2005). In mammals, 20 genes encoding Rho GTPases belonging to 8 subfamilies have been described so far: RhoA, B and C, Rac1 – 3, RhoG, Cdc42, RhoQ/TC10, RhoJ/TCL, RhoD, RhoF/Rif, Rnd1/Rho6, Rnd2/RhoN, Rnd3/RhoE, RhoH/TTF, RhoV/Chp, RhoU/Wrch-1, RhoBTB1 and RhoBTB2/DBC-2. Rho GTPases are found in all eukaryotic cells, but expression of the individual members of the family varies.

Like other regulatory GTPases, Rho proteins act as molecular switches and most of them cycle between an active, GTP-bound conformation and an inactive, GDP-bound conformation (Fig. 1.3). Rho proteins can exchange nucleotides and hydrolyse GTP *in vitro*, but at a very slow rate and to achieve rapid and efficient signalling these reactions are catalysed by guanine nucleotide exchange factors (GEFs) and GTPase-activating proteins (GAPs), respectively. Additionally, some Rho GTPases are regulated by binding to guanine-nucleotide dissociation inhibitors (GDIs), which prevent plasma membrane localisation but not necessarily interaction with downstream targets (DerMardirossian and Bokoch, 2005). Most family members contain a CAAX motif (C denotes cysteine, A represents any aliphatic amino acid and X may be any amino acid) at their C-terminus, which serves as a

Figure 1.2: Actin polymerisation at the leading edge
Extracellular stimuli activate receptors (1) leading to activation of Rho GTPases and PIP2 production (2). Rho GTPases activate Arp2/3 complex via WAVE proteins leading to actin filament branching (3/4). Polymerisation of actin filaments at the barbed ends (5) pushes the membrane forward (6), while capping proteins terminate filament elongation (6). Actin filaments age by ATP hydrolysis (white to yellow subunits), which is followed by the dissociation of the γ phosphate (red subunits) (8). ADP/cofilin promotes this phosphate dissociation and severs ADP-actin filaments (9). Finally, profilin catalyses the exchange of ADP for ATP and monomeric actin enters the cytoplasmic pool and is available again for filament polymerisation (11). Actin polymerisation is regulated by Rho GTPase-activated PAK and LIM kinase-induced inhibition of ADF/cofilin (12). Adapted from (Pollard and Borisy, 2003)

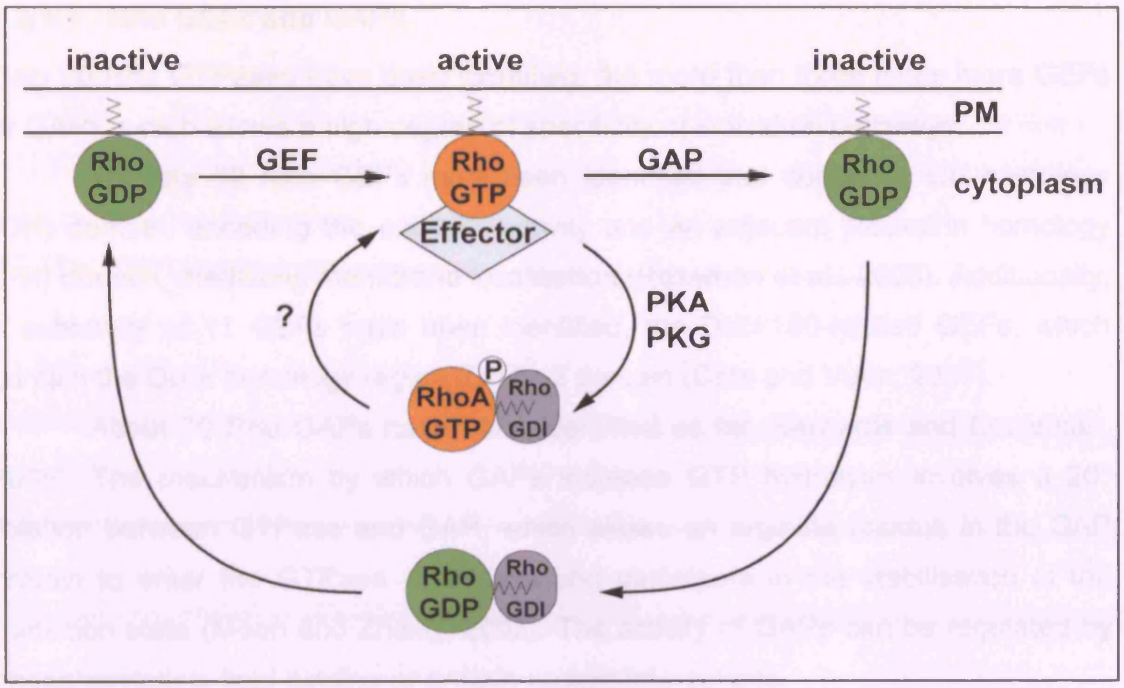

Figure 1.3: Regulation of Rho GTPases
Rho GTPases are molecular switches that contain a lipid modification to allow insertion into the plasma membrane and cycle between GTP-bound (active) and GDP-bound (inactive) forms. In their active state Rho GTPases interact with downstream effectors and regulate a range of cellular processes. Nucleotide exchange and GTP hydrolysis are catalysed by GEFs and GAPs, respectively. Additionally, Rho GTPases can be sequestered away from the membrane by interacting with RhoGDI, which prevents interaction with downstream effectors. Abbr.: Plasma membrane (PM); protein kinase A (PKA); protein kinase G (PKG).

substrate for post-translational modifications (Konstantinopoulos et al., 2007). These modifications include the covalent attachment of a non-sterol isoprenoid (either farnesyl pyrophosphate or predominantly geranylgeranyl pyrophosphate) to the cysteine residue of the CAAX motif by prenylation. This lipidated hydrophobic domain allows insertion of the Rho GTPase into the lipid bilayer of membrane (mainly the plasma membrane) as well as binding to RhoGDIs. When active, membrane-bound Rho GTPases can interact with down-stream effectors, including serine/threonine kinases, tyrosine kinases, lipid kinases, lipases, oxidases and scaffold proteins and are involved in a variety of biological processes (Bishop and Hall, 2000). Rho GTPases are important for actin polymerisation, MAP kinase pathway signalling, activation of transcription factors (SRF, NF-κB), regulation of nicotinamide adenine dinucleotide phosphate (NADPH) oxidase, cell-cycle progression, regulation of cell-cell contacts, secretion, polarity and transformation (Bishop and Hall, 2000).

1.3.1.1 Rho GEFs and GAPs

Only 20 Rho GTPases have been identified, but more than three times more GEFs or GAPs, which allows a high degree of specificity of individual pathways.

To date 69 Rho GEFs have been identified that contain a Dbl-homology (DH) domain, encoding the catalytic activity and an adjacent pleckstrin homology (PH) domain, mediating membrane localisation (Rossman et al., 2005). Additionally, a subfamily of 11 GEFs have been identified, the Dock180-related GEFs, which contain the Dock homology region (DHR)-2 domain (Cote and Vuori, 2007).

About 70 Rho GAPs have been identified so far (Bernards and Settleman, 2005). The mechanism by which GAPs increase GTP hydrolysis involves a 20° rotation between GTPase and GAP, which allows an arginine residue in the GAP protein to enter the GTPase active site and participate in the stabilisation of the transition state (Moon and Zheng, 2003). The activity of GAPs can be regulated by phosphorylation, lipid binding or protein-protein interactions.

1.3.1.2 Rho GDIs

So far three human Rho GDIs have been identified: the ubiquitously expressed RhoGDI (GDIα/GDI1), the hematopoietic cell-selective Ly/D4GDI (GDIβ/GDI2) and RhoGDIγ (GDI3), which is expressed in the lung, brain and testis (DerMardirossian and Bokoch, 2005). RhoGDI and D4GDI, hereafter referred to as GDIs, are cytosolic proteins that form 1:1 complexes with Rho GTPases. RhoGDIγ is associated with vesicular membranes and specifically binds RhoB and RhoG (Zalcman et al., 1996). GDIs form high-affinity complexes with Rho GTPases, mainly in their GDP-bound, but also to a lesser extent in their GTP-bound conformation, by shielding the geranylgeranyl membrane-targeting moiety at the C-terminus of the GTPases in a hydrophobic pocket formed by an immunoglobulin-like β sandwich (DerMardirossian and Bokoch, 2005). GDI binding serves three functions: 1) when bound to GDP-bound proteins, it prevents the dissociation of GDP from the Rho GTPase, keeping it inactive and preventing the activation by GEFs; 2) when bound to GTP-bound proteins, the intrinsic- and GAP-catalysed GTPase activity is inhibited and binding to downstream targets is blocked; 3) it sequesters Rho GTPases away from the membrane.

The GTPase:GDI complex can be influenced either by GDI dissociation factors (GDFs) or by phosphorylation of either the GDI, the GTPase or both (DerMardirossian and Bokoch, 2005). Several biologically relevant lipids, including saturated and unsaturated fatty acids, phosphatidic acids and phosphoinositides

have been reported as GDFs (Chuang et al., 1993). Phosphorylation of RhoGDI in neutrophils has been shown to stabilize the RhoA-RhoGDI-complex (Bourmeyster and Vignais, 1996), while p21-activated kinase 1 (PAK1)-mediated phosphorylation of RhoGDI at Ser101 and Ser174 results in the dissociation of Rac1-RhoGDI-complexes (DerMardirossian et al., 2004). Src kinase-mediated phosphorylation of RhoGDI at Tyr156 on the other hand leads to decreased complex formation with RhoA, Rac1 and Cdc42 (DerMardirossian et al., 2006). Phosphorylation of Rho GTPases also affects binding to GDIs; phosphorylation of RhoA at Ser188 by cyclic adenosine monophosphate (cAMP) and cyclic guanosine monophosphate (cGMP)-dependent kinases (protein kinase A (PKA) and protein kinase G (PKG)) has been shown to increase binding to RhoGDI, independent of the nucleotide binding status (Ellerbroek et al., 2003; Rolli-Derkinderen et al., 2005). PKA has also been shown to enhance Cdc42-RhoGDI interaction by phosphorylation at Ser188 (Forget et al., 2002).

The complex regulation of Rho GTPase-RhoGDI interaction by phosphorylation at multiple sites ensures specificity of the GTPase activation and also provides a mechanism for specific termination of signals.

1.3.2 Regulation of cell migration

Cell migration is usually initiated by extracellular cues, including diffusible factors such as growth factors (GFs) and signals from neighbouring cells and/or the extracellular matrix (ECM). Steps of cell migration are the extension of a leading edge protrusion or lamellipodium, the establishment and turnover of adhesion sites, the contraction and translocation of the cell body and tail detachment (Fig. 1.4) (Lauffenburger and Horwitz, 1996). Other mechanisms of migration have been detected for zebrafish primordial germ cells, where bleb-like protrusions are formed by cytoplasmic flow (Blaser et al., 2006). A gradient of the chemokine SDF-1/CXCL 12 induces calcium (Ca^{2+}) influx leading to contraction of myosin associated with the actin cortex and separation of the membrane from the cell cortex. At these sites of membrane detachment, cytoplasmic flow leads to the formation of protrusions. This type of migration has also been observed in 3D for some cancer cells (Sahai and Marshall, 2003).

Figure 1.4: Cell migration
Cell migration can be divided into distinct steps of leading edge protrusion, including extension of lamellipodium and filopodia, formation of new adhesion sites, contraction and translocation of the cell body and detachment of the tail. Adapted from (Lauffenburger and Horwitz, 1996)

1.3.2.1 Leading edge protrusion

The leading edge of migrating cells is characterised by the protrusion of a lamellipodium and filopodia. The lamellipodium is composed of a dense network of actin filaments and displays a treadmilling mechanism, with actin polymerisation at the interface between the growing filaments and the protruding plasma membrane, while the turnover is balanced by nucleation and capping at the front and disassembly occurring at the rear (Pollard and Borisy, 2003). Rac1 and Cdc42 have been shown to be important for membrane protrusions (Ladwein and Rottner, 2008), with Rac1 being the main driver in lamellipodium formation and Cdc42 being implicated in filopodium formation. GF-induced Rac1 activation by tyrosine kinases and G-protein-coupled receptors (GPCRs) is often dependent on PI3K activity (Rickert et al., 2000; Sander et al., 1998). Rac1 can also be activated in response to integrin engagement (del Pozo et al., 2000), which involves Vav family exchange factors (del Pozo et al., 2003; Moores et al., 2000). Rac1 regulates lamellipodium extension by stimulating new actin polymerisation through the Arp2/3 complex, which initiates actin branching by forming new actin filaments on the side of existing ones (Pollard and Borisy, 2003). Rac1 signals to Arp2/3 via a IRSp53 (insulin receptor substrate p53) and WASP/WAVE (Wiscott-Aldrich syndrome protein/WASP-family verprolin homology protein) proteins (Fig. 1.5) (Miki et al., 2000). WASP/WAVE proteins are potent nucleation promoting factors that differ in

their activation and regulation (Vartiainen and Machesky, 2004). WAVEs are kept inactive in a complex with four other proteins, PIR121/Sra-1, Nap125, HSPC300 and Abl interactor (Abi). In response to stimuli, this complex is disassembled and WAVEs can signal to Arp2/3. WASP proteins on the other hand are autoinhibited and need activation, e.g. phosphatidylinositol (4,5)-bisphosphate (PtdIns(4,5)P_2), which unmasks the verprolin-homology-connecting acidic (VCA) domain.

Rac1 can also stimulate actin polymerisation by promoting the uncapping of proteins, by phosphatidylinositide 4-phosphate 5-kinase (PI(4)P5-K)-induced formation of PtdIns(4,5)P_2, which binds to capping proteins, thereby removing them from the barbed ends of actin filaments (Carpenter et al., 1999; Tolias et al., 2000). Myosins are important players in cell migration and Rac1 has been shown to affect phosphorylation of myosin II heavy chain and myosin light chain (MLC) via PAK (Daniels and Bokoch, 1999; van Leeuwen et al., 1999). Considering the importance of Rac1 in migration, it is surprising that Rac1-deficient fibroblasts are able to migrate, extending pseudopodia-like protrusions without development of lamellipodia (Vidali et al., 2006). Deletion or inhibition of Rac2, which is only expressed in haematopoietic cells, compromises cell migration and adhesion in different haematopoietic cells, except for macrophages (Gu et al., 2003; Wheeler et al., 2006). Interestingly, double deletion of Rac1 and Rac2 in macrophages does not compromise migration and cells are able to perform chemotaxis normally (Wheeler et al., 2006). Cdc42 might compensate for the loss of Rac in activating Arp2/3 via IRSp53 and WAVE proteins (Vartiainen and Machesky, 2004). RhoG, another member of the Rac subfamily, is thought to contribute to Rac1-mediated lamellipodium protrusion by binding to its downstream effector genes in engulfment and motility (ELMO), which in turn binds to the Rac1 activator Dock180 (Cote and Vuori, 2007).

As opposed to the network organisation of actin in the lamellipodium, filopodia are relatively stiff rods with parallel bundles of actin filaments (Small et al., 2002). In neuronal growth cones, filopodia play a pivotal role as sensors of the extracellular milieu, steering the direction of the axon growth (Gordon-Weeks, 2004). The Arp2/3 complex is excluded from filopodia, whose rod-like structure is generated by fascin- and fimbrin-mediated bundling of actin filaments (Small et al., 2002). Cdc42 has been shown to play a major role in mediating filopodium formation by binding to the formin mDia2 (Faix and Rottner, 2006), which accumulates at the tips of filopodia (Mallavarapu and Mitchison, 1999). Additionally,

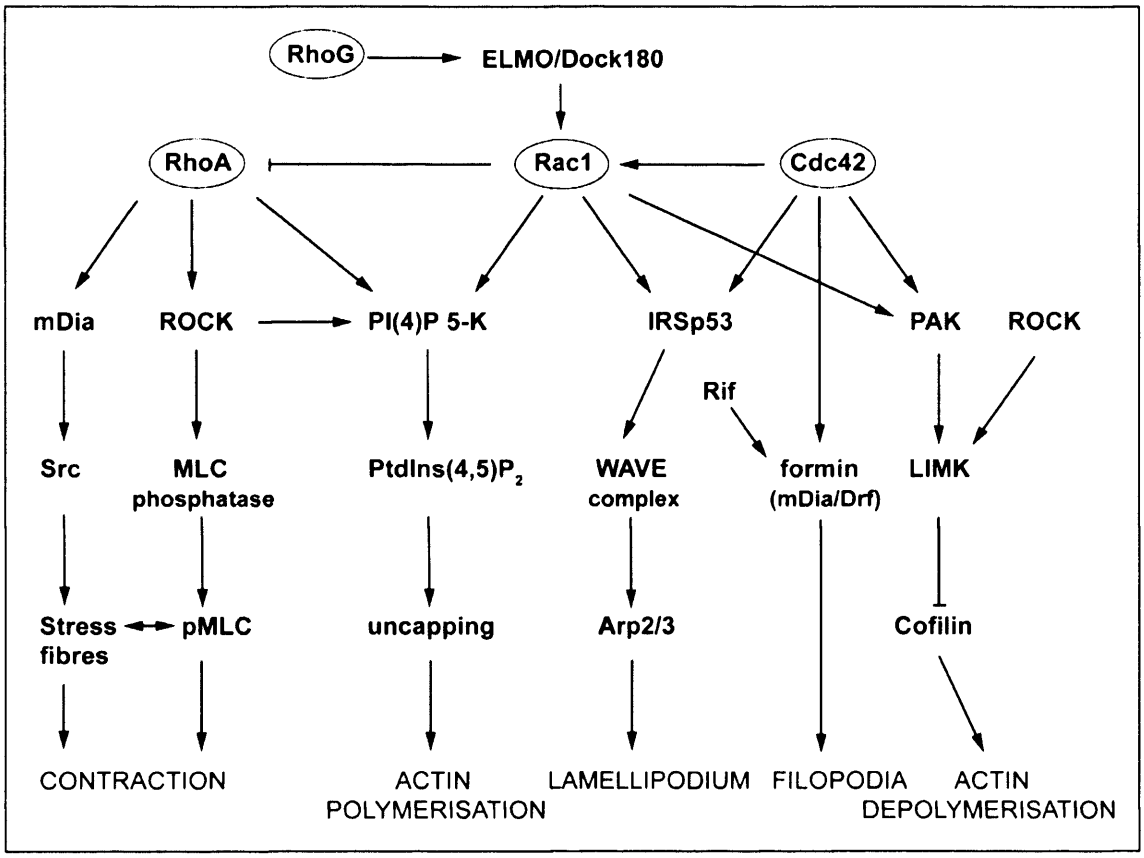

Figure 1.5: Regulation of cell migration by Rho GTPases
Cell migration is regulated by Rho GTPases and their downstream effectors. Lamellipodium protrusion is mainly regulated by Rac1, which activates the WAVE complex via IRSp53 and leads to Arp2/3-mediated actin branching and filament polymerisation. Cdc42, which induces filopodium formation via the formin mDia2/Drf, has also been shown to interact with IRSp53, feeding into the Arp2/3 pathway. Rac1 is additionally activated by RhoG, which interacts with its downstream effector ELMO, leading to Dock180-mediated activation of Rac1. Finally, Rac1 and Cdc42 both activate LIM kinase (LIMK) via PAK, thereby inhibiting cofilin-mediated actin depolymerisation. ROCK, a RhoA effector, has also been shown to activate LIMK. RhoA and Rac1 both regulate the activity of PI(4)P5-K to induce increases in PtdIns(4,5)P_2 levels, thereby affecting capping proteins and actin polymerisation. RhoA activity also leads to increased contractility and stress fibre formation by ROCK-induced inhibition of MLC phosphatase and subsequent MLC phosphorylation. Additionally, RhoA interacts with mDia to contribute to stress fibre formation, which is dependent on Src kinase.

mDia has been implicated in filopodium formation triggered by the Rho GTPase RhoF/Rif (Rho in filopodia) (Pellegrin and Mellor, 2005). Interestingly, Cdc42 has also been shown to interact directly with the Arp2/3-complex activator WASP, thereby linking Cdc42 into the lamellipodium formation pathway (Vartiainen and Machesky, 2004). This pathway is also important for membrane trafficking during endocytosis.

1.3.2.2 Formation and turnover of adhesions

Adhesion to the ECM or neighbouring cells is mediated by adhesion sites that vary in morphology, size and subcellular distribution depending on the cell type and substratum, but share two common features: they are integrin-mediated and interact with the actin cytoskeleton (Geiger et al., 2001). Focal adhesions (FA) are the best characterised adhesions; they are flat and elongated structures mostly at the periphery of cells and mediate adhesion to the substrate by anchoring the actin cytoskeleton through a plaque of many different proteins, including vinculin, talin and paxillin (Geiger et al., 2001). However, this form of FAs has only been observed in slow moving cells. During cell migration the co-ordinated assembly and disassembly of FAs is vital for efficient translocation. FAs act as substrate-anchoring points for stress fibres and can also act as mechanosensors, maturing with increasing tension as the cell moves along. Rac1 and RhoA have been shown to be involved in FA assembly and maturation. Rac1 mediates FA assembly in the lamellipodium (Allen et al., 1997; Nobes and Hall, 1995), while RhoA-induced contractility via Rho-kinase (ROCK) and myosin II leads to FA maturation (Rottner et al., 1999; Totsukawa et al., 2000). Rac1 is also involved in FA disassembly, either directly through PAK (Zhao et al., 2000), or by antagonising RhoA activity (Sander et al., 1998). Integrin-mediated adhesion seems to be required for Rac1 binding to PAK (del Pozo et al., 2000), indicating that a critical level of integrin engagement ultimately leads to FA disassembly. However, adhesion turnover involves additional regulatory signals, including FAK and Src (Jones et al., 2000).

1.3.2.3 Cell body contraction

The contraction of the cell body is believed to be dependent on Rho-mediated actomyosin contractility (Mitchison and Cramer, 1996). Rho acts via ROCKs to induce MLC phosphorylation, by inhibiting MLC phosphatase and directly phosphorylating MLC (Kaibuchi et al., 1999). MLC is also phosphorylated by MLC-kinase (MLCK) in response to Ca^{2+} and extracellular signal-regulated kinase (ERK) activation (Hansen et al., 2000). RhoA is also linked to the actin cytoskeleton via mDia, which interacts with Src to induce stress fibre formation (Tominaga et al., 2000). Inhibiting Rho proteins has two opposing effects on cell migration depending on adherence and cell type: it promotes migration by lowering adhesion due to decreased stress fibres, and it reduces migration by reducing contractility.

1.3.2.4 Tail detachment

Migrating leukocytes exhibit a more or less triangular shape with a 'uropod' at the rear. A uropod is an actively produced structure that is important in the interplay between leukocytes (Fais and Malorni, 2003). Slow migrating fibroblasts have a tail, which is formed passively (Lauffenburger and Horwitz, 1996). The mechanism regulating uropod or tail detachment depends on the type of cell and strength of adhesion (Palecek et al., 1998). The protease calpain, which degrades FA components at the rear, plays an important role in tail detachment (Glading et al., 2000; Palecek et al., 1998). Rho inhibition by C3 transferase has been shown to inhibit tail detachment through decreased contractility, leading to the development of long tails (Cox and Huttenlocher, 1998; Worthylake et al., 2001). Regulated assembly as well as disassembly of adhesions is therefore pivotal for efficient migration.

1.3.3 Cell-type specific variations in cell migration mechanisms

Most cell types of the body are capable of migration at a given time and tissue space. However, the mechanism of migration can differ between cell types. A large range of migration studies have been carried out in mouse fibroblasts and fish keratocytes (see reviews by (Geiger et al., 2001; Lauffenburger and Horwitz, 1996; Pollard and Borisy, 2003). Fish keratocytes are fast migrating cells that do not complete the typical stepwise migration sequence (see Chapter 1.3.2) observed in fibroblasts (Svitkina et al., 1997). However, their large lamellipodium makes them ideal candidates for studying actin dynamics (Pollard and Borisy, 2003). Additionally, a lot of the basic actin biochemistry has been studied *in vitro* (Pollard and Borisy, 2003). Other cellular systems used to study single cell migration include leukocytes (Allen et al., 1998; del Pozo et al., 2003; Gu et al., 2003; Moores et al., 2000; Rickert et al., 2000; Wheeler et al., 2006; Worthylake et al., 2001), epithelial cells (Hansen et al., 2000; Sander et al., 1998), COS7 (Miki et al., 2000), PC12 and melanoma cells (van Leeuwen et al., 1999), HeLa (Pellegrin and Mellor, 2005), and Chinese hamster ovary cells (CHO) (Palecek et al., 1998). Regulatory pathways have also been extensively studied in non-mammalian organisms such as *Caenorhabditis elegans*, *Drosophila*, *Saccharomyces cerevisae* and *S. pombe* (Vartiainen and Machesky, 2004).

Although the basic mechanisms regulating cell migration, e.g. actin polymerisation or actomyosin-mediated contraction, are believed to be very similar between cell types, two distinct mechanisms for single cell migration have been

described: mesenchymal and amoeboid migration (Friedl, 2004). However, variations of these migration mechanisms are possible and cells can change their migration behaviour when differentiating or in response to stimuli. Mesenchymal migration is relatively slow (0.1 – 2 µm/min) and is characteristic for fibroblasts, myoblasts, single endothelial or sarcoma cells (Grinnell, 1994; Tamariz and Grinnell, 2002) and is accomplished by completing the complete five-step migration sequence (including protase-dependent degradation of ECM). Amoeboid migration, which mimics the migration behaviour of the amoeba *Dictyostelium discoideum*, is fast (2 – 30 µm/min) and is carried out by haematopoietic stem cells, leukocytes and certain tumour cells (Francis et al., 2002; Friedl et al., 2001; Wang et al., 2002). Amoeboid migration can be described as a four-step process: 1) leading edge protrusion by actin flow; 2) interaction of surface receptors with substrate; 3) actomyosin-mediated contraction of the cell body; 4) forward movement of rear of cell. While mesenchymal migration is dependent on focalised integrin-mediated adhesion in FAs (Ballestrem et al., 2001; Maaser et al., 1999; Sims et al., 1992; Tamariz and Grinnell, 2002) and requires local proteolysis of ECM proteins, amoeboid migration is driven by short-lived and relatively weak interactions with the substrate (Friedl, 2004). This lack of stable focal contacts and the use of protease-independent physical mechanisms to overcome matrix barriers by squeezing through narrow spaces (Wolf et al., 2003) allow the highly deformable leukocytes to move at high velocities. Migration of lymphocytes and neutrophils has been shown to be completely or partially independent of β1 integrin, both *in vitro* (Friedl et al., 1998) and *in vivo* (Brakebusch et al., 2002; Werr et al., 1998).

1.4 The innate immune response and inflammation

The recognition of pathogens by the innate immune system is dependent on Toll-like receptors (TLRs) (Murphy et al., 2008). In mammals, 10 TLR genes are expressed, forming eight different receptors, which can be either heterodimers, homodimers or monomers. TLRs recognise diacyl lipopeptides, triacyl lipopeptides, flagellin, lipopolysaccharide (LPS), double and single stranded ribonucleic acid (dsRNA and ssRNA, respectively), guanine-rich oligonucleotides and unmethylated deoxyribonucleic acid (DNA). The initial stages of the innate immune response rely on mobilisation of existing leukocytes to the site of infection or damage. This is achieved through inflammation and subsequent extravasation of leukocytes from the blood to the tissue, termed transendothelial migration (TEM). Inflammation is a complex response and involves various cell types and numerous pro-inflammatory

mediators. These pro-inflammatory mediators are produced upon tissue damage and infection and regulate the migration of leukocytes into the sites of inflammation. Pro-inflammatory cytokines include tumor necrosis factor-α (TNF-α), TNF-β, IL-1 and IL-6 and are produced by a variety of activated cell types, including endothelial cells (ECs), platelets, leukocytes and fibroblasts (Huang et al., 2006b). Inflammation leads to the disruption of vascular integrity which can be potentially harmful and is known to be a contributing factor in the pathogenesis of a range of diseases, including atherosclerosis, cancer and neurodegenerative diseases (Lin and Karin, 2007; Napoli and Palinski, 2005).

1.4.1 TNF-α induces an inflammatory response in ECs

TNF-α is predominantly produced by macrophages and monocytes, but ECs are also capable of TNF-α production (Kofler et al., 2005). TNF-α has several effects on the endothelium, including protein-synthesis-independent changes such as increases in monolayer permeability and cell motility, facilitating leukocyte extravasation, but also leading to vascular leakage and oedema formation (Friedl et al., 2002).

TNF-α exerts its effects via two cell surface receptors, TNFR1 (p50) and TNFR2 (p75) (MacEwan, 2002). TNF-α binding induces activation of nuclear factor-κB (NF-κB) and MAPKs, including ERK, p38 and c-Jun N-terminal kinase (JNK) among other responses (MacEwan, 2002; Paul et al., 1997).

1.4.2 NF-κB activation

At least 150 genes are regulated by the transcription factor NF-κB. It is composed of homo- and hetero-dimeric complexes of Rel family polypeptides, which include five related DNA binding family members: Rel-A (p65), Rel-B, c-Rel, NF-κB1/p50 and NF-κB2/p52 (Beinke and Ley, 2004). NF-κB activity is tightly regulated by the inhibitor of NF-κB (IκB) family, including IκB-α, IκB-β, IκB-γ, p100 and p105, which bind NF-κB in the cytosol and prevent it from activating target genes. Two distinct NF-κB activation pathways exist: the classical pathway and the alternative pathway (Fig. 1.6) (Karin and Greten, 2005). The classical pathway is triggered by pro-inflammatory cytokines, such as TNF-α, bacterial wall components, viruses and DNA-damaging agents and activates the IκB kinase (IKK) complex. This complex consists of three components, two catalytic subunits IKK-α and IKK-β, as well as a regulatory subunit IKK-γ. The IKK complex phosphorylates IκB leading to its

Figure 1.6: Classical and alternative pathway of NF-κB activation
A: In the classical pathway activation of cellular receptors by pro-inflammatory cytokines or other stimuli activates the IKK complex, which is composed of IKK-α, IKK-β and IKK-γ. The IKK complex phosphorylates IκB, which is bound to and inhibits the NF-κB complex made up of p50 and Rel-A in the cytoplasm, leading to its proteasomal degradation. The p50/Rel-A dimer can enter the nucleus and up-regulate target gene transcription. In the alternative pathway, cellular receptors are activated by TNF family members leading to IKK-α-dependent phosphorylation of p100 (a p52 precursor) and its proteasomal degradation to p52. Dimers of p52 and Rel-B can enter the nucleus and activate downstream targets. **B**: NF-κB target genes include genes involved in inflammation, innate immunity and survival. From (Karin and Greten, 2005)

polyubiquitination and subsequent proteasomal degradation. The liberated NF-κB dimers, which are mostly p50-Rel-A dimers, are translocated to the nucleus where they mediate transcription of target genes. The alternative pathway is triggered by certain TNF-family members and leads to an IKK-α-dependent phosphorylation of p100, resulting in its proteasomal degradation to p52 and translocation of p52-Rel-B dimers to the nucleus, where target genes are activated.

TNF-α-mediated adhesion molecule expression plays a central role in the inflammatory response. TNF-α-mediated NF-κB activation leads to transcriptional upregulation of E-selectin, P-selectin, intercellular adhesion molecule-1 (ICAM-1), vascular adhesion molecule-1 (VCAM-1), mucosal addressin adhesion molecule-1 (MadCAM-1) and others (De Martin et al., 2000; Zeiffer et al., 2004). The distinct roles of the two TNF receptors in this process are controversial. Studies using receptor-specific antibodies and TNF-α mutants have shown that TNFR1 (p55) and not TNFR2 (p75) is important in mediating the TNF-α response (Paleolog et al., 1994; Zhou et al., 2007), while mouse studies have shown that TNFR2 (p75) is critical for ICAM-1 upregulation at mRNA and protein level and P-selectin at the mRNA level (Chandrasekharan et al., 2007; Lucas et al., 1997). TNFR1 (p55)-mediated adhesion molecule upregulation is entirely NF-κB-dependent and no cross-talk with the MAPK pathway occurs (Zhou et al., 2007).

1.4.3 Leukocyte adhesion cascade and transendothelial migration

Leukocyte adhesion and TEM are active and tightly regulated mechanisms that involve many molecules on the endothelial and the leukocyte surface as well as cytoskeletal rearrangements and signalling events. The leukocyte adhesion cascade can be divided into distinct steps: tethering and rolling, arrest and firm adhesion, locomotion, and diapedesis or transmigration (Fig. 1.7) (Ley et al., 2007).

1.4.3.1 Leukocyte rolling

The initial steps of adhesion are mediated by L-selectin on leukocytes and/or E- and P-selectin on ECs, causing the leukocyte to be captured from the fast flowing bloodstream and to roll slowly along the endothelial surface (Hogg and Landis, 1993). L-selectin, which is expressed by most leukocytes, interacts with sialylated ligands on the endothelial surface (McEver, 2002). L-selectin is localised to microvilli, which is mediated by its binding to moesin, a member of the ezrin-radixin-moesin (ERM) family (Ivetic et al., 2004). P-selectin glycoprotein ligand 1 (PSGL1)

Figure 1.7: The leukocyte adhesion cascade and transendothelial migration
The leukocyte adhesion cascade is a multi-step process, involving a multitude of molecules on the endothelium as well as the leukocytes. The steps are: 1) Tethering and rolling, which involves P-selectin and E-selectin on the endothelial cells, as well as L-selectin and selectin ligands PSGL1, CD44 and ESL1 on the leukocytes. Rolling can also be mediated by integrins, where VLA-4 binds to VCAM-1 and LFA-1 binds to ICAM-1. 2) Leukocyte arrest and firm adhesion is mediated by chemokine-induced activation of integrins, including Mac-1, LFA-1, VLA-4, binding to ICAM-1 and VCAM-1. 3) Locomotion is, depending on the cell type, mediated by Mac-1 or LFA-1 binding to ICAM-1 and VCAM-1, respectively. 4) Transmigration is mediated by LFA-1 binding to ICAM-1, and additionally by PECAM-1, CD99 and JAMs during paracellular TEM. Dark blue font: leukocyte receptors; light blue font: endothelial receptors. Adapted from figure provided by Dr R.J. Cain.

is a ligand for all three selectins and is anchored to the actin cytoskeleton by ezrin and/or moesin (Ivetic et al., 2004; McEver, 2002). Binding of PSGL1 to L-selectin mediates leukocyte-leukocyte interaction, thereby allowing leukocytes without ligands for E- or P-selectin to reach sites of inflammation (Eriksson et al., 2001). Other selectin ligands include glycosylated CD44 and E-selectin ligand 1 (ESL1), which are both ligands for E-selectin (Hidalgo et al., 2007). Selectins have been shown to display catch bonds behaviour, where increasing force first prolongs and then shortens the lifetime of selectin binding (Marshall et al., 2003). This phenomenon allows deceleration of the leukocytes and increases proximity between leukocytes and the endothelium, a prerequisite for chemokine-induced signalling and firm adhesion.

Leukocyte rolling can also be mediated by integrins and their ligands: very late antigen-4 (VLA-4; α4β1)-mediated rolling on VCAM-1 has been seen for several leukocytes (Chan et al., 2001; Singbartl et al., 2001), while leukocyte function-associated antigen-1 (LFA-1; CD11a/CD18 or $\alpha_L\beta2$)-mediated rolling by binding to

ICAM-1 has been observed in neutrophils (Chesnutt et al., 2006). The latter requires partial LFA-1 activation induced by E-selectin binding.

1.4.3.2 Leukocyte arrest and firm adhesion

The close proximity between rolling leukocytes and the endothelium allows modulation of the adhesiveness by chemokines presented on the apical surface of the ECs (Campbell et al., 1998). These chemokines can be produced by the endothelium in response to pro-inflammatory stimuli and are transported to the apical surface (Mordelet et al., 2007). Additionally, thrombin-activated platelets deposit CC-chemokine ligand 5 (CCL5; previously known as RANTES) as well as CXC-chemokine ligand 4 (CXCL4) and CXCL5 on the surface of inflamed vasculature (Huo et al., 2003; von Hundelshausen et al., 2001). Endothelium-bound chemokines and chemokine receptors on the leukocytes are localised to microvilli to facilitate their interaction. The chemokines presented on the ECs differ depending on the site of vasculature allowing recruitment of specific leukocyte subsets, for example to sites of inflammation or secondary lympoid organs (Muller and Lipp, 2003).

Chemokines exert their effect by binding to GPCRs, thereby dissociating Gα and Gβγ subunits of the heterotrimeric G proteins (Viola and Luster, 2008). Chemokine receptors can signal through different Gα families, activating distinct signalling pathways. During TEM, exposure to chemokines induces arrest of rolling leukocytes (Huo et al., 2003; von Hundelshausen et al., 2001). The activation of chemokine receptors in endothelium-bound leukocytes has multiple effects, including direct or indirect stimulation of members of the Rho GTPase family and activation of leukocyte integrins (Wittchen et al., 2005).

1.4.3.2.1 Integrins

Integrins are heterodimers containing non-covalently linked α and β chains (Takada et al., 2007). Each subunit has a large extracellular domain, a single transmembrane domain and a short cytoplasmic domain. In mammals, combination of 18 α and 8 β subunits forms 24 integrins, which bind to various substrates, mediating cell-cell and cell-ECM contacts. The N-terminal portions of the α and β subunit form a globular head containing the ligand-binding region. Nine of the α subunits contain a domain of about 200 amino acids, which is termed the inserted or I domain and is the major or exclusive ligand-binding site in these integrins (Takada et al., 1997). Ligand binding requires divalent cations, and integrins have

several putative cation binding sites. Non-αI integrin binding is mediated by specific regions of the N-terminal portions of both α and β subunits.

For leukocyte TEM, β2-containing integrins are most important, particularly LFA-1 and myeloid-specific integrin Mac-1 (CD11b/CD18 or $\alpha_M\beta2$), but α4 containing integrins also play a role, including VLA-4 and α4β7 (Barreiro et al., 2007). The ligands mediating cell-cell contacts belong mainly to the immunoglobulin superfamily, LFA-1 binds to members of the ICAM family (Hayflick et al., 1998), but also junctional adhesion molecule-A (JAM-A) (Ostermann et al., 2002). Mac-1 binds to ICAM-1, JAM-C and the endothelial receptor for advanced glycation end products (RAGE) (Chavakis et al., 2003; Lamagna et al., 2005), while VLA-4 interacts with VCAM-1 and JAM-B (Cunningham et al., 2002; Elices et al., 1990).

1.4.3.2.2 Integrin activation

During TEM, integrin adhesiveness is modulated by chemokines acting through leukocyte GPCRs. Integrin activation has long been thought to occur due to integration of successive GPCR signals encountered by rolling leukocytes until a threshold is reached. Shamri et al. have shown, though, that endothelium-bound chemokines induce instantaneous extension of LFA-1 in the absence of ligand (Shamri et al., 2005). The immediate binding of the ligand ICAM-1 then induces the fully active high-affinity conformation. GPCR-induced integrin activation is referred to as 'inside-out signalling', in contrast to signalling downstream of ligand binding, which is referred to as 'outside-in signalling'.

How GPCRs exert their effects on integrin activation is not fully understood, but two members of the Ras GTPase family, RhoA and Rap1 have been implicated in this process (Bos, 2005) (Fig. 1.8). Rap1 has been shown to activate integrins in a RapL-dependent manner, where RapL is recruited by Rap1 to associate with and activate LFA-1 (Katagiri et al., 2003). The importance of RapL in integrin activation has been confirmed by the RapL knock-out phenotype, in which leukocytes show decreased binding to ICAM-1 (Katagiri et al., 2004). The role of RhoA in integrin activation is likely to be downstream of Rap1, since loss of RhoA function has been shown to prevent integrin activation induced by Rac1 and Rap1A *in vivo* (Vielkind et al., 2005). Additionally, RhoA is also involved in LFA-1 extension triggered by SDF-1 (Pasvolsky et al., 2008). Rap1 has also been shown to activate integrins by a

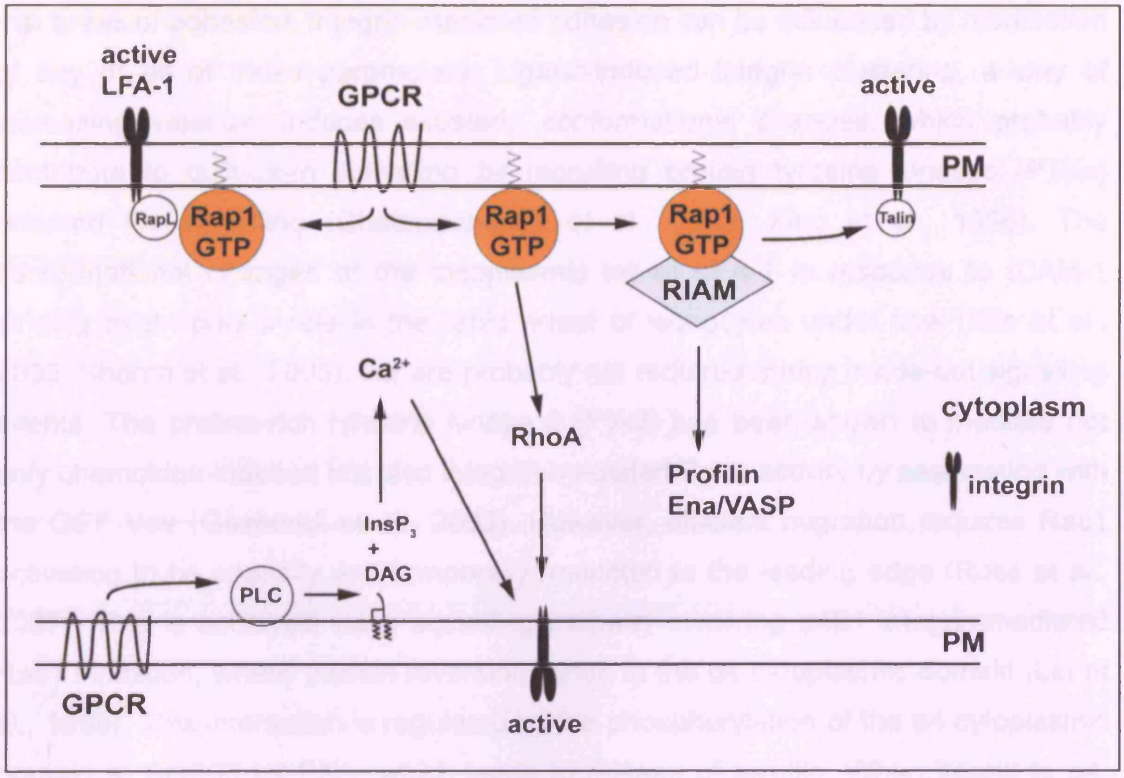

Figure 1.8: Integrin activation downstream of GPCRs
Integrin activation downstream of GPCRs involves the activation of the GTPase Rap1, which leads to RapL localisation to LFA-1, thereby inducing activation. Additionally, the Rap1 effector RIAM induces localisation of Talin to integrins, thereby mediating integrin activation by wedging in between the two cytoplasmic tails. RhoA is also likely to play a role in integrin activation and has been shown to be downstream of Rap1. Integrin activation downstream of GPCRs is also induced via PLC-generated $InsP_3$ and DAG generation, leading to increased intracellular Ca^{2+} levels.

profilin- and vasodilator-stimulated phosphoprotein (VASP)-binding protein termed Rap-interacting adapter molecule (RIAM) (Lafuente et al., 2004), which recruits talin to the vicinity of integrins, thereby inducing integrin activation (Han et al., 2006). Talin inserts between the α- and β-cytoplasmic tails of integrins, thereby increasing adhesion (Kim et al., 2003; Tadokoro et al., 2003). Integrin activation downstream of GPCRs has also been shown to be dependent on activation of phopholipase C (PLC), 1,4,5-trisphophate receptors, Ca^{2+} influx and activation of calmodulin (CaM) (Hyduk et al., 2007).

The overall strength of adhesion is referred to as 'avidity' and is defined by the intrinsic affinity of the receptor-ligand bond and the number of bonds, the 'valency' (Carman and Springer, 2003). The valency is defined by the density and distribution of the receptors on the cellular surface, as well as the ability to move

into areas of adhesion. Integrin-mediated adhesion can be influenced by modulation of any or all of these parameters. Ligand-induced integrin clustering, a way of increasing valency, induces allosteric conformational changes, which probably contribute to outside-in signalling by recruiting protein tyrosine kinases (PTKs) required for signalling (Chatzizacharias et al., 2008; Xiao et al., 1996). The conformational changes of the cytoplasmic tail of LFA-1 in response to ICAM-1 binding might play a role in the rapid arrest of leukocytes under flow (Kim et al., 2003; Shamri et al., 2005), but are probably not required during inside-out signalling events. The proline-rich tyrosine kinase 2 (Pyk2) has been shown to mediate not only chemokine-induced but also integrin-mediated Rac1 activity by associating with the GEF Vav (Gismondi et al., 2003). However, efficient migration requires Rac1 activation to be spatially and temporally restricted to the leading edge (Rose et al., 2007). This is achieved via a signalling pathway involving α4β1 integrin-mediated Rac1 inhibition, where paxillin reversibly binds to the α4 cytoplasmic domain (Liu et al., 1999). This interaction is regulated by the phosphorylation of the α4 cytoplasmic domain at Ser988 by PKA, which leads to release of paxillin. When bound to α4, paxillin binds to other signalling molecules including the adenosine diphosphate (ADP)-ribosylation factor (Arf)-GAP, G protein-couples receptor kinase-interactor-1 (GIT1) (Nishiya et al., 2005). GIT inhibits Rac1 by inhibiting the activation of another small GTPase, Arf6 (Vitale et al., 2000). The interaction between α4 integrin and paxillin is therefore an important regulator of the spatial and temporal activation of Rac1 during cell migration. Selective paxillin phosphorylation in the leading edge is likely to be achieved by PKA localisation and activation at the leading edge (Goldfinger et al., 2003).

Integrin-mediated firm adhesion, elicited by chemokine-mediated inside-out signalling, and leukocyte activation initiate the next step of TEM, migration on the endothelium (locomotion).

1.4.3.3 Locomotion

Only recently, Schenkel et al. have identified the importance of locomotion, a process in which leukocytes move from sites of firm adhesion to the nearest junction to transmigrate (Schenkel et al., 2004). This step is dependent on LFA-1 and Mac-1 on the leukocyte surface, since blocking with specific antibodies prevents directed movement to the junctions and TEM. Similar results have been found with Mac-$1^{-/-}$ mice, where locomotion of neutrophils was reduced (Phillipson et al., 2006). In LFA-$1^{-/-}$ mice, however, neutrophils did not exhibit a locomotion defect, but adhesion was significantly reduced. These data suggest that LFA-1 and Mac-1 have different

functions in TEM *in vivo*, where LFA-1 is important for adhesion and Mac-1 in locomotion. However, further studies should clarify if this effect is neutrophil-specific or is valid for other leukocytes too.

1.4.3.4 Transmigration

Diapedesis or transmigration refers to the process whereby leukocytes traverse the endothelium and can be rapid, involving different sets of molecules depending on the transmigrating cell. Leukocytes have been shown to transmigrate using two distinct pathways, either by penetrating endothelial junctions, using a 'paracellular route', or by transmigrating directly through ECs in a process termed 'transcellular' TEM.

1.4.3.4.1 Endothelial cell-cell junctions

During paracellular TEM leukocytes have to transmigrate through endothelial cell-cell junctions to reach the underlying tissue. Endothelial cell-cell junctions have specialised regions that are comparable to adherens junctions (AJs) and tight junctions (TJs) in epithelia (Dejana, 2004). TJs and AJs are formed by different molecules, but have common features, such as the formation of homophilic interactions. TJ-associated transmembrane proteins include JAMs, endothelial selective adhesion molecule (ESAM), claudins and occludin, while AJ-associated proteins include VE-cadherin (Fig. 1.9). Junctional adhesion proteins are anchored to the actin cytoskeleton by binding to various adapter molecules, which often have additional signalling functions (Matter and Balda, 2003; Wheelock and Johnson, 2003). Some of these adaptor molecules function as scaffolding proteins, by binding several effector proteins and enabling their reciprocal interaction. Examples of such scaffolding proteins are the TJ components zona occludens-1 (ZO-1), ZO-2 and ZO-3, which can associate with many transmembrane proteins, including claudins, occludin or JAMs, with cytoskeletal binding proteins such as cortactin, cingulin, α-catenin, and indirectly with vinculin and β-catenin (Matter and Balda, 2003). VE-cadherin, like most other cadherins, binds catenins; β- and γ-catenin (plakoglobin) connect VE-cadherin with α-catenin, which binds to actin filaments (Vestweber, 2008), but possibly not when bound to β-catenin (Drees et al., 2005). The nectin-afadin system plays an important role in both junction types. Nectin is a member of the immunoglobulin family and is linked to actin via afadin (or AF6) and ponsin (Takahashi et al., 1999). Outside specialised junctional structures, ECs express

Figure 1.9: Organisation of endothelial cell-cell junctions
Endothelial junctions are made up of transmembrane adhesion proteins and their intracellular binding partners. TJs are formed by Claudins, Occludin, JAMs and ESAM, while adherens junctions AJs are composed of VE-cadherin. Nectin is part of both junction types. PECAM-1 is also present in the junctions, but outside of specialised junctional structures. Many intracellular binding partners mediate direct or indirect association to actin filaments, e.g. ZO-1/2, α-catenin, β-catenin, α-actinin, plakoglobin, vinculin, cingulin and Ca^{2+}/calmodulin-dependent serine protein kinase (CASK), afadin, ponsin, while others, such as vascular endothelial protein tyrosine phosphatase (VE-PTP), modulate cadherin and catenin phosphorylation, thereby regulating vascular permeability. Adapted from (Dejana, 2004)

additional adhesion molecules capable of forming homophilic interactions, which include CD99 and platelet EC adhesion molecule-1 (PECAM-1 or CD31) (Dejana, 2004). PECAM-1 belongs to the immunoglobulin superfamily and is not confined to any type of junctions.

1.4.3.4.2 Paracellular TEM

During paracellular TEM adherens junctions have to be transiently opened to allow passage of leukocytes. Binding of leukocytes to the endothelium has been shown to induce signalling events in the ECs, leading to remodelling of the actin cytoskeleton and loosening of the junctions (Millan and Ridley, 2004). This event is accompanied by formation of stress fibres, via RhoA/ROCK and Ca^{2+}-dependent phosphorylation of MLC by MLCK, leading to increased contractility (Hixenbaugh et al., 1997; Huang et al., 1993; Wojciak-Stothard et al., 1999). Binding of leukocytes to ICAM-1 and

VCAM-1 on the EC activates this pathway (Adamson et al., 1999; Thompson et al., 2002; Wojciak-Stothard et al., 1999), possibly via the involvement of ERM proteins (Barreiro et al., 2002; Bretscher et al., 2002). Disruption of adherens junctions also occurs through VCAM-1-clustering and downstream Rac1 activation, leading to subsequent reactive oxygen species (ROS) production (Cook-Mills, 2002; van Buul and Hordijk, 2004). This process is dependent on VCAM-1-induced Ca^{2+} influx (Cook-Mills et al., 2004).

During diapedesis VE-cadherin is transiently removed from the junctions in order to allow leukocytes to pass (Shaw et al., 2001; Su et al., 2002), while endothelial junctional proteins that are also expressed on leukocytes (e.g. PECAM-1 and JAM-A) actually facilitate TEM (Muller, 2003). PECAM-1 has been shown to localise to a membrane network just below the plasma membrane at the cell borders, which is connected to the junctional surface (Mamdouh et al., 2003). These structures have been referred to as 'subjunctional reticulum', 'reticular junctions' or 'lateral border recycling compartment' (LBCR) (Mamdouh et al., 2003; Mamdouh et al., 2008). When leukocytes transmigrate, PECAM-1 in the endothelium recycles from these structures and concentrates around the migrating leukocyte. This process, which is dependent on kinesin family molecular motors and requires normally functioning endothelial microtubules, is a requirement for TEM, since disruption of microtubules and inhibition of kinesin motor domain blocked diapedesis (Mamdouh et al., 2008). VE-cadherin and CD99 have also been shown to localise to this compartment (Mamdouh et al., 2003).

As well as PECAM-1, ICAM-1, ICAM-2, JAM-A, JAM-B, JAM-C, ESAM and CD99 contribute to leukocyte TEM (Muller, 2003; Vestweber, 2002). These molecules are involved in binding to leukocyte integrins (ICAM-1 and -2 bind LFA-1), mediate homophilic interactions between leukocyte and endothelium (PECAM-1 and CD99), or do both (JAMs).

Following leukocyte extravasation endothelial junctions are rapidly resealed to prevent vascular leakage (Shaw et al., 2001; Su et al., 2002). VE-cadherin appears to be pushed aside during TEM and returns to the junctions within 5 min.

1.4.3.4.3 Transcellular TEM

Leukocytes have long been thought to transmigrate through endothelial cell-cell junctions only. However, *in vivo* EM studies have shown that leukocytes can also follow a transcellular route by transmigrating directly through ECs (Feng et al., 1998). Transmigrating cells form channels through the EC by fusion of vesicles resembling vesiculo-vacuolar organelles (VVOs) with the plasma membrane. More

recent studies have shown that TEM via the transcellular route also occurs *in vitro*, although only a minority of cells uses this pathway and the rate is dependent on endothelial as well as leukocyte cell type (Carman and Springer, 2004; Millan et al., 2006). VVOs have not been observed *in vitro*. Instead, clustering of ICAM-1 has been shown to trigger signalling events leading to translocation of ICAM-1 and caveolae in F-actin-enriched areas, and it is postulated that caveolae fuse to form a channel through which leukocytes can transmigrate (Millan et al., 2006). Carman et al. have demonstrated the importance of invasive podosomes, actin-dependent protrusive structures at the basal surface of leukocytes, during transcellular TEM (Carman et al., 2007). Lymphocytes use these protrusions to probe the EC surface and form the transcellular pore. The formation of podosomes is dependent on Src kinase and the actin regulatory protein WASP, while the formation of the transcellular pore is dependent on membrane fusion.

Adherent leukocytes have been shown to induce the formation of 'transmigratory cups' or docking structures in ECs (Barreiro et al., 2002; Carman and Springer, 2004). These structures play a role in the firm adhesion of leukocytes and are composed of microvillus-like projections from the ECs that surround transmigrating leukocytes. The projections are rich in ICAM-1 and VCAM-1, and VCAM-1 interacts directly with activated moesin and ezrin (Barreiro et al., 2002). Cytoskeletal components such as α-actinin, vinculin and VASP are also present, and phosphoinositides and the Rho/ROCK pathway participate in the activation of ERM proteins. The VCAM-1-rich vertical projections lead to a redistribution of leukocyte integrins and disruption of these structures leads to inhibition of TEM (Carman and Springer, 2004). However, the importance of these structures in TEM is still controversial.

In $Mac1^{-/-}$ mice, neutrophils predominantly transmigrate using the transcellular route, which takes 20 -30 minutes longer than the paracellular route in wild-type (wt) mice (Phillipson et al., 2006). Interestingly, $Mac1^{-/-}$ mice did not display higher vascular permeability than wt mice. In both wt and $Mac1^{-/-}$ mice, transmigrating neutrophils were enveloped by a dome-like structure (Phillipson et al., 2008). This structure could be an extension of the 'transmigratory cup' or docking structure and seems to prevent vascular leakage during TEM.

1.5 Reactive oxygen species

ROS is a collective term that describes chemical species that are formed upon incomplete reduction of oxygen (O_2). ROS include radicals and non-radical species such as superoxide anion (O_2^-), hydrogen peroxide (H_2O_2) and the hydroxyl radical

($OH^{\bullet}$) among others (Table 1.1). In cellular systems, ROS can be converted into 'secondary' ROS, e.g. by the Fenton reaction ($Fe^{2+} + H_2O_2 \rightarrow Fe^{3+} + OH^{\bullet} + OH^-$), or harmless molecules, such as water. ROS, in particular $OH^{\bullet}$, can react with all biological macromolecules, including lipids, proteins, DNA and carbohydrates. Free radicals react with other molecules in order to gain a stable electron configuration; their reaction with cellular macromolecules starts a chain reaction that propagates until two radicals meet to form a covalent bond. In cells, these chain reactions can have devastating effects, leading to damage of macromolecules. Other ROS induce oxidation of their targets, which can lead to addition of groups (e.g. glutathione groups (S-glutathionylation) (Hayes and McLellan, 1999)), cross-linking or fragmentation of proteins (Halleen et al., 1999) and modifications of nucleotide bases, single-strand breaks or cross-linking of DNA (Bertram and Hass, 2008). Despite their damaging properties, ROS, in particular H_2O_2, have been shown to have signalling properties and to be involved in mediating a variety of cellular processes (Droge, 2002; Veal et al., 2007). One of the first reports of ROS signalling properties was the activation of guanylate cyclase by H_2O_2 (Mittal and Murad, 1977). The signalling properties of ROS were first met with scepticism since signalling require a high level of specificity, whereas ROS were thought to react unspecifically due to their reactive nature. Specificity in signalling is achieved through non-covalent binding of two (or more) molecules through complementary structures. ROS on the other hand, mediate signalling by chemically reacting with specific atoms of the target molecule, thereby inducing covalent protein modifications (Nathan, 2003). ROS signalling therefore occurs at the atomic and not the macromolecular level. This mechanism is similar to signalling mediated by nitric oxide (NO) and reactive nitrogen species (RNS) (see Chapter 1.6).

The imbalance of pro-oxidants (high) and antioxidants (low) has been defined as oxidative stress (Jones, 2006) and has been implicated as being important in aging (Finkel and Holbrook, 2000) and the pathogenesis of several major diseases, including cardiovascular and pulmonary diseases, diabetes, neurogenerative diseases and cancer (Droge, 2002).

Radicals		Non-radicals	
Superoxide	O_2^-	Hydrogen peroxide	H_2O_2
Hydroxyl	$OH^•$	Hypochloric acid	HOCl
Nitric oxide	$NO^•$	Peroxynitrite	$ONOO^-$
Thyl	$RS^•$	Singlet oxygen	$^{-1}O_2$
Peroxyl	$RO_2^•$	Ozone	O3
Lipid peroxyl	Lipid-$OO^•$	Lipid peroxide	Lipid-OOH

Table 1.1: Radical and non-radical ROS

1.5.1 Sources of ROS

In a cellular system, ROS production can occur as a by-product of metabolism or be induced by exogenous or endogenous stimuli (Fig. 1.10) (Finkel and Holbrook, 2000).

1.5.1.1 Exogenous stimuli of ROS production

Exogenous stimuli of ROS production include ultraviolet (UV) light, ionising radiation, chemotherapeutics and environmental pollution/toxins. Diverse chemotherapeutic agents have been shown to increase oxidative stress by inducing ROS production thereby inducing cell death (Mansat-de Mas et al., 1999; Schumacker, 2006). Air pollution with ultrafine and nano-particles can lead to increased oxidative stress (Stone et al., 2007). Additionally, alcohol has not only been shown to be directly involved in the production of ROS, but additionally reduces antioxidant activity (Das and Vasudevan, 2007). Cigarette smoke contributes to oxidative stress by directly or indirectly (via upregulation of cytokines) increasing ROS production (El-Zayadi, 2006; Perlstein and Lee, 2006). Environmental conditions and personal life-style choices can therefore affect oxidative stress levels and personal health.

1.5.1.2 ROS as a by-product of metabolism

In eukaryotes, low levels of ROS are constantly produced as a by-product of metabolism (Finkel and Holbrook, 2000). The majority is produced in mitochondria, where the production occurs mainly at two points in the electron transport chain, at complex I (NADH dehydrogenase) and more importantly at complex III (ubiquinone-

Figure 1.10: Cellular generation of ROS
Cellular ROS production mainly occurs at three sites: 1) ROS generation in the mitochondria at complexes I and III of the respiratory chain as a by-product of the metabolism. 2) Regulated production of O_2^- via the NADPH oxidase complex, which assembles at the plasma membrane and is composed of the two membrane components $gp91^{phox}$ and $p22^{phox}$ and the cytoplasmic components $p40^{phox}$, $p67^{phox}$, $p47^{phox}$ and Rac1 (in the case of the phagocytic NADPH oxidase). 3) O_2^- production also occurs via 5-lipoxygenase (5-lox) during the conversion of arachidonic acid (AA) to hyroperoxyeicosatetraenoaic acid (HPETE), an intermediate in the conversion to leukotriene. Different isoforms of SOD convert O_2^- to H_2O_2. Adapted from (Chiarugi and Fiaschi, 2007)

cytochrome c reductase) (Echtay, 2007). ROS production at complex III can occur when the semiquinone anion species is formed as an intermediate during coenzyme Q regeneration. The semiquinone anion species can transfer electrons to molecular oxygen, leading to the generation of superoxide anion ($O_2 + e^- \rightarrow O_2^-$), which can rapidly be transformed into other ROS. Additionally, electrons can leak away at every step of the electron transport chain and reduce oxygen to the superoxide anion. The generation of mitochondrial ROS is therefore dependent on the metabolic rate and it is not surprising that organisms with a high metabolic rate have greater production of ROS and a shorter life span (Finkel and Holbrook, 2000).

In vitro experiments with isolated mitochondria have shown that 1 – 2% of oxygen molecules are used to produce ROS under conditions with high oxygen concentrations (Boveris and Chance, 1973). The *in vivo* rate will undoubtedly be much smaller. Cellular mechanisms to reduce mitochondrial ROS production

include a process known as metabolic uncoupling (Skulachev, 1996), where oxygen consumption is uncoupled from ATP generation and heat is produced. This process is mediated by the family of uncoupling proteins (UCP-1, -2 and -3) (Echtay, 2007).

1.5.1.3 Regulated cellular ROS production

Regulated ROS production has long been thought to be confined to phagocytic immune cells which produce ROS to promote killing of phagocytosed microorganisms by means of NADPH oxidase (Quinn et al., 2006). However, members of the Nox family of NADPH oxidases have now been found in a variety of cells and tissues (Geiszt and Leto, 2004).

1.5.1.3.1 The Nox family of NADPH oxidases

The phagocytic oxidase (phox), which has been studied extensively, consists of a membrane-bound flavocytochrome b_{558}, several molecular cytosolic regulators ($p47^{phox}$, $p67^{phox}$, $p40^{phox}$) and Rac1 or Rac2 (Geiszt and Leto, 2004). The cytochrome is a complex of two proteins, a flavin- and heme-binding glycoprotein ($gp91^{phox}$ or Nox-2) and a smaller subunit ($p22^{phox}$). In resting cells the NADPH oxidase complex is unassembled and only assembles at the membrane upon stimulation. The activity of NADPH oxidase can be induced by microbial products such as bacterial lipopolysaccharide or N-formylated peptides such as fMetLeuPhe (fMLP) (DeLeo et al., 1998; Karlsson et al., 1995). NADPH oxidase in other cell types, e.g. ECs, has been shown to be activated in response to various agonists, including angiotensin II (ang II), TNF-α, and vascular endothelial growth factor (VEGF) (Alom-Ruiz et al., 2008). Other, non-physiological stimuli include phorbol 12-myristate 13-acetate (PMA), which is commonly used in biomedical research as a tumour promoter (Jagnandan et al., 2007; Liu and Heckman, 1998).

The Nox family of oxidases consists of seven members, which have different expression patterns (Geiszt and Leto, 2004). Nox-1 is highly expressed in colon and at lower levels in the uterus, prostate and vascular smooth muscle cells (Suh et al., 1999). Nox-1 knock-out mice are healthy, reproduce normally and do not exhibit a spontaneous phenotype, but have a moderately decreased blood pressure (Gavazzi et al., 2006). However, they show an almost complete loss of the sustained blood pressure response when treated with ang II, while the initial response is conserved. This suggests a role of Nox-1 in blood pressure regulation and vascular ang II response. Overexpression of Nox-1 in NIH-3T3 cells leads to increased cell proliferation and tumour formation when injected into mice. These data fit with previous findings linking enhanced ROS generation to enhanced growth triggered

by growth factor stimulation or tumourigenesis (Sundaresan et al., 1995; Szatrowski and Nathan, 1991). Nox-1 over-expressing cells also show increased VEGF expression, indicating a role of ROS in angiogenesis in these tumours (Arbiser et al., 2002). Nox-2 or $gp91^{phox}$ is highly expressed in phagocytic cells, but also the endothelium (Alom-Ruiz et al., 2008; Geiszt and Leto, 2004). Mice deficient in Nox-2 have been used as a model for chronic granulomatous disease (CGD) (Pollock et al., 1995). CGD is a rare genetic childhood disease in which phagocytes do not produce ROS, leading to severe recurring infections with bacteria and fungi (Seger, 2008). In addition, patients display aberrant inflammatory response and tissue granuloma formation. The X-linked form of human CGD is caused by mutations in $gp91^{phox}$ (60% of cases), while the autosomal recessive forms are caused by mutations in $p47^{phox}$ (30% of cases), $p67^{phox}$ (5% of cases) and $p22^{phox}$ (5% of cases). Nox-2 knock-out mice show an increased susceptibility to infections with *Staphylococcus aureus* and *Aspergillus fumigatus*, two CGD-typical infections (Pollock et al., 1995). Mice deficient in $p47^{phox}$ have also been used as a model for CGD: $p47^{phox-/-}$ mice produce no superoxide and kill *staphylococci* ineffectively, they develop lethal infections and granulomatous inflammation similar to those encountered in humans (Jackson et al., 1995).

Nox-3 is predominantly expressed in fetal tissue, including kidney, liver, lung and spleen (Cheng et al., 2001; Kikuchi et al., 2000). Nox-4 is highly expressed in the kidney, and has been shown to induce cellular senescence when overexpressed in NIH-3T3 cells (Geiszt et al., 2000; Shiose et al., 2001). Nox-4 expression has also been shown for HUVECs (van buul 2005). Nox-5 is more distantly related and can be detected in spermatozoa and the spleen (Banfi et al., 2001). The dual oxidases Duox1 and Duox2 contain an N-terminal extracellular peroxidase-like domain and a $gp91^{phox}$-like oxidase domain (Dupuy et al., 1999; Edens et al., 2001). These oxidases are thought to serve as a source of H_2O_2 supporting anti-microbial activity during mucosal surface host defense (Geiszt et al., 2003).

1.5.1.3.2 5-lipoxygenase

ROS production in the cell can also occur via lipoxygenases (Chiarugi and Fiaschi, 2007). The enzyme 5-lipoxygenase (5-Lox) is involved in production of leukotrienes from arachidonic acid in response to several GFs and cytokines (Radmark et al., 2007). During the conversion of arachidonic acid to leukotrienes, O_2^- is produced during one of the intermediate steps and can be converted to other ROS (Zuo et al., 2004).

1.5.2 ROS induces various biological responses

In their function as signalling mediators, ROS have been shown to induce a variety of biological responses (Droge, 2002; Veal et al., 2007). These include activation of the cellular antioxidant defence system and induction of redox-signalling pathways leading to regulation of various redox-regulated processes, including cell proliferation, differentiation, migration and apoptosis.

1.5.2.1 Cellular antioxidant defence system

Since ROS can have damaging effects on cells it is vital to have a cellular defence system able to deal with increasing ROS levels. In unicellular organisms the ROS-induced damage can be lethal, and one important response to increasing ROS level is therefore the upregulation of antioxidants (Lushchak, 2006; Scandalios, 2005). Similarly, antioxidants are also upregulated in certain cell types of multicellular organisms in response to ROS (An and Blackwell, 2003; Sablina et al., 2005). The concentration of ROS required to induce a response can vary significantly between cell types, e.g. concentration differences of up to 20-fold have been shown to be required to induce H_2O_2-mediated apoptosis in mammalian cells (Choi et al., 2006; Sablina et al., 2005). Moreover, different ROS levels have been shown to induce distinct, sometimes opposing responses. For example, mild oxidative stress leads to p53-induced upregulation of several genes with antioxidant properties, while high levels of ROS have pro-oxidant effects (Sablina et al., 2005).

The cellular antioxidant defence system comprises non-enzymatic antioxidants such as carotenoids, vitamins C and E and enzymes with antioxidant activities (Borek, 2004; Droge, 2002). The major antioxidant enzymes involved in the catalytic breakdown of ROS are superoxide dismutase (SOD), catalase, glutathione peroxidase (Gpx) and thioredoxin (Trx) peroxidases (peroxiredoxins, Prx) (Fig. 1.11). SOD is the only mammalian enzyme that converts O_2^- to H_2O_2 (Kinnula and Crapo, 2004). Three different isoforms are expressed in mammalian cells, copper-zinc SOD (CuZnSOD), manganese SOD (MnSOD) and extracellular SOD (ECSOD). CuZnSOD is mainly localised in the cytosol, but also to a lesser extent in organelles, and protects against cytosolic produced O_2^-. MnSOD is produced as a precursor in the cytosol and is then transported to mitochondria, where is plays an important role in mediating oxidative resistance. ECSOD is synthesised in the cytosol and is secreted into the extracellular space, where it binds to ECM components via its four heparin-binding domains. H_2O_2 can be

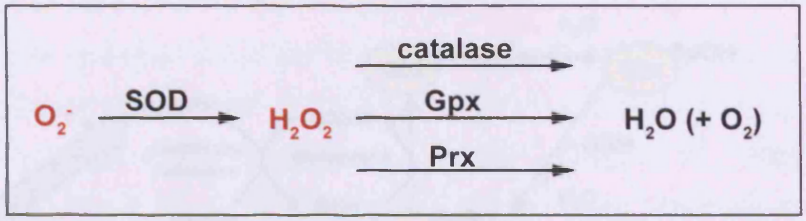

Figure 1.11: Enzymatic antioxidant defence mechanisms
Intracellular ROS can be rapidly converted into secondary ROS or harmless substances such as H_2O and O_2 by several enzymes with antioxidative properties. SOD converts O_2^- into H_2O_2 which can be further broken down by three parallel mechanisms: the enzyme catalase or the GSH and thioredoxin system involving Gpx and Prx.

catalytically broken down to H_2O by three parallel processes: via catalase, the glutathione (GSH) system involving Gpx, or the thioredoxin system involving Prx (Veal et al., 2007). Catalase is a highly efficient enzyme that is widely expressed in peroxisomes, but can also be found in the cytosol and mitochondria, and uses its heme prosthetic group to convert H_2O_2 to H_2O (van den Bosch et al., 1992). The GSH and thioredoxin system are similar in their functionality: the catalytic reduction of H_2O_2 involves the oxidation of Gpx or Prx and their recovery via reduced GSH or Trx, respectively (Fig. 1.12).

However, since ROS have been shown to have important signalling functions, it is important for the cells to allow enough ROS to induce signalling, but prevent damage due to high levels by inducing an antioxidant response.

1.5.2.2 ROS-sensitive targets in signalling cascades

ROS have been shown to be involved in several signalling cascades, including increasing protein phosphorylation, activating MAPKs, inducing intracellular Ca^{2+} and activation of transcription factors.

1.5.2.2.1 Inhibition of protein tyrosine phosphatases

Several protein tyrosine phosphatases (PTPs) have been shown to be regulated by ROS. Redox-sensitive PTPs include cysteine-based phosphatases (CBPs), which hydrolyse phospho-ester bonds via a cysteine-based mechanism (Salmeen and Barford, 2005). The environment in their catalytic site allows the thiol (or sulphydryl) group of a cysteine (Cys-SH) to be deprotonated (Cys-S^-) at physiological pH, which makes it susceptible to reactions with mild oxidizing reagents such as H_2O_2 to form

Figure 1.12: The catalytic removal of H_2O_2 by the GSH and thioredoxin systems
The catalytic reduction of H_2O_2 to H_2O mediated by the GSH and thioredoxin systems involves the oxidation of thiol groups on selenocysteine (SeH) or cysteine (SH) residues in Gpx or cysteine residues in Prx to Gpx-SeOH, Gpx-SOH and Prx-SOH, respectively. The recycling of the oxidised peroxidase enzymes involves the oxidation of reduced GSH or thioredoxin (Trx) to their oxidised counterparts, while the recycling of GSH and Trx are dependent on $NADPH+H^+$ and glutathione reductase or thioredoxin reductase, respectively. $NADPH+H^+$ is provided by the pentose phosphate pathway, hence coupling the antioxidant defence to cellular metabolism. The typical 2-Cys Prx contains two conserved cysteine residues, which are both involved in the reduction of H_2O_2 to H_2O. The cysteine residue is oxidised to sulphenic acid (SOH), which can either form a disulphide bridge with the cysteine of a partner protein, preventing further oxidation, or, since the disulphide formation is a slow process, the sulphenic acid is further oxidised to form sulphinic acid (SOOH), which can be reduced by either sulphiredoxin or sestrin enzymes. From (Veal et al., 2007)

a sulphenic acid intermediate (Cys-SOH). This modification renders the cysteine residue unable to act as a nucleophile, and the phosphatase looses its enzymatic activity. CBPs include PTPs, dual-specificity PTPs (dephosphorylate serine and threonine, as well as tyrosine), Cdc25 phosphatases and low-molecular-weight phosphatases (LMW-PTPs).

1.5.2.2.2 Activation of protein kinases

Protein kinases are often regulated via phosphorylation and binding of regulatory proteins. However, protein serine-threonine kinases and protein tyrosine kinases (PTKs) also appear to be under redox control (Rhee et al., 2000). Protein phosphorylation, induced by ROS-mediated phosphatase inhibition is therefore additionally increased by activation of protein kinases. The mechanism of activation involves cysteine oxidation, as has been shown for the receptor tyrosine kinase (RTK) c-Ret (Kato et al., 2000) and the non-receptor tyrosine kinase c-Abl (Leonberg and Chai, 2007). Certain serine/threonine kinase protein kinase C (PKC) isoforms, which are typically activated by the lipid second messenger diacylgylcerol (DAG) (Yang and Kazanietz, 2003), can be activated by H_2O_2 in a phospholipid-independent process that involves tyrosine phosphorylation of the catalytic domain (Gopalakrishna and Anderson, 1989; Konishi et al., 1997).

1.5.2.2.3 Activation of MAPK cascade and apoptosis

H_2O_2 induces sustained activation of all three major MAPK pathways (i.e. ERK1/2, JNK and p38 MAPK) in HeLa cells and caradiomyocytes (Purdom and Chen, 2005; Wang et al., 1998). JNK is involved in programmed cell death by regulating a number of proteins involved in apoptosis, including Bcl-2 family proteins (i.e. Bcl-X_L, Bax) (Shen and Liu, 2006). The pro-apoptotic signal from H_2O_2 is transmitted via TNF-R1 and recruitment of TRADD and TRAF2 (Pantano et al., 2003). Activation of apoptosis signali-regulating kinase 1 (or apoptosis-stimulated kinase 1 (ASK1)) after TNF-α-induced NADPH oxidase activation (Liu et al., 2000; Saitoh et al., 1998) seems to be one major mechanism by which ROS stimuli regulate JNK (Matsukawa et al., 2004; Shen and Liu, 2006). ASK1, a MAPKKK, binds to the reduced form of Trx. ROS induced oxidation of Trx leads to its dissociation from ASK1 allowing interaction with TNF receptor associated factor-2 (TRAF2) and activation of downstream targets, including JNK and p38.

1.5.2.2.4 Induction of intracellular Ca^{2+} and activation of transcription factors

Changes in intracellular Ca^{2+} level play a role in a variety of cellular processes, including transcription, cell contraction and migration (Ermak and Davies, 2002; Touyz, 2005). Cytosolic Ca^{2+} level can be increased by ROS either through mobilisation of intracellular Ca^{2+} stores or the influx of extracellular Ca^{2+} (Yan et al., 2006). The increase in Ca^{2+} contributes to the activation of PKC-γ, observed under conditions of oxidative stress (Wang et al., 2001) and the transcriptional induction of AP-1 (Wu, 2006). AP-1 is typically composed of c-Fos and c-Jun proteins and has

been implicated in differentiation processes. In T lymphocytes AP-1 regulates expression of IL-2 and other immunological relevant genes (Altman and Villalba, 2003). c-Fos and c-Jun mRNA are increased with a variety of ROS and other inducers of oxidative stress (Droge, 2002). The transcription factor NF-κB is involved in inflammatory reactions (see Chapter 1.4.1.1), growth control and apoptosis (Karin and Greten, 2005). ROS-mediated NF-κB activation has been shown in several cell types, including epithelial cells (de Oliveira-Marques et al., 2007), monocytes (Lu and Wahl, 2005) and smooth muscle cells (Robbesyn et al., 2003).

1.5.2.2.5 H_2O_2 as endothelium-derived hyperpolarising factor

Endothelial cells control the tone of the underlying vascular smooth muscle cells (VSMC) by releasing active vasodilators and vasoconstrictors (Furchgott and Vanhoutte, 1989). Prostacyclin (PGI_2), a cyclooxygenase-dependent metabolite of arachidonic acid, and NO were identified as the major endothelium-derived vasodilators (Dusting et al., 1977; Palmer et al., 1987). However, other endothelium-dependent, but PGI_2- and NO-independent agonist-induced relaxation has suggested the existence of additional mechanisms/factors (Feletou and Vanhoutte, 1988; Komori et al., 1988). The endothelium-dependent relaxation occurs simultaneously with VSMC hyperpolarisation and the mediator(s) responsible have been termed endothelium-derived hyperpolarising factor(s) (EDHF) (Taylor and Weston, 1988). Two general pathways explaining EDH have been proposed (Sandow, 2004): 1) mediated by diffusible factors; 2) mediated by direct contact between cells, e.g. via gap junctions (Hill et al., 2002). Several endothelial-derived substances have been proposed as diffusible EDHF, e.g. epoxyeicosatrienoic acid, lipoxygenase metabolites, carbon monoxide and H_2O_2 (Feletou and Vanhoutte, 2007). H_2O_2 has been suggested due to the evidence that EC-derived H_2O_2 can hyperpolarise and relax pig VSMC (Beny and von der Weid, 1991). Catalase has been shown to abolish EDHF-mediated hyperpolarisation and relaxation in mesenteric arteries from mice (Matoba et al., 2000) and coronary arteries from human (Matoba et al., 2002) supporting this hypothesis. However, other studies have failed to confirm the existence of a catalase-sensitive pathway in small mesenteric arteries from the same strain of mice (Ellis et al., 2003). Meanwhile, H_2O_2 might function as an endothelium-derived vasodilator, since recent work has shown that eNOS-derived H_2O_2 can act as a vasodilator in pressurised cerebral arteries from mice and shares similar dilatory pathways as NO (Drouin et al., 2007).

1.5.3 ROS in the immune system

ROS have long been known to play an important role in host defence, where ROS kill invading pathogens, but additionally, ROS plays an important role as a signalling mediator in inflammation, in particular in TEM.

1.5.3.1 Oxidative burst

The ability of phagocytic leukocytes to produce ROS is a vital component of host defence. Activated macrophages and neutrophils can produce large amounts of O_2^- via the NADPH oxidase (Quinn et al., 2006). The rapid production and release of antimicrobial ROS by leukocytes is referred to as 'respiratory or oxidative burst' (Murphy et al., 2008). Invading mircoorganisms are phagocytosed and killed by releasing antimicrobial proteins from specific granules into the phagosome (Hampton et al., 1998), while NADPH oxidase on the membrane releases ROS into the phagosome. In phagocytes, the combined activity of NADPH oxidase and myeloperoxidase also leads to the production of secondary ROS, including hypochlorous acid (HClO), one of the strongest physiological oxidants and a powerful antimicrobial agent (Hampton et al., 1998). However, release of ROS into the phagosome induces a rise in the pH and has been shown to be important for pathogen killing (Segal et al., 1981).

1.5.3.2 ROS in transendothelial migration

ROS have been suggested to play important roles at different stages of TEM, including EC activation, leukocyte adhesion, regulation of endothelial permeability and leukocyte diapedesis. However, so far only the role of ROS in ECs has been investigated.

Many of the key signal transduction molecules involved in cytokine-induced endothelial activation such as various MAPKs and transcription factors AP-1 and NF-κB are known to be redox-sensitive (see Chapter 1.5.2.2.4). TNF-α and other pro-inflammatory cytokines induce upregulation of adhesion molecules, including ICAM-1 and VCAM-1, through an NF-κB-dependent redox-sensitive mechanism, which can be inhibited by antioxidants or NADPH oxidase inhibitors (Postea et al., 2006; True et al., 2000). TNF-α-mediated upregulation of E- and P-selectin have also been shown to be mediated via NADPH oxidase-produced ROS (Chen et al., 2003; Takano et al., 2002). ECs express Nox2 and Nox4 oxidase isoforms and TNF-α stimulation results in assembly of these complexes and ROS production (Alom-Ruiz et al., 2008). Adhesion of leukocytes to the endothelium is not only influenced by the ROS-mediated expression of adhesion molecules, but can also be

directly influenced by ROS-induced modifications of the leukocyte surface ligands (Eguchi et al., 2005). Treatment of the human promyelocyte leukaemia cell line HL60 with ROS reduces E-selectin-mediated adhesion to the endothelium due to reduction of cell surface levels of sialyl LewisX. This mechanism allows a very fast regulation of adhesion, independent of transcripitional downregulation or internalisation of adhesion receptors.

Treatment of ECs with ROS has been shown to induce phosphorylation of PECAM-1 and increase HL60 cell TEM, which can be inhibited by antioxidants (Rattan et al., 1997). ROS have also been shown to be important in mediating VCAM-1 signalling following leukocyte binding (Deem and Cook-Mills, 2004; Keshavan et al., 2005). Engagement of VCAM-1 by leukocytes rapidly activates NADPH oxidase in ECs and subsequent ROS production is necessary for activation of matrix-metalloproteases (MMPs). Exogenous addition of ROS rapidly activates MMPs, whereas inhibition of NADPH oxidase or scavengers of ROS prevent MMP activation and block leukocyte TEM. Activated MMPs degrade ECM components, cell surface receptors in cell-cell junctions and tight junction proteins (Verma and Hansch, 2007).

ROS have also been shown to be important in the regulation of endothelial permeability, altering the blood-brain barrier (BBB) integrity, inducing cytoskeletal rearrangements and redistribution and disappearance of TJ proteins claudin-5 and occludin (Schreibelt et al., 2007). These events can be prevented by specific inhibitors for RhoA and PI3K, indicating their involvement in ROS signalling. Van Buul et al. have suggested a role of the redox-sensitive tyrosine kinase Pyk2 in regulating endothelial cell-cell adhesion (van Buul et al., 2005). Loss of VE-cadherin from the junctions is dependent on Rac1-induced ROS production, leading to activation and recruitment of Pyk2 to the junctions, where β-catenin is phosphorylated leading to loss of VE-cadherin.

How leukocyte signalling and subsequent adhesion and TEM are influenced by ROS is subject of the present study.

1.6 Nitric oxide

The development of many cardiovascular disorders including hypertension, atherosclerosis, heart failure and stroke has been shown to be a result of excess production of ROS, decreased NO bioavailability due to ROS-mediated oxidative modification and decreased antioxidant capacity of the vasculature (Paravicini and Touyz, 2008).

In addition to its well known function in regulating vascular tone, NO has been shown to exert multiple modulating effects on inflammation (Guzik et al., 2003). NO is a hyper-reactive radical that is generated in the tissue by the action of NO synthases (NOS) (Alderton et al., 2001). NOS enzymes are usually referred to as dimeric, although in their active form, they are composed of two NOS monomers associated with two molecules of calmodulin (CaM). They contain relatively tightly-bound cofactors (6R)-5,6,7,8-tetrahydrobiopterin (BH_4), flavin adenine dinucleotide (FAD), flavin mononucleotide (FMN) and iron protoporphyrin IX (heme), and probably catalyse a reaction of L-arginine, NADPH and O_2 to give NO, citrulline and NADP, although the exact mechanism is not clear (Fig. 1.13). NO is synthesised in a large number of tissues, playing a role in a variety of physiological processes. In mammalian cells, there are three NOS isoforms: neuronal NOS (nNOS, NOS-1), which is predominantly expressed in neurons, inducible NOS (iNOS, NOS-2), which is inducible in a wide range of tissues and cells, and endothelial NOS (eNOS, NOS-3), which is mainly expressed in the vasculature (Alderton et al., 2001).

The high reactivity of NO makes a tight temporal and spatial regulation indispensable. Spatial regulation is achieved by membrane anchorage through lipid modifications (myristoylation and palmytoylation) and by specific protein-protein interactions (Oess et al., 2006). NO production via NOS and availability in cellular compartments can be regulated by transcriptional and post-transcriptional regulation (Alderton et al., 2001). NOS activity can be regulated by the availability of Ca^{2+}: the dependency on Ca^{2+} is different for the isoforms though; while nNOS and eNOS require high Ca^{2+} concentrations, iNOS forms an active complex with CaM even at low Ca^{2+} levels. nNOS and eNOS have also been shown to be regulated by phosphorylation; in the case of eNOS via an Akt-dependent pathway (Dimmeler et al., 1999; Fulton et al., 1999), and iNOS by Src-mediated phosphorylation (Hausel et al., 2006).

NO is normally produced constitutively by eNOS in the endothelium, is responsible for maintaining low vascular tone and preventing leukocytes and platelets from adhering to the vascular wall (Ignarro, 2002; Sun et al., 2006). Low levels of NO, produced by the constitutive NOS, interact with guanylate cyclase, which leads to increased cGMP level and subsequent activation of PKGs (Hofmann et al., 2000). PKGI and PKGII mediate various processes, including vasorelaxation, increase in vascular permeability as well as anti-proliferative, anti-platelet and antioxidant effects (Hofmann et al., 2000).

Figure 1.13: NO production by NOS
Active NOS is composed of two NOS subunits, bound to two CaM molecules. NADPH donates electrons (e^-) to the reductase domain of NOS, which are then transferred to the oxygenase domain via FAD and FMN redox carriers. In the oxygenase domain electrons interact with the heme ion and BH_4 to catalyse the reaction of L-arginine with O_2 to generate citrulline and NO. Adapted from (Alderton et al., 2001)

In the inflammatory response NO, which is produced by iNOS in macrophages and other cells, has been shown to play multiple roles (Guzik et al., 2003). At high concentrations, NO is an important toxic defence molecule that kills microorganisms. Under inflammatory conditions, NO is usually produced together with O_2^-, leading to formation of peroxynitrite ($ONOO^-$) (Guzik et al., 2002), which has been shown to be involved in S-nitrosylation of proteins, e.g. NF-κB (Park et al., 2005). S-nitrosylation is the covalent attachement of NO to the thiol group of a cysteine (to form an S-nitrosothiol, SNO) and has emerged as an important regulatory mechanism for a range of proteins (Hess et al., 2005). S-nitrosylation has been shown for a number of metabolic enzymes, oxidoreductases, proteases, protein kinases and phosphatases, as well as respiratory proteins, receptor/ion channels and transporters, cytoskeletal and structural components, transcription factors, regulatory elements (including G proteins) and others (Hess et al., 2005). In addition to regulating protein function, S-nitrosylation can promote or inhibit the formation of disulphide bonds within or between proteins.

NO is therefore an important signalling molecule that is involved in a range of processes, including TEM where endothelial NO has been shown to inhibit neutrophil and T cell extravasation (Oka et al., 2005; Sun et al., 2006).

1.7 Role of ecto-enzymes in leukocyte transendothelial migration

In addition to the classical adhesion molecules (Fig. 1.14), a number of additional molecules have been suggested to be involved in different steps of the leukocyte adhesion cascade. Among these are several enzymes, which are expressed on the surface of leukocytes and ECs with their catalytic site in the extracellular space, and are termed ecto-enzymes (Salmi and Jalkanen, 2005).

1.8 Ecto-enzymes

Ecto-enzymes are a large and diverse class of proteins, which mediate a variety of functions, e.g. proteolytic maturation of chemokines or purine signalling (Goding, 2000). The strongest evidence for involvement of ecto-enzymes in the leukocyte adhesion cascade is available for nucleotidases and related proteins (CD39, CD73 and Autotaxin (CD203)) (Fig. 1.14) (Salmi and Jalkanen, 2005).

Ecto-enzymes are usually large glycoproteins that belong to different groups of membrane protein types (Goding, 2000): 1) type II integral membrane proteins with a short N-terminal cytoplasmic domain, single transmembrane domain and a large extracellular C-terminal catalytic domain (e.g. CD26, CD38); 2) type I integral membrane proteins with N-terminal cleavable signal sequence, large extracellular N-terminal catalytic domain, a single transmembrane domain and short C-terminal cytoplasmic domains; 3) proteins with two transmembrane domains (CD39); 4) proteins with a glycosylphosphatidyl inositol (GPI)-anchor (e.g. CD73) (Zimmermann, 1992). Ecto-enzymes are involved in the leukocyte adhesion cascade by modulating the purinergic signalling cascade, thereby inducing or terminating inflammatory stimuli. Additionally, many ecto-enzymes have enzyme-independent functions that are involved in the leukocyte adhesion cascade.

1.8.1 Ecto-enzymes as modulators of purinergic signalling

Adenosine triphosphate (ATP) and other nucleotides are powerful extracellular signalling molecules (Yegutkin, 2008). Nucleotide release occurs under several conditions: cell lysis due to organ injury, traumatic shock or certain inflammatory conditions (Bours et al., 2006). Under non-pathological conditions, nucleotide release occurs from various tissues including the epithelium (Burnstock, 2007), endothelium (Bodin and Burnstock, 2001), fibroblasts (Gerasimovskaya et al., 2002), neutrophils (Eltzschig et al., 2006), monocytes/macrophages (Wong et al., 2006) and other hematopoietic cells (Bours et al., 2006). These cells have been

Figure 1.14: Role of ecto-enzymes in the leukocyte adhesion cascade
The different steps of the leukocyte adhesion cascade are mediated by a large number of molecules on the endothelium as well as the leukocyte surface. The molecules in green boxes are well characterised participants in the leukocyte TEM cascade. The molecules in the centre panel display the best characterised ecto-enzymes involved in the process, while the relevance of the involvement of the molecules in the lowest panel needs further confirmation. Adapted from (Salmi and Jalkanen, 2005).

shown to release ATP in response to a variety of stimuli, including shear stress, hypotonic swelling, hypoxia, stretching, hydrostatic pressure, bradykinin, serotonin and other Ca^{2+}-mobilising agonists. ATP and ADP exerted their effects via two major receptor subfamilies, P2X and P2Y (Ralevic and Burnstock, 1998). Engagement of these receptors has many pro-thrombotic and pro-inflammatory effects, including cytokine secretion and dendritic cell (DC) activation (Di Virgilio et al., 2001; Idzko et al., 2002). In neutrophils and monocytes, ATP has been shown to stimulate adhesion to the endothelium, which is achieved by upregulation of Mac-1 but also E-selectin upregulation on the endothelium (Bours et al., 2006).

1.8.1.1 CD39 and CD73

In the endothelial-leukocyte microenvironment, the ecto-nucleotidases CD39 and ecto-5'-nucleotidase (CD73) act in concert to degrade extracellular nucleotides,

thereby terminating pro-inflammatory stimuli. Extracellular ATP is dephosphorylated by CD39, a nucleoside triphosphate diphosphohydrolase, in a sequential hydrolysis from ATP to ADP and AMP (Dombrowski et al., 1998). CD39 is expressed on many leukocytes, including B and T cells, monocytes and Langerhans cells, but also on the endothelium. CD39 deficient mice ($CD39^{-/-}$) have been shown to have severe platelet dysfunction with prolonged bleeding times and impaired platelet aggregation in response to ADP, thrombin and collagen, despite the fact that they have normal ATP and ADP plasma levels (Enjyoji et al., 1999). This platelet dysfunction is reversible and associated with a receptor P2Y1 desensitisation. Migration of $CD39^{-/-}$ monocytes or macrophages through ECs towards ATP or CCL2 is impaired *in vivo* (Goepfert et al., 2001). Additionally, $CD39^{-/-}$ mice show exacerbated skin inflammation in response to irritant chemicals (Mizumoto et al., 2002), demonstrating the importance of extracellular nucleotide degradation in attenuating inflammation.

In the nucleotide breakdown cascade (Fig. 1.15), AMP is further hydrolysed by CD73, a GPI-anchored protein that is expressed abundantly on ECs and on a subset of leukocytes (Airas et al., 1993; Thomson et al., 1990). So far, seven human 5'-nucleotidases have been identified, five in the cytoplasm (gene symbols NT5C, NT5C1A, NT5C1B, NT5C2, NT5C3), one in the mitochondrial matrix (gene symbol NT5M) and one extracellular isoform (gene symbol NT5E) (Bianchi and Spychala, 2003). NT5E, NT5C and NT5M form dimers, NT5C1A and NT5C2 form tetramers, while NT5C3 is a monomer. The protein structure for NT5C1B has not been characterised yet. The term 'CD73' will be used throughout to refer to the extracellular protein (NT5E) only. The intracellular enzymes have broader substrate specificity, hydrolysing 5'-ribonucleoside monophosphates, 5'- (deoxy) nucleoside monophosphates (NMPs) and 2'- and 3'-NMPs, whereas CD73 hydrolyses only 5'-AMP efficiently (Hunsucker et al., 2005; Zimmermann, 1992). CD73 has a molecular mass of 70 kDa and consists of two (glyco)protein subunits, which are tethered by non-covalent binding (Martinez-Martinez et al., 2000). The N-terminal domain binds two catalytic divalent metal ions and the C-terminal domain contains the substrate specificity pocket, while the substrate binds at the interface of the two domains (Strater, 2006). The enzymatic activity of CD73 produces adenosine, which has anti-inflammatory properties and exerts its effects via the G-protein-coupled P1 purinergic receptors A_1, A_{2A}, A_{2B} and A_3 (Yegutkin, 2008). A_{2A} and A_{2B} activate adenylate cyclase, thereby increasing intracellular cAMP levels, while A_1 and A_3 inhibit cAMP production (Shryock and Belardinelli, 1997). In ECs, stimulation of A_{2B}

Figure 1.15: Nucleotide breakdown cascade in the leukocyte-endothelial microenvironment
The pro-inflammatory mediators ATP and ADP are broken down to AMP by the endothelial diphosphohyrolase CD39. AMP is then further hydrolysed to adenosine (ado) by the GPI-anchored nucleotidase CD73 on the endothelial surface. Endothelium-bound lymphocytes inhibit CD73 via an unknown mechanism. Adenosine, an anti-inflammatory mediator, is degraded to inosine by adenine deaminase (ADA), which is bound to CD26 on the lymphocyte surface. From (Salmi and Jalkanen, 2005).

receptors increases endothelial barrier function by decreasing actomyosin contractility of the cytoskeleton and strengthening the intercellular junctions (Comerford et al., 2002; Srinivas et al., 2004). Adenosine has also been shown to inhibit neutrophil adhesion to the endothelium via neutrophil A_2 receptors (Cronstein, 1994). This effect is mediated by preventing upregulation of β2 integrins and shedding of L-selectin from the neutrophil surface, necessary for successful binding (Thiel et al., 1996). The concerted activity of CD39 and CD73 therefore not only terminates pro-inflammatory stimuli of ATP/ADP, but also acts as an anti-inflammatory signal, leading to increased endothelial barrier function and decreased leukocyte binding.

1.8.1.2 Adenosine deaminase and autotaxin

Binding of lymphocytes to the endothelium has been shown to inhibit endothelial CD73, likely by selectively masking the catalytic site (Henttinen et al., 2003). This

mechanism is thought to be important to decrease vascular barrier function in order to facilitate TEM. Residual adenosine is rapidly degraded by lymphocyte-bound adenosine deaminase (ADA) (Yegutkin, 2008). ADA hydrolyses the irreversible deamination of adenosine and 2'-deoxyadenosine to inosine and 2'-deoxyinosine respectively and is widely expressed (Spychala, 2000). On the surface of lymphocytes, ADA is often associated with CD26 (Gorrell et al., 2001; Martin et al., 1995). CD26 belongs to the group of ecto-peptidases and cleaves N-terminal dipeptides from polypeptides with either proline or alanine residues in the penultimate position (De Meester et al., 1999). CD26 has a range of substrates, including several chemokines, e.g. CCL5, CCL11, CXCL9, CXCL10, CXCL11, CXCL12 (De Meester et al., 1999; Lambeir et al., 2001). The effects of chemokine processing have been shown to be cell type- and chemokine-dependent, and include downregulation, termination and even potentiation of the inflammatory response (De Meester et al., 1999). CD26 is therefore an important modulator of chemokine-mediated inflammatory reactions.

The degradation of ATP to ADP, AMP and adenosine, thus the termination of pro-inflammatory signals, can also be accomplished by the action of nucleotide pyrophosphatases and nucleotide phosphodiesterases, one of which is autotaxin (ATX, CD206, NNP2) (Goding et al., 2003). ATX also has lysophospholipase D activity, which generates lysophosphatidic acid (LPA) from lysophosphatidylcholine and hydrolyses sphingosylphosphorylcholine to produce sphingosine 1-phosphate (S1P) (Clair et al., 2003; Tokumura et al., 2002; Umezu-Goto et al., 2002). LPA and S1P induce a variety of responses in many cell types by activating a family of five GPCRs and they are chemoattractants for certain types of leukocytes (Mills and Moolenaar, 2003; Rosen and Goetzl, 2005). However, there are other biosynthetic pathways producing LPA and S1P and autotaxin is not found in lymphoid tissue (Goding et al., 2003). The exact role and importance of autotaxin during inflammation therefore requires further investigation.

The interplay between ATP-consuming and ATP-regenerating pathways is what determines the inflammatory status. The nucleotide breakdown is counterbalanced by the re-synthesis of high-energy phosphoryls through backward phosphotransfer reactions (Yegutkin et al., 2002). Ecto-enzymes responsible for these reactions include adenylate kinase (AK), NDP kinase and ATP synthase (Yegutkin, 2008). The latter has only recently been found to be expressed on the outer plasma membrane in addition to its known localisation in mitochondria (Moser et al., 2001).

Taken together, in the endothelial-leukocyte microenvironment pro-inflammatory stimuli in the form of ATP/ADP are rapidly terminated mainly by combined activity of CD39 and CD73. The resulting adenosine mediates anti-inflammatory effects and can be further degraded to inosine by lymphocyte-bound ADA.

1.8.2 Non-enzymatic functions of ecto-enzymes

Ecto-enzymes are important modulators of the purinergic signalling cascade, thereby acting as regulators of pro- and anti-inflammatory signals. Additionally, many ecto-enzymes have enzyme-independent functions, which can be regulated at transcriptional, translational and post-translational levels. For example CD26 increases migration in many cell types by binding to ECM proteins (such as fibronectin and collagen) and soluble molecules (such as type II plasminogen and adenosine) and by binding other proteins, such as ADA, at the cell surface (Boonacker and Van Noorden, 2003; Gonzalez-Gronow et al., 2005; Kameoka et al., 1993). Engagement of leukocyte CD73 promotes leukocyte binding to the endothelium by LFA-1 clustering via a yet unknown ligand (Airas et al., 1995; Airas et al., 2000; Airas et al., 1993).

1.8.3 CD73 as a modulator of inflammation

$CD73^{-/-}$ mice have been used to demonstrate a role for CD73 in tubuloglomerular feedback and renal function (Castrop et al., 2004; Huang et al., 2006a), lung protection (Eckle et al., 2007a; Volmer et al., 2006), cardioprotection during myocardial ischemia (Eckle et al., 2007b) and vasoprotection (Koszalka et al., 2004; Thompson et al., 2004; Zernecke et al., 2006). $CD73^{-/-}$ mice are viable and do not show significant differences in systolic blood pressure or cardiac output (Koszalka et al., 2004). Zernecke et al. reported increased neointimal plaque formation in $CD73^{-/-}$ mice and increased monocyte adhesion due to upregulation of VCAM-1 on the endothelium (Zernecke et al., 2006). Additionally, $CD73^{-/-}$ mice display significantly increased vascular leakage after subjection to hypoxia (8% O_2) (Thompson et al., 2004). In the cremaster model of ischaemia-reperfusion, leukocyte attachment to the endothelium is significantly increased in $CD73^{-/-}$ mice (Koszalka et al., 2004).

Hypoxia, e.g. as a result of ischaemia, is known to result in tissue accumulation of polymorphonuclear cells (PMNs) (Eltzschig et al., 2004). However, hypoxia is also associated with increased intravascular adenosine levels, due to upregulation of CD73, which can be reversed by reoxygenation (Li et al., 2006). It is thought that adenosine production via CD39/CD73 is upregulated on the

endothelium during hypoxia as an anti-inflammatory response to dampen damaging effects (Eltzschig et al., 2004). CD73 expression and activity has also been shown to be induced by IFN-α in HUVECs (Niemela et al., 2004) and by IFN-β in mice, thereby improving the vascular barrier function after intestinal ischemia-reperfusion injury (Kiss et al., 2007). IFN-α levels are usually low, but are increased in inflammatory conditions. Since adenosine is highly anti-inflammatory, CD73-mediated production of adenosine presents a way to reduce detrimental effects of inflammatory conditions in the endothelial microenvironment. An additional regulatory mechanism has been shown to involve the transcriptional induction of CD73 by its enzymatic product (Narravula et al., 2000). Adenosine acts via A_{2B} receptor and elevated cAMP level to induce CD73 mRNA, surface expression and function. On the other hand TNF-α reduces CD73 surface levels (Kalsi et al., 2002). Since no changes in mRNA level could be detected, TNF-α is thought to activate PI-PLC, leading to cleavage of the GPI-anchor, which results in loss of CD73 from the surface.

These findings demonstrate the importance of CD73-derived adenosine in the maintenance of vascular barrier function and anti-inflammatory conditions.

1.8.4 Ecto-enzymes as therapeutic targets

Ecto-enzymes are attractive therapeutic targets to influence leukocyte trafficking, since their activity can be modulated by monoclonal antibodies or specific inhibitors. Their extracellular location means that enzyme inhibitors do not need to be cell membrane permeable and can therefore be administered orally. Some ecto-enzymes have already been targeted in early clinical trials; VAP-1 can be blocked by administration of the mouse monoclonal antibody Vepalimomab in patients with nickel-induced allergic contact dermatitis lesions, which resulted in decreased inflammation (Vainio et al., 2005). Other ecto-enzymes need to be stimulated in order to reduce inflammation. Increased adenosine production might be achieved by providing additional substrate in form of ADP, to increase the anti-inflammatory signal. CD73 is upregulated *in vivo* specifically on the vasculature of urinary bladder cancer patients when treated with IFN-α (Niemela et al., 2004). This upregulation can not be observed in lymphocytes present in the tumour or in CD73-positive malignant cells. However, CD73-positive leukaemia cells are thought to have a better chance of survival, when patients are treated with anti-metabolites that block *de novo* synthesis of purines (Pieters and Veerman, 1988). The use of CD73 inhibitors in combination with anti-metabolites could therefore be used in therapies,

especially since CD73 inhibitors have been shown to reverse multi-drug resistance to doxorubicin in a T lymphoma cell line (Ujhazy et al., 1994).

Many solid tumours are characterised by hypoxia due to insufficient blood supply (Harris, 2002; Vaupel et al., 2001). Hypoxia-induced upregulation of adenosine production (Eltzschig et al., 2004) in the tumour can stimulate cell proliferation (Braganhol et al., 2007) and is therefore associated with poor prognosis. Additionally, the accumulation of adenosine in the tumour and subsequent diffusion into the extracellular space leads to increased adenosine levels in the tumour microenvironment (Eltzschig et al., 2004; Ohta et al., 2006). Tumour-released adenosine protects the cancerous tissue by inhibiting anti-tumour T cells in the close environment (Ohta et al., 2006). T cell inhibition occurs through occupation of the adenosine receptor A2A and genetic deletion of A2AR in mice resulted in rejection of established immunogenic tumours by T cells (Ohta et al., 2006). A2AR-deficient mice also developed autoimmunity, which has to be taken into consideration when developing an A2AR-antagonist-based cancer therapy. Prevention of tumour-induced adenosine production could therefore be a possible approach to increase tumour rejection by T cells and to prevent pro-proliferative signals, which could be achieved by downregulating CD39 and CD73 activity with specific inhibitors or by RNAi.

Taken together, ecto-enzymes such as CD39 and CD73 offer several prospects for therapeutic modification of potentially harmful purinergic signalling during inflammation as well as the pathogenesis of cancer.

1.9 Aims of this project

Transendothelial migration has been extensively studied, but the signalling pathways involved in mediating leukocyte extravasation are not yet fully understood. The regulation of TEM involves not only endogenously generated signals, but can also be influenced by exogenous factors. This study aims to investigate novel aspects of leukocyte TEM, in particular the influence of oxidative stress. Oxidative stress can affect a range of diseases, and can be increased by several exogenous factors. The role of ROS, as an inducer of oxidative stress, on leukocyte TEM will be investigated with respect to morphological changes induced in leukocytes and signalling pathways involved. While chapters three and four investigate the role of ROS in TEM, chapter five is concerned with the role of the ecto-enzyme CD73 in TEM. A range of ecto-enzymes have been proposed as new 'players' in the process of leukocyte TEM, but detailed investigations have not been carried out yet. In this study, the role of endothelial CD73 will be investigated in leukocyte adhesion and TEM, and in maintaining the endothelium in a non-inflammatory state.

In this study I aim to further the understanding of mechanisms involved in leukocyte TEM by investigating poorly understood aspects of this process.

2

Materials and methods

2.1 Materials

Chemicals for solutions were purchased from Sigma-Aldrich unless otherwise stated.

2.1.1 Reagents and kits

[2-3H]Adenosine 5'-monophosphate, ammonium salt	GE Healthcare www.gehealthcare.com
adenosine	Sigma-Aldrich www.sigmaaldrich.com
adenosine-5'-monophosphate disodiumsalt	Fluka www.sigmaaldrich.com
3-amino-1,2,4-triazole (AT)	Calbiochem www.merckbiosciences.co.uk
4-amino-5-methylamino-2',7'-difluorofluorescein diacetate	Molecular Probes www.invitrogen.com
angiotensin II	Sigma-Aldrich
Annexin V-FLUOS staining kit	Roche www.roche.com
BioMax MS Film	Kodak www.sigmaaldrich.com
BioMax TRANSSCREEN LE Intensifying Screen	Kodak
calcium ionophore A23187	Sigma-Aldrich
carboxy-H_2DCFDA	Molecular Probes
carboxy-H_2DFFDA	Molecular Probes
CellTracker Green CMFDA (5-chloromethylfluorescein diacetate)	Molecular Probes
complete Mini EDTA-free (PI-mix)	Roche
CXCL12/SDF-1α human recombinant	R & D systems www.rndsystems.com
2',7'-dicholorofluorescin diacetate	Sigma-Aldrich

Dynabeads® Protein A	Dynal www.invitrogen.com
Dynabeads® Protein G	Dynal
Dynal MCP®-S, magnetic particle concentrator	Dynal
EBM-2 bullet kits	Lonza www.lonza.com
ECL Reagent	GE Healthcare
fetal bovine serum (FBS)	biosera www.biosera.com
fibronectin from human plasma	Sigma-Aldrich
filipin III from *Streptomyces filipinensis*	Sigma-Aldrich
FITC-dextran, Mr 42 000	Sigma-Aldrich
fluorescent mounting medium	Dako Cytomation www.dako.com
GDP 100x	Upstate www.millipore.com
GTPγS 100x	Upstate
human sera type AB	Lonza
hydrogen peroxide 3% in H_2O (H_2O_2)	Sigma-Aldrich
ICAM-1 human recombinant	R & D systems
interleukin-2, human	Roche
isopropyl β-D-1-thiogalactopyranoside	Sigma-Aldrich
MagneGST™ glutathione particles	Promega www.promega.com
MCP-1/CCL2 human recombinant	Peprotech www.peprotech.com
MG132	Calbiochem
N-acetyl-L-cysteine	Sigma-Aldrich
n-formyl-MET-LEU-PHE	Sigma-Aldrich
n-octyl glucoside	Sigma-Aldrich
NuPAGE® 4 - 12% Bis-Tris Gel	Invitrogen
NuPAGE® LDS sample buffer (4×)	Invitrogen
NuPAGE® MES SDS running buffer (20×)	Invitrogen
NuPAGE® transfer buffer (20×)	Invitrogen
n^{ω}-nitro-L-arginine methyl ester (L-NAME)	Sigma-Aldrich
Oligofectamine™	Invitrogen
OPI media supplement	Sigma-Aldrich

Opti-MEM +GlutaMax™-I	Gibco www.invitrogen.com
PBS (phosphate buffered saline) (-) $CaCl_2$ (-) $MgCl_2$	Gibco
PBS (+) $CaCl_2$ (+) $MgCl_2$	Gibco
penicillin/streptomycin (10 000 U/ml/10 000 µg/ml)	Gibco
phorbol-12-myristate-13-acetate	Cell Signaling www.cellsignal.com
phosphatidylinositol-specific phospholipase C	Molecular Probes
phytohaemagglutinin (PHA)	Roche
Precision PlusProtein™ standards	Bio-Rad
Rac/cdc42 assay reagent (PAK1 PBD, agarose)	Upstate
Re-Blot Plus	Chemicon www.millipore.com
rhotekin-RBD protein GST beads	Cytoskeleton www.cytoskeleton.com
RMPI 1640, (+) L-glutamine	Gibco
silica gel 60 ADAMANT™ on TLC plates	Sigma-Aldrich
s-nitroso-N-acetylpenicillamine (SNAP)	Sigma-Aldrich
Super RX medical X-ray film	Fuji www.fujimed.com
TNF-alpha/TNFSF1A	R & D systems
Transwell™ Permeable Supports, 0.4 µm pore size, 12 mm	Costar www.colepalmer.com
Transwell™ Permeable Supports, 5 µm pore size, 6.5 mm	Costar
trypsin/EDTA 0.05%	Gibco
VCAM-1 human recombinant	R & D systems
VEGF 165 human recombinant	R & D systems

2.1.2 Buffers and solutions

Fluorescence-activated cell sorting (FACS) buffer	PBS (-) $CaCl_2$ (-) $MgCl_2$	
	BSA	0.2%
	N_3Na	0.1%

Glutaraldehyde fixative	Na_2HPO_4 x $2H_2O$	73.1 mM		
	NaH_2PO_4	21.8 mM		
	pH 7.35 then add			
	glutaraldehyde	2.5%		
Glutaraldehyde wash solution	Na_2HPO_4 x $2H_2O$	51.2 mM		
	NaH_2PO_4	15.2 mM		
	pH 7.35 then add			
	sucrose	250 mM		
HEPES buffer	HEPES	20 mM		
	NaCl	140 mM		
	glucose	2 mg/ml		
	pH 7.4			
Homogenising buffer	Tris, pH 7.4	25 mM	add fresh	
	$MgCl_2$	5 mM	Na_3VO_4	1 mM
	NaCl	150 mM	PI-mix	
Integrin activation buffer	HEPES buffer			
	$MgCl_2$	5 mM		
	EGTA	1 mM		
Lysis buffer	Triton X-100	1%		
	SDS	0.1%		
	Tris, pH 7.5	20 mM	add fresh	
	NaCl	150 mM	Na_3VO_4	1 mM
	EDTA	10 mM	PI-mix	
Magne-GST buffer	Na_2HPO_4	4.2 mM		
	KH_2PO_4	2 mM		
	NaCl	140 mM		
	KCl	10 mM		
	pH 7.2			
MES buffer	MES	25 mM		
	pH 5.5			

Mg^{2+} lysis buffer (5×)	HEPES, pH 7.5	125 mM	add fresh	
	NaCl	750 mM	NaF	25 mM
	NP-40 substitute	5%	Na_3VO_4	1 mM
	$MgCl_2$	50 mM	Aprotinin	10 µg/ml
	EDTA	5 mM	Leupeptin	10 µg/ml
			PMSF	100 µM
			Glycerol	10%
Osmium tetroxide fixative	NaH_2PO_4	1.68%		
	NaOH	0.38%		
	glucose	0.54%		
	pH 7.3 then add			
	OsO_4	1%		
Rho lysis buffer (2×)	Tris, pH 7.4	100 mM	add fresh	
	EDTA	4 mM	NaF	2 mM
	NaCl	1 M	Na_3VO_4	0.4 mM
	$MgCl_2$	20 mM	PMSF	2 mM
	SDS	0.2%	DTT	2 mM
	Triton X-100	2%	Aprotinin	1 µg/ml
	Glycerol	20%	Leupeptin	1 µg/ml
	Na-deoxycholate	1%		
	β-mercaptoethanol	1%		
RIPA buffer	Tris pH 7.5	20 mM		
	NaCl	150 mM		
	EDTA	1 mM		
	NP-40	1%	add fresh	
	Na-deoxycholate	0.5%	Na_3VO_4	1 mM
	SDS	0.1%	PI-mix	
STE buffer	Tris, pH 8	10 mM		
	NaCl	150 mM		
	EDTA	1 mM		
TBS (10×)	Tris	200 mM		
	NaCl	1.5 M		
	pH 7.4			

TST buffer	Tris, pH 7.4	25 mM
	NaCl	150 mM
	Triton X-100	0.2%

2.1.3 Antibodies and oligonucleotides

Table 2.1: Primary antibodies

Antigen	Species	Dilution	Supplier
β-actin	mouse	western blotting (WB) 1/1000	Sigma-Aldrich
active β1 integrin (12G10)	mouse	FACS 1/100	Chemicon
active β2 Integrin (mAb 24)	mouse	FACS 1/100	Generous gift from Dr N. Hogg
α-catenin	rabbit	immunofluores-cence (IF) 1/100	Sigma-Aldrich
α-tubulin-FITC	mouse	IF 1/200	Sigma-Aldrich
β-catenin	mouse	IF 1/100	BD Biosciences www.bdbeurope.com
β-catenin	rabbit	IF 1/100	Sigma-Aldrich
Cadherin 5 (VE-cadherin)	mouse	IF 1/100	BD Biosciences
Catalase	rabbit	WB 1/200	Calbiochem
Caveolin-1	rabbit	IF 1/100	Santa Cruz www.scbt.com
CD11a/α_L integrin (LFA-1)	mouse	IF 1/100	BD Biosciences
CD11b/α_M integrin	mouse	IF 1/100	Serotec www.serotech.com
CD11c/α_X integrin	mouse	IF 1/100	Serotec
CD18 / β2 Integrin	mouse	FACS 1/100	BD Biosciences
CD29 / β1 Integrin	mouse	FACS 1/100	Serotec
CD44	mouse	FACS undiluted	Generous gift from Dr I. Dransfield
CD59 (MEM43)	mouse	IF 1/100	Generous gift from Dr Horejsi
CD59 (MEM43/5)	mouse	WB 1/1000	Generous gift from Dr Horejsi

CD73 (4G4)	mouse	IF, FACS 1/2000	Generous gift from Dr S. Jalkanen
CD73 (H-300)	rabbit	WB 1/500	Santa Cruz
Cdc42	rabbit	WB 1/1000	Cell Signaling
c-Myc	rabbit	IP 2 ug	Santa Cruz
ERK1	rabbit	WB 1/1000	Santa Cruz
E-selectin	mouse	FACS 1/100	Santa Cruz
GAPDH	mouse	WB 1/5000	Chemicon
ICAM-1	mouse	WB 1/500 FACS 1/1000	R&D Systems
IgG1 negative (neg) control	mouse	FACS 1/100	Serotech
IgG2a neg control	mouse	FACS 1/100	Serotech
IκB-α	rabbit	WB 1/200	Santa Cruz
iNOS / NOS type II	mouse	WB 1/500	BD Biosciences
JAM-A	rabbit	IF 1/100	Zymed www.invitrogen.com
MnSOD	rabbit	WB 1/1000	Stressgen www.nventacorp.com
PECAM-1	mouse	WB 1/500	Santa Cruz
P-selectin	mouse	FACS 1/100	BD Biosciences
p-tyrosine (clone 4g10)	mouse	WB 1/1000	Upstate
Rac1	mouse	WB 1/1000	Upstate
RhoA	mouse	WB 1/100	Santa Cruz
RhoE	mouse	FACS undiluted	generated in mice against recombinant full-length RhoE (Riento et al., 2003)
RhoGDI	rabbit	WB 1/1000 IP 2 µg	Santa Cruz
VCAM-1	mouse	FACS 1/500	BD Biosciences
ZO-1	rabbit	IF 1/100	Zymed

Table 2.2: Secondary antibodies

Antigen	Species	Conjugate	Dilution	Supplier
mouse IgG	sheep	HRP	1/10 000	GE Healthcare
rabbit IgG	goat	HRP	1/10 000	Dako Cytomation
mouse IgG (H+L)	goat	AlexaFluor® 488	1/200	Molecular Probes
mouse IgG (H+L)	goat	AlexaFluor® 594	1/200	Molecular Probes
rabbit IgG (H+L)	goat	AlexaFluor® 488	1/200	Molecular Probes
rabbit IgG (H+L)	goat	AlexaFluor® 594	1/200	Molecular Probes
phalloidin		TRITC	1/400	Sigma-Aldrich
phalloidin		FITC	1/400	Sigma-Aldrich
phalloidin		Cy5	1/200	Molecular Probes

Table 2.3: Oligonucleotides

Gene		Sense Sequence	Concen-tration	Supplier
siControl	onTARGET plus # 1	sequence not known	25 – 50 nM	Dharmacon www.dharmacon.com
NT5E (CD73)	siGENOME duplex 1	GAACCUGGCUG CUGUAUUGUU	25 – 50 nM	Dharmacon
NT5E (CD73)	siGENOME duplex 2	GGAAGUCACUG CCAUGGAAUU	25 – 50 nM	Dharmacon
NT5E (CD73)	siGENOME duplex 3	UGAAAUCACUG CAUUACAAUU	25 – 50 nM	Dharmacon
NT5E (CD73)	siGENOME duplex 4	GGACUUUAUUU GCCAUAUAUU	25 – 50 nM	Dharmacon
NT5E (CD73)	Silencer™ pre-designed siRNA	GGAAUUAGGGA AAACAAUUtt	25 nM	Ambion www.ambion.com
NT5E (CD73)	GeneSolution #1	CAGGACTTTATT TGCCATATA	25 nM	Quiagen www.quiagen.com
NT5E (CD73)	GeneSolution #2	CAGCAAGAGGC TAGCACTGAA	25 nM	Quiagen

NT5E (CD73)	GeneSolution #4	TAGGGTAAATCC TATTAGAAA	25 nM	Quiagen
NT5E (CD73)	GeneSolution #5	CAACGTGGTTTC TACATATAT	25 nM	Quiagen

2.2 Methods: cell biology

2.2.1 Mammalian cell culture

2.2.1.1 Endothelial cells

Pooled human umbilical vein endothelial cells (HUVECs) were cultured in EBM-2 medium with growth factors (EGM-2) containing 2% FBS. All cell culture vessels were coated with 10 µg/ml fibronectin (FN) for 1 h at 37°C (Table 2.1). Cells were passaged by washing once in PBS and incubating with 3 ml trypsin/EDTA at 37°C until all cells detached. Trypsin/EDTA was inactivated by addition of 7 ml EGM-2 and cells pelleted by centrifugation at 200 g. Unless otherwise indicated, cells were stimulated with 10 ng/ml TNF-α for 8 – 15 h. HUVECs were used until passage five.

Table 2.4: HUVEC usage in various experimental set-ups

Experiment	Cell culture vessel	Cell number	Used after
Immunoblotting	6-well dish	400 000	24 h
FACS	6-well dish	400 000	24 h
RNAi	6-well dish	150 000	24 h
Immunofluorescence	coverslips 13 mm	100 000	48 h
CD73 Activity Assay	24-well dish	100 000	48 h
Microscopy-based transmigration assay	24-well dish	100 000	48 h
Permeability Assay	12 mm Transwell™ filter	100 000	48 h
Transwell™ trans-migration assay	6.5 mm Transwell™ filter	30 000 50 000	48 h 24 h
Adhesion Assay	96-well dish	30 000 50 000	48 h 24 h

2.2.1.2 T lymphoblasts (T cells)

T lymphoblasts were thawed and transferred to a cell culture flask containing RPMI-1640 medium supplemented with 10% human plasma, penicillin (100 U/ml), streptomycin (100 µg/ml) and 0.5% PHA. To induce proliferation, the medium was replaced after 48 h with RPMI-1640 medium containing 10% human plasma, penicillin (100 U/ml), streptomycin (100 µg/ml) and 10 U/ml IL-2. Cells were passaged by pelleting at 120 g for 5 min and resuspended in fresh medium. Cells were used between passage 4 and 10.

2.2.1.3 THP-1 cells

The human monocytic cell line THP-1 was cultured in RPMI-1640 medium supplemented with 2 mM (+) L-glutamine, 10% heat-inactivated FBS, penicillin (100 U/ml) and streptomycin (100 µg/ml). For passaging, cells were pelleted at 200 g, resuspended in fresh medium at 2 - 5 x 10^5 cells/ml and transferred to a fresh cell culture flask. THP-1 cells were frozen down at a density of 5 x 10^6 cells/ml in growth medium, containing 60% FBS and 10% DMSO.

2.2.1.4 CCRF-CEM cells

The T lymphoplastoid cell line CCRF-CEM was cultured in RPMI-1640 medium with 2 mM (+) L-glutamine, 25 mM HEPES, 1 mM sodium pyruvate, 10% heat-inactivated FBS, penicillin (100 U/ml) and streptomycin (100 µg/ml). Cells were passaged by pelleting at 200 g and resuspending in fresh medium at 2 - 5 x 10^5 cells/ml before being transferred to a fresh cell culture flask.

2.2.1.5 MonoMac6 cells

The human monocytic cell line MonoMac6 (MM6) was cultured in RPMI-1640 medium containing 2 mM (+) L-glutamine, 10% heat-inactivated FBS, 1× non-essential amino acids, 1 mM oxaloacetate, 0.45 mM pyruvate, 0.2 U/ml insulin, penicillin (100 U/ml) and streptomycin (100 µg/ml). For passaging, cells were pelleted at 200 g, resuspended in fresh medium and transferred to a fresh cell culture flask.

2.2.2 siRNA transfection of HUVECs

HUVECs (1.5 x 10^5) were plated onto FN-coated 6-wells in EGM-2 medium without antibiotics 24 h prior to transfection. For each transfection sample, 50 nM CD73 (NT5E) or control siRNA were diluted into 175 µl Opti-MEM whilst 4 µl Oligofectamine was diluted in 15 µl Opti-MEM. To knock-down CD73 five different

oligonucleotides were used separately. Dilutions were mixed and incubated for 5 – 10 min at RT. Diluted oligonucleotides and lipids were then combined, mixed and incubated for 20 min at RT. While the complexes were forming, the growth medium was removed from the cells and replaced with 800 µl Opti-MEM. The siRNA transfection mixture was added drop wise to the cells and incubated for 4 h, before growth medium containing 3 x the normal concentration of serum, but no antibiotics was added. After transfection for 24 h the medium was replaced with normal EGM-2 medium and cells subsequently split after 48 h into appropriate dishes. Cells were used for endpoint assays 72 h after transfection.

2.2.3 Transmigration assays

Transmigration of leukocytes across HUVECs was assessed either by time-lapse microscopy or a Transwell™-based assay.

2.2.3.1 Transwell™-based assay

HUVECs were grown to confluency on FN-coated Transwell™ filters (6.5 mm diameter, 5 µm pore size) and either stimulated with TNF-α prior to the experiment or left unstimulated. THP-1 or CCRF-CEM cells were treated with biochemical reagents or left untreated, pelleted and resuspended in fresh medium before 2 x 10^5 cells were added per filter. Chemoattractants were added to the lower chamber (THP-1: 100 ng/ml monocyte chemotactic protein-1 (MCP-1); CCRF-CEM: 50 ng/ml SDF-1α) and cells were allowed to transmigrate for 2 h at 37°C and 5% CO_2. Cells from the lower chamber were counted using a CASY® cell counter (Schärfe System GmbH).

2.2.3.2 Time-lapse-microscopy-based assay

HUVECs were grown to confluency in FN-coated 24-well dishes and stimulated with TNF-α prior to experiments. THP-1 cells were either treated with biochemical reagents or left untreated and then pelleted and resuspended in fresh medium before addition of 1.5 x 10^5 cells per 24-well. Movies of cells were generated using Metamorph software and a Nikon Eclipse TE2000-E microscope with a Hamamatsu Orca-ER digital camera for 2 h at 37°C and 5% CO_2 at 1 frame/min. The movies were analysed using ImageJ analysis software (http://rsb.info.nih.gov/ij/) and counting transmigrating cells manually. The results were normalised to the untreated cells.

2.2.3.3 Migration analysis

Migration data were recorded on a Nikon TE2000-E time-lapse microscope using Methamorph software as a series of images, and Motion analysis software (Andor Technologies) was used to track the individual THP-1 cells migrating on the HUVEC surface. The movement of the cells was followed with a mouse pointer and x-y coordinates were recorded for each cell, at each frame. The resulting series of x and y coordinates was analysed using a Mathematica (Wolfram Research) notebook, written by Dr D. Zicha (Allen et al., 1998). This notebook uses a calibration of the pixel size of the images and the actual size of the images in µm. In this way, coordinates relating to image pixels were used to calculate the actual distance between points in the image. With reference to the time between each frame, the migration speed was calculated.

2.2.4 Adhesion assay

HUVECs were grown to confluency in FN-coated black 96-well dishes with clear bottom (Corning Inc.) and TNF-α-stimulated prior to experiments. THP-1 cells were stained with 1 µM CellTracker™ Green CMFDA for 30 min, washed once with PBS and subsequently treated with biochemical reagents or left untreated. 5 x 10^4 THP-1 cells were added for 15 min to wells containing HUVECs or wells coated with ICAM-1 or VCAM-1 (5 µg/ml, 1 h at 37°C). The wells were washed twice with PBS and fluorescence measured in RPMI-1640 medium without phenol-red in a Fusion™ α-FP plate reader (Perkin Elmer) at 485 nm excitation wavelength and a 535/25 nm emission bandpass filter. To determine absolute cell numbers a standard curve was constructed.

2.2.5 Permeability assays

Untreated or siRNA-treated HUVECs were cultured to confluency on FN-coated Transwell™ filters (12 mm diameter, 0.4 µm pore size) and either stimulated with TNF-α or left unstimulated. siRNA-treated cells were used 72 h after transfection. THP-1 cells were incubated with or without H_2O_2 for 30 min at 37°C and 1 x 10^6 cells added to the upper chamber. After a 25 min incubation 100 µg/ml FITC-dextran was applied to the upper chamber. Samples of the medium from the lower chamber were subsequently removed at 40 and 80 min time points and were measured in black clear-bottom 96-well plates using a Fusion™ α-FP plate reader (Perkin Elmer) at 485 nm excitation wavelength and a 535/25 nm emission bandpass filter. To maintain the volume in the lower chamber over the course of the experiment, an

equivalent volume of fresh medium was added to the lower chamber after each removal. Each condition was performed in triplicate.

2.2.6 FACS analysis

FACS analysis was used to detect cell surface levels of adhesion proteins in leukocytes and ECs, to determine intracellular ROS and NO levels and the fraction of apoptotic/necrotic cells after H_2O_2 treatment. FACS analysis was carried out using a BD FACSCanto™ and BD FACSCalibur™ flow cytometer (www.bdeurope.com) at 488 nm excitation wavelength and a 530/30 nm emission bandpass filter for AlexaFluor®488 and AnnexinV-FITC, and 488 nm excitation wavelength and a 610/20 nm emission bandpass filter for propidium iodide (PI).

2.2.6.1 Immunolabelling

Control or siRNA-treated HUVECs were cultured in FN-coated 6-well dishes. HUVECs were detached by washing once with PBS, addition of 0.2 ml typsin/EDTA, incubation for 1 min and pelleting by centrifugation at 200 g for 5 min. Suspension cells such as THP-1, MM6 and CCRF-CEM cells were pelleted by centrifugation at 200 g for 5 min.

Cells were washed once with FACS buffer and pelleted by centrifugation at 200 g for 5 min. For staining of active β1 integrin, cells were fixed in 70% ethanol (30 min, 4°C) prior to labelling, since the antibody activates β1 integrin. Cells were then incubated with 10 µl of 2% BSA in FACS buffer on ice for 10 – 30 min to block unspecific binding. Primary antibodies, including negative isotype controls, were diluted in FACS buffer and 50 µl was added to the cells before incubation on ice for 30 min. For detection of active integrins, positive (pos) and negative (neg) activation controls were additionally carried out. For β1 activity detection, cells were treated with 200 µM Mn^{2+} (pos) or 5 mM EDTA (neg) for 15 min prior to fixation, whereas for active β2 integrin activity antibody labelling was carried out in the presence of 200 µM Mn^{2+} or 5 mM EDTA. To remove the antibody, 100 µl of FACS buffer was added and cells were pelleted at 200 g for 5 min. This step was then repeated. A 1/200 dilution of AlexaFluor488 antibody was added (50 µl) and incubated on ice for 20 min. To remove the antibody, 100 µl of FACS buffer was added and cells were pelleted at 200 g for 5 min. This step was then repeated. The cells were resuspended in 300 µl of FACS buffer and transferred into FACS tubes. Controls for this assay included unstained and IgG isotype negative control stained cells.

2.2.6.2 ROS and NO detection

THP-1 cells were centrifuged at 200 g for 5 min and resuspended in fresh medium. For ROS detection, cells were treated with various concentrations of H_2O_2 for 30 min. H_2O_2 was removed by centrifugation and cells were subsequently incubated with 10 µM DCF or H_2DCFDA for 60 min. The reagent was removed by centrifugation and cells resuspended in 300 µl FACS buffer before transferring to FACS tubes.

For NO detection, cells were incubated with 10 µM DAF for 60 min. The reagent was removed by centrifugation and cells subsequently incubated with various concentrations of H_2O_2 for 30 min. Hydrogen peroxide was removed by centrifugation and cells were resuspended in 300 µl FACS buffer before transfering to FACS tubes.

As the dyes used are light sensitive, all experiments were carried out with as little exposure to light as possible.

2.2.6.3 Apoptosis/necrosis assay

THP-1 and CCRF-CEM cells were treated with various concentrations of H_2O_2 for 30 min (THP-1: 0 – 100 mM; CCRF-CEM cells: 0 – 5 mM). H_2O_2 was removed by centrifugation at 200 g for 3 min. Cells were resuspended in fresh medium and allowed to recover (2 h, 37°C, 5% CO_2). Control cells were either treated with 1 µM staurosporine for 2.5 h (positive control for apoptosis) or briefly heated to 70°C (positive control for necrosis).

For the assay, 8 x 10^5 cells were centrifuged at 200 g and resuspended in Annexin V buffer. Cells were stained with Annexin V (dilution 1/500) for 10 min on ice. Samples were transferred to FACS tubes in this buffer and 1 µM PI was added just before measuring.

2.2.7 Ca^{2+} detection assay

To detect a potential Ca^{2+} influx after H_2O_2 treatment, the Fluo-4 NW assay kit (Molecular Probes) was used. For the assay, 1.25 x 10^5 THP-1 cells were pelleted per condition, resuspended in 50 µl assay buffer and transferred to a 96-well plate. The cells were allowed to settle for 60 min (37°C and 5% CO_2). The reagents were prepared according to the manufacturer's instructions and 50 µl 2x loading dye was added to each well and incubated for 30 min (37°C and 5% CO_2). THP-1 cells were then treated with H_2O_2 (0 – 5 mM) for 30 min and fluorescence measured using a Fusion™ α-FP plate reader (Perkin Elmer) at 485 nm excitation wavelength and a

535/25 nm emission bandpass filter. As a positive control 10 µM Ca^{2+} ionophore A23187 was added to one of the untreated samples before measuring.

2.2.8 Immunofluorescence microscopy

For immunofluorescence labelling, HUVECs were grown to confluency on FN-coated coverslips and treated either with or without TNF-α. For THP-1 cell labelling, treated or untreated THP-1 cells were allowed to adhere to FN- or VCAM-1-coated coverslips (5 µg/ml, 15 h, 4°C).

For monocultures, cells were washed once with PBS and fixed with 4% PFA in PBS (20 min, room temperature (RT)). For co-cultures, HUVECs were incubated with THP-1 cells for 25 min or with T cells for 10 min, before fixation with 4% PFA in PBS (20 min, RT). After fixation cells were permeabilised when appropriate with 0.1% Triton X-100 in PBS (5 min, 4°C), washed three times with PBS, and incubated with 2% BSA in PBS (30 – 60 min). Coverslips were then sequentially incubated with various dilutions of the appropriate polyclonal or monoclonal antibodies, AlexaFluor488- or AlexaFluor568-conjugated anti-rabbit or anti-mouse IgG secondary antibodies and counterstained with TRITC- or Cy5-conjugated phalloidin to visualise F-actin. Coverslips were mounted onto slides using fluorescent mounting Medium, and visualised using a LSM 510 laser scaning confocal microscope (Zeiss).

For CD73 staining, HUVECs were washed with PBS and incubated sequentially with undiluted 4G4 hybridoma supernatant on ice for 30 min and an AlexaFluor488-conjugated anti-mouse antibody for 20 min on ice. Cells were fixed subsequently with 4% PFA in PBS (20 min, RT) and either further stained or mounted onto slides.

2.2.9 Protrusion assay

THP-1 cells were treated with 1 µM CellTracker™ Green CMFDA (30 min, 37°C). Excess dye was removed by centrifugation at 200 g before subsequent treatment with 0, 0.1, 0.5, 1, 2 and 5 mM of H_2O_2 (30 min, 37°C). Cells were centrifuged for 3 min at 200 g to remove H_2O_2 and 3 x 10^6 cells were added to a TNF-α stimulated HUVEC monolayer, grown to confluency on FN-coated coverslips. After 25 min of incubation at 37°C, cells were washed with PBS and fixed with 4% PFA in PBS (20 min, RT). Co-cultures were either counterstained with TRITC- or Cy5-conjugated phalloidin to visualise F-actin or directly mounted onto glass slides. The number of cells with protrusions was determined by capturing images using a Zeiss Axiophot with a Q-Imaging Retiga SRV camera and counting cells manually.

2.2.10 Transmission electron microscopy

In order to visualise the interaction between THP-1 cells and the HUVEC monolayer in the y-z plane in greater detail, HUVECs were grown to confluency on FN-coated coverslips, stimulated with TNF-α for 15 -18 h then 3 x 10^5 THP-1 cells were added per coverslip for 25 min. Co-cultures were washed twice with PBS and fixed with 2.5% glutaraldehyde fixative at RT for 1 h. Coverslips were washed three times with glutaraldehyde wash solution.

The following procedures were carried out by Ken Brady at the Centre for Ultrastructural Imaging at King's College London. In order to enhance the contrast in the resulting images, the cells were post-fixed in osmium tetroxide fixative (15 – 30 min, RT). The samples were sequentially dehydrated at RT in 10% ethanol for 10 min, 70% ethanol for 15 min and three times 100% ethanol for 15 min. TAAB premix medium resin was made up according to the manufacturer's instructions and one drop applied to one glass slide per sample. The coverslips were placed onto the resin drop with the glass surface facing down and covered immediately with a few drops of resin which were allowed to penetrate the sample for 2 h at RT. BEEM® capsules in a rack were filled to the brim with resin and inverted onto the coverslip ensuring that resin did not get under the coverslip. The slides were placed into an embedding oven and allowed to polymerise for 24 h at 60°C. Cooled samples were placed onto a hot plate for 30 sec, glass slide facing down, the BEEM® capsules snapped off the coverslip. BEEM® capsules were sawn in half in order to obtain block faces of suitable size. The blocks were then cut on a Leica Ultra-cut machine (Leica, www.leica-microsystems.com) to semi-thin thickness (0.75 – 2 µm). These sections were stained with toluidine blue to select appropriate areas for transmission electron microscopy. Ultra-thin sections (100 – 120 nm) of the selected viewing area were cut on the Leica Ultra-cut machine and placed onto 200 mesh gilder grids with a support film of pioloform. The grids were stained with uranyl acetate and lead citrate to further enhance the contrast and viewed on a Hitachi H7600 transmission electron microscope (Hitachi, www.hht-eu.com).

2.2.11 Cholesterol-depletion of HUVECs

To deplete cholesterol from the plasma membrane, HUVECs grown on FN-coated coverslips or 24-well dishes were incubated with 4 mg/ml methyl-β-cyclodextrin (MβCD) (15 min, 37°C). MβCD was removed and cells were washed with PBS and used in various experiments.

To visualise cholesterol by light microscopy, coverslips with either cholesterol-depleted or untreated HUVEC monolayers were incubated with 5 µg/ml filipin for 15 min at 37°C and subsequently mounted onto coverslips. The staining and mounting procedure was carried out in the dark as filipin is highly sensitive to light. The samples were visualised using a Zeiss Axiophot with a Q-Imaging Retiga SRV camera.

2.2.12 Phosphatidylinositol-specific phospholipase C (PI-PLC)-induced shedding of CD73

In order to shed CD73 from the cell surface, HUVECs were treated with 0.2 U/ml of PI-PLC (15 min, 37°C). PI-PLC was removed and cells were used in various experiments.

2.2.13 Antibody-mediated cross-linking of ICAM-1, VCAM-1 and CD73

HUVECs were grown to confluence in FN-coated 24-well dishes and stimulated with TNF-α for 15 – 18 h. Cells were washed once with EGM-2 and cross-linking was carried out for 30 min on ice using 50 µl IgG_1 negative control (1/100), ICAM-1 (1/100), VCAM-1 (1/100), RhoE (undiluted) or CD73 (undiluted) antibodies or no antibody as a control. Monolayers were washed twice with PBS and either incubated for 20 min at 37°C with 50 µl FITC-conjugated anti-mouse antibody (1/100) or PBS only. Cells were washed twice with EGM-2 and used for determination of CD73 activity.

2.2.14 CD73 activity assay (radio-thin layer chromatography)

To measure CD73 enzymatic activity, treated or untreated HUVECs were grown in FN-coated 24-well dishes until confluency and either treated with or without TNF-α. For leukocyte binding experiments, THP-1 cells were treated with 0, 0.5, 1 and 5 mM H_2O_2 for 30 min and 3 x 10^5 THP-1 cells were added per well for 25 min. For CD73 inhibition experiments, various concentrations of AMP-CP were added for 1 h. Cells were washed once with EGM-2 before adding 250 µl EGM-2, containing 180 µM [2-^{3}H] adenosine 5'-monophosphate (specific activity per well: 37 µBq) and 20, 200 or 900 µM unlabelled adenosine 5'-monophosphate for 5 – 45 min at 37°C. Aliquots of the medium (6 – 8 µl) were applied to silica 60 gel thin layer chromatography (TLC) plates and were separated using isobutyl alcohol / isoamyl alcohol / 2-ethoxyethanol / ammonia / H_2O (ratio 9:6:18:9:15) as a solvent. The TLC plates were developed by exposing to tritium-sensitive film (Kodak BioMax MS film)

together with a BioMax TranscreenLE intensifying screen (Kodak) for 110 – 150 h at -80°C.

2.3 Methods: biochemistry

2.3.1 Western immunoblotting

Protein samples were prepared by lysing 3 – 5 x 10^6 cells/ml in lysis buffer for 20 min at 4°C with rotation. Cell lysates were centrifuged at 18 500 g for 15 min to remove insoluble material. Cleared lysates were boiled for 5 min with 4× sample buffer either with or without 4 mM DTT and 20 µg of total protein was applied to NuPAGE 4 – 12% Bis-Tris gels. Proteins were separated using a constant voltage of 120 V, in NuPAGE MES running buffer. After electrophoresis proteins were transferred to Immobilon-P membranes for immunoblotting. Protein transfer was carried out for 90 min at constant voltage of 100 V in NuPAGE transfer buffer.

Immunoblotting was performed using various monoclonal and polyclonal antibodies (see Chapter 2.1.3). Membranes were sequentially blocked in Tris-buffered saline containing 0.03% Tween-20 (TBS-T) and either 5% (weight/volume) milk powder or 2% BSA for 1 h at RT, incubated with primary antibody either for 1 h at RT or for 15 – 18 h at 4°C, washed with TBS-T and incubated with secondary antibodies for 1 h at RT. Membranes were washed with TBS-T and immunodetection performed using an ECL detection kit according to the manufacturer's instruction and Super RX medical X-ray film (Fuji).

Immunoblots were quantified by densitometry using VisionWorks®LS analysis software (UVP, www.uvp.com), subtracting the background from the reading and normalising to the loading control.

2.3.2 Proteasome inhibition

In order to inhibit proteasome-mediated degradation, THP-1 cells were treated for 15 - 18 h with 10 µM of the proteasome inhibitor MG132. The inhibitor was removed by centrifugation at 200 g for 3 min and cells washed once with PBS before they were lysed in lysis buffer. Samples were separated by gel electrophoresis.

2.3.3 Co-immunoprecipitation

For antibody immobilisation, 15 µl of protein A+G Dynabeads® were washed three times with MES buffer, and incubated with 2 µg of RhoGDI or c-Myc antibody in 70 µl MES buffer for 15 - 18 h at 4°C and washed with MES three times. To cross-link the antibody to the beads, the beads were sequentially washed twice with 0.2 M

triethanolamine (TEA), pH 8.2, resuspended in fresh 20 mM dimethyl pimelimidate x 2HCl (DMP) in 0.2 M TEA and incubated for 30 min at RT with rotational mixing. The supernatant was discarded and the reaction stopped by adding 50 mM Tris, pH 7.5 for 15 min with rotational mixing. The beads were washed three times with 0.1% Tween-20 in PBS.

Cell lysates were prepared by homogenising 5 x 10^6 treated or untreated THP-1 cells in homogenising buffer using a BioSpec Tissue-Tearor homogeniser (www.biospec.com) and centrifuged at 18 500 g for 30 min at 4°C. A small aliquot of the cleared homogenate was kept for western blotting (whole cell lysate; WCL); the remainder was incubated with the antibody cross-linked beads at RT for 2 h. To remove unbound protein, the beads were washed three times with homogenising buffer and proteins eluted by boiling the beads for 5 min with 2× sample buffer. Samples were separated by gel electrophoresis.

2.3.4 GST-Pull-downs

To detect GTPase activity in treated and untreated THP-1 cells, GST-fusion proteins of rhotekin, the p21-binding domain (PBD) of PAK and the Cdc42/Rac interactive binding (CRIB) domain of WASP were used for RhoA, Rac1 and Cdc42 pull-downs respectively.

2.3.4.1 GST-Pull-down for suspension THP-1 cells

2.3.4.1.1 Preparation of GST-proteins

E. coli transformed with plasmids encoding GST-fusion proteins were plated onto Luria broth (LB) agar containing 50 µg/ml ampicillin. One colony was used to inoculate 100 ml of LB medium containing 100 µg/ml ampicillin and grown for 15 - 18 h at 37°C. The overnight culture was diluted 1/20 into fresh LB medium with ampicillin and grown at 37°C to an optical density of 0.7 (OD_{600}). To induce protein expression, isopropyl β-D-1-thiogalactopyranoside (IPTG) was added at a concentration of 0.5 mM for 2 h at 30°C. To collect the cells, the culture was centrifuged at 600 g for 20 min at 4°C and pellets were either stored at -40°C for future use or used the same day. Bacterial pellets derived from 50 ml of culture were resuspended in ice-cold STE buffer with 1 mM phenylmethylsulphonyl fluoride (PMSF), homogenised with a 19G needle and 100 µg/ml lysozyme added before incubation on ice for 15 min with gentle mixing. In order to further lyse the bacteria, 5 mM dithiothreitol (DTT), 1% Tween-20 and 0.03% sodium dodecyl sulfate (SDS)

were sequentially added. The lysate was then centrifuged at 18 500 g for 20 min at 4°C.

In the meantime, 10 µl MagneGST beads per condition were washed three times with MagneGST buffer and resuspended in 100 µl MagneGST buffer containing 1% BSA to reduce non-specific binding. Bacterial lysate was added to the beads and incubated at 4°C for 1 h with rotation. The supernatant was removed and the beads washed three times with MagneGST buffer and resuspended in 10 µl.

2.3.4.1.2 Pull-down assay

THP-1 cells were treated with 0, 0.1, 0.5, 1, 2 and 5 mM H_2O_2 (5 x 10^6 cells per condition) for 30 min, washed once with PBS and lysed with 1× Mg^{2+} buffer for 5 min on ice. Lysates were centrifuged for 5 min at 18 500 g and a small aliquot of each was kept for immunoblotting as WCL. The remaining lysate was either incubated with the prepared beads for 1 h at 4°C or subjected to GTPase activation or inactivation reactions (positive and negative controls).

To generate positive and negative controls, the pre-cleared lysate was incubated with 10 mM EDTA and either 100 µM GTPγS or 1 mM of GDP at 30°C for 15 min. The reaction was stopped by adding 60 mM $MgCl_2$ and the lysate added to the MagneGST beads for 1 h at 4°C.

After incubation, the supernatant was removed and beads were washed with MagneGST buffer 5 times. In order to elute the bound proteins, beads were incubated with 2× sample buffer with DTT for 5 min at RT. Beads were removed and supernatants and WCL in sample buffer were boiled for 5 min. The pull-down samples were separated in parallel with the WCL samples by gel electrophoresis.

2.3.4.2 GST-Pull-down for adherent THP-1 cells

To detect Rho GTPase activity in adherent THP-1 cells, 5 x 10^6 THP-1 cells per experimental condition were treated with 0, 0.1, 0.5, 1, 2 and 5 mM H_2O_2 for 30 min. Cells were pelleted, resuspended in 800 µl integrin activation buffer, divided in two parts and each centrifuged onto a FN-coated 6-well for 5 min at 170 g. Cells were then lysed by addition of an equal volume of 2× Rho lysis buffer and passed through a 19G needle several times. In order to remove cellular debris and insoluble material the lysate was centrifuged at 18 500 g at 4°C for 10 min. A small sample of the supernatant was kept for immunoblotting as WCL, while the rest was added to 20 µl GST-Rhotekin-RBD beads (RhoA; Cytoskeleton) or 10 µl GST-PAK1-PBD conjugated agarose beads (Rac1 and Cdc42; Upstate) and incubated at 4°C for 1 h

with rotation. The beads were washed three times with Rho lysis buffer and pelleted by centrifugation for 1 min at 2 500 g at 4°C. Protein was eluted by boiling in 2× sample buffer. The pull-down samples were separated in parallel with the WCL samples by gel electrophoresis.

2.3.5 Raft fractionation by n-octylglucoside (OG)-selective solubility

Raft fractionations were carried out at 4°C, at all stages using only pre-chilled pipette tips. HUVECs were grown to confluency on FN-coated 6-well dishes, washed twice with ice-cold PBS and lysed with 100 µl of TST buffer. Cells were harvested by thorough scraping and incubated with occasional agitation for 20 min. The supernatant (soluble fraction, S) was separated from the pellet by centrifugation at 18 500 g for 3 min. The pellet was resuspended in 100 µl TST containing 60 mM OG and incubated on ice for 15 min followed by a 10 min incubation at 37°C. To separate the raft fraction from the pellet, the lysate was centrifuged again for 3 min at 18 500 g and supernatant (raft fraction, R) was separated. In order to solubilise the final pellet, 100 µl of TST was added. The three fractions were boiled with 4× sample buffer and sonicated before loading equal volumes of each fraction onto a NuPAGE gel.

2.4 Statistical analysis

Statistical analysis was carried out where three or more independent experiments were available. In order to determine statistical significance, Student's t-test and analysis of variants (ANOVA) with Bonferroni post-test was carried out using GraphPad Prism software (www.graphpad.com).

3

Role of reactive oxygen species in leukocyte transendothelial migration

3.1 Introduction

The intra- and intercellular signalling pathways involved in regulating TEM have yet to be fully elucidated. Additionally, how external factors, including environmental pollution and life-style choices such as diet, alcohol consumption and smoking influences leukocyte TEM has not been investigated in detail. These exogenous factors have been shown to increase oxidative stress, a condition defined as an imbalance between ROS and antioxidants (Jones, 2006). Several studies have investigated the role of endothelium-derived ROS in TEM. ROS have been shown to be important in the endothelium during TNF-α-mediated upregulation of adhesion molecules (Alom-Ruiz et al., 2008), VCAM-1 signalling following leukocyte binding (Deem and Cook-Mills, 2004; Keshavan et al., 2005) and also in regulating endothelial monolayer permeability (Schreibelt et al., 2007; van Buul et al., 2005). However, very few studies have investigated the effects of ROS on leukocytes during TEM. Eguchi et al. have shown that treatment of HL60 cells with ROS reduces E-selectin-mediated adhesion to the endothelium by decreasing cell surface level of sialyl LewisX (Eguchi et al., 2005). Also, overexpression of UCP-2, a protein involved in metabolic uncoupling, in a monocytic cell line leads to decreased adhesion and TEM due to reduced intracellular ROS and β2 integrin levels (Ryu et al., 2004). In addition, an increasing number of studies have investigated the involvement of ROS in adhesion and the regulation of the actin cytoskeleton in experimental settings other than inflammation. Fraticelli et al. have demonstrated a ROS-induced upregulation of β2 and αM in PMNs (Fraticelli et al., 1996), while ROS-induced rearrangements of the actin cytoskeleton have been observed in different cell types, including rat hepatocytes and ECs (Huot et al., 1998; Perez et al., 2006). Actin itself undergoes direct oxidative modifications during integrin-mediated adhesion, promoting spreading and actin rearrangements (Fiaschi et al., 2006). Additionally, localised ROS production due to subcellular targeting of

NADPH oxidase has been shown to be important in directional migration (Ushio-Fukai, 2006).

Since rearrangements of the actin cytoskeleton and actin-dependent processes, such as migration, play a crucial role in leukocyte extravasation, it was interesting to investigate if and how ROS affect leukocyte TEM. The aim of this chapter was therefore to set up an *in vitro* model for leukocyte TEM and to investigate the transmigration behaviour of ROS-treated leukocytes.

3.2 *In vitro* transendothelial migration assays

3.2.1 Characterisation of leukocytes

Leukocytes express different patterns of cell surface proteins, including adhesion molecules such as integrins. Integrins constitute a family of over 20 heterodimers whose ligand-binding activity can be rapidly regulated by conformational changes, clustering, and redistribution from surface and intracellular pools (Carman and Springer, 2003; Dustin et al., 2004). The most relevant integrins for leukocyte adhesion to the endothelium are α4β7 integrin and β1 and β2 containing integrins, including ICAM-1-binding LFA-1 (αLβ2), MAC-1 (αMβ2) and VCAM-1-binding VLA-4 (α4β1) (Barreiro et al., 2007). FACS analysis was used in order to characterise a number of different leukocyte lines to be used in *in vitro* TEM assays. The human monocytic leukaemia cell lines THP-1 and MM6 and the T lymphoblastoid cell line CCRF-CEM were chosen, as they have been well characterised in TEM models (Cabrero et al., 2006; Ryu et al., 2004; Weber et al., 1998). Cells with different properties were chosen in order to provide a range of responses in the system.

In order to characterise the leukocytes, FACS analysis was carried out in which cells were stained for: CD44 (phagocytic glycoprotein 1, Pgp-1), which binds to hyaluronic acid (HA) in the ECM; integrins such as β1 (CD29), β2 (CD18), CD11a (αL, α subunit of LFA-1), CD11b (αM, α subunit of Mac-1) and CD11c (αX). Representative FACS traces show, that β1 integrin levels were high and uniform for THP-1 and CCRF-CEM cells, whereas MM6 cells showed two distinct populations, one with high, and the other with levels at negative control intensity (Fig. 3.1A). The β2 integrin was highly expressed on THP-1 and CCRF-CEM cells, but only a portion of MM6 cells showed staining above negative control levels (Fig. 3.1B). CD44 was highly expressed in all three cell lines, but MM6 cells additionally showed a second

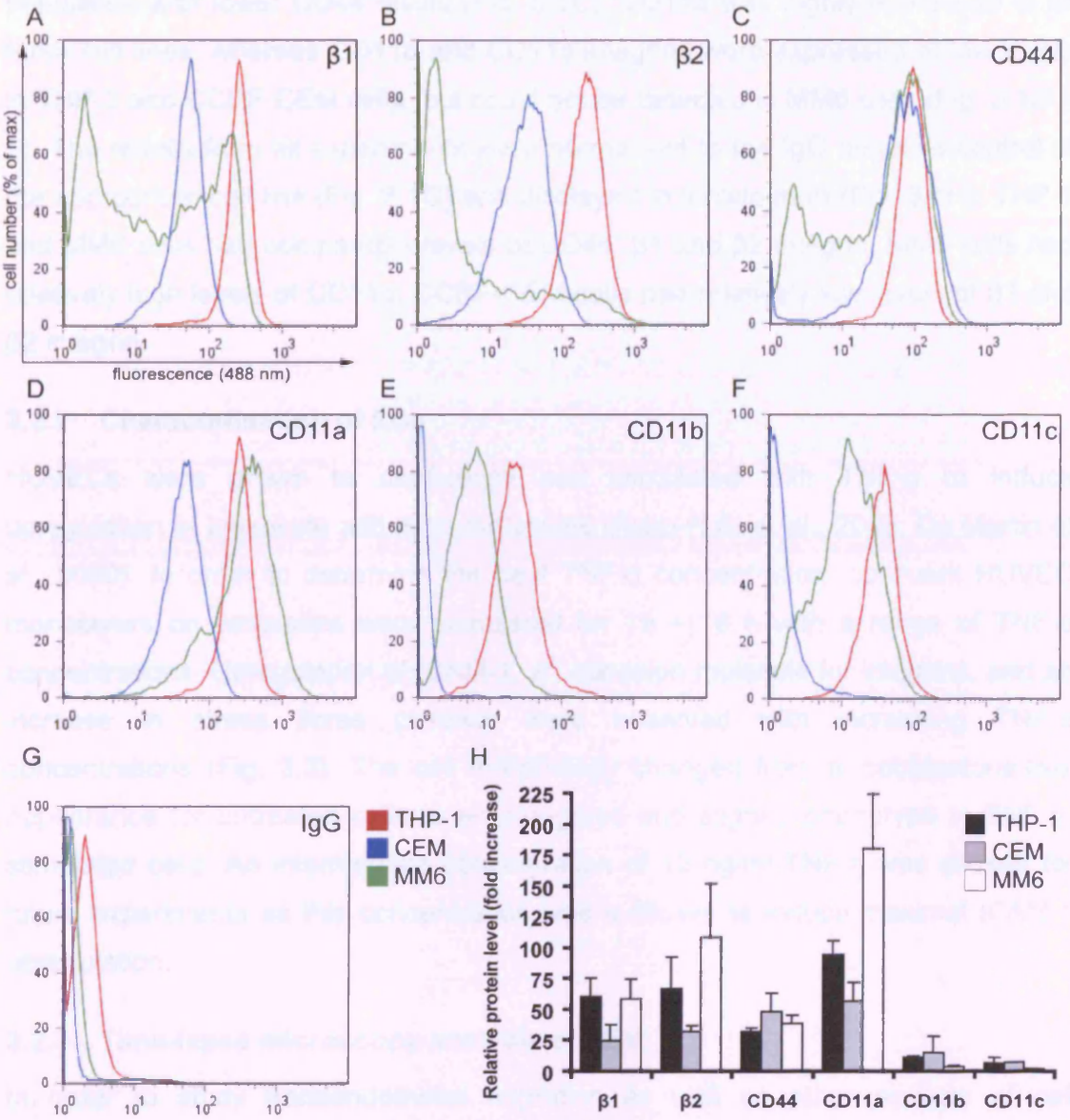

Figure 3.1: Characterisation of leukocyte surface marker expression by flow cytometry

FACS analysis was carried out on untreated THP-1, CCRF-CEM and MM6 cells. Cells were labelled with antibodies against β1 and β2 integrin, CD44, CD11a (αL), CD11b (αM) and CD11c (αX) and FITC-conjugated secondary antibodies. Mouse IgG was used as negative control. **A - G**: Representative FACS traces for individual antibodies and cell lines. **H**: Graphical display of all experiments. Fold increase is calculated over each respective IgG control. Bars represent SEM. n = 3.

population with lower CD44 levels (Fig. 3.1C). CD11a was highly expressed in all three cell lines, whereas CD11b and CD11c integrins were expressed at low levels in THP-1 and CCRF-CEM cells, but could not be detected in MM6 cells (Fig. 3.1D – F). The results from all experiments were normalised to the IgG negative control of the appropriate cell line (Fig. 3.1G) and displayed in a histogram (Fig. 3.1H). THP-1 and MM6 cells had comparable levels of CD44, β1 and β2 integrin. MM6 cells had relatively high levels of CD11a; CCRF-CEM cells had relatively low levels of β1 and β2 integrin.

3.2.2 Characterisation of ECs

HUVECs were grown to confluency and stimulated with TNF-α to induce upregulation of leukocyte adhesion molecules (Alom-Ruiz et al., 2008; De Martin et al., 2000). In order to determine the best TNF-α concentration, confluent HUVEC monolayers on coverslips were stimulated for 15 – 18 h with a range of TNF-α concentrations. Upregulation of ICAM-1, an adhesion molecule for integrins, and an increase in stress fibres (arrows) were observed with increasing TNF-α concentrations (Fig. 3.2). The cell morphology changed from a 'cobblestone-like' appearance for untreated cells to an elongated and aligned phenotype in TNF-α-stimulated cells. An intermediate concentration of 10 ng/ml TNF-α was chosen for future experiments as this concentration was sufficient to induce maximal ICAM-1 upregulation.

3.2.3 Time-lapse microscopy analysis of TEM

In order to study transendothelial migration as well as other aspects of cell behaviour, a time-lapse-microscopy (TLM)-based assay was set up. The microscopy based assay allows not only the determination of the transmigration rate, but also analysis of cell morphology and behaviour after various treatments. Movies of transmigrating THP-1 cells were recorded over 2 h and the transmigration rate was calculated from the movies and amounted to 16.3 ± 2% and 15.8 ± 2.3% (of input) for untreated THP-1 and CCRF-CEM cells respectively (see Fig. 3.14). Phase-contrast images from these movies show that cells did not exhibit a clear polarised phenotype with lamellipodium and uropod during their migration on the HUVEC surface and instead had a rounded morphology with dynamic protrusions at multiple sites of the migrating cell (Fig. 3.3A – D). During the early phase of TEM, cells extended these protrusions to invade the junctions between neighbouring ECs. In transmigrating cells, these exploratory protrusions evolved into a lamella (Fig. 3.3B, C, arrow) and squeezed into the monolayer gap, finally followed by the

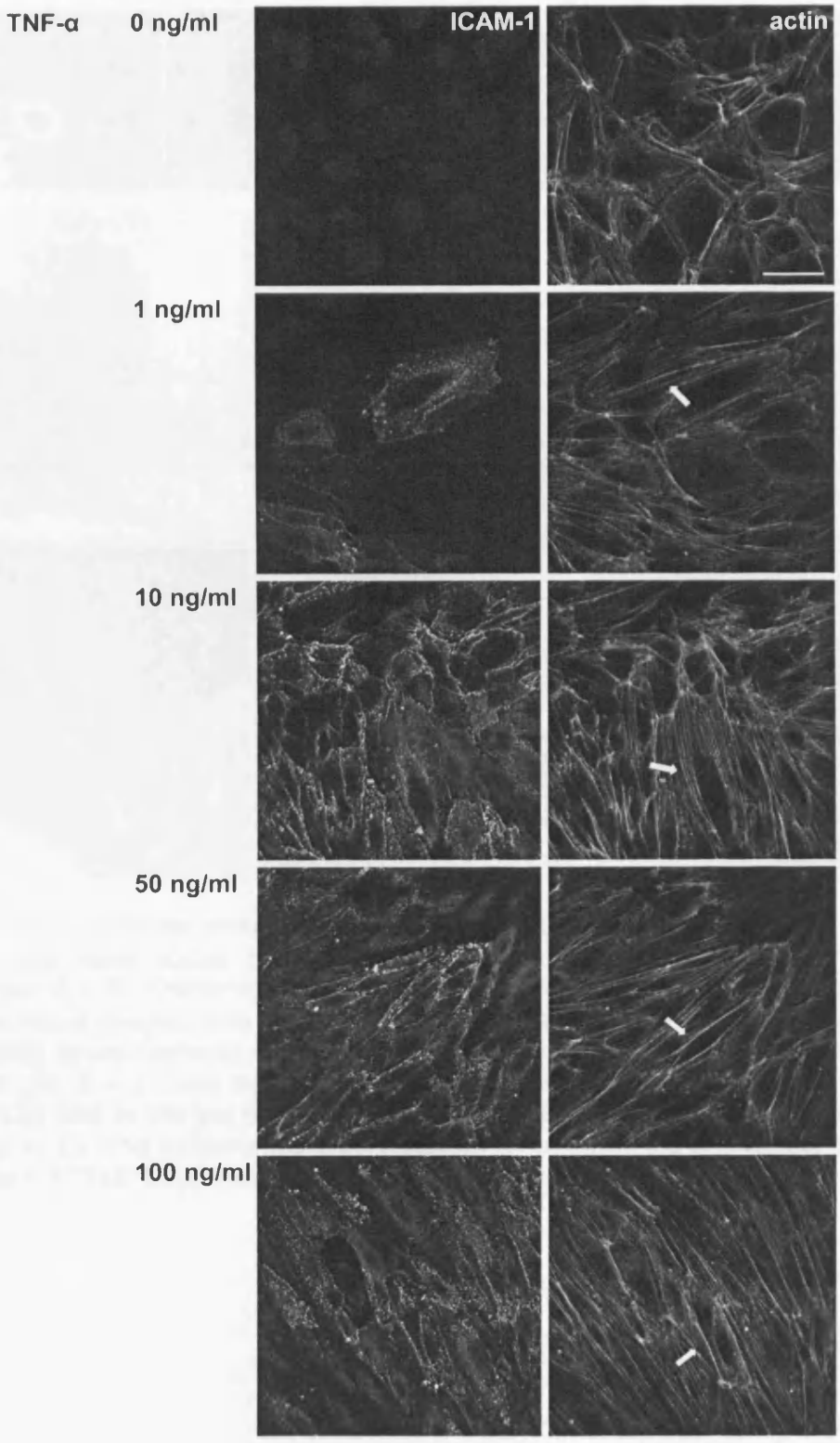

Figure 3.2: TNF-α response in HUVECs
HUVECs were grown to confluency on coverslips and stimulated for 15 – 18 h with 0, 1, 10, 50 or 100 ng/ml TNF-α. Monolayers were fixed and stained for ICAM-1 and F-actin. Arrows indicate stress fibres. Bar = 50 µm.

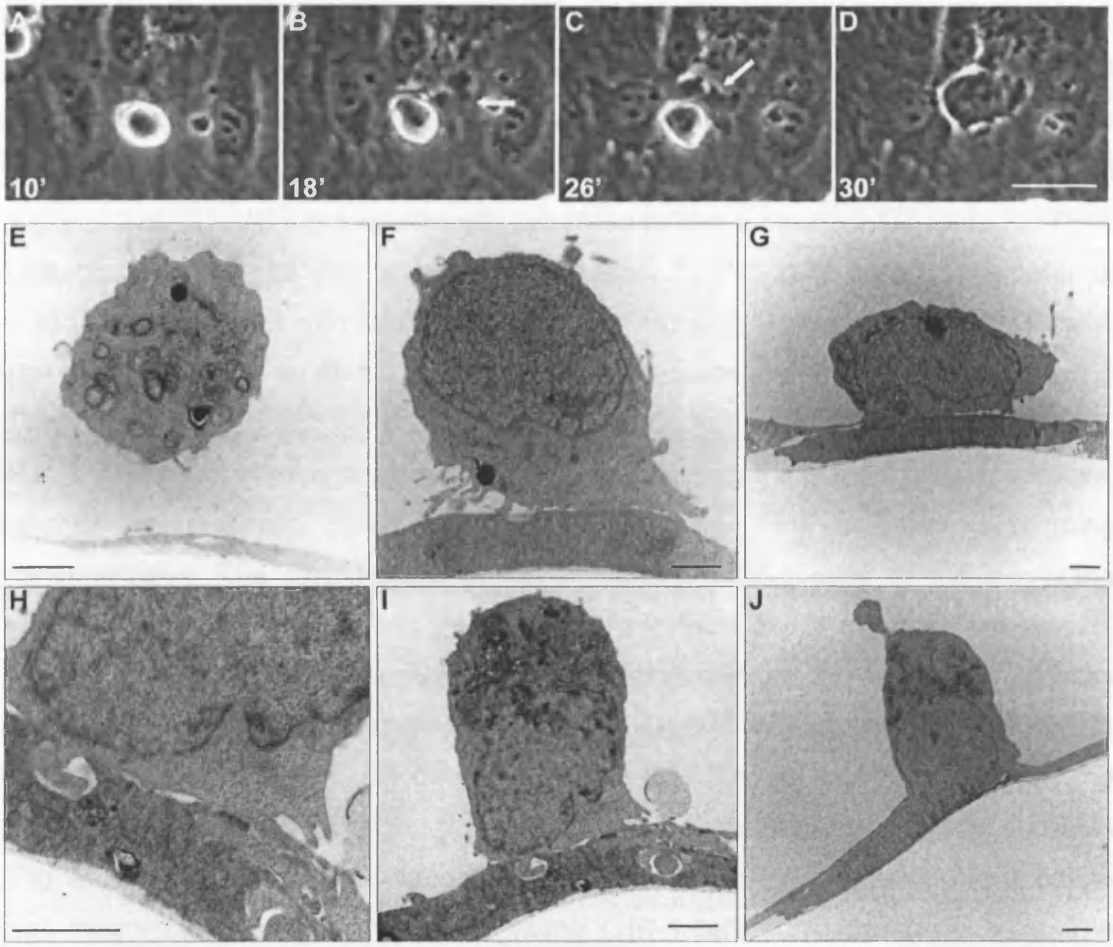

Figure 3.3: Leukocyte transendothelial migration
THP-1 cells were added to a TNF-α-activated (10 ng/ml, 15 - 18 h) HUVEC monolayer. **A – D**: Transmigration was monitored using time-lapse microscopy and phase contrast images from the movies at the indicated timepoints (min) are shown. Phase-dark areas (arrows) of THP-1 cells are underneath the HUVEC monolayer. Bar = 20 µm. **E – J**: Cells were fixed after 25 min, embedded and ultra-thin sections (100 – 120 nm) in the y-z plane were cut by Ken Brady (Centre for Ultrastructural Imaging, KCL). The sections were post-stained to enhance the contrast and viewed in a Hitachi H7600 transmission electron microscope. Bars = 2 µm.

cell body (Fig. 3.3D). Most transmigrating THP-1 cells underwent reverse TEM (i.e. reappeared on the HUVEC surface) after 5 – 10 min. This is a phenomenon that has been observed *in vivo* as well, but not at this high rate, which is likely to be due to the lack of underlying matrix (i.e. ECM) in this system into which the cells could migrate. THP-1 cells were exclusively observed to use a paracellular route for TEM. This could be due to their relatively large size; THP-1 cells have a diameter of ~ 15 µm (determined with CASY® cell counter, Schärfe Systems), whereas T cells, which are known to be able to use a transcellular route (Millan et al., 2006), have a diameter of only ~ 6 µm.

To further investigate the cell morphology during the transmigration process, electron microscopy (EM) was carried out on THP-1 cells undergoing transmigration. The EM images of transmigrating THP-1 cells in the z-y plane confirm the observations made from the TLM movies: THP-1 cells are not spread, but exhibit a rather rounded morphology during the whole transmigration process (Fig. 3.3E - J). The diameter of THP-1 cells is large in comparison to the flat ECs (1 – 3 µm). THP-1 cells exhibited only small lamellipodia while crawling on the endothelium (Fig. 3.3F) and protrusions could be seen probing junctions and ECs (Fig. 3.3G – I). Even during diapedesis, THP-1 cells were not spread (Fig. 3.3J) as high magnification images of transmigrating THP-1 cells confirmed (Fig. 3.4A). The details of the transmigrating cell illustrate the close proximity of the endothelial and the leukocyte plasma membrane during paracellular TEM (Fig. 3.4 B – D). The sites of interaction are not continuous, but rather 'button-like'. These areas are likely sites of adhesion, which could be demonstrated by immunogold-labelling of cell-cell adhesion molecules.

3.2.4 Transwell™ assay of migration

The disadvantage of the TLM-based TEM is the relatively small number of cells that can be recorded (~ 100 THP-1 cells per field of view). In order to provide a more rapid quantification of cell TEM rate, a second TEM assay was set up, using Transwell™ cell culture inserts. These cell culture inserts provide a two chamber system, which is separated by a porous membrane. This membrane can be coated with cell substrates, such as VCAM-1, or used to grow HUVECs on. In order to induce efficient migration in the Transwell™-based assay a chemotactic gradient using CCL2 (MCP-1) was applied. To determine the most efficient concentration of MCP-1 for THP-1 migration, concentrations from 0 – 200 ng/ml were tested.

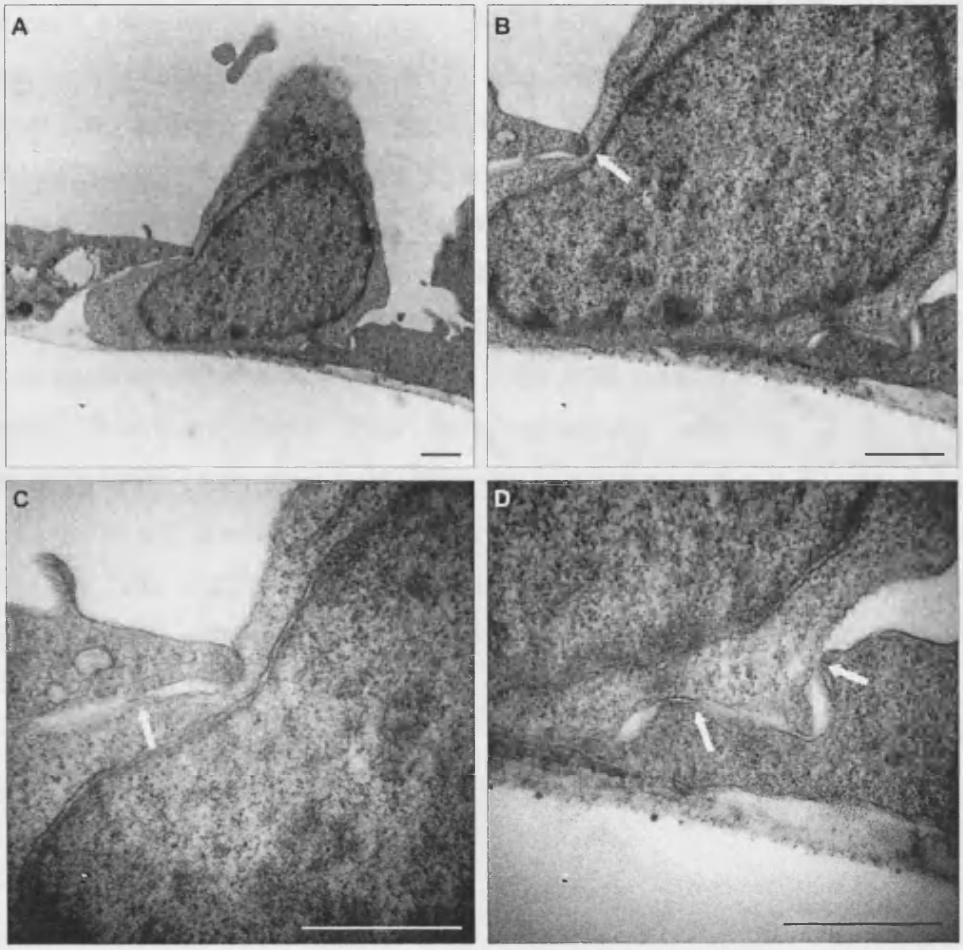

Figure 3.4: EM details of a transmigrating THP-1 cell
THP-1 cells were added to a TNF-α-activated (10 ng/ml, 15 - 18 h) HUVEC monolayer. Cells were fixed after 25 min, embedded and ultra-thin sections (100 – 120 nm) in the z-y plane were cut by Ken Brady (Centre for Ultrastructural Imaging, KCL). The sections were post-stained to enhance the contrast and viewed in a Hitachi H7600 transmission electron microscope. **A**: Overview of a transmigrating THP-1 cell. **B – D**: Details of leukocyte-endothelial interaction sites. Arrows indicate areas of close contact between leukocyte and EC. Bar = 2 µm.

Transwell™ filters were coated with VCAM-1 since adhesion of THP-1 cells was highest for this substrate (see Fig. 3.12), and THP-1 cells were added to the upper chamber and allowed to transmigrate for 2 h in response a range of MCP-1 concentrations. Cells from the lower chamber were counted and the migration rate calculated (Fig 3.5). THP-1 cells displayed increased migration in response to MCP-1, with most effective migration at 100 ng/ml MCP-1. This concentration was used in future experiments. The migration rate was calculated by counting the cells from the lower chamber and amounted to 7.4 ± 1.9% and 20.4 ± 11.7% (of input) for untreated THP-1 and CCRF-CEM cells respectively (see Fig. 3.14). A similar response to MCP-1 with a peak at 100 ng/ml has been seen in a Transwell™-based TEM assay in the presence of HUVECs (R.J. Cain, unpublished data). Similarly, CCRF-CEM cells migrated in response to CXCL12 (SDF-1) in Transwells™, with a peak at 50 ng/ml without or 100 ng/ml with HUVECs (S.J. Heasman, unpublished data).

The TLM and Transwell™ assays provided complementary approaches for studying *in vitro* TEM.

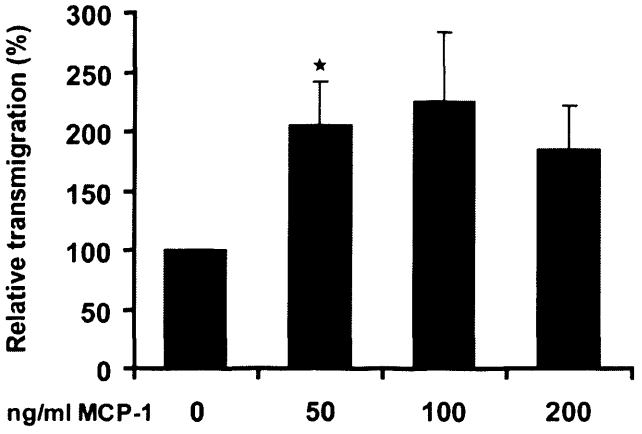

Figure 3.5: Determination of MCP-1 concentration for Transwell™-based migration assay
Untreated THP-1 cells were added to a VCAM-1-coated (5 µg/ml) Transwell™ filter. MCP-1 was added to the lower chamber at 0, 50, 100 and 200 ng/ml to provide a chemoattractant gradient across the filter. Cells from the lower chamber were counted after 2 h. Results were normalised to untreated control. Bars represent SEM. ★ $p < 0.05$ determined by Student's t-test and Bonferroni post-test. $n = 5$.

3.3 H_2O_2 application decreases leukocyte transendothelial migration

To determine the role of H_2O_2 in TEM, H_2O_2 treatment was chosen as a model for ROS exposure (see Chapter 1.5). THP-1, CCRF-CEM, and MM6 cells were treated independently from HUVECs with a range of H_2O_2 concentrations and H_2O_2 was removed by centrifuging and resuspending the cells in fresh medium. The treated leukocytes were used in the TLM- and Transwell™-based assays, except for MM6, which were only used in TLM-based assays. Phase-contrast images from time-lapse movies with treated or untreated THP-1, CCRF-CEM, or MM6 cells after 5 and 120 min are shown in Figure 3.6. THP-1 cells did not show an obvious change in morphology with H_2O_2 treatment (Fig. 3.6A – D), whereas CCRF-CEM cells appeared more rounded after H_2O_2 treatment (Fig. 3.6E – H). The rounded morphology could indicate a defect in polarisation. The effect might only be detectable in CCRF-CEM cells, as THP-1 cells do not exhibit a clearly polarised phenotype which impedes the identification of a polarisation defect without analysing specific markers. The reason for this rounding remains to be determined, but could contribute significantly to the observed decrease in TEM.

The analysis of time-lapse movies revealed that no MM6 cells transmigrated during the 2 h of recording, neither in treated nor untreated conditions. The cells appeared to be rounded throughout the 2 h of recording (Fig. 3.6I - L), which could contribute to the lack of TEM. This finding is surprising as MM6 cells have been used for TEM experiments by other groups (Weber et al., 1998). The transmigration of MM6 cells was not pursued further.

Analysis of the THP-1 and CCRF-CEM cell movies showed a significant decrease in TEM from 0.5 mM H_2O_2 for both cell types (Fig. 3.7A, B). The transmigration rate was calculated as a percentage of untreated cells in all following experiments. TEM was inhibited by a maximum of 54.5 ± 14.7% (0.5 mM) in THP-1 cells and 95.2 ± 2.6% (5 mM) in CCRF-CEM cells. THP-1 TEM was not inhibited at lower H_2O_2 concentrations ranging from 0 – 100 µM (Fig. 3.7C).

The TEM results were confirmed using the Transwell™-based assay (Fig. 3.7D, E). However, THP-1 TEM was inhibited less efficiently, needing higher concentrations to reach a maximum inhibition of 61 ± 4.5% at 5 mM H_2O_2. CCRF-CEM TEM showed a very similar trend to the TLM-based assay, but lower concentrations (0.1 and 0.5 mM) were move effective at reducing TEM.

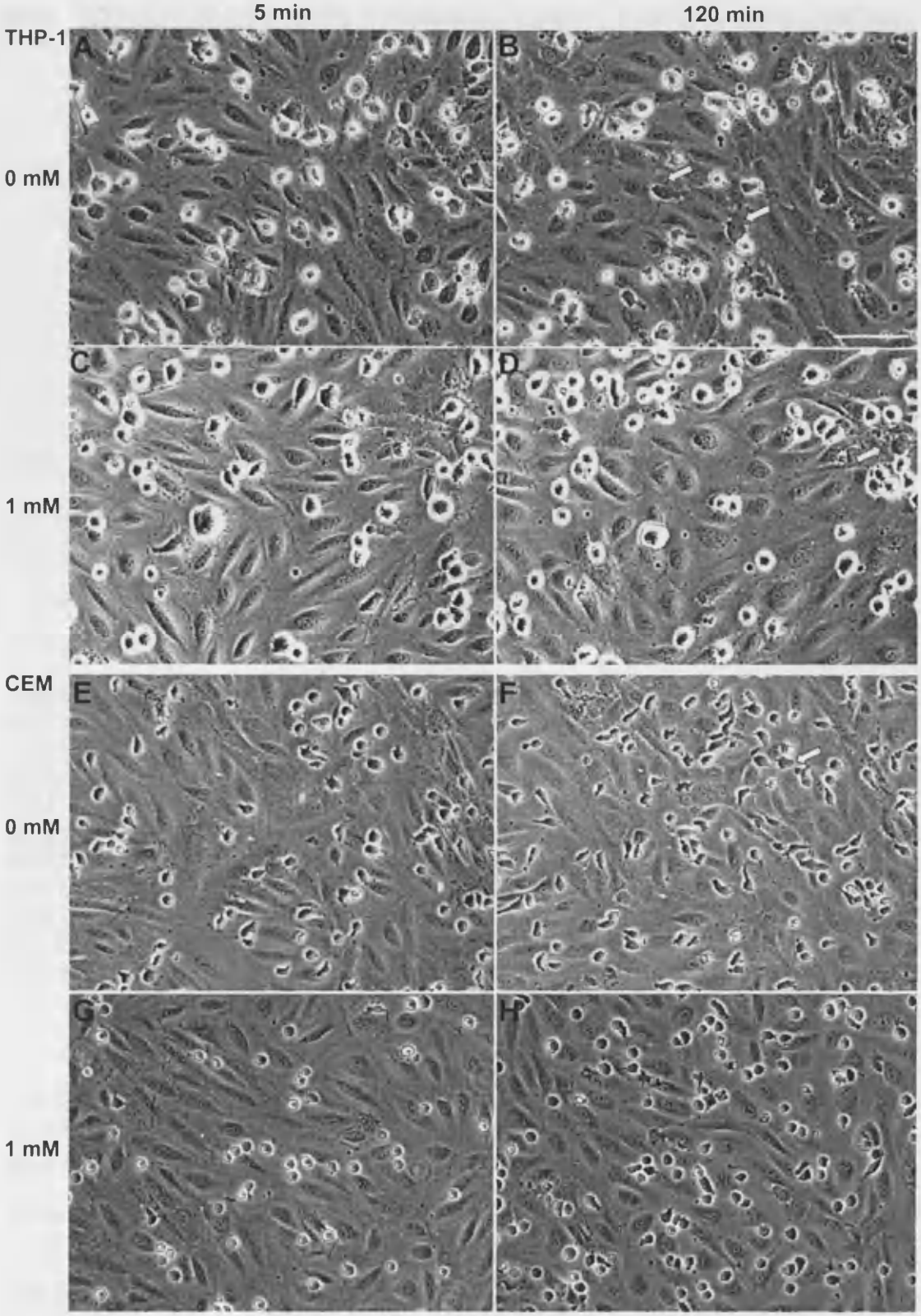
5 min
120 min
THP-1
0 mM
1 mM
CEM
0 mM
1 mM
A
B
C
D
E
F
G
H

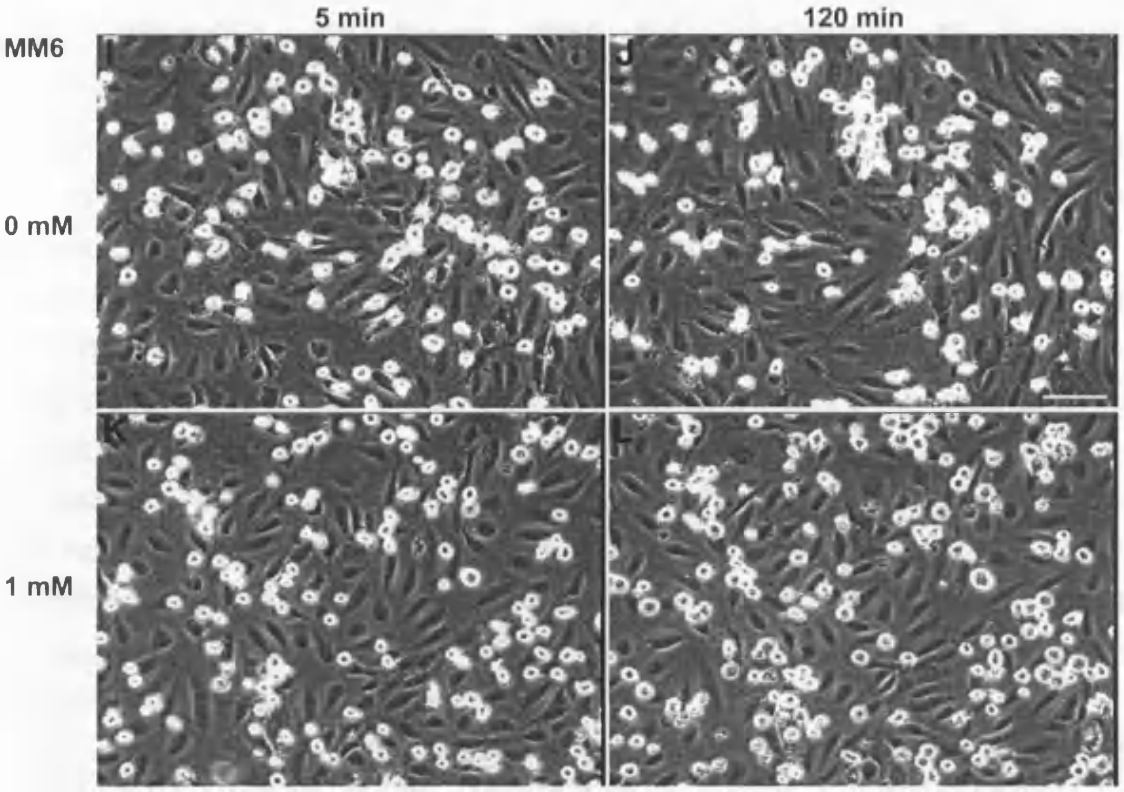

Figure 3.6: Phase-contrast images of transmigrating H_2O_2-treated leukocytes
THP-1, CCRF-CEM and MM6 cells were treated with 0 and 1 mM H_2O_2 (30 min, 37°C). H_2O_2 was removed by centrifugation and cells were allowed to transmigrate across TNF-α-activated (10 ng/ml, 15 - 18 h) HUVECs for 2 h and monitored by TLM. To promote CCRF-CEM cell TEM, HUVECs were additionally incubated with 50 ng/ml CXCL12 (SDF-1) for 15 min, then SDF-containing medium was removed and CCRF-CEM cells were added. Phase-contrast images of THP-1, CCRF-CEM and MM6 cells, taken from movies (1 frame/min) started 10 min after leukocyte addition, are shown for untreated conditions after 5 (**A, E, I**) and 120 min (**B, F, J**) and cells treated with 1 mM H_2O_2 after 5 (**C, G, K**) and 120 min (**D, H, L**). Arrows indicate examples of transmigrated leukocytes. Bars = 50 µm.

To investigate whether the chemotactic response and the ability to deform the cell, e.g. by remodelling the actin cytoskeleton, in order to transmigrate through confined areas was compromised in H_2O_2-treated THP-1 cells, the Transwell™-based migration assay was carried out without HUVECs. The pore size of 5 µm is small enough to force the THP-1 cells (diameter 15 µm) to remodel the cytoskeleton and nucleus extensively in order to migrate through the pores. The results show a significant inhibition of migration at 1 and 5 mM H_2O_2, but only by a maximum of 23.7 ± 6% (Fig. 3.7F), indicating that neither changes in chemotaxis nor the ability to deform the cells are able to explain the detected defect in TEM. The reduction in TEM seems to be specific for the interaction of leukocytes with the endothelium.

3.4 Leukocytes are viable after H_2O_2 treatment at working concentrations

H_2O_2 has been shown to be an inducer of apoptosis in several cell types (Cook et al., 1999; Kazzaz et al., 1996; Lee et al., 2002). JNK has been shown to be activated in response to ROS, which is mediated via Src kinase and ASK-1 (Shen and Liu, 2006). JNK is an important mediator of apoptosis, and is required for mitochondrial cytochrome C release (Tsuruta et al., 2004). To determine if H_2O_2 induced apoptosis in THP-1 and CCRF-CEM cells at working concentrations, an apoptosis assay was carried out. Apoptotic cells can be detected by Annexin V and PI staining. Annexin V binds to phosphatidylserine (PS), which usually is confined to the inner leaflet of the plasma membrane in viable cells (Koopman et al., 1994), but is translocated to the outer leaflet of the plasma membrane during apoptosis. PI staining of the DNA is used to distinguish between cells with intact and compromised membranes (Nicoletti et al., 1991).

H_2O_2-treated cells were allowed to recover for 2 h before being labelled with Annexin V and PI. Controls for apoptosis were staurosporine treatment (Nicotera et al., 1999) and briefly heated THP-1 cells for necrosis. In this assay, apoptosis is defined by positive Annexin V staining and lack of PI uptake, while necrosis is defined by positive Annexin V staining and uptake of PI (Fig. 3.8A). With these markers, it is not possible to distinguish between normal necrosis and secondary necrosis. Secondary necrotic cells are late apoptotic cells and can be distinguished by the presence of nuclear condensation and/or fragmentation along with PI uptake (Kelly et al., 2003).

The assay revealed no significant increase in apoptosis or necrosis for THP-1 cells at working concentrations of H_2O_2 (Fig. 3.8). THP-1 cells showed an increase in necrosis from 50 mM H_2O_2 upwards. CCRF-CEM cells were more susceptible to the damaging effects of H_2O_2, showing an increase in necrosis, with 22.4 ± 4.9% at 5 mM compared to 6.4 ± 0.3% at 0 mM H_2O_2. Results with 5 mM H_2O_2 on CCRF-CEM cells should therefore be treated with caution.

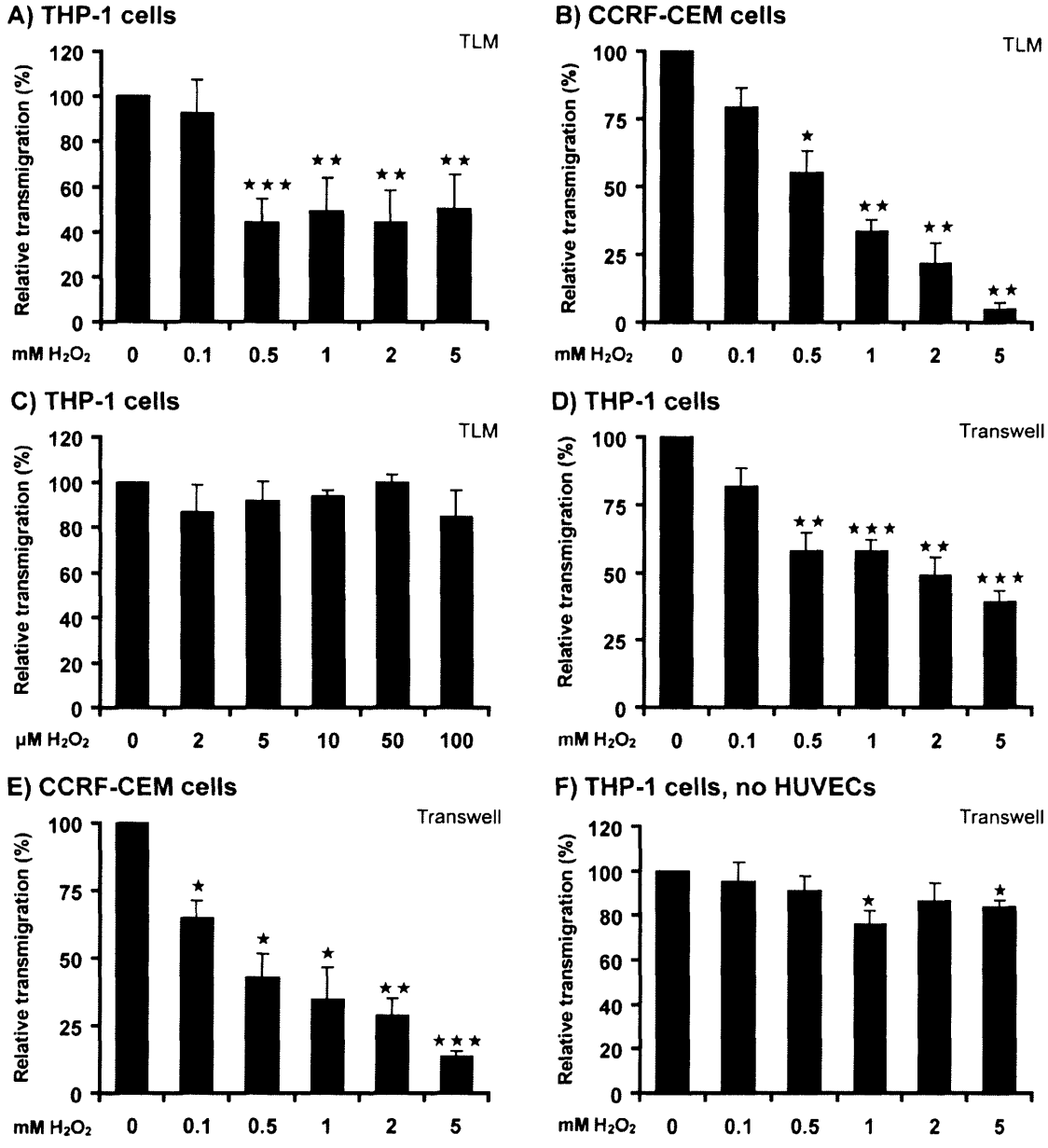

Figure 3.7: H_2O_2 decreases THP-1 and CCRF-CEM cell TEM
THP-1 and CCRF-CEM cells were treated with 0 - 100 µM H_2O_2 or 0 - 5 mM H_2O_2 (30 min, 37°C). H_2O_2 was removed by centrifugation and cells were added to HUVECs for 2 h. TEM rate was normalised to untreated samples. THP-1 (**A, C**) and CCRF-CEM (**B**) cell TEM across HUVECs was monitored by TLM and movies were analysed to calculate TEM rate. n = 7 (A); 5 (B); 3 (C). THP-1 (**D**) and CCRF-CEM (**E**) cell TEM across HUVECs was detected using a Transwell™-based system. Transmigrated cells from the lower chamber were counted after 2 h. n = 6 (D) or 5 (E). Migration across a VCAM-1-coated Transwell™ filter (**F**) was determined by counting cells from the lower chamber after 2 h of transmigration. n = 5.
Results are normalised to untreated control. Bars represent SEM. ⋆⋆⋆ $p < 0.001$, ⋆⋆ $p < 0.01$, ⋆ $p < 0.05$ determined by Student's t-test and Bonferroni post-test, as compared to untreated control.

3.5 TEM of T lymphoblasts and primary monocytes is not significantly altered after H_2O_2 treatment

To investigate if primary leukocytes had the same response to H_2O_2 as leukaemic cell lines, T lymphoblasts and primary monocytes were subjected to H_2O_2 treatment and subsequent TLM-based TEM assays. The two cell types displayed different susceptibility to oxidative damage after H_2O_2 treatment as determined by Trypan blue staining. Trypan blue is a diazo dye that is excluded from cellular uptake in viable cells, but stains dead cells (Rodrigues et al., 2007). Different H_2O_2 concentrations were chosen for the TEM assays. T cells were treated with concentrations ranging from 0 – 500 µM H_2O_2, which is lower than the range used for THP-1 cells, but overlaps with concentrations that reduce TEM in THP-1 cells. T cells died at concentrations higher than 500 µM. Control T cells transmigrated at a high rate of up to 48.3 ± 5.5% (compared to THP-1 cells at 16.3 ± 2%; see Fig. 4.8) and exhibited a highly polarised morphology with long tails (Fig. 3.9A, B). The analysis of the movies showed a trend towards a decrease in TEM for high concentrations, but these results were not statistically significant due to the high variability between assays (Fig. 3.9E).

Primary monocytes were even more susceptible to the toxic effects of H_2O_2 and lower concentrations from 0 – 60 µM were therefore used. These concentrations have been shown to have no effect on THP-1 cells (Fig. 3.7C). Primary monocyte TEM rate for untreated cells was 11.1 ± 3%, similar to THP-1 cells (see Fig. 4.8). The cell morphology was relatively rounded throughout the 2 h of recording (Fig. 3.9C, D). Again, a trend towards a decrease in TEM was detectable, but due to the high variability, changes were not statistically significant (Fig. 3.9F).

Together these data indicate a trend towards a reduction in TEM for primary leukocytes, although they are more susceptible to the toxic effects of H_2O_2 and show a higher variability in the transmigration rate than leukaemic cell lines.

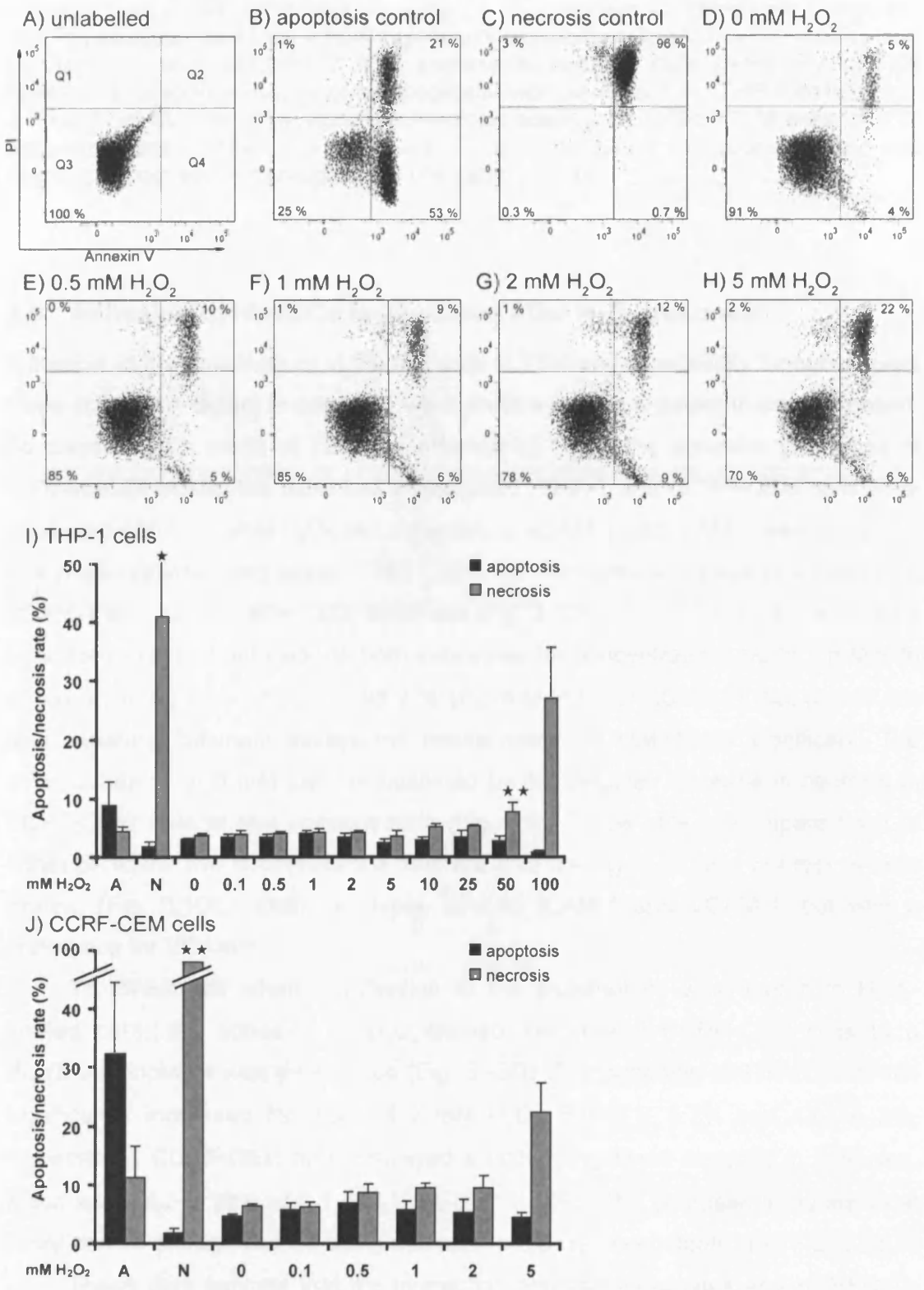

Figure 3.8: Working concentrations of H_2O_2 do not induce a significant increase in apoptosis or necrosis

Cells were treated with H_2O_2 concentrations from 0 – 100 mM or 0 – 5 mM (30 min, 37°C) and allowed to recover for 2 h. Controls for apoptosis (A) were cells treated with staurosporine (1 µM, 2.5 h, 37°C) or cells briefly heated for necrosis (N). The apoptosis and necrosis rates were determined by Annexin V-binding and PI staining respectively, which were detected by FACS analysis. **A – H**: Representative FACS

dot plots from CCRF-CEM cells. Quadrant 3 (Q3) represents viable cells (AnnexinV and PI negative), quadrant 4 (Q4) represents apoptotic cells (AnnexinV positive and PI negative) and quadrant 2 (Q2) represents necrotic cells (AnnexinV and PI positive). **I**: Graphical display of all apoptosis/necrosis assays for THP-1 cells. n = 7. **J**: Graphical display of all apoptosis/necrosis assays for CCRF-CEM cells. n = 3. Bars represent SEM.** $p < 0.01$, * $p < 0.05$ determined by Student's t-test and Bonferroni post-test, as compared to untreated control.

3.6 Adhesion to HUVECs is increased after H_2O_2 treatment

Adhesion to the endothelium is the first step of TEM and a necessity for subsequent steps of TEM. A defect in adhesion will therefore lead to a defect in transmigration. To dissect which steps of TEM are affected by H_2O_2, the adhesive properties of H_2O_2-treated leukocytes were first investigated. THP-1 and CCRF-CEM cells were incubated with 0 – 5 mM H_2O_2 and adhesion to VCAM-1 and ICAM-1 was measured in a plate-reader-based assay. THP-1 cells did not show a change in adhesion to VCAM-1 and ICAM-1 after H_2O_2 treatment (Fig. 3.10A). CCRF-CEM cells showed a trend for increased adhesion to both substrates for concentrations up to 2 mM with a maximum increase of 53.3 ± 35.2 % (0.5 mM H_2O_2 on ICAM-1), but due to the high variability between assays the results were not statistically significant. The lower adhesion at 5 mM can be explained by the detected increase in necrosis in CCRF-CEM cells at this concentration (Fig. 3.8). To be able to compare level of adhesion to the two substrates the data are also displayed as total number of cells binding (Fig. 3.10C). Both cell types bind to ICAM-1 and VCAM-1, but with a preference for VCAM-1.

To investigate whether adhesion to the endothelium was altered in H_2O_2-treated cells, the adhesion of H_2O_2-treated THP-1 and CCRF-CEM cells to a HUVEC monolayer was determined (Fig. 3.10D). The adhesion of THP-1 cells was significantly increased for 0.5 and 2 mM H_2O_2, by 24 ± 5.7% and 13.1 ± 2%, respectively. CCRF-CEM cells displayed a higher significant increase in adhesion, which was 48.3 ± 13% at 0.1 mM H_2O_2 (Fig. 3.10E). The decrease in adhesion at 5 mM can be disregarded as being due to an increase in cell death (see Fig. 3.8J).

These data indicate that the interaction between leukocytes and HUVECs is influenced by H_2O_2, leading to an increase in adhesion.

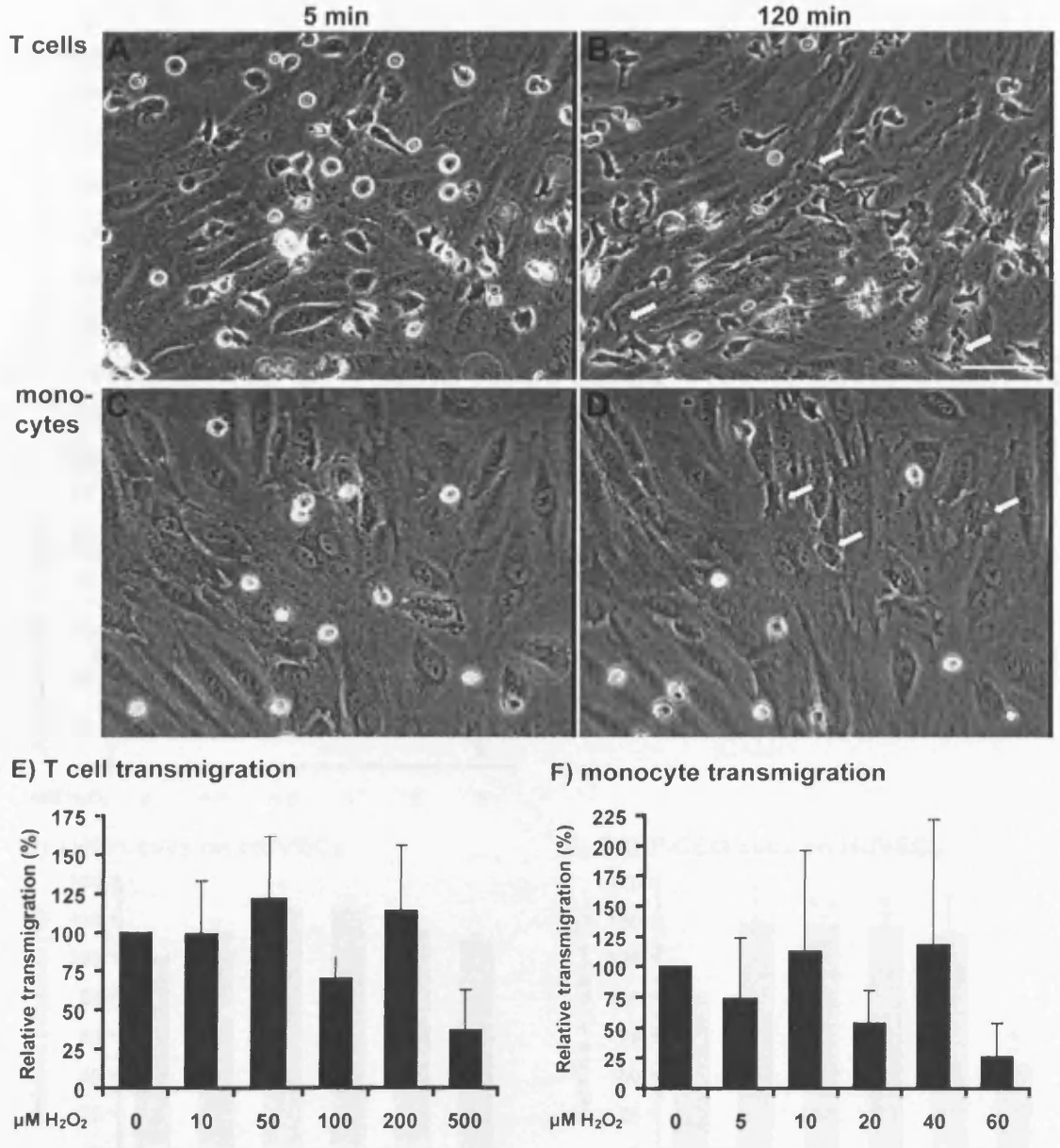

Figure 3.9: Effects of H_2O_2 on TEM of T lymphoblasts and monocytes
T lymphoblasts and monocytes were treated with H_2O_2 (30 min, 37°C): T lymphoblasts: 0 – 500 µM; monocytes: 0 – 60 µM. H_2O_2 was removed by centrifugation and cells were added to a TNF-α-activated (10 ng/ml, 15 - 18 h) HUVEC monolayer for 2 h. TEM rate was determined by TLM. Phase-contrast images of untreated T lymphoblasts and monocytes after 5 (**A, C**) and 120 min (**B, D**) are taken from movies (1 frame/min) started 10 min after cell addition. Arrows indicate examples of transmigrated cells. Bar = 50 µm. **E, F**: Graphical illustration of results from all T lymphoblast and monocyte transmigration experiments. Results are normalised to untreated control. Bars represent SEM. n = 3.

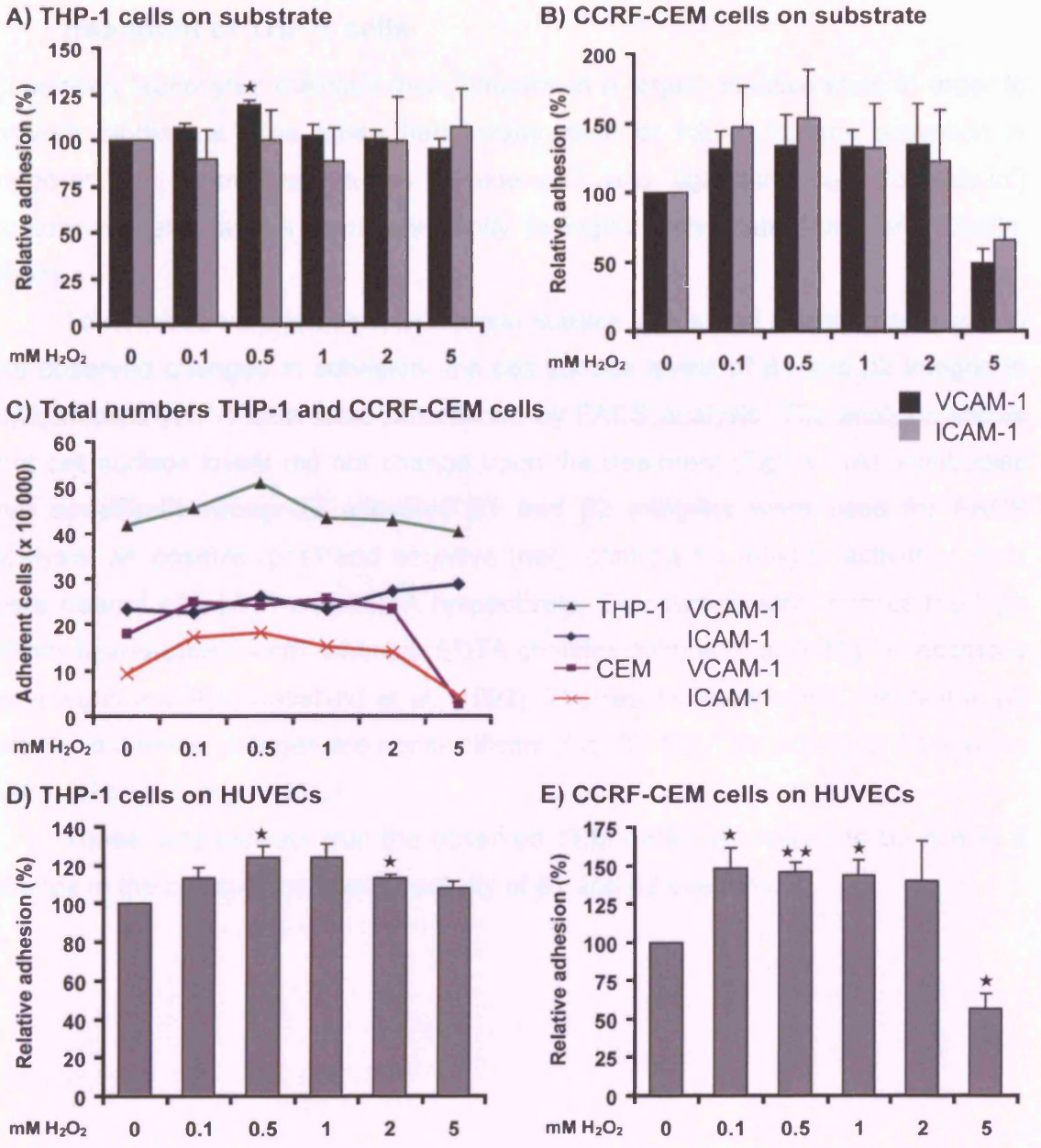

Figure 3.10: THP-1 and CCRF-CEM cell adhesion to HUVECs is increased by H_2O_2 treatment

THP-1 and CCRF-CEM cells were labelled with green CellTracker™ dye (1 µM, 30 min, 37°C), cells were washed and treated with 0 – 5 mM H_2O_2 (30 min, 37°C). Cells were washed and allowed to adhere for 15 min to either VCAM-1- or ICAM-1-coated 96-well plates or TNF-α-activated (10 ng/ml, 15 - 18 h) HUVECs. Unattached cells were washed off and fluorescence was measured using a Fusion™ α-FP plate reader. THP-1 (**A**) and CCRF-CEM (**B**) cell adhesion to VCAM-1- and ICAM-1-coated 96-well plates. n = 4. **C**: Total numbers of THP-1 and CCRF-CEM cells adhering to VCAM-1- and ICAM-1. n = 4. Error bars are omitted for clarity. **D**, **E**: THP-1 and CCRF-CEM cell adhesion to HUVECs. n = 3.

Results are normalised to respective untreated control. Bars represent SEM. ⋆⋆ $p < 0.01$, ⋆ $p < 0.05$ determined by Student's t-test and Bonferroni post-test, as compared to untreated control.

3.7 Integrin level and activity are not significantly changed upon H_2O_2 treatment of THP-1 cells

Circulating leukocytes maintain their integrins in a largely inactive state in order to prevent binding at sites other than inflammation or injury. Integrin activation is triggered by chemokine-induced ('inside-out') and ligand-induced ('outside-in') conformational changes from low-affinity to high-affinity state (Alon and Dustin, 2007).

To determine if alterations in integrin surface levels and activity play a role in the observed changes in adhesion, the cell surface levels of β1 and β2 integrin in H_2O_2-treated THP-1 cells were determined by FACS analysis. The analysis shows that cell surface levels did not change upon the treatment (Fig. 3.11A). Antibodies that specifically recognize activated β1 and β2 integrins were used for FACS analysis; as positive (pos) and negative (neg) controls for integrin activation cells were treated with Mn^{2+} and EDTA respectively. Exposure to Mn^{2+} mimics the high affinity ligand-bound form, whereas EDTA chelates cations (mainly Mg^{2+}) necessary for integrin activity (Dransfield et al., 1992). The results show some variation in β2 activity, but these changes are not significant (Fig. 3.11B). The activity of β1 integrin was unchanged (Fig. 3.11C).

These data indicate that the observed TEM defect is unlikely to be due to a change in the cell surface level or activity of β1 and β2 integrins.

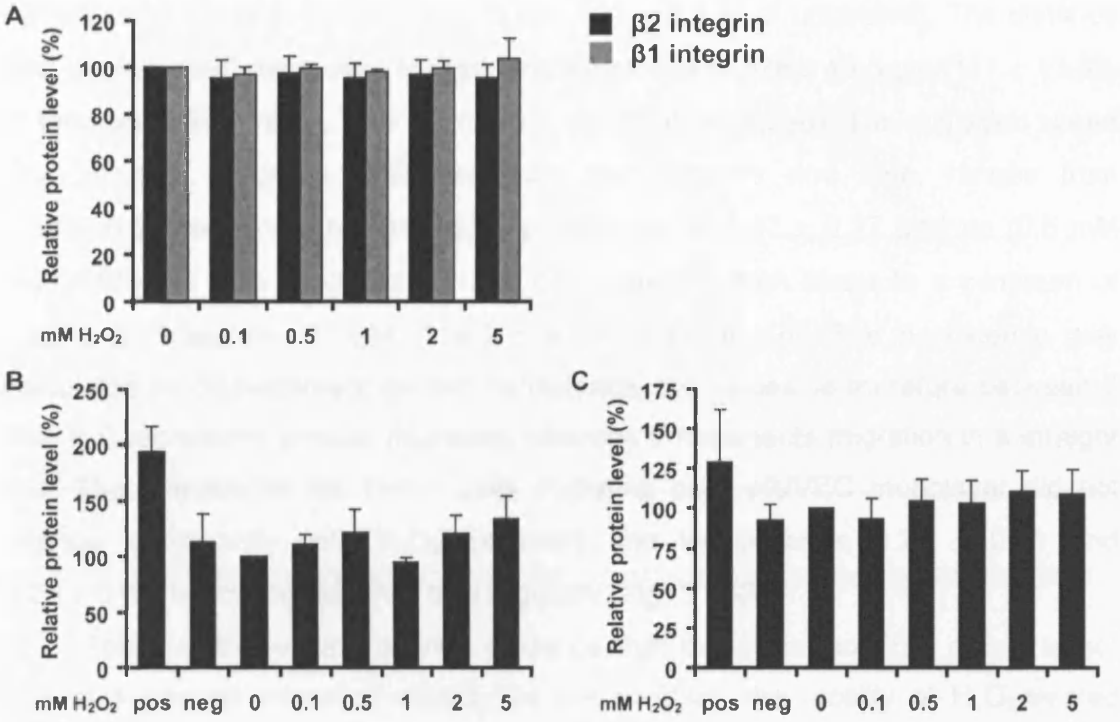

Figure 3.11: Integrin levels and activity are unchanged upon H_2O_2 treatment of THP-1 cells
THP-1 cells were treated with 0 – 5 mM H_2O_2 (30 min, 37°C) and integrin levels were determined by FACS analysis using specific antibodies for total and active β1 and β2 integrin. **A**: Total surface level of β1 and β2 integrin. n = 4. **B**, **C**: Positive (pos) and negative (neg) controls for active β2 (B) and β1 (C) integrin labelling were cells treated with 200 µM Mn^{2+} or 5 mM EDTA respectively. β1 integrin-labelled cells were fixed prior to staining with antibodies. n = 8 (B); 5 (C).
Results are normalised to respective untreated control. Bars represent SEM.

3.8 H_2O_2 treatment increases THP-1 cell motility on HUVECs

To identify possible mechanisms involved in the TEM defect caused by H_2O_2, some of the time-lapse movies of THP-1 cells were analysed further. Fifteen THP-1 cells per condition and experiment were tracked on the surface of HUVECs and tracks were analysed using a Mathematica notebook written by D. Zicha (Allen et al., 1998). The migration tracks are shown as vector plots with all tracks beginning at the origin (0,0) of a Cartesian coordinate system (Fig. 3.12). The coloured bars represent the time, starting at the left hand side.

The distance migrated and total displacement was determined from the migration tracks, and migration speed and persistence were calculated (Fig. 3.13). The distance migrated by H_2O_2-treated was significantly increased at 1 mM H_2O_2 (441 ± 52 µm, 127 ± 10.4% of untreated), while the displacement was significantly

increased at 2 mM H_2O_2 (96.1 ± 8.23 µm, 123 ± 8.8 % of untreated). The distance and displacement decreased for high concentrations to 378 ± 49.5 µm (117 ± 13.3% of untreated) and 79.2 ± 12.6 µm (98.8 ± 16.3% of untreated). The migration speed (Fig. 3.13C), which is calculated from the distance and time, ranges from 1.38 ± 0.08 µm/min (0 mM H_2O_2) to a maximum of 1.87 ± 0.17 µm/min (0.5 mM H_2O_2; 136.7 ± 13% of untreated) and decreased for high levels to a minimum of 1.63 ± 0.11 µm/min (2 mM; 119.3 ± 8.1% of untreated). The persistence was calculated as displacement divided by distance, the values lie therefore between 0 and 1; 0 represents circular migration, whereas 1 represents migration in a straight line. The persistence for THP-1 cells migrating on a HUVEC monolayer did not change significantly with H_2O_2 treatment and lay between 0.22 ± 0.01 and 0.28 ± 0.02, indicating that they turn regularly (Fig. 3.13D).

Together these data provide evidence that the observed TEM defect is not due to a general migration defect. On the contrary, the motility of H_2O_2-treated THP-1 cells was significantly increased, as was the distance migrated and the total displacement. The mechanisms involved in cell turning were not influenced by H_2O_2, as seen from the unchanged persistence.

It is worth noting that all adhesion and motility effects were highest for intermediate H_2O_2 concentrations unlike TEM itself which shows strongest effects for high H_2O_2 concentrations. This will be further discussed in Chapter 4.

3.9 Data spread for TEM and adhesion assays

To illustrate the actual percentage of leukocytes transmigrating or adhering to substrate and the endothelium, Box-and-Whisker plots were constructed for untreated THP-1 and CCRF-CEM cells. The Box-and-Whisker plot for THP-1 cells illustrates, that transmigration was more efficient in the TLM-based TEM assay, but with higher variability than the Transwell™-based system (Fig. 3.14A). All adhesion assays had high variability; the adhesion to VCAM-1 was highest, intermediate to HUVECs and lowest to ICAM-1. CCRF-CEM cells had comparable levels of TEM for TLM- and Transwell™-based TEM assays, but variability was higher for the Transwell™-based assay (Fig. 3.14B). Adhesion was low compared to THP-1 cells for substrates, as well as adhesion to HUVECs. Levels of adhesion were similar for VCAM-1 and HUVECs, whereas adhesion to ICAM-1 was low. The variability was lower for CCRF-CEM cells, compared to THP-1 cells.

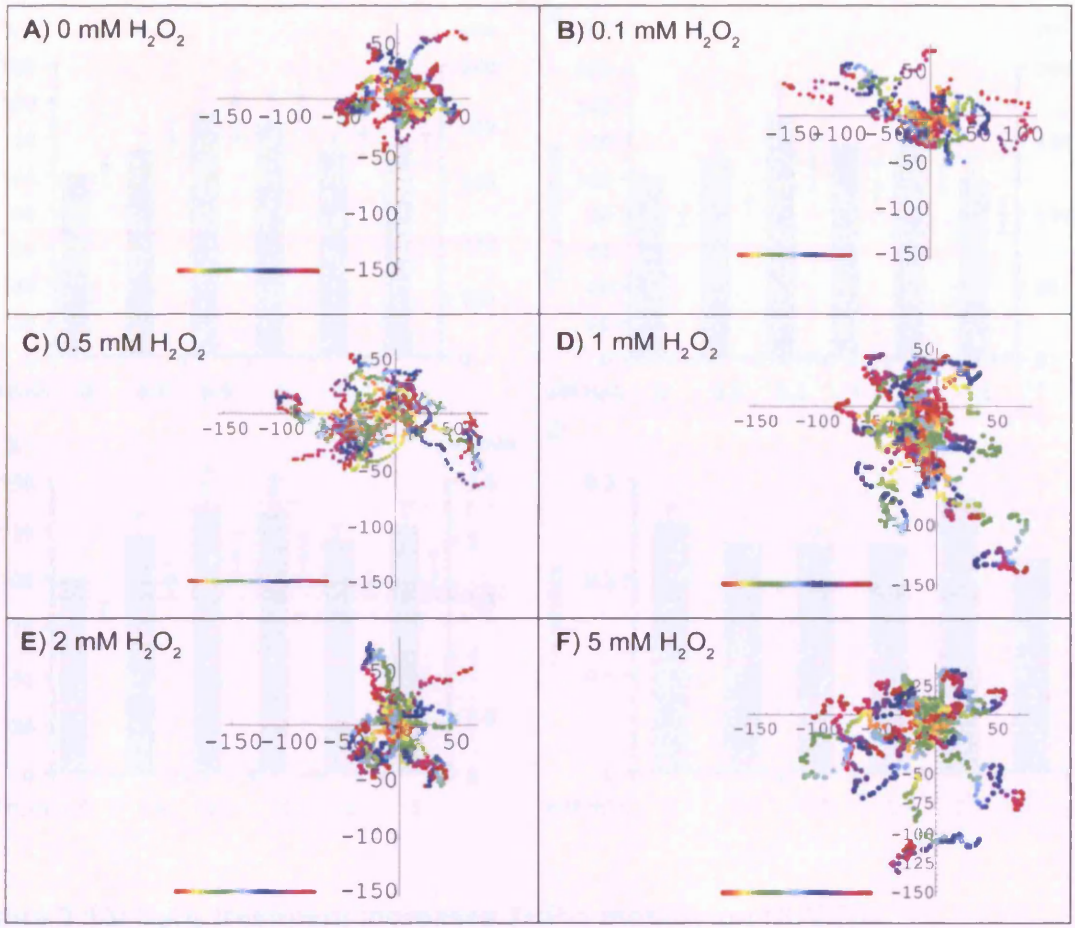

Figure 3.12: Analysis of THP-1 cell migration on HUVECs
THP-1 cells were treated with 0 – 5 mM H_2O_2 (30 min, 37°C), added to TNF-α-activated (10 ng/ml, 15 - 18 h) HUVECs and monitored using time-lapse microscopy (1 frame/min) for 2 h. 15 randomly chosen THP-1 cells per movie were tracked with Motion Analysis software (Andor Biotechnology) and tracks were analysed using a Mathematica notebook written by Dr D. Zicha. **A – F**: Representative migration tracks for treated and untreated THP-1 cells are shown as vector plots with tracks beginning at the origin of a Cartesian coordinate system. The migration tracks are colour coded to indicate the progression during the movie.

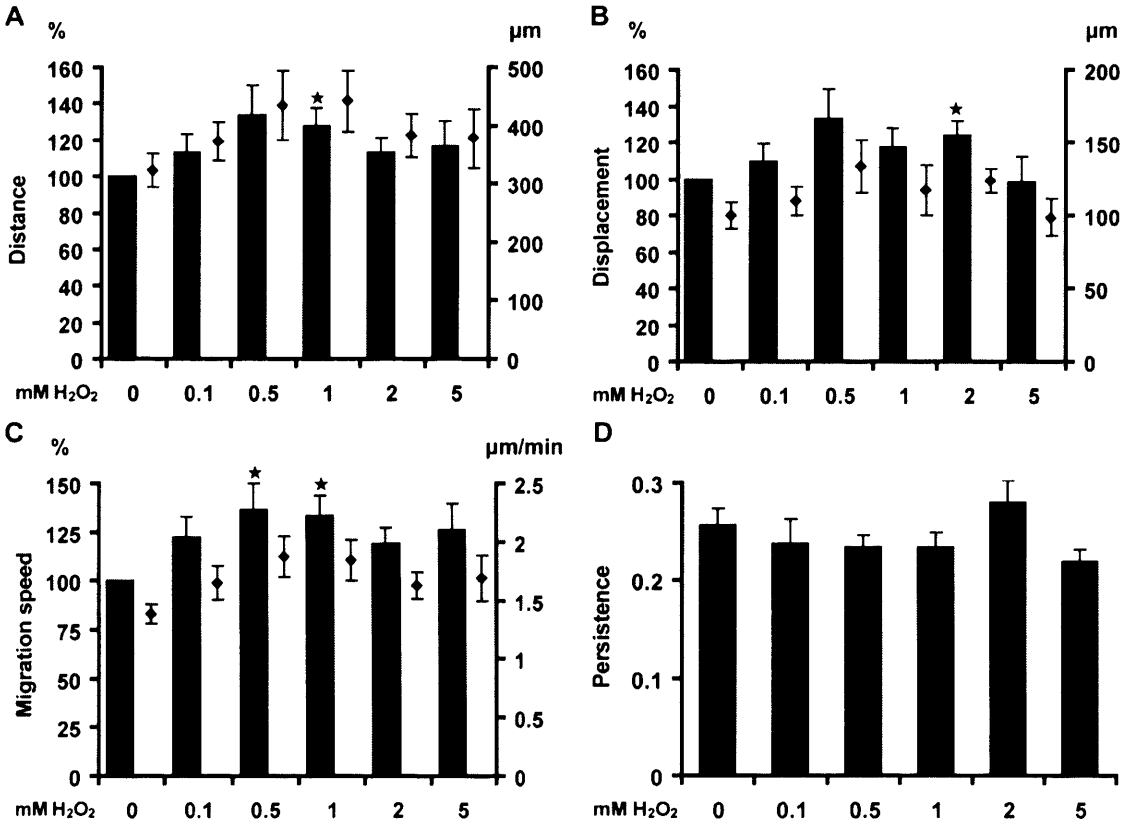

Figure 3.13: H_2O_2 treatment increases THP-1 motility on HUVECs
Histograms with two y-axes are shown, the black bars represent 'percentage of untreated' (left axis), while the diamonds represent µm or µm/min (right axis). Distance migrated (length of track) and the total displacement (direct distance from start to endpoint) was determined from the migration tracks of H_2O_2-treated THP-1 cells on TNF-α-activated (10 ng/ml, 15 - 18 h) HUVECs (**A, B**). The migration speed (**C**) and the persistence (**D**) were calculated from these measurements. The persistence is defined as the displacement/distance; it is 0 for migration in a complete circle and 1 for migration in a straight line. n = 7 with 15 cells/experiment. Results are normalised to untreated control. Bars represent SEM. ⋆ $p < 0.05$ determined by Student's t-test and Bonferroni post-test, as compared to untreated control.

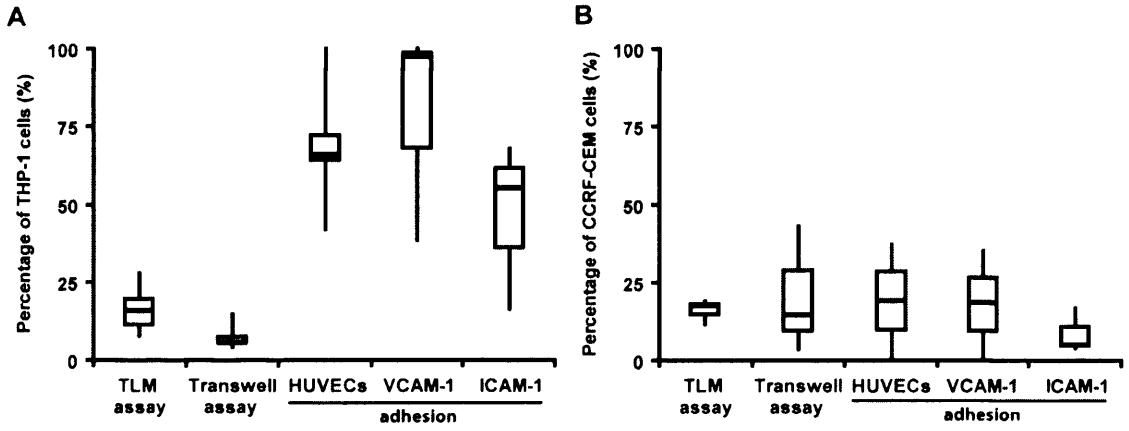

Figure 3.14: Data spread for TEM and adhesion in THP-1 and CCRF-CEM cells
The box-and-whisker plots illustrate the data range for untreated THP-1 (**A**) and CCRF-CEM cells (**B**) in TEM and adhesion experiments as percentage of input. The horizontal bar indicates the median, the box indicates the upper and lower quartile, and the vertical bars the largest and smallest observation. $n \geq 4$.

3.10 THP-1 cell morphology on substrate is not altered

To understand the effect of H_2O_2 on leukocytes, the morphology of treated THP-1 cells was assessed. To this end, THP-1 cells were incubated with varying H_2O_2 concentrations, allowed to adhere to VCAM-1 coated coverslips and stained for F-actin and tubulin (Fig. 3.15). Most THP-1 cells did not exhibit a very polarised phenotype with a clear lamellipodium and uropod. This morphology seems to be typical for THP-1 cells, as it was also observed in the time-lapse movies of untreated THP-1 cells. The immunofluorescence images did not reveal a clear trend, although differences in the actin cytoskeleton and microtubule network could be observed. All samples had cells with actin accumulations at multiple sites around the cell, which are likely to be the dynamic protrusions that were observed in the time-lapse movies. Samples treated with 1 – 2 mM H_2O_2 seemed to have ruffles around the cells, which were less frequent in other samples. The microtubule network appeared to be denser and less organised in the cells treated with 5 mM H_2O_2.

This data indicates that the overall actin organisation is not influenced by H_2O_2, whereas the microtubule network is.

3.11 H_2O_2 treatment might lead to a decrease in THP-1 cellular protrusions

During TEM leukocytes extend cellular protrusions to probe the endothelium for suitable sites of diapedesis (see Fig. 3.3). These exploratory protrusions can be retracted or developed into lamellae which allow the cells to transmigrate. These protrusions are therefore important structures and impairment of their development could lead to a decrease in TEM. During the process of protrusion extension and lamella development, LFA-1 plays a prominent role. Therefore, H_2O_2-treated and CellTracker-stained THP-1 cells were allowed to transmigrate across a HUVEC monolayer, before the cells were fixed and stained for LFA-1 and F-actin. The immunofluorescence images show LFA-1 localisation in the cell protrusions underneath the HUVECs as well as in the cell body above the endothelium (Fig. 3.16). White arrows indicate areas of ring-like LFA-1 clusters at the leukocyte-endothelial interface. More of these accumulations could be detected with increasing H_2O_2 concentration. The LFA-1 staining as well as the CellTracker™ dye labelling possibly suggests a decrease in the number of cells with protrusions (red arrowheads) with increasing H_2O_2 concentration. Quantification of the number of cells with protrusions should be carried out to confirm these preliminary observations.

This potential decrease in cellular protrusions could to play a crucial role in the decrease of leukocyte TEM after H_2O_2 treatment.

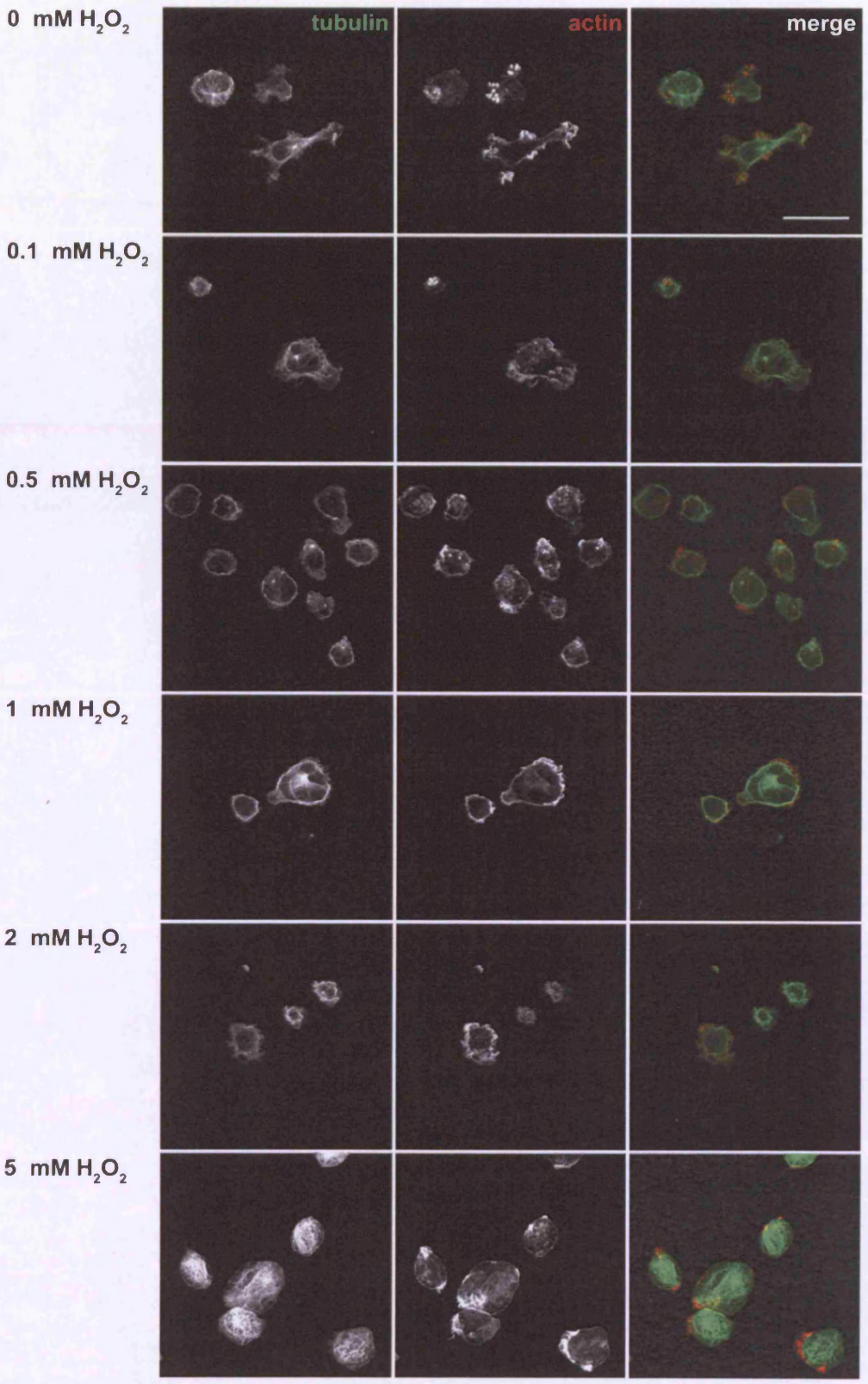

Figure 3.15: The actin cytoskeleton is not altered by H_2O_2
THP-1 cells were treated with 0 – 5 mM H_2O_2 (30 min, 37°C). H_2O_2 was removed and cells were allowed to adhere to VCAM-1-coated coverslips. After 60 min, cells were fixed and stained for F-actin and tubulin. Bar = 20 µm.

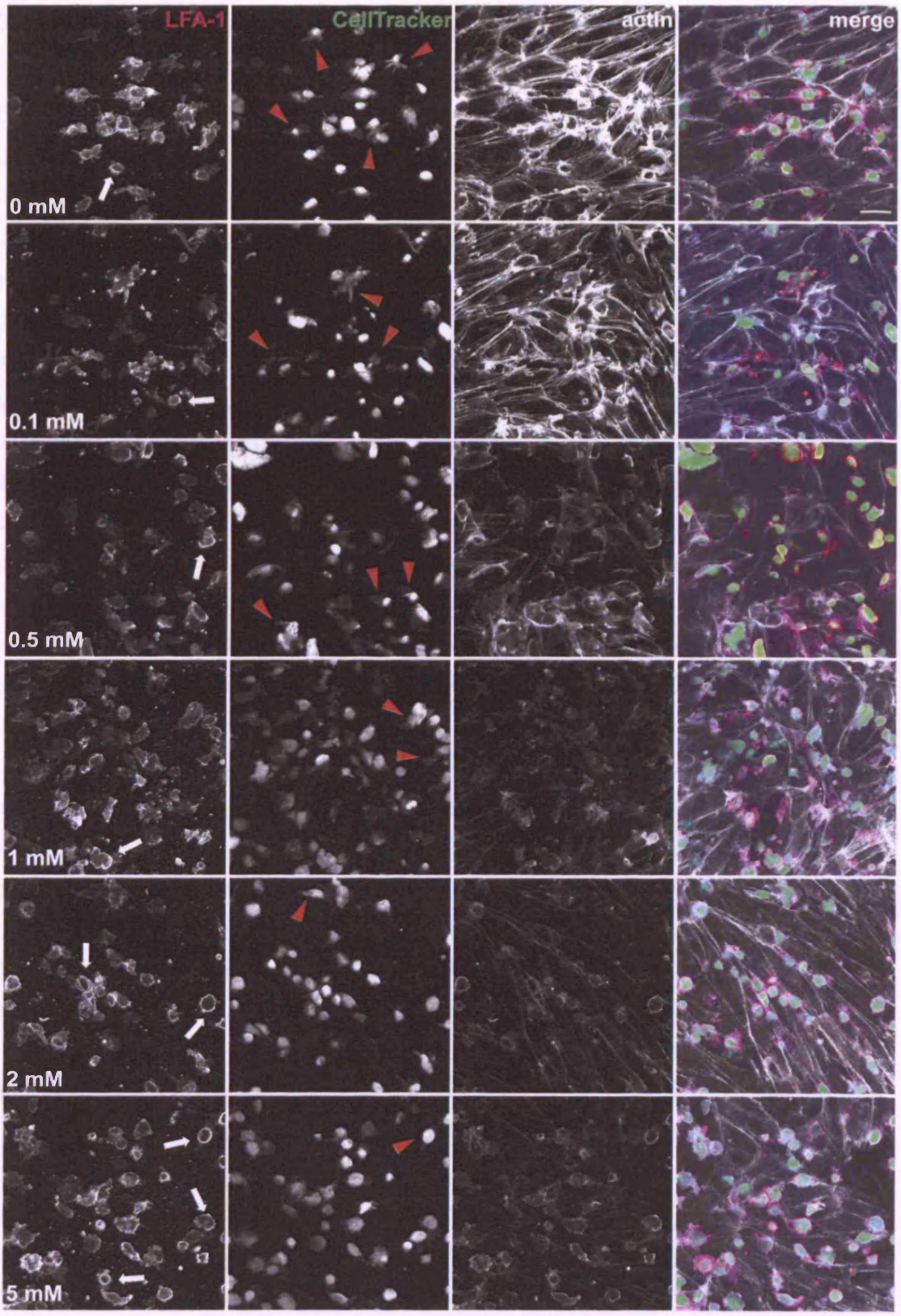

Figure 3.16: LFA-1 staining of H_2O_2-treated THP-1 cells on HUVECs
THP-1 cells were labelled with green CellTracker™ dye (1 µM, 30 min, 37°C), treated with 0 – 5 mM H_2O_2 (30 min, 37°C) and added to TNF-α-activated (10 ng/ml, 15 - 18 h) HUVECs for 25 min before cells were fixed and stained for LFA-1 and F-actin. White arrows indicate LFA-1 accumulation, red arrowheads indicate cells with protrusions. Bar = 20 µm.

3.12 HUVEC monolayer permeability is increased when H_2O_2-treated THP-1 cells are bound

Endothelial cell-cell junctions need to be disrupted when leukocytes transmigrate using the paracellular route. THP-1 cells exclusively use the paracellular pathway (see Chapter 3.2.3); endothelial junction remodelling therefore is a critical event during TEM. If the ability to induce reversible opening of adherens junctions in endothelial monolayers was impaired in H_2O_2-treated THP-1 cells, the resulting transmigration rate would be decreased. To test if bound H_2O_2-treated THP-1 cells are able to induce a reversible reorganisation of endothelial junctional structures, VE-cadherin and F-actin staining of transmigrating THP-1 cells was carried out. In a co-culture with untreated THP-1 cells, VE-cadherin was localised in reticular (red arrowheads) as well as non-reticular junctions (Fig. 3.17A). Reticular junctions have been described as PECAM-1-bearing membranes that can serve as a recycling compartment (Mamdouh et al., 2003). The arrows indicate sites of transmigration where VE-cadherin is reorganised. Non-quantitative analysis of the immunofluorescence images showed few gaps between ECs (white arrow heads) with untreated THP-1 cells. For H_2O_2 concentrations of 0.5 and 1 mM a decrease in the width of the junctions, hence fewer reticular junctions, might be observed (Fig. 3.17D, G). Concurrently, the number of gaps between cells at sites without transmigrating cells appears to be increased. For 5 mM H_2O_2 the portion of reticular junctions was possibly increased, but at sites of non-reticular junctions more gaps between ECs appeared to open (Fig. 3.17J). The F-actin staining also showed this potential increase in gaps for HUVEC monolayers with H_2O_2-treated THP-1 cells (Fig. 3.17B, E, H, K; white arrow heads). H_2O_2-treated THP-1 cells also seemed to induce an increase in the formation of actin stress fibres in HUVECs.

These data possibly suggest a differential influence of H_2O_2-treated and untreated THP-1 cells on endothelial junction remodelling after leukocyte binding. However, this potential regulation is usually thought to support TEM and is therefore controversial to the observed decrease in TEM. Further investigations, including the role of reticular junction in TEM, the quantification of number of gaps and proportion of reticular to non-reticular junctions, are needed to confirm these preliminary results an to draw conclusions about their impact on THP-1 cell TEM.

To further investigate the influence of H_2O_2-treated THP-1 cells on HUVEC remodelling after leukocyte binding, a permeability assay was carried out. This assay measures paracellular integrity by applying fluorescently labelled dextran to the upper chamber of Transwells™ coated with a HUVEC monolayer. Samples from

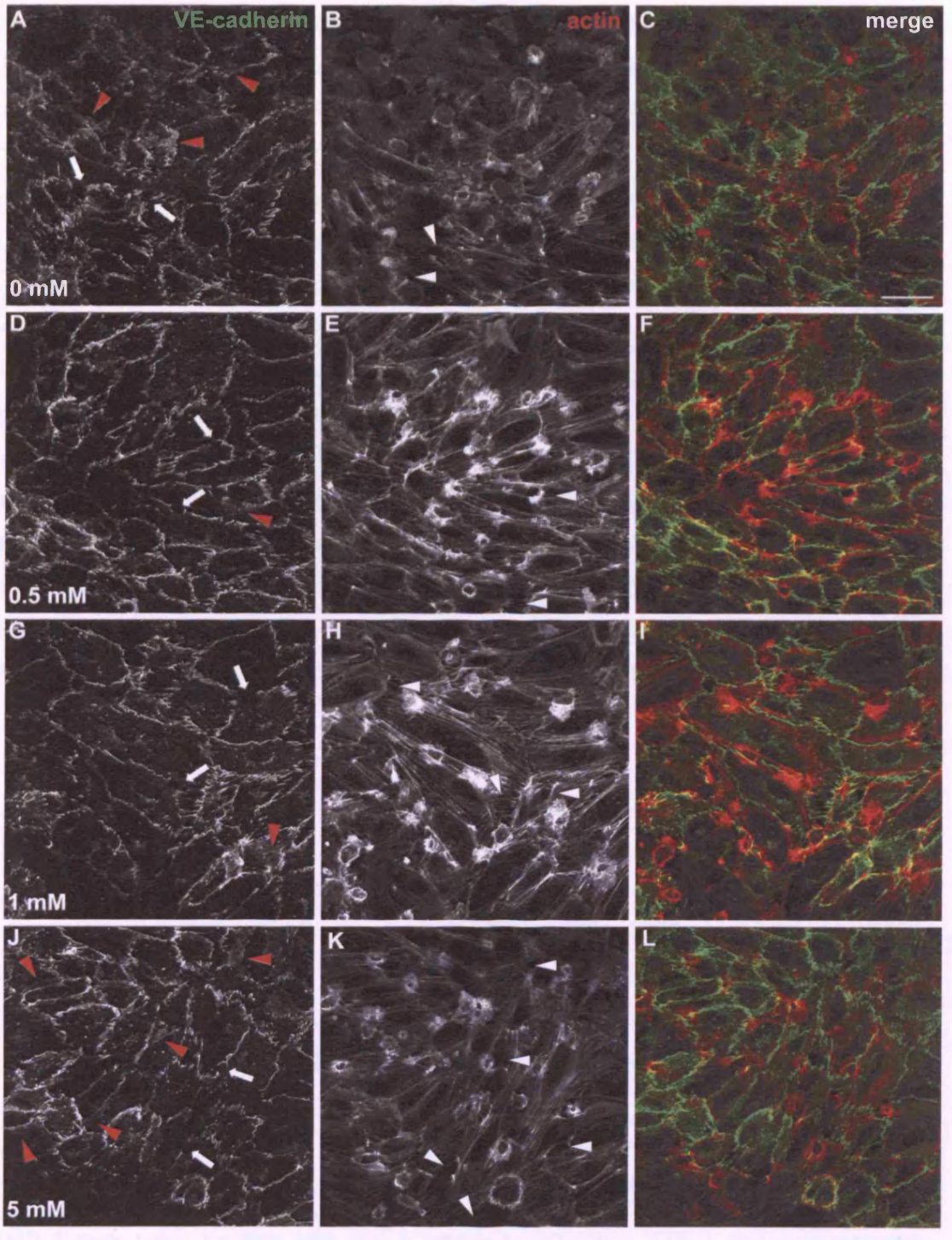

Figure 3.17: Modulation of endothelial adherens junctions after adhesion of H_2O_2-treated THP-1 cells

THP-1 cells were treated with 0 – 5 mM H_2O_2 (30 min, 37°C) and allowed to transmigrate across TNF-α-activated (10 ng/ml, 15 - 18 h) HUVECs. Cells were fixed and stained for VE-cadherin and F-actin. White arrows indicate VE-cadherin reorganisation at sites of THP-1 transmigration; red arrow heads indicate reticular junctions; white arrow heads indicate intercellular gaps. Bar = 40 µm.

the lower chamber were taken and measured for fluorescence after 40 and 80 min (Fig. 3.18). The assay was carried out with either H_2O_2-treated or untreated THP-1 cells and HUVECs alone as a negative control. Untreated THP-1 cells were able to increase the permeability by 28.1 ± 23.2% (40 min). H_2O_2-treated THP-1 cells increased the permeability even further, by a maximum of 154 ± 40.8% (1 mM H_2O_2; 40 min). The increase in endothelial permeability with THP-1 cells treated with 1 mM H_2O_2 was statistically significant, when compared to untreated THP-1 cells (40 min).

Together these results demonstrate that H_2O_2-treated THP-1 cells are capable of inducing adherens junction remodelling. In fact they induce stronger actin remodelling then untreated THP-1 cells, as becomes apparent from the increased number of gaps between neighbouring ECs. This was confirmed by the permeability assay, which demonstrated a significant increase in permeability between untreated and H_2O_2-treated THP-1 cells bound to the endothelium. This indicates that the decrease in TEM is not due to an inability of H_2O_2-treated THP-1 cells to remodel the adherens junctions and the endothelial actin cytoskeleton.

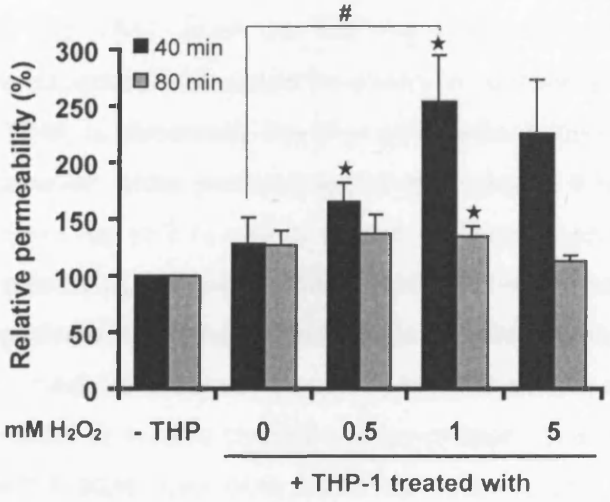

Figure 3.18: Endothelial permeability is significantly increased when H_2O_2-treated THP-1 cells are bound
THP-1 cells were treated with 0 – 5 mM H_2O_2 (30 min, 37°C) and then added to TNF-α-activated (10 ng/ml, 15 - 18 h) HUVECs grown on Transwell™ filters. To determine monolayer permeability, 100 µg/ml FITC-dextran was added to the upper chamber and samples of media from the lower chamber were measured for fluorescence using a Fusion™ α-FP plate reader after 40 and 80 min. HUVECs without THP-1 cells were used as a control and samples were normalised to this. Significance was determined against samples without THP-1 cells unless otherwise indicated.
Results are normalised to untreated control. Bars represent SEM. n = 5. ⋆ $p < 0.05$ determined by Student's t-test and Bonferroni post-test, as compared to '- THP-1' sample. # $p < 0.05$ determined by two-way ANOVA and Bonferroni post-test.

3.13 Discussion

In this chapter, the experimental conditions for two *in vitro* TEM assays were set-up and used to assess the effects of H_2O_2 on leukocyte TEM. Adhesion, motility and integrin surface levels and activity of H_2O_2-treated cells were determined in the appropriate assays. Additionally, the morphology of H_2O_2-stimulated leukocytes their influence on endothelial actin reorganisation and monolayer permeability were also investigated.

All leukocytes tested, except MM6 cells, showed a trend of decreased TEM with increasing H_2O_2 level, but only the results for the cell lines THP-1 and CCRF-CEM were statistically significant. Primary cells displayed a higher variability in TEM rates, which makes it much harder to reach statistical significance, unless sample size is high. MM6 cells were non-transmigratory under the experimental settings used, although they have been reported to transmigrate by other groups (Weber et al., 1998), which may reflect experimental differences or differences in the cell line itself, which can occur with increasing length of culture. ROS have been shown to have multiple targets and effects (Droge, 2002). H_2O_2 could inhibit leukocyte TEM by direct modification of cell surface proteins or by inducing/inhibiting signalling pathways important for TEM, such as the regulation of actin dynamics (see Chapter 4). In future experiments it would be useful to perform a time course for the effects of H_2O_2 on TEM, to determine the time point where the maximum response can be reached. However, when performing this time course it has to be taken into account, that short-term (up to 2 h) and long-term treatment can have very different effects. While the effects of short-term treatment are more likely to involve early responses such as direct oxidative modification of molecules, e.g. inhibition of phosphatases and subsequent increase in phosphorylation, the effects of long-term treatment are more likely to involve changes in expression level as well as oxidative modifications. Since this study was more interested in short-term effects a time point of 30 min was chosen, that was sufficiently long to allow the development of those early responses. An additional limitation to the approach taken is to look at one time point of TEM only. For future experiments it could be interesting to look at longer time points to see if the H_2O_2-treated THP-1 cells eventually transmigrate and only display a delay or if the decrease in TEM is irrevocable.

Different leukocytes displayed varying susceptibility to the oxidative damage caused by H_2O_2. The leukaemia cell lines THP-1 and CCRF-CEM showed low susceptibility, whereas the primary cells were damaged at lower H_2O_2 concentrations. It remains to be determined if these discrepancies are due to cell

type differences or arise from the fact that the less sensitive cells are leukaemia cell lines. Cancer cells have been shown to have increased ROS production, but also display upregulation of antioxidant enzymes such as Catalase, MnSOD and CuZnSOD (Chowdhury et al., 2007; Kattan et al., 2008; Trachootham et al., 2006). Cancer cells, including the leukaemia cell lines tested here, might therefore be better prepared to deal with exogenous H_2O_2 than non-cancerous cells.

Previous studies have shown that in THP-1 cells, overexpression of UCP2, a protein belonging to the mitochondrial anion carrier family, reduces the steady state level of intracellular ROS (Ryu et al., 2004). Overexpression reduced β2 integrin-mediated firm adhesion and TEM across human aortic endothelial cells (HAEC). These TEM results are inconsistent with the H_2O_2-dependent decrease in leukocyte TEM observed in the present study. These apparent differences could be due to differences in the EC type, but more importantly, overexpression of UCP2 might induce changes in addition to the reported changes in ROS level that influence adhesion and TEM. If a decrease in intracellular ROS indeed decreases adhesion and TEM (Ryu et al., 2004), it would be predicted that the application of H_2O_2 would lead to increased adhesion and TEM. The former is true for H_2O_2-treated THP-1 as well as CCRF-CEM cells; but the latter was reduced. This could be due to the interdependency of adhesion and diapedesis. While adhesion is independent of TEM, diapedesis depends on successful adhesion. It is therefore inevitable that defects in adhesion will ultimately lead to a diapedesis defect. The reverse conclusion that H_2O_2 should lead to an increase in adhesion and a decrease in diapedesis is therefore not necessarily tenable.

The findings from Ryu et al. (2004) are mainly interpreted as being dependent on the decrease in β2 integrin levels caused by the reduced intracellular ROS level. It has been shown for PMNs that ROS lead to an upregulation of CD18 (β2 integrin) and CD11b within 15 min (Fraticelli et al., 1996). The upregulation is accompanied by shedding of L-selectin from the surface and 0.1 mM H_2O_2 is sufficient to exert the effects. This is contrary to findings of the present study, where β2 and β1 integrin surface levels were unchanged after H_2O_2 treatment. Since the upregulation of surface integrins reported by Fraticelli et al. occurs within 15 min it is probable that increased delivery of integrin-containing vesicles is responsible for this effect, rather than upregulation of gene expression. FACS analysis in the present study has shown that in THP-1 cells, β1 and β2 integrin levels are high compared to CCRF-CEM. This could indicate that a high proportion of the total pool of integrin molecules is located at the plasma membrane and therefore H_2O_2-induced delivery

of vesicles would not lead to an increase in integrin level. The reported upregulation of integrin gene expression (Ryu et al., 2004) has not been detected by the FACS analysis at the timepoints tested here. It would therefore be interesting to look at the integrin levels at later time points, e.g. 6 h after H_2O_2 treatment.

In control cells, β1 and β2 integrins were mainly inactive. The activity of β2 integrin showed some variability with H_2O_2 treatment, while β1 activity remained unchanged. Other integrins would need to be investigated to determine changes in surface levels and activation, since small changes in multiple integrins could lead to the observed changes in adhesion. Activation of VLA-4 has been shown to be directly dependent on redox modification of the α4 subunit (Liu et al., 2008). Ligand binding of VLA-4 induces exposure of a thiol group and subsequent S-glutathionylation in the presence of H_2O_2 and GSH, which plays a role in integrin activation.

Interestingly, only adhesion to the endothelium was increased, whereas no change could be observed for adhesion to VCAM-1 or ICAM-1. These data indicate that the endothelium provides particular conditions that can be utilised by H_2O_2-treated cells to strengthen their adhesion, which are not present on substrate. These could include clustering of ICAM-1 and VCAM-1 on the endothelial surface and/or chemokine presentation. How H_2O_2-treated leukocytes increase their adhesion remains to be determined, but chemokine signalling leading to integrin activation could play a role. The activation status of leukocyte integrins could thus be changed in H_2O_2-treated cells only when bound to the endothelium, but not in suspension as was tested in this study.

The signalling events involved in mediating leukocyte adhesion have been extensively studied. The H_2O_2-mediated increase in adhesion could be dependent on the activation of the FAK family member Pyk2, which has been shown to be activated by ROS (Frank et al., 2000). The signalling involved in the H_2O_2-mediated TEM defect in THP-1 cells will be discussed in Chapter 4.

To determine if the TEM defect in H_2O_2-treated THP-1 and CCRF-CEM cells was due to the compromised ability to deform the cell, e.g. by remodelling the actin cytoskeleton, a Transwell™-based TEM assay without HUVECs was carried out. The results demonstrate that the ability of cells to deform in order to transmigrate through confined spaces was not compromised. In addition, the actin cytoskeleton of H_2O_2-treated THP-1 cells on VCAM-1 did not appear to be changed. However, further investigations, including quantifications of actin structures are needed to draw firm conclusions about any changes to the actin cytoskeleton. Findings by

others have suggested a role of ROS in a variety of actin-based mechanisms in various cell types. For example Perez et al. proposed a role for ROS in the induction of actin-cytoskeletal rearrangements and tight-junction impairment in rat hepatocytes in a PKC-mediated and Ca^{2+}-dependent mechanism (Perez et al., 2006). It is worth mentioning that hepatocytes are slow moving cells, whereas leukocytes are fast moving, which might require a different regulation of the actin cytoskeleton. In ECs, H_2O_2 induces formation of focal adhesion complexes and a major reorganisation of the actin cytoskeleton, causing the disappearance of membrane ruffles with disruption of cortical actin filaments and formation of a dense transcytoplasmatic stress fibre network (Huot et al., 1998). Since THP-1 cells are not very spread, displaying only cortical F-actin and do not form obvious ruffles actin changes are more difficult to detect. Investigating the distribution of actin-regulating proteins in H_2O_2-treated THP-1 cells could allow us to analyse further whether H_2O_2 regulates the actin cytoskeleton in THP-1 cells.

Although no obvious difference in the actin cytoskeleton was detectable in cells adherent to ICAM-1 and VCAM-1, the increased motility of THP-1 cells on endothelium at intermediate H_2O_2 concentrations suggests H_2O_2-induced changes in actin dynamics. The role of H_2O_2 in regulating actin cytoskeletal dynamics and cellular motility has been the subject of many studies. ROS can affect the activity of signalling pathways by direct modification of regulatory proteins via disulphide bond formation, nitrosylation, carbonylation or glutathionylation (England and Cotter, 2005). Actin can also undergo direct redox regulation by glutathionylation of Cys^{374} during integrin-mediated cell adhesion in NIH-3T3 fibroblasts (Fiaschi et al., 2006). The impairment of this redox modification leads to the inability of cells to spread and organise the cytoskeleton in response to ECM and the inhibition of the disassembly of the actomyosin complex. These findings suggest that this redox modification is a key step in the dynamic contraction of the actin cytoskeleton during cell spreading. Moldovan et al. showed that migrating ECs produce ROS, which contribute to the actin cytoskeletal reorganisation required for migration (Moldovan et al., 2000). Their results suggest that ROS induce the uncovering of new barbed ends, thereby increasing the actin polymerisation rate. The positive regulation of cell motility observed in the present study is therefore in accordance with findings from other groups, although the exact mechanisms involved in THP-1 cells remain to be determined.

Cell migration also involves reorganisation of the microtubule network (Watanabe et al., 2005). During leukocyte TEM the relatively rigid microtubules are

retracted into the uropod to increase the deformability of the cells and to facilitate their migration through confined spaces (Ratner et al., 1997). Preliminary and non-quantitative data suggest that microtubules are altered in H_2O_2-treated THP-1 cells on VCAM-1. Not much is known about the effects of ROS on the microtubule network and most studies have been carried out in porcine brain. There, tubulin has been shown to be oxidised by peroxynitrite, leading to a dose-dependent inhibition of microtubule polymerisation (Landino et al., 2002). Cysteine oxidation of Tau and microtubule-associated protein-2 (MAP-2), two neuron-specific MAPs, has been reported in response to peroxynitrite and H_2O_2 (Landino et al., 2004). This cysteine oxidation prevents the assembly of microtubules in porcine brain extracts. These results are contrary to findings in the present study, where there appear to be more microtubules after H_2O_2 treatment. The differences could be attributed to the different cells types used, as it is known that the effects of ROS can depend on the cell type (Droge, 2002). Rho GTPases have been implicated in the regulation of microtubule dynamics during cell migration (Watanabe et al., 2005). If and how Rho GTPases are affected by H_2O_2 treatment in THP-1 cells will be determined in the next chapter. Quantification of the immunofluorescence images should reveal if H_2O_2 induces a change in the microtubule network. How the observed changes in microtubule network integrate into the H_2O_2-induced TEM defect remains to be determined.

It appears that H_2O_2 has multiple effects on THP-1 cells, regulating cell motility, adhesion and TEM. The interdependency of these events and the sensitive regulatory mechanisms make TEM a highly adaptable process, but also renders it susceptible to environmental influences such as exogenous H_2O_2.

It is noticeable that changes in adhesion and migration speed follow the same pattern, both display a peak at intermediate H_2O_2 concentration followed by a decrease to approximate control levels at high H_2O_2 concentrations. The interdependency of migration speed and adhesion strength has been well studied. DiMilla et al. proposed a mathematical model which predicted that migration speed would exhibit a biphasic response to increasing adhesion strength (DiMilla et al., 1991). This model has since been experimentally confirmed by modulating ECM ligand density, integrin expression levels or integrin-ECM affinity (DiMilla et al., 1993; Huttenlocher et al., 1996; Palecek et al., 1997). The increased migration speed observed in the present study could therefore be a result of the increased adhesion to the endothelium, optimising the conditions for a higher migration velocity.

The increased cell motility at intermediate H_2O_2 concentrations did not affect the migration persistence, i.e. the turning frequency of the cells, leading to greater displacement from the migration origin. The unchanged persistence indicates that the regulatory mechanisms involved in cellular turning are not affected by H_2O_2 treatment. The increased migration speed might contribute to the TEM defect, by preventing the probing of the endothelium for suitable sites of diapedesis. This process might be less efficient when cells migrate faster, leading to a decrease in TEM. The leukocytes probably have to slow down or arrest to extend the exploratory protrusions which are necessary for TEM. However, migration was only significantly increased at intermediate H_2O_2 concentrations, while TEM was significantly decreased at concentrations ≥ 0.1 mM, indicating that other regulatory mechanisms are playing a role.

The importance of cellular protrusions for TEM was further investigated. Preliminary and non-quantitative date suggests a dose-dependent decrease in cellular protrusion in H_2O_2-treated leukocytes when bound to HUVECs. Migrating THP-1 cells do not normally exhibit typical lamellipodia or filopodia, which complicates the characterisation of cellular protrusions. Cellular protrusions are essential for cell motility and are particular important during TEM where filopodia have an exploratory function (Barreiro et al., 2007). During transcellular TEM, podosomes play an important role in forming the transcellular pore (Carman et al., 2007; Millan et al., 2006). The potential decrease in protrusions could play a crucial role in the H_2O_2-mediated TEM defect. Additionally, it might also contribute to the increase in migration speed. Although cellular protrusions, in particular the lamellipodium, are essential structures for migration, extensive protrusive activity might decrease migration velocity. This could be particularly true for exploratory protrusions that probe the endothelium for suitable sites of TEM. The potential decrease in protrusion formation will be further investigated in the next Chapter 4.

Preliminary and non-quantitative data suggest that binding of H_2O_2-treated THP-1 cells leads to alterations in the junctions of HUVECs. Reticular junctions appeared to increase with binding of H_2O_2-treated THP-1 cells. Reticular junctions, also termed the 'subjunctional reticulum', have been described as PECAM-1-bearing membranes that can serve as a recycling compartment (Mamdouh et al., 2003). Other junctional proteins such as VE-cadherin and CD99 also localise to these structures. The role of these structures is unclear, but they have been suggested to play a role in endothelial barrier function (Millan et al. unpublished). This potential increase in reticular structures in HUVECs with H_2O_2-treated THP-1

cells bound could therefore increase the endothelial barrier function and decrease TEM. However, preliminary and non-quantitative data suggest that HUVECs with H_2O_2-treated THP-1 cells also display more intercellular gaps. This could indicate that two different, H_2O_2-induced, mechanisms are acting on the HUVECs, one to induce the formation of reticular structures and another to induce retraction of the ECs, leading to intercellular gaps. The exact mechanism of how these two responses are induced remains to be determined.

ROS are known to induce a variety of biological responses (Droge, 2002; Veal et al., 2007). However, the responses are not only dependent on the type of ROS, but also the concentration. There are various examples, where differences in concentration can lead to different and sometimes opposing effects: while H_2O_2 concentrations of up to 0.4 mM increase protein degradation, 1 mM H_2O_2 inhibits this process (Grune et al., 1997). Small amounts of damage, e.g. one or two oxidised amino acids, increase the proteolytic susceptibility, while damage further than an optimal degree (which is different for each protein) will lead to a decrease in protein degradation. Also, Sablina et al. have shown that while mild oxidative stress leads to p53-induced upregulation of several genes with antioxidant properties (e.g. SESN1 and SESN2, both encoding sestrins, and GPX1, encoding glutathione peroxidase 1), high levels of ROS induce upregulation of genes with pro-oxidant effects (e.g. TP53I3, encoding a quinine oxidoreductase homologue, or BBC3, encoding PUMA) (Sablina et al., 2005). In the latter study, H_2O_2 concentrations of up to 0.4 mM are considered mild oxidative stress, while 1 mM H_2O_2 is considered a high level. In cells, low micromolar concentrations (up to 10 µM) of ROS have been measured under physiological conditions (Deem and Cook-Mills, 2004; Nathan and Root, 1977). The exposure of cells to high micromolar and particularly millimolar concentrations of H_2O_2 are therefore unlikely to be physiological, but can prove useful to provoke a response. However, high H_2O_2 concentrations (1 – 5 mM) in this study might give rise to not only multiple, but also potentially opposite effects. Examples would be the potential induction of more gaps in the endothelial monolayer, while TEM is decreased.

H_2O_2-treated THP-1 cells bound to HUVECs not only seemed to induce more junctional gaps but also a higher increase in permeability than untreated THP-1 cells. Leukocyte binding has been shown to induce stress fibre formation in ECs (Millan and Ridley, 2004), and is often accompanied by an increase in endothelial permeability (Wedmore and Williams, 1981). The leukocyte-induced stress fibre formation is induced via a RhoA/ROCK and Ca^{2+}-dependent MLCK-induced

phosphorylation of MLC, and is important for leukocyte TEM (Adamson et al., 1999; Hixenbaugh et al., 1997; Huang et al., 1993; Wojciak-Stothard et al., 1999); (Millan et al., 2006). This pathway is activated by binding of leukocytes to ICAM-1 and VCAM-1 on the endothelial surface (Adamson et al., 1999; Thompson et al., 2002; Wojciak-Stothard et al., 1999), possibly via the involvement of ERM proteins (Barreiro et al., 2002; Bretscher et al., 2002). Clustering of VCAM-1 has also been shown to induce disruption of adherens junctions through Rac1 activation and subsequent ROS generation (Cook-Mills, 2002; van Buul and Hordijk, 2004), which has been reported to be necessary for TEM (Matheny et al., 2000; van Buul et al., 2002). The concerted activation of RhoA and Rac1 in response to leukocyte engagement of ICAM-1 and VCAM-1, leading to actomyosin contractility and disruption of endothelial junctions, is therefore thought to facilitate leukocyte TEM. These events also seem to occur, and are probably even more pronounced, after binding of H_2O_2-treated THP-1 cells, but do not enhance THP-1 TEM. This emphasises the strength of the effects of H_2O_2 on THP-1 cells. The potential increase in stress fibres and intercellular gaps in the endothelium might arise due to the increased adhesion and migration on the endothelial surface, leading to increased ICAM-1 and VCAM-1 interactions and subsequent RhoA and Rac1 activation in the endothelium. Inadvertent carryover of small amount of H_2O_2 could also lead to the increase in stress fibres and intercellular gaps, as ROS have been shown to induce cytoskeletal rearrangements in ECs (Matheny et al., 2000).

Future experiments that lie outside of the time-frame of this study should use alternative approaches to investigate the role of ROS in leukocyte TEM. In particular, other ways to deliver and increase ROS in cells should be explored. These approaches could include the use of different ROS species and ROS delivery systems, e.g. the xanthine oxidase/hypoxanthine system. Xanthine oxidase uses hypoxanthine as substrate to produce O_2^-, which subsequently becomes converted to H_2O_2 and OH^- and $^{\bullet}OH$ (Sato et al., 2008). Additionally, H_2O_2 could be administered together with glucose oxidase. This approach allows the establishment of a steady-state level of H_2O_2, since glucose oxidase compensates for the H_2O_2 loss by oxidising O_2 to H_2O_2 (Antunes et al., 2001). Intracellular ROS could also be increased by knocking-down UCP2 using siRNA. Also, the transmigration behaviour of cells that have inhibited intracellular ROS production, e.g. the use of THP-1 cells transfected with siRNA against components of the NADPH oxidase (e.g. $gp91^{phox}$ or $p47^{phox}$), or leukocytes from mice deficient in one these components, in response to H_2O_2 treatment could be studied. Other approaches to inhibit production or

decrease levels of intracellular ROS are the overexpression of UCP2 or ROS-converting enzymes, such as Catalase. The effectiveness of these measures to increase/reduce ROS should be determined by using dyes that specifically measure intracellular ROS (see Chapter 4.6). The use of these alternative approaches should not only allow the confirmation of previous results with H_2O_2, but also elucidate more general aspects of how ROS regulates TEM or distinguish between specific roles of different ROS.

The results from this chapter show that H_2O_2 negatively regulates TEM in different cell types, which is probably due to effects on multiple stages of the TEM process, including adhesion, migration and protrusion formation. To further elucidate the mechanisms involved in H_2O_2-mediated decrease in TEM, the underlying signalling pathways will be assessed in the next chapter.

4

Redox-signalling in leukocyte transendothelial migration

4.1 Introduction

The results from the previous chapter have shown that treating leukocytes with H_2O_2 inhibited TEM. H_2O_2 has been shown to induce a range of signalling processes (see Chapter 1.5.2.2), which could play a role in the observed TEM defect, including protein phosphorylation, activation of MAPK pathways, changes in intracellular Ca^{2+} levels and activation of transcription factors with subsequent transcriptional upregulation of target genes (Droge, 2002). Due to the length of the H_2O_2-treatment (30 min) and the immediacy with which the effects can be seen, it is likely that early signalling responses, involving non-transcriptional modifications, play an important role in mediating the TEM defect. These could include changes in protein phosphorylation, which is known to play a role in a wide range of signalling pathways. ROS have been shown to modify protein phosphorylation in two ways: by activating protein kinases, and by inhibiting protein phosphatases (Rhee et al., 2000). One example of a ROS-regulated process involving inhibition of protein phosphatases is the Rac1-induced downregulation of RhoA: Rac1 induces ROS production via NADPH oxidase, which increases phosphorylation of p190RhoGAP by inhibiting the LMW-PTP, thereby reducing RhoA activity (Nimnual et al., 2003). Rho GTPases have additionally been shown to be ROS-regulated via direct oxidation of cysteine residues (Heo and Campbell, 2005).

Since ROS have been shown to play a role in the development of a variety of diseases, several clinical studies have been carried out involving the administration of antioxidants or ROS scavengers (Mandel et al., 2004; Slemmer et al., 2008). One commonly used antioxidant in clinical studies and basic research is the synthetic cysteine and GSH precursor NAC. NAC has been shown to increase intracellular GSH level and prevent ROS induced signalling (Hashimoto et al., 2001). It was therefore interesting to investigate the effects of antioxidants, specifically NAC, under the experimental conditions set up in Chapter 3.

A common feature of many vascular diseases is not only the contribution of ROS, but also RNS to vascular injury. Signalling pathways involving NADPH oxidase-derived ROS and NOS-derived RNS, in particular NO, have been shown to be linked in several processes, and ROS may participate in NF-κB-dependent upregulation of iNOS (Ginnan et al., 2008; Mendes et al., 2003). NO may play a role in TEM by modulating adhesion molecule expression level. Under basal conditions both nNOS- and eNOS-deficient mice exhibit significantly increased P-selectin expression levels, leukocyte rolling and adhesion, whereas iNOS-deficient mice do not (Lefer et al., 1999). NO constitutively produced by nNOS and eNOS therefore seems to inhibit P-selectin expression. In addition, neutrophil and T cell TEM has been shown to be negatively regulated by NO. Neutrophil TEM is at least partly inhibited by activating soluble guanylate cyclase (sGC) (Oka et al., 2005), while T cell adhesion and migration is reduced due to downregulation of MMP-9 production and β1 integrin expression (Sun et al., 2006).

The aim of this chapter was to investigate the role of NO and H_2O_2-mediated signalling events in the observed TEM defect. In particular the involvement and regulation of Rho GTPases in H_2O_2-treated leukocytes was of interest, since Rho GTPases are key players in the regulation of TEM.

4.2 H_2O_2-induced secretion of anti-inflammatory mediators is not responsible for reduced TEM

Inflammatory mediators such as TNF-α and IL-1β alter endothelial morphology through changes in the actin cytoskeleton and the junctional composition, which leads to decreased barrier function, necessary for efficient TEM. Anti-inflammatory mediators, which increase endothelial barrier function, include nucleotides such as ATP, AMP or adenosine (Yegutkin, 2008), which can be secreted from a range of cells, including leukocytes.

To investigate if H_2O_2-induced secretion of anti-inflammatory mediators was responsible for the observed changes in TEM and adhesion, conditioned medium from H_2O_2-treated THP-1 cells was used in Transwell™-based TEM and adhesion assays. Neither TEM nor adhesion of untreated THP-1 cells were significantly changed by the presence of conditioned media over the duration of the assay (Fig. 4.1A, B), in fact TEM was actually significantly increased at 5 mM H_2O_2.

These results suggest that H_2O_2 did not induce secretion of anti-inflammatory mediators. In fact, conditioned medium from THP-1 cells treated with 5 mM H_2O_2 induced an increase in TEM, indicating that the conditions for TEM are favourable, but defects in the H_2O_2-treated leukocytes are dominant in preventing TEM.

4.3 H_2O_2 has long-term effects on TEM and adhesion to HUVECs

To investigate the characteristics of the H_2O_2-induced TEM defect, long-term effects of transient H_2O_2 treatment on leukocyte TEM and adhesion were investigated. THP-1 cells were incubated for 30 min with H_2O_2 and then allowed to recover for 0, 6 or 12 h. After 6 h of recovery, the dose-dependent TEM defect could still be detected (Fig. 4.2A, grey bars). The maximum decrease was 37.5 ± 12.8% (5 mM), which was smaller than in H_2O_2-treated cells without recovery (Fig. 4.2A, black bars), but the trend was the same. The TEM defect was not abolished until 12 h after treatment (Fig. 4.2A, white bars). At this time-point only 0.5 mM H_2O_2 induced a 20.2 ± 6.7% decrease in TEM.

Adhesion of THP-1 cells that had recovered for 6 h (Fig. 4.2B, grey bars) had an even more pronounced increase with rising H_2O_2 level than unrecovered cells (Fig. 4.2B, black bars). Recovered THP-1 cells also displayed a response with a peack at intermediate concentrations to H_2O_2, with highest adhesion at 0.1 mM (133 ± 16.8% of untreated). After 12 h of recovery the peak at intermediate concentrations was no longer present; 0.1, 1 and 5 mM H_2O_2 displayed a similar adhesion increase of about 16%, whereas adhesion for 0.5 mM was at control level and for 2 mM at 144 ± 17% (of untreated). The higher adhesion in THP-1 cells after recovery for 6 h suggests that the effect needs time to develop, which could indicate that *de novo* synthesis of adhesion molecules plays a role.

The expression levels of proteins involved in redox homeostasis were determined in H_2O_2-treated THP-1 cells with or without recovery. These were two important enzymes of the cellular antioxidant defence system: MnSOD, an enzyme catalysing the dismutation of two molecules of superoxide anion (O_2^-) into H_2O_2 and oxygen (O_2), and catalase, a H_2O_2-scavenging protein (Droge, 2002). No differences in their expression could be detected (Fig. 4.2C), suggesting that H_2O_2 treatment does not induce upregulation of ROS-scavenging proteins in THP-1 cells. This is surprising since ROS have been shown to induce upregulation of antioxidants in other cells (An and Blackwell, 2003; Sablina et al., 2005). These

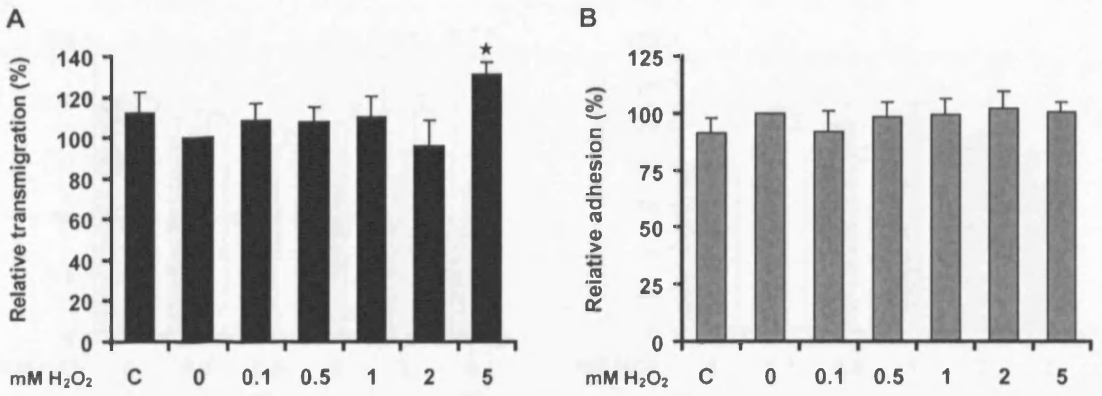

Figure 4.1: Conditioned medium from H_2O_2-treated THP-1 cells does not inhibit TEM or induce adhesion

THP-1 cells were incubated with 0 – 5 mM H_2O_2 (30 min, 37°C) and H_2O_2 was removed by centrifugation before incubation with fresh medium for 2 h. Cells were pelleted and the supernatant (conditioned medium) used for subsequent TEM and adhesion experiments with untreated THP-1 cells. **A**: THP-1 cells were allowed to transmigrate across TNF-α-activated (10 ng/ml, 15 - 18 h) HUVECs in a Transwell™-based TEM assay for 2 h in the absence (C) or presence of THP-1-conditioned medium. **B**: THP-1 cells labelled with CellTracker™ dye (1 µM, 30 min, 37°C) were allowed to adhere to TNF-α-activated (10 ng/ml, 15 - 18 h) HUVECs for 15 min. Non-adherent cells were washed off and remaining fluorescence detected using a Fusion™ α-FP plate reader.

Results were normalised to untreated control. Bars represent SEM. n = 3. ⋆ $p < 0.05$ determined by Student's t-test and Bonferroni post-test, as compared to untreated control.

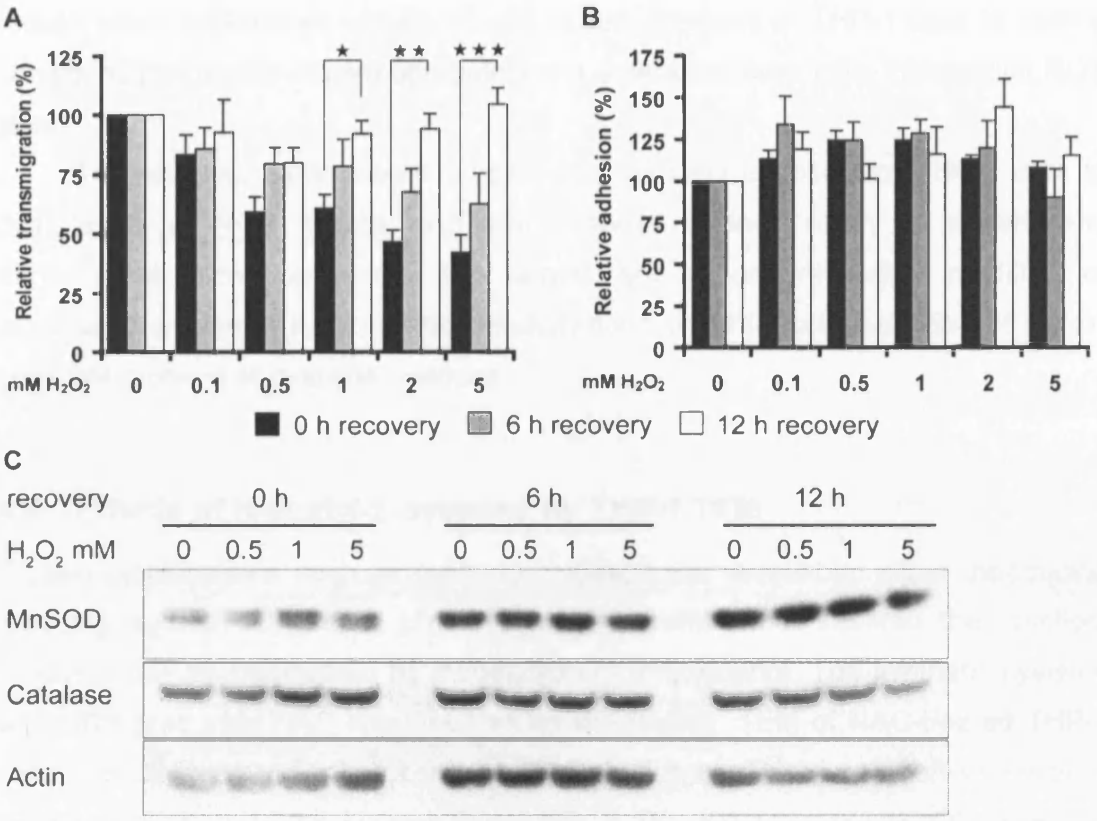

Figure 4.2: Recovery of THP-1 cells from H_2O_2 treatment
H_2O_2-treated THP-1 cells (0 – 5 mM, 30 min, 37°C) were allowed to recover for 0, 6 or 12 h. **A**: A Transwell™-based TEM assay across TNF-α-activated (10 ng/ml, 15 - 18 h) HUVECs was carried out. Cells from the lower chamber were counted after 2 h and transmigration rate was calculated. **B**: THP-1 cells labelled with CellTracker™ dye (1 µM, 30 min, 37°C) were allowed to adhere to TNF-α-activated (10 ng/ml, 15 - 18 h) HUVECs for 15 min. Non-adherent cells were washed off and remaining fluorescence detected using a Fusion™ α-FP plate reader. **C**: Cell lysates were immunoblotted with antibodies against MnSOD, Catalase and β-Actin (loading control).
Results were normalised to respective untreated control. Bars represent SEM. n = 3. ★★★ $p < 0.001$, ★★ $p < 0.01$, ★ $p < 0.05$ determined by two-way ANOVA and Bonferroni post-test.

results could indicate an excess of antioxidant enzymes in THP-1 cells at resting conditions that do not require upregulation in order to prevent toxic intracellular ROS level.

The recovery experiments indicate that transient exposure of THP-1 cells to high levels of ROS induce long-term changes in their ability to adhere and transmigrate, which suggests that targets are either irreversibly modified or modifications have a long half-life. Modifications could include oxidation of redox-sensitive proteins at cysteine residues.

4.4 Effects of N-acetyl-L-cysteine on THP-1 TEM

Protein modifications such as cysteine oxidation are reversible: either introducing reducing agents or removal of the oxidant is sufficient to reverse the reaction. Oxidants can be neutralised by introduction of antioxidants. The synthetic cysteine and GSH precursor NAC was used as an antioxidant. TEM of NAC-treated THP-1 cells was unchanged for low concentrations and only slightly and non-significantly increased by 11 ± 18.3% for high levels (Fig. 4.3A). Adhesion to HUVECs was also only marginally increased (max. 8.5 ± 3.1%) (Fig. 4.3B). These data indicate that NAC treatment has little significant effect on THP-1 cell TEM and adhesion.

To determine if treatment with antioxidants could rescue the H_2O_2-induced TEM defect, THP-1 cells were treated with H_2O_2 before subsequent treatment with NAC. THP-1 cells treated with H_2O_2 and NAC did not display a higher TEM rate than THP-1 cells treated with H_2O_2 alone (Fig. 4.3C). The increase in adhesion observed in H_2O_2-treated cells was not observed in samples treated with H_2O_2 and NAC (Fig. 4.3D), although no statistically significant difference could be determined between H_2O_2 only and H_2O_2 and NAC treated samples. These data indicate that NAC has little significant effect on the response of THP-1 cells to H_2O_2.

4.5 PMA and AT inhibit THP-1 cell TEM

In the previous chapter the effects of exogenous H_2O_2 on leukocyte TEM were characterised. Although H_2O_2 is able to diffuse across membranes, exogenously added H_2O_2 has been shown to be less effective at mediating intracellular signalling responses than endogenously produced ROS (Choi et al., 2005a). To determine how changes in intracellular ROS level influence TEM and adhesion, THP-1 cells were treated with PMA, a stimulus of NADPH oxidase-induced ROS production,

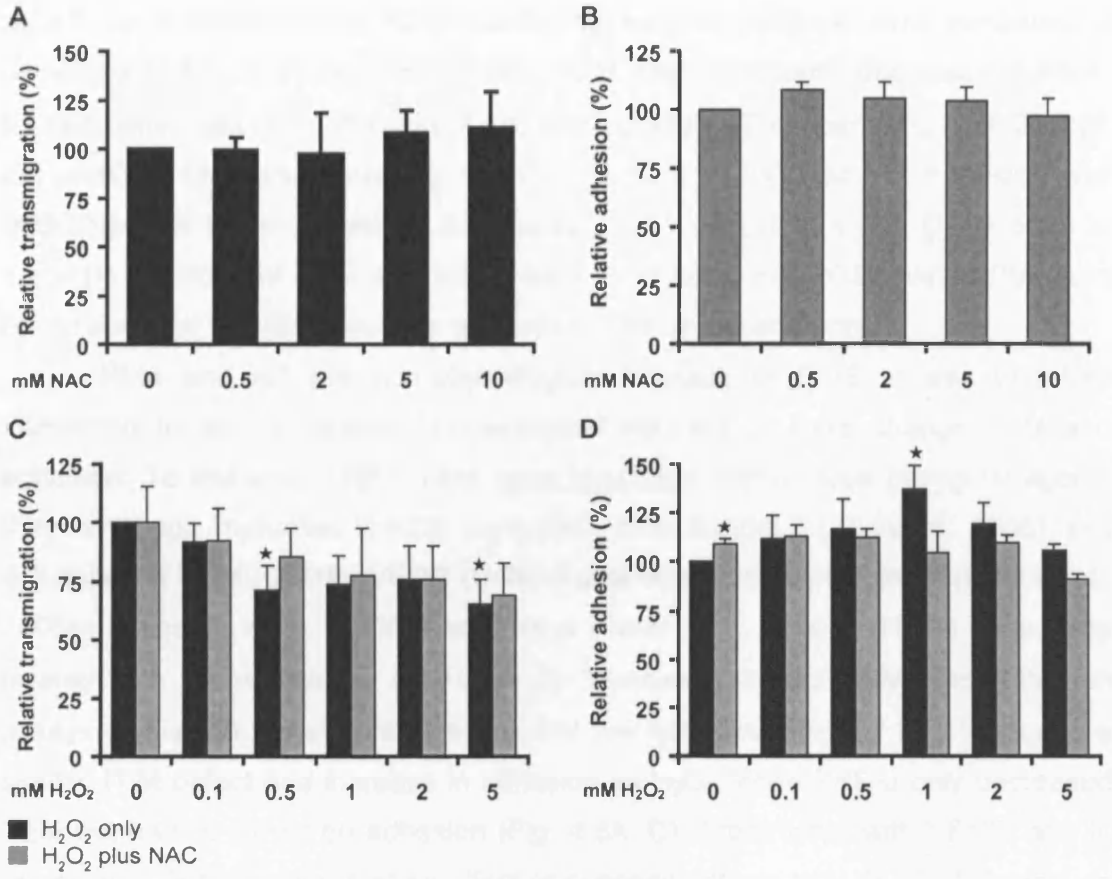

Figure 4.3: Effects of N-acetyl-L-cysteine on THP-1 TEM and adhesion
NAC-treated THP-1 cells (0 – 10 mM, 30 min, 37°C) were either allowed to transmigrate across TNF-α-stimulated HUVECs for 2 h in a Transwell™-based TEM assay (**A**) or were pre-treated with CellTracker™ dye (1 µM, 30 min, 37°C) and allowed to adhere to HUVECs for 15 min (**B**). n = 4 (A) or 5 (B). **C, D**: H_2O_2-treated THP-1 cells (0 – 5 mM, 30 min, 37°C) were incubated with or without 10 µM NAC (30 min, 37°C). Cells were either allowed to transmigrate across TNF-α-stimulated HUVECs for 2 h in a Transwell™-based TEM assay (**C**) or were pre-treated with CellTracker™ dye (1 µM, 30 min, 37°C) and allowed to adhere to HUVECs for 15 min (**D**). n = 4 (C) or 6 (D).
Results were normalised to untreated control. Bars represent SEM. ⋆ $p < 0.05$ determined by Student's t-test and Bonferroni post-test, as compared to untreated control.

or AT, an inhibitor of the ROS-scavenging enzyme catalase, and compared to untreated and H_2O_2-treated THP-1 cells. TEM was significantly decreased in PMA-treated cells (max. 97 ± 3%, Fig. 4.4A), and for high AT concentrations (≥ 20 mM; Fig. 4.4C). TEM was completely inhibited at 50 and 100 mM AT. Adhesion was unchanged for PMA- as well as AT-treated THP-1 cells (Fig. 4.4 B, D). In order to correlate inhibition of TEM with intracellular ROS level, the ROS level in PMA and AT-treated THP-1 cells should be quantified in future experiments.

PMA and AT are non-physiological inducers of ROS, it was therefore interesting to look at whether physiological inducers of ROS change TEM and adhesion. To this end, THP-1 cells were incubated with various biological agents that have been implicated in ROS production, including fMLP (Zhu et al., 2005), ang II (Lassegue et al., 2001), VEGF (Ushio-Fukai et al., 2002), thrombin (Choi et al., 2005b) (Begonja et al., 2005) and TNF-α (Defer et al., 2007). THP-1 cells were treated with these agents and used in Transwell™-based TEM and adhesion assays. Preliminary results suggested that low concentrations of fMLP induced a similar TEM defect and increase in adhesion as H_2O_2, while TNF-α only decreased TEM but had no effect on adhesion (Fig. 4.5A, C). Treatments with VEGF, ang II, thrombin or DMSO either had no effect or opposing effects to H_2O_2. To follow up on these results, lower concentrations of fMLP and the same concentrations of TNF-α and H_2O_2 were used in Transwell™-based TEM and adhesion assays. The effect of fMLP on TEM was not reproducible, which suggests that it does not affect TEM (Fig. 4.5D). TNF-α induced a small and statistically not significant reduction in TEM.

Further investigations are needed to determine how effective these reagents are at inducing intracellular ROS and whether they influence TEM.

4.6 High intracellular ROS levels coincide with low TEM

To elucidate whether application of H_2O_2 alters intracellular ROS levels, THP-1, MM6 cells, monocytes and T lymphoblasts were treated with H_2O_2 levels that were previously determined to be non-toxic (see Chapter 3.5) and intracellular ROS levels determined by FACS analysis using carboxy-H_2DCFDA. H_2O_2 induced a dose-dependent increase in intracellular ROS in THP-1 and MM6 cells, with maximal increases of 62.1 ± 30.6% and 28.1 ± 23.6%, respectively at 5 mM (Fig. 4.6A). While monocytes did not show a change in intracellular ROS levels, T lymphoblasts displayed significantly decreased ROS level for H_2O_2 concentrations ≥ 0.1 mM (max. 40 ± 3.5%).

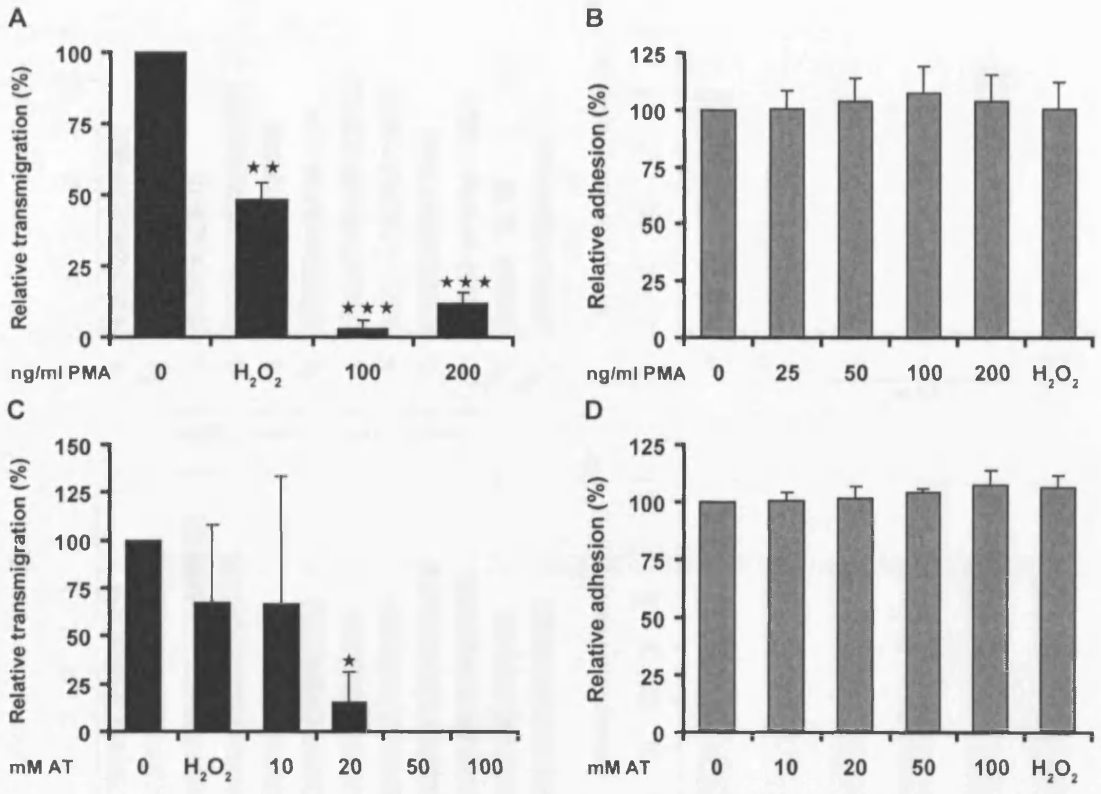

Figure 4.4: PMA and AT inhibit THP-1 cell TEM
THP-1 cells were either treated with 1 mM H_2O_2 (30 min, 37°C) and 100 or 200 ng/ml PMA or 1 mM H_2O_2 and 10 – 100 mM AT (60 min, 37°C). **A, C**: H_2O_2- and PMA- or AT-treated THP-1 cells were allowed to transmigrate across TNF-α-activated (10 ng/ml, 15 - 18 h) HUVECs for 2 h and TEM rate was determined from the time-lapse movies. **B, D**: CellTracker™-labelled (1 µM, 30 min, 37°C) and subsequently H_2O_2- and PMA- or AT-treated THP-1 cells were allowed to adhere to TNF-α-activated (10 ng/ml, 15 - 18 h) HUVECs for 15 min. Adhesion was detected measuring fluorescence using a Fusion™ α-FP plate reader.
Results were normalised to untreated control. Bars represent SEM. $n \geq 3$. ★★★ $p < 0.001$, ★★ $p < 0.01$, ★ $p < 0.05$ determined by Student's t-test and Bonferroni post-test, as compared to untreated control.

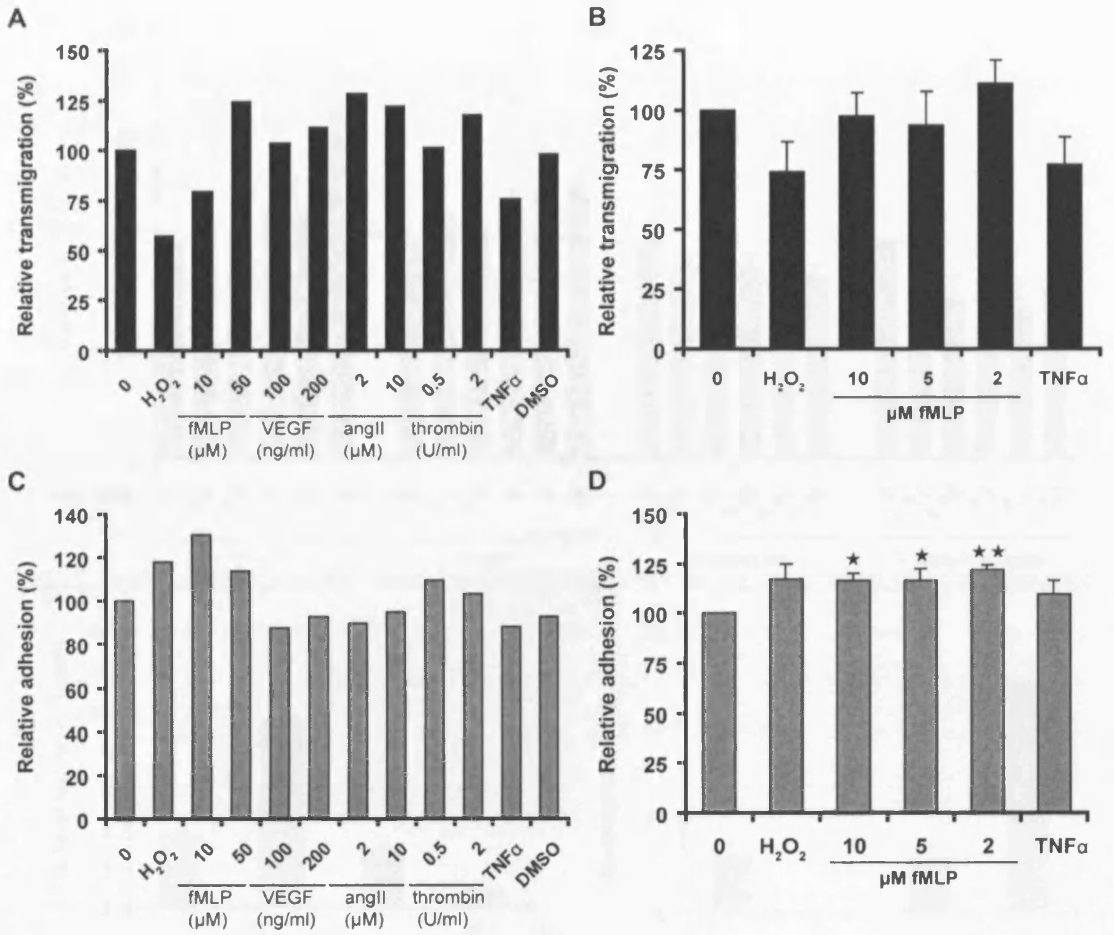

Figure 4.5: Effect of various stimuli on TEM and adhesion
THP-1 cells were treated with H_2O_2 (1 mM, 30 min, 37°C), or for 60 min (37°C) with fMLP (2, 5, 10 or 50 µM), VEGF (100 or 200 ng/ml), ang II (2 or 10 µM), thrombin (0.5 or 2 U/ml), TNF-α (10 ng/ml) or DMSO (0.5%) before being used in Transwell™-based TEM and adhesion assays. **A, B**: Cells were allowed to transmigrate across TNF-α-activated (10 ng/ml, 15 - 18 h) HUVECs for 2 h. Transmigration rate was determined by counting cells from the lower chamber. n = 1 (A) or 4 (B). **C, D**: Prior to exposure to ROS-stimulating reagents cells were labelled with CellTracker™ dye (1 µM, 30 min, 37°C) before adhering to HUVECs for 15 min. Adhesion was detected measuring fluorescence using a Fusion™ α-FP plate reader. n = 1 (C) or 5 (D).
Results were normalised to untreated control. Bars represent SEM. ⋆⋆ $p < 0.01$, ⋆ $p < 0.05$ determined by Student's t-test and Bonferroni post-test, as compared to untreated control.

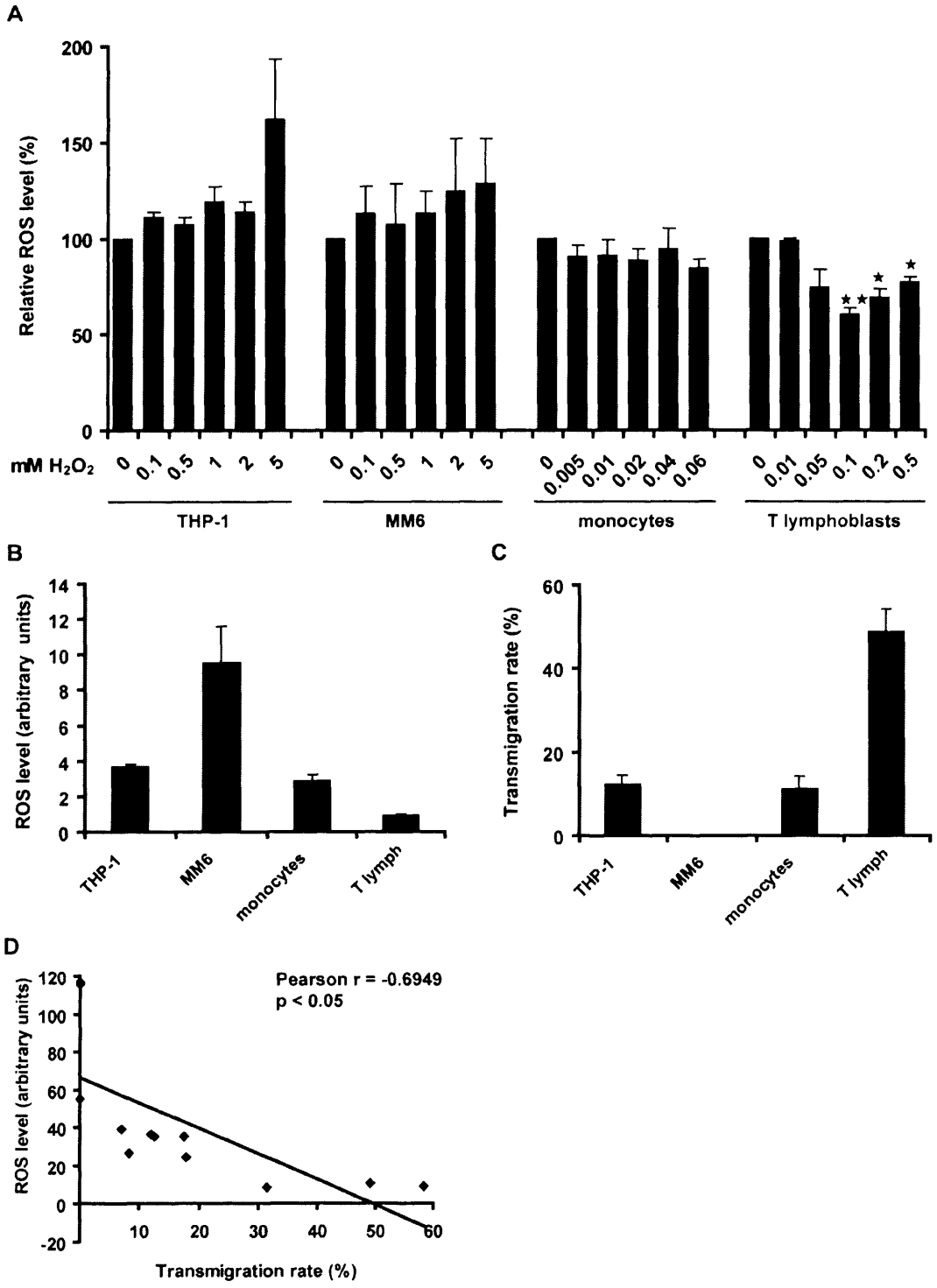

Figure 4.6: High intracellular ROS levels correlate with low TEM rate
A: THP-1, MM6 cells, monocytes and T lymphoblasts were treated with 0 – 5 mM H_2O_2 before labelling with 5 µM H_2DCFDA (30 min, 37°C). ROS level were determined by FACS analysis and normalised to the respective untreated control. $n \geq 3$. ⋆⋆ $p < 0.01$, ⋆ $p < 0.05$ determined by Student's t-test and Bonferroni post-test. **B**: THP-1, MM6 cells, monocytes and T lymphoblasts were labelled with 5 µM H_2DCFDA (30 min, 37°C) before ROS level were determined by FACS analysis. $n \geq 3$. **C**: Transmigration rate of THP-1, MM6 cells, monocytes and T lymphoblasts was determined by TLM-based TEM assays and displayed as percentage of input. **D**: Correlation analysis of ROS level vs. TEM rate. $p < 0.05$ determined by Student's t-test.

These results show that different leukocytes react differently in response to H_2O_2. While 0.1 and 0.5 mM H_2O_2 led to a small increase in intracellular ROS in the monocytic cell lines THP-1 and MM6, it led to a significant decrease in T lymphoblasts. When interpreting these results it has to be taken into account that not only H_2O_2, but also peroxynitrite and peroxyl radicals will be detected by this method. This apparent discrepancy could be due to differences in the cellular redox state of unstimulated leukocytes and in the production of secondary ROS, e.g. peroxynitrite.

To investigate the relationship between intracellular ROS levels and TEM, ROS levels in untreated leukocytes were determined and compared to their TEM rate. ROS levels were detected using carboxy-H_2DCFDA and FACS analysis (Fig. 4.6B). The transmigration rates were determined by TLM-based TEM assays and calculated as percentage of total cell input (Fig. 4.6C). Leukocytes with similar ROS levels displayed similar TEM rates, whereas high levels of ROS coincided with low TEM and *vice versa*. This observation was confirmed by statistical analysis, revealing a significant negative correlation between ROS level and TEM, with a Pearson's coefficient of $r = -0.6949$ and $r^2 = 0.4829$. The Pearson's coefficient is a measure for correlation, where $r = 1$ is a perfect positive correlation and $r = -1$ a perfect negative correlation. The coefficient $r^2 = 0.4829$ can be interpreted as 48% of the variance in TEM can be explained by variations in ROS levels. The assumption that different redox states in leukocytes could be responsible for the differences in intracellular ROS after H_2O_2 treatment could not be confirmed from this experiment. THP-1 cells and primary monocytes had similar levels of resting ROS, but unlike to THP-1 cells, primary monocytes did not display an increase in intracellular ROS at the H_2O_2 concentrations tested. However, since different H_2O_2 level had to be used for the leukocytes tested, it is difficult to compare them directly.

4.7 Role of NO in transmigration

ROS have been reported to stimulate NO production in ECs via transient activation of eNOS (Boulden et al., 2006). In chondrocytes, ROS has been shown to induce iNOS expression (Mendes et al., 2003). Leukocytes also express iNOS, but nothing is known about its regulation by ROS in these cells. To investigate if the intracellular level of NO changed with H_2O_2 treatment and how this compared to intracellular ROS, THP-1 cells were either treated with H_2O_2 or PMA before labelling with carboxy-H_2DCFDA to visualise ROS, or were first incubated with DAF before incubation with H_2O_2 or PMA to visualise NO. PMA, a known stimulator of NADPH oxidase (Jagnandan et al., 2007), was used as a positive control for intracellular

ROS production. ROS and NO level were detected using FACS analysis (Fig. 4.7A, B). Intracellular ROS levels were only increased for 5 mM H_2O_2, whereas NO levels were increased for H_2O_2 concentrations ≥ 0.5 mM (Fig. 4.7C). PMA induced high levels of ROS but no production of NO. NO displayed a dose-dependent increase in response to H_2O_2. The higher responsiveness of the NO increase suggests that NO might play a critical role in mediating the effects of H_2O_2.

NO is produced by NOS; with iNOS being the predominant isoform in leukocytes. The expression of iNOS was determined by immunoblotting, and increased in a dose-dependent manner after H_2O_2 treatment in THP-1 cells with or without 6 h of recovery, by maximal 228% and 219% for 0 and 6 h recovery respectively (Fig. 4.8). Twelve hours after removal of H_2O_2, iNOS levels were lower in H_2O_2-treated than in control THP-1 cells. From these results, it is feasible to assume that elevated iNOS levels after 30 min of H_2O_2 treatment lead to the observed increase in NO.

4.7.1 Effects of NOS inhibition and an NO donor on THP-1 TEM and adhesion

To elucidate if NO is a mediator of H_2O_2-induced TEM and adhesion changes, the effects of a non-selective NOS inhibitor (L-NAME) (Oka et al., 2005) and a NO donor (SNAP) (Sun et al., 2006) on THP-1 TEM and adhesion were determined. Pre-treatment with L-NAME did not prevent the dose-dependent decrease in TEM after H_2O_2 treatment. However, SNAP treatment inhibited leukocyte TEM significantly by 22.2 ± 5.6% (Fig. 4.9A). Similarly, L-NAME treatment did not prevent the increase in adhesion after H_2O_2 incubation (Fig. 4.9B) but SNAP induced an increase in adhesion to a similar level as 1 mM H_2O_2 (108 ± 7.1% vs. 105 ± 8.2%).

Although pre-treatment of THP-1 cells with L-NAME did not prevent the H_2O_2-induced alterations in TEM and adhesion, the results of the NO donor indicate that NO is likely to play a role in the observed H_2O_2 phenotype. The efficiency of the inhibitor has to be tested before it is possible to draw conclusions about the actual involvement of NO in this process.

4.7.2 Formation of THP-1 cellular protrusions is prevented by SNAP

Previous results (see Fig. 3.16) have indicated that H_2O_2 inhibits the formation of cellular protrusions. NO has also been shown to play a role in regulating cellular protrusions (Lee et al., 2005; Lindsay et al., 2007). The preliminary results from Chapter 3 were verified and quantified and the involvement of NO in this process was investigated. The cellular protrusions from THP-1 cells treated with H_2O_2 or

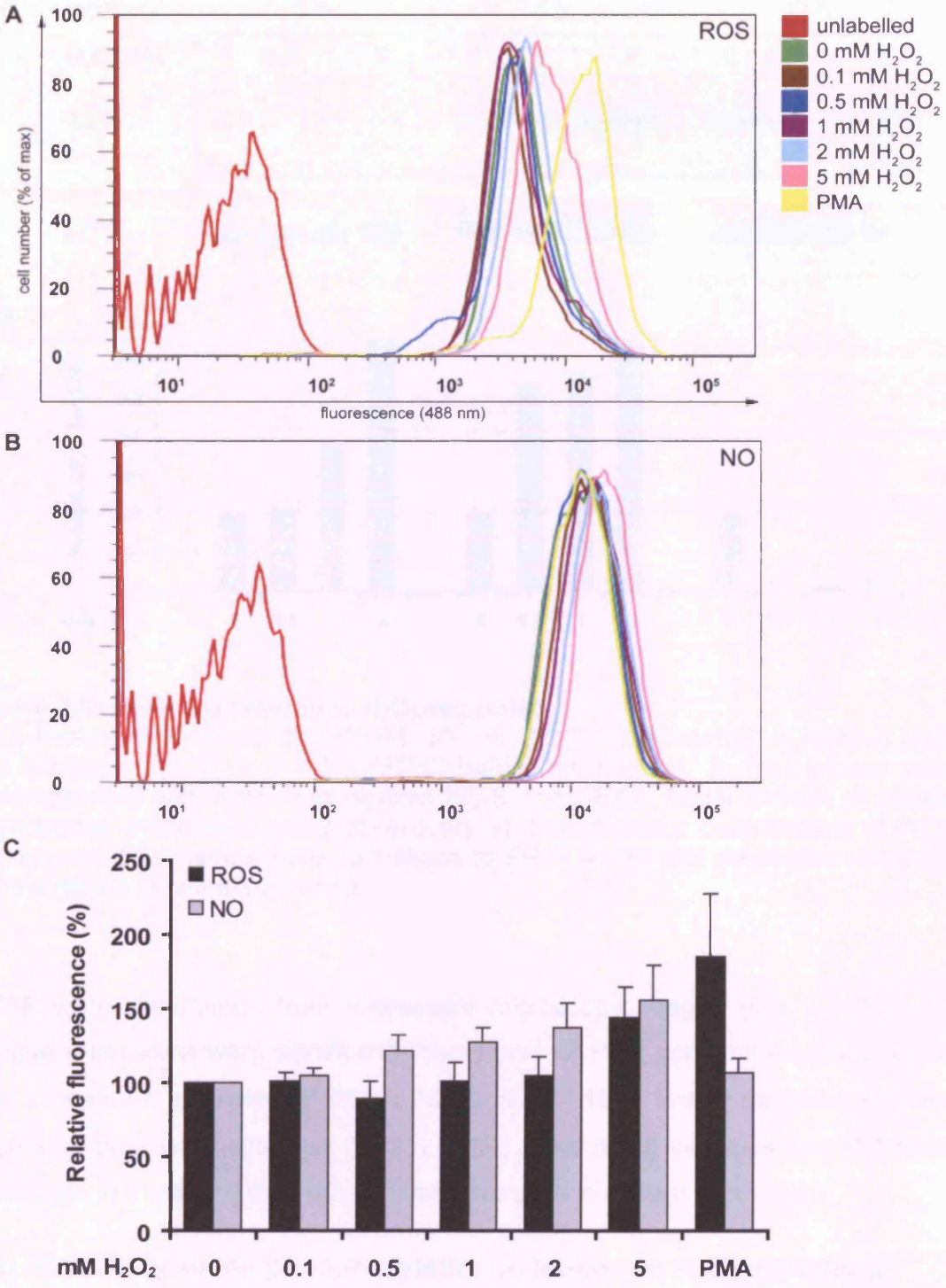

Figure 4.7: Intracellular NO levels are increased upon H_2O_2 treatment
THP-1 cells were treated with 0 – 5 mM H_2O_2 (30 min, 37°C) or 100 ng/ml PMA (60 min, 37°C). **A**: Representative FACS trace for cells labelled with 5 µM H_2DCFDA (30 min, 37°C) to detect ROS. **B**: Prior to incubation with H_2O_2 and PMA, THP-1 cells were incubated with 5 µM DAF (30 min, 37°C). NO levels were detected using FACS analysis and representative FACS trace is shown. **C**: Graphical display of all experiments. Results are normalised to the respective untreated control. n = 7.

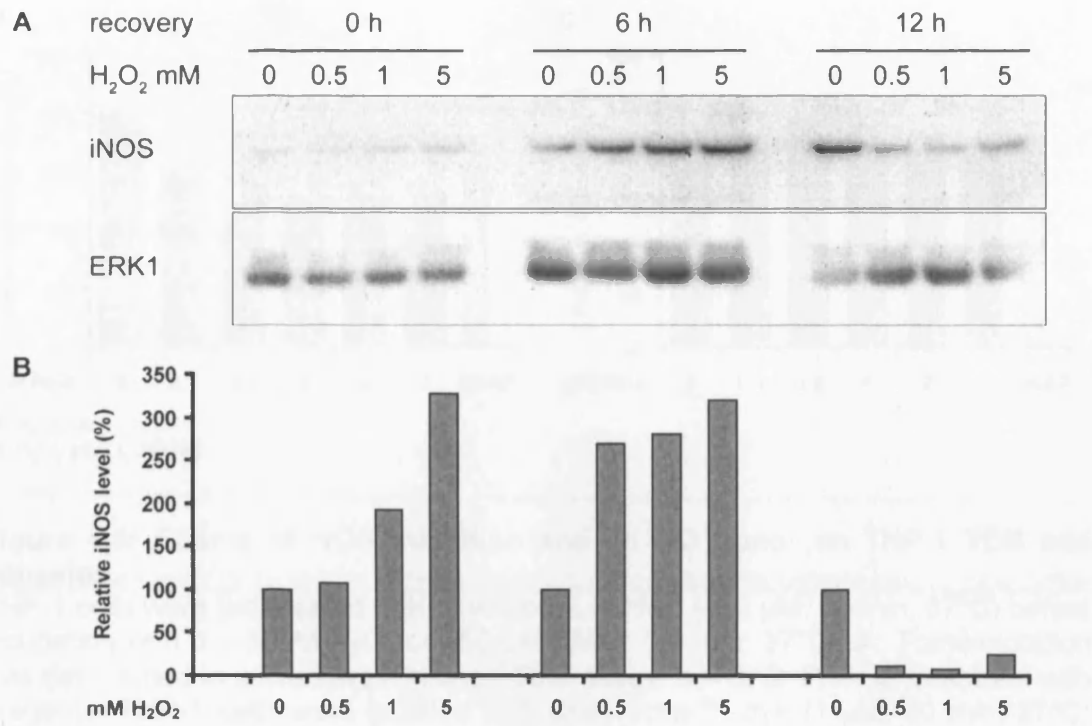

Figure 4.8: iNOS expression is H_2O_2-regulated
H_2O_2-treated THP-1 cells (0 – 5 mM, 30 min, 37°C) were washed to remove H_2O_2 and incubated for 0, 6 or 12 h (37°C) before being lysed. **A**: Cell lysates were immunoblotted with antibodies against iNOS and ERK1. Equal amount of protein were loaded within each group of recovery. **B**: Densitometric quantification of iNOS expression. iNOS levels were normalised to ERK1 levels and respective untreated control. Mean of two experiments.

SNAP were determined from fluorescent microscopy images (Fig. 4.10A – G). Cellular protrusions were significantly decreased for H_2O_2 concentrations ≥ 0.5 mM, with a maximum decrease of 46.1 ± 10.5% (Fig. 4.10H). SNAP exhibited a similar degree of protrusion inhibition (33.2 ± 2.1%). This result indicates that NO could participate in mediating the H_2O_2-induced decrease in cellular protrusions.

4.8 Role of tyrosine phosphorylation in leukocyte H_2O_2 signalling

As previously mentioned, some proteins are prone to cysteine oxidation and redox regulation. This phenomenon has been well studied for phosphatases, where oxidation leads to protein inactivation, resulting in an increase in protein phosphorylation (Salmeen and Barford, 2005). Protein serine-threonine kinases and PTKs also appear to be under redox control (Rhee et al., 2000). Although the mechanism has not been elucidated yet, it is also likely to involve cysteine oxidation.

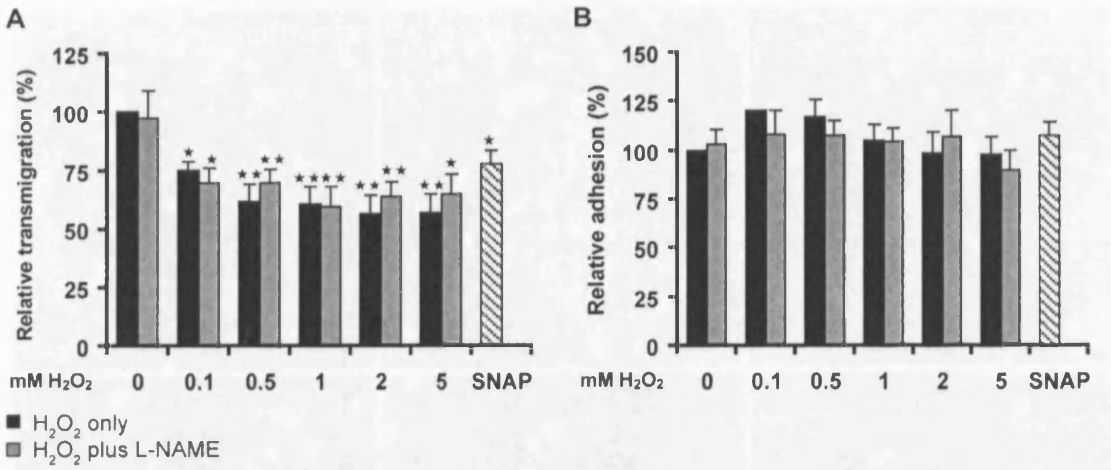

Figure 4.9: Effects of NOS inhibition and an NO donor on THP-1 TEM and adhesion
THP-1 cells were pre-treated with or without L-NAME (400 µM, 60 min, 37°C) before incubation with 0 – 5 mM H_2O_2 or 250 µM SNAP (30 min, 37°C). **A**: Transmigration was determined in a Transwell™-based TEM assay. n = 6. **B**: Prior to treatment with reagents, THP-1 cells were labelled with CellTracker™ dye (1 µM, 30 min, 37°C) before adhesion to TNF-α-activated (10 ng/ml, 15 - 18 h) HUVECs was measured using a Fusion™ α-FP plate reader. n = 5.
Results were normalised to untreated control. Bars represent SEM. ⋆⋆ $p < 0.01$, ⋆ $p < 0.05$ determined by Student's t-test and Bonferroni post-test, as compared to untreated control.

Phospho-tyrosine (pTyr) levels and localisation were determined by immunofluorescence in H_2O_2-treated THP-1 cells adherent to VCAM-1 or HUVECs. On VCAM-1 pTyr staining was found throughout the cell, with intense punctate staining, mainly in clusters, at the basal surface (Fig. 4.11). This staining is likely to represent podosomes, adhesive structures found in cells of the monocyte lineage. The amount of pTyr-containing structures displayed a dose-dependent increase with H_2O_2 treatment. On HUVECs, no punctate pTyr staining could be observed in THP-1 cells; pTyr staining was found throughout the cell with accumulations at the leading edge (Fig. 4.12 arrows). Levels of THP-1 pTyr were highest at 1 and 2 mM. HUVECs also displayed pTyr staining in particular in the junctions, where junctional proteins such as VE-cadherin and β-catenin are known to be tyrosine phosphorylated, thereby regulating junction disassembly (Allingham et al., 2007; van Buul et al., 2005).

These preliminary data indicate that pTyr levels are changed upon H_2O_2 treatment. While pTyr is accumulated in adhesive structures on VCAM-1, pTyr is found in the leading edge in THP-1 cells adherent to HUVECs.

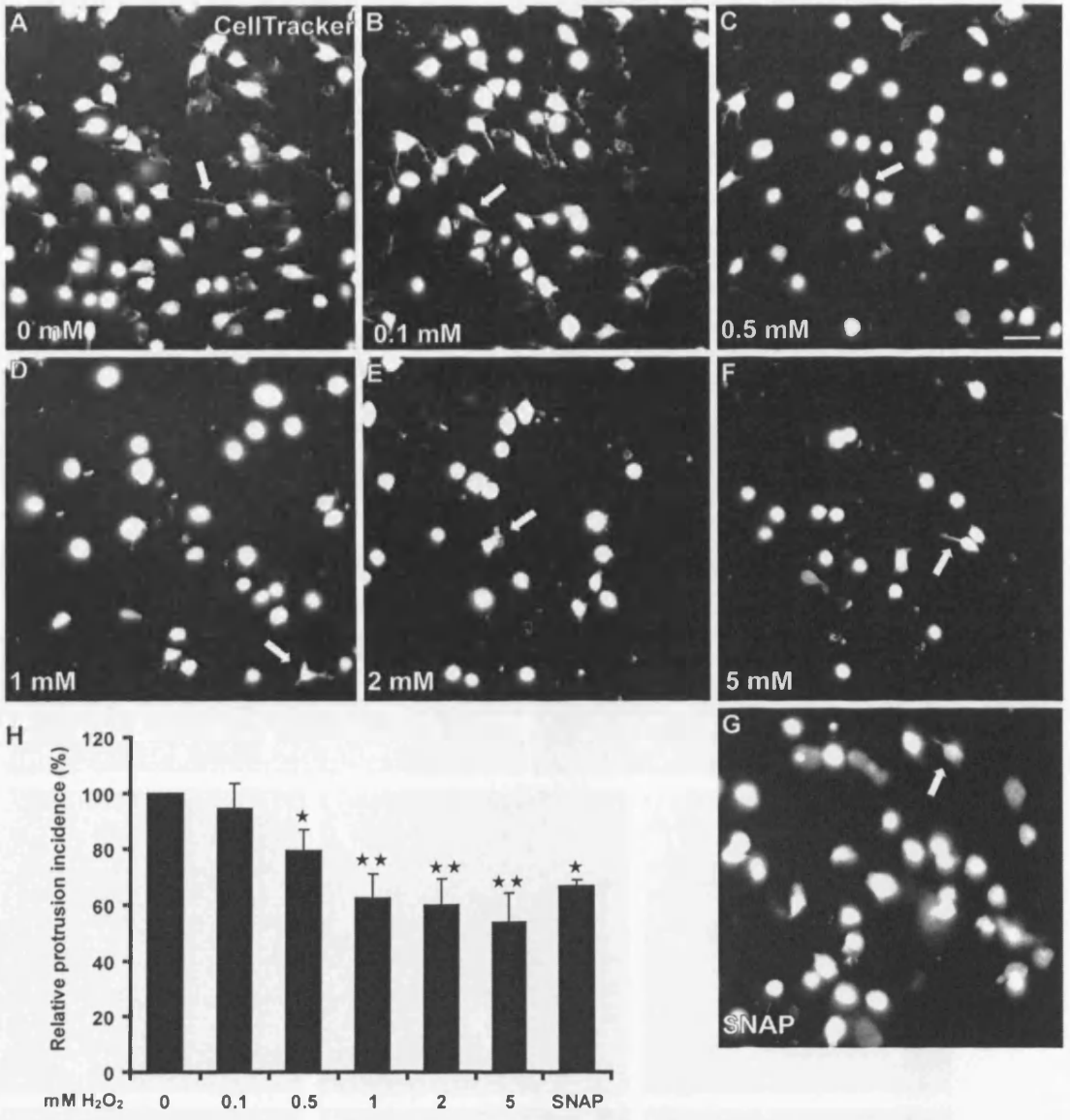

Figure 4.10: Number of cells with cellular protrusions is significantly reduced with H_2O_2 and SNAP treatment
CellTracker™-labelled THP-1 cells (1 µM, 30 min, 37°C) were treated with 0 – 5 mM H_2O_2 or 250 µM SNAP (30 min, 37°C) and added to TNF-α-activated (10 ng/ml, 15 - 18 h) HUVECs for 25 min. **A** – **G**: Fixed cells were visualised using a Zeiss Axiophot. Bar = 20 µm. **H**: The percentage of cells with protrusions (arrow) was determined from the fluorescent images. Results were normalised to untreated control. Bars represent SEM. $n \geq 3$. ⋆⋆ $p < 0.01$, ⋆ $p < 0.05$ determined by Student's t-test and Bonferroni post-test.

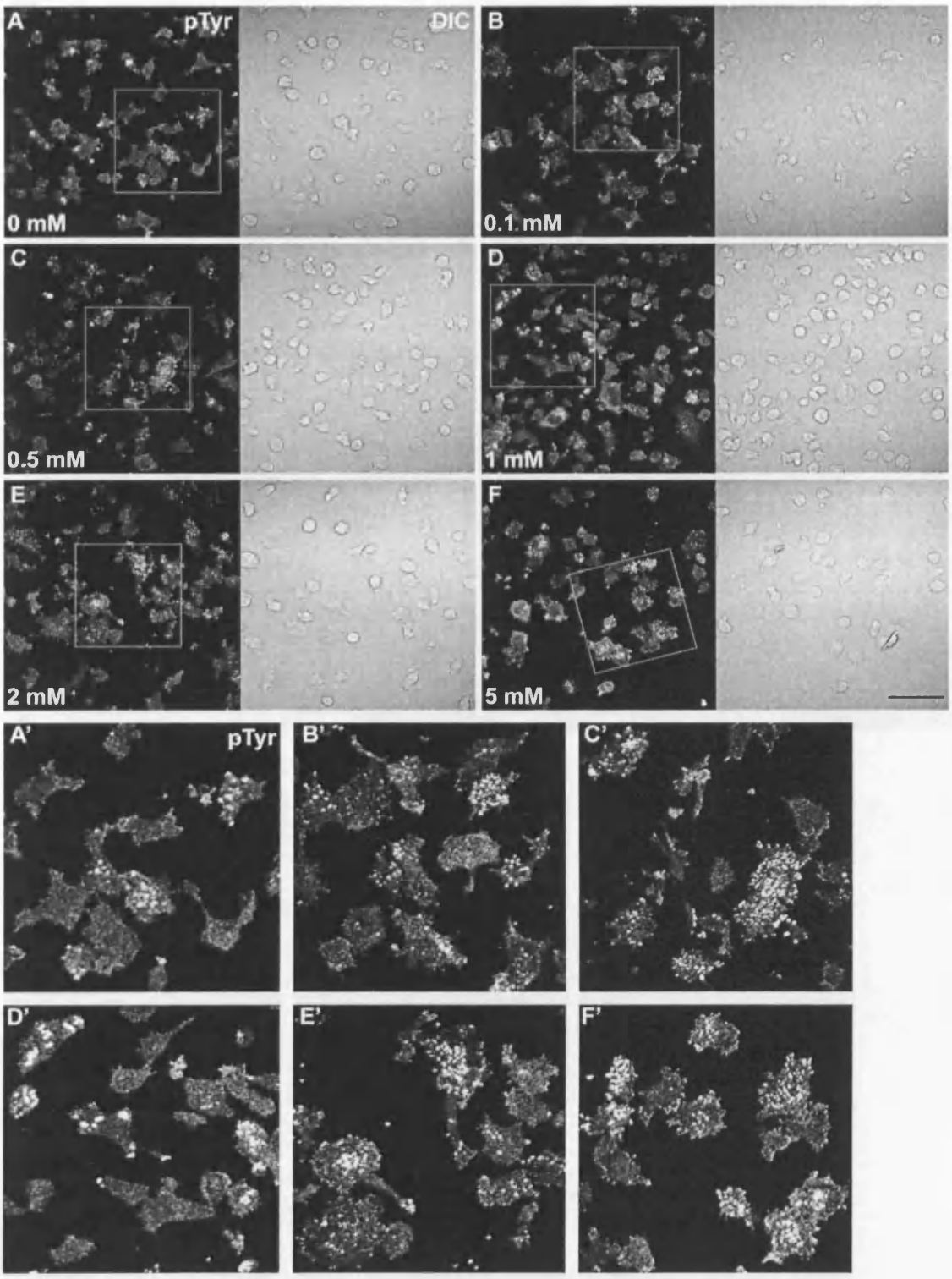

Figure 4.11: H_2O_2 treatment increases pTyr levels in adhesive structures when bound to VCAM-1

THP-1 cells were incubated with H_2O_2 (0 – 5 mM, 30 min, 37°C). H_2O_2 was removed and cells were allowed to adhere to VCAM-1-coated coverslips for 1 h, before cells were fixed and stained for pTyr. **A – F**: Additionally, differential interference contrast (DIC) images were taken to visualise outline of the cells. Bar = 50 µm. **A' – F'**: Details of images A – F, localisation is indicated by white box.

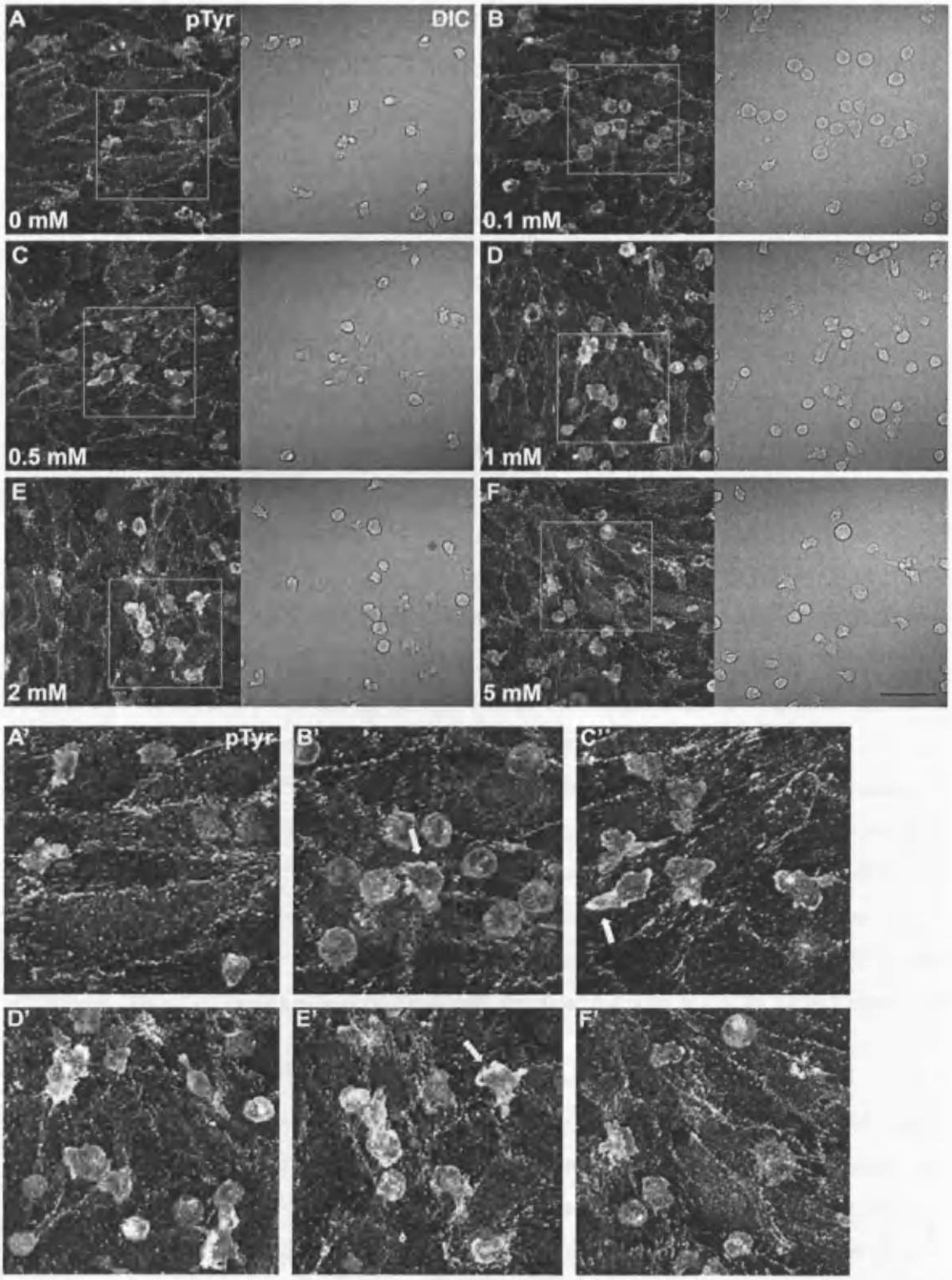

Figure 4.12: pTyr levels are increased in H_2O_2-treated THP-1 cells on ECs THP-1 cells were incubated with H_2O_2 (0 – 5 mM, 30 min, 37°C). H_2O_2 was removed and cells were added to TNF-α-stimulated HUVECs for 25 min, before cells were fixed and stained for pTyr. **A – F**: Additionally, differential interference contrast (DIC) images were taken to visualise outline of the cells. White arrows indicate pTyr accumulation at the leading edge. Bar = 50 µm. **A' – F'**: Details of images A – F, localisation in is indicated by white box.

4.9 Role of Rho GTPases in H_2O_2-mediated decrease in leukocyte TEM

Rho GTPases play distinct roles in every step of TEM from adhesion to translocation and diapedesis (see Chapter 1.4.2). The most studied Rho GTPases, RhoA, Rac1 and Cdc42, have recently been postulated to be redox-sensitive due to a unique Cys, Cys^{18} (Rac1 numbering), located at the end of the P-loop (G*XXXX*GK(S/T), residues 10 to 17, Rac1 numbering) (Heo and Campbell, 2005). It was therefore crucial to look into the regulation of Rho GTPases in THP-1 cells after H_2O_2 treatment.

4.9.1 Rho GTPase expression level in response to H_2O_2

As a starting point to investigating the roles of Rho GTPases in H_2O_2-mediated TEM decrease, total levels of Rho GTPases after H_2O_2 treatment were determined. Specific antibodies against RhoA, Rac1 and ERK1 (loading control) were used. Preliminary results suggest that RhoA levels display a dose-dependent increase with H_2O_2 treatment, while Rac1 showed some variability but no obvious trend (Fig. 4.13 left panel and histogram). Cdc42 was not detectable under these experimental conditions, which could be due to differences in the composition of the lysis buffer.

Some proteins are known to undergo redox-mediated changes in their susceptibility towards proteasomal degradation (Grune et al., 1997). To elucidate if Rho GTPase stability was redox-regulated in THP-1 cells, cells were incubated with the proteasome inhibitor MG132 prior to treatment with H_2O_2. These preliminary results suggest that RhoA levels peak at 1 mM H_2O_2, while Rac1 level were decreased slightly (Fig. 4.13 right panel and histogram). These results might tentatively suggest that RhoA stability could be regulated by H_2O_2 in THP-1 cells.

4.9.2 Rho GTPase activity is modified by H_2O_2 treatment

To investigate whether H_2O_2 affects Rho GTPase activity, GST-pull-downs of active RhoA, Rac1 and Cdc42 were carried out using H_2O_2-treated adherent or suspension THP-1 cells and appropriate GST-fusion proteins. Upon H_2O_2 treatment, suspension cells displayed a small increase in activity at low concentrations, followed by a decrease for RhoA, Rac1, Cdc42 (Fig. 4.14A, C). RhoA activity peaked at 1 mM with 122 ± 63% (of untreated) and was decreased by 45 ± 22% at 5 mM. Rac1 activity was only increased for 0.5 mM H_2O_2 (130 ± 60% of untreated), while all other concentrations led to a decrease in activity (max. 23 ± 17%). Cdc42 activity peaked at 0.5 mM with 123% (of untreated) and was decreased by 39% at 2 mM.

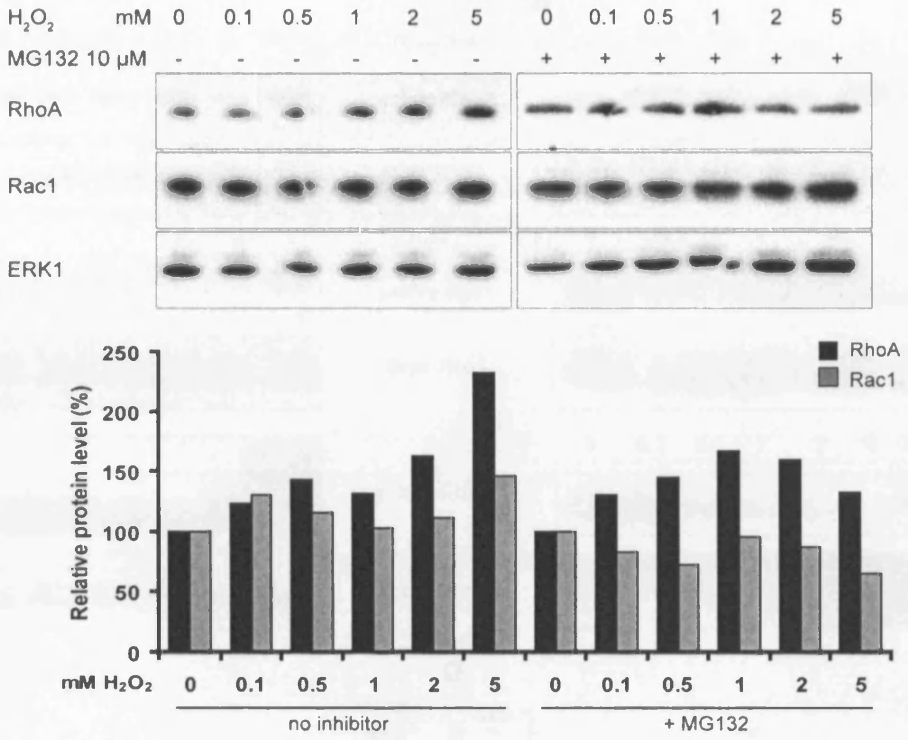

Figure 4.13: Rho GTPase expression levels in H_2O_2 treated cells
THP-1 cells in suspension were either treated with or without MG132 (10 µM, 24 h, 37°C) before incubation with 0 – 5 mM H_2O_2 (30 min, 37°C). Cells were then lysed and immunoblotting using antibodies against RhoA, Rac1 and ERK1 (loading control) was carried out. Representative immunoblots of two experiments are shown. Histogram shows densitometric quantification of two experiments. Results were normalised to ERK level and control without H_2O_2.

Adherent THP-1 cells exhibited similar changes in RhoA activity as suspension cells, with an slight increase at 0.5 mM H_2O_2 with 142 ± 55% (of untreated) and a maximal decrease of 45 ± 26% at 5 mM (Fig. 4.14B, D), whereas Rac1 activity was differently regulated in these cells. Rac1 activity displayed a high activation peak of 207 ± 123% (of untreated) at 1 mM. Rac1 activation level decreased by 15 ± 25% for high H_2O_2 concentrations. Cdc42 activity was only slightly increased for low H_2O_2 concentrations (109 ± 37% of untreated, 0.1 mM) and decreased for high H_2O_2 concentrations, by a maximum of 68 ± 17% (5 mM).

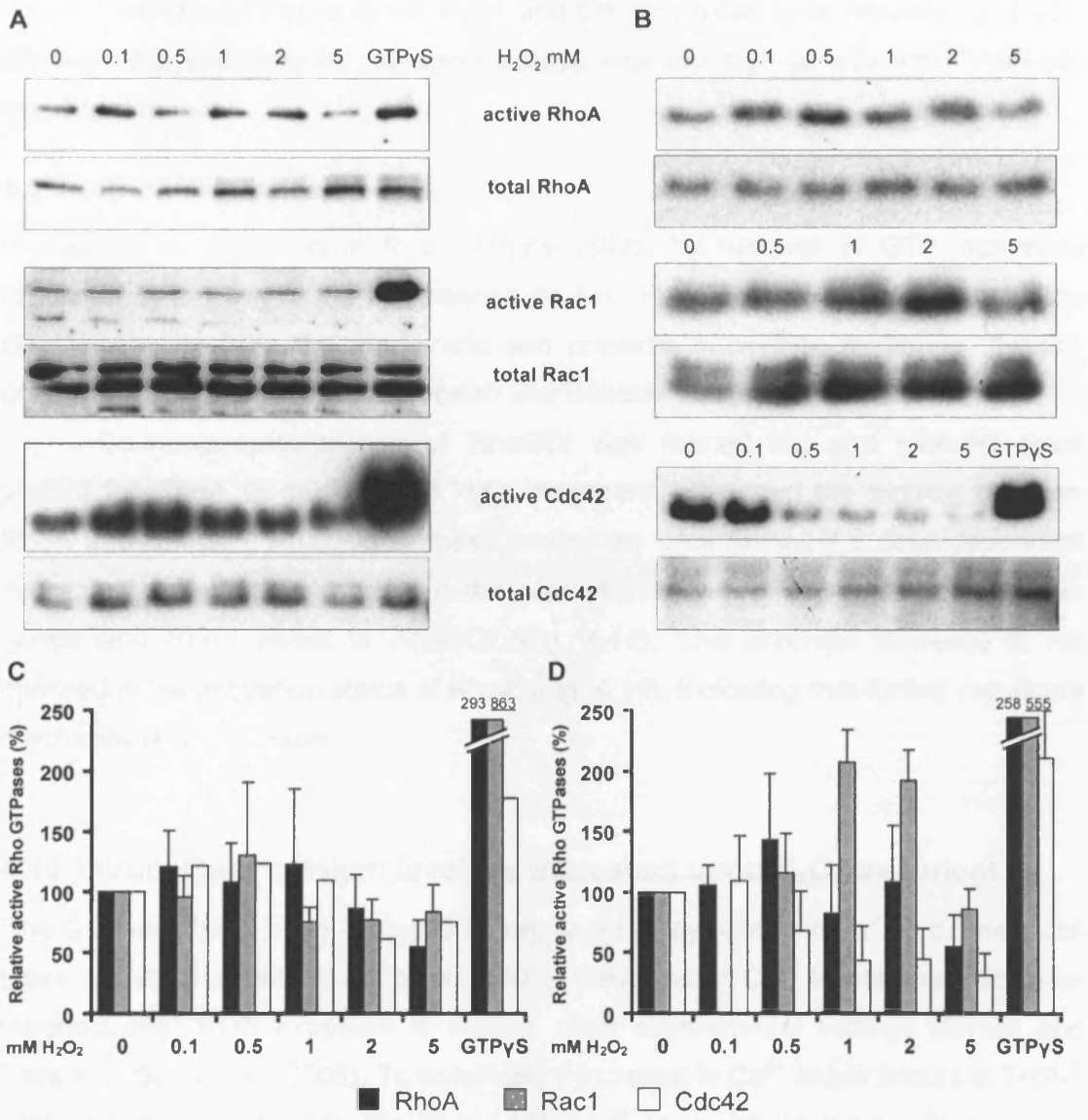

Figure 4.14: RhoA, Rac1 and Cdc42 activities are altered by H_2O_2
H_2O_2-treated THP-1 cells (0 – 5 mM, 30 min, 37°C) were either centrifuged onto FN-coated 6-well dishes or used in suspension. Control cell lysates were treated with 100 µM GTPγS (15 min, 30 °C) before incubation with immobilised GST-fusion proteins (60 min, 4 °C). GST-fusion proteins of rhotekin Rho-binding domain (RhoA) and the p21-binding domain (PBD) of PAK (Rac1 and Cdc42) were used. **A, B**: Representative western blots for GST-pull-downs with suspension (A) and adherent (B) THP-1 cells. **C, D**: Densitometric quantification of GST-pull-down experiments from suspension (C) and adherent (D) cells. Results are normalised to respective untreated control. Bars represent SEM. n ≥ 3, except suspension Cdc42, where the means of two experiments are displayed. Numbers above GTPγS samples (C, D) indicate values of discontinued bars for RhoA and Rac1 (underlined).

The Rho GTPases RhoA, Rac1 and Cdc42 appear to be regulated by H_2O_2, although the variability in pull-down assays was too high to achieve statistically significant results.

4.9.3 RhoA regulation by H_2O_2

In addition to regulation of Rho GTPase activity by turnover of GTP, activity is regulated by binding to the cytoplasmic inhibitor RhoGDI. RhoGDI sequesters Rho GTPases away from the membrane and prevents nucleotide exchange, thereby preventing activation (DerMardirossian and Bokoch, 2005).

Co-immunoprecipitation of RhoGDI was carried out and samples were probed for RhoA to determine if H_2O_2 treatment influenced the binding between RhoA and RhoGDI. Analysis of these preliminary data revealed a dose-dependent decrease by a maximum of 85% in the interaction between RhoA and RhoGDI after normalising RhoA levels to RhoGDI (Fig. 4.15). This potential decrease is not mirrored in the activation status of RhoA (Fig. 4.14), indicating that further regulatory mechanisms are in place.

4.10 Intracellular calcium level are increased upon H_2O_2 treatment

Rho GTPases have been shown to be regulated by cytoplasmic Ca^{2+} in different cell types (Jin et al., 2005; Price et al., 2003). Elevation of Ca^{2+} levels has also been reported after ROS exposure in various other experimental settings (Ermak and Davies, 2002; Touyz, 2005). To determine if increase in Ca^{2+} levels occurs in THP-1 cells after H_2O_2 treatment, the Fluo-4 NW Ca^{2+} assay kit (Molecular Probes) was used with H_2O_2-treated THP-1 cells. After H_2O_2 treatment, Ca^{2+} levels increased in a dose-dependent manner, with a maximal increase of 276 ± 75% (5 mM; Fig. 4.16). Changes in Ca^{2+} levels could play an important role in the regulation of Rho GTPases in response to H_2O_2.

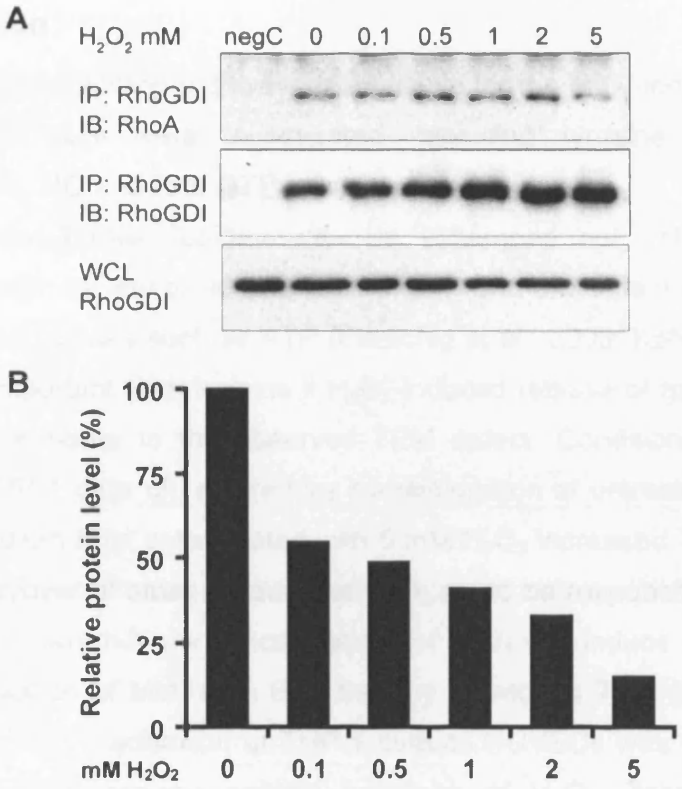

Figure 4.15: Interaction between RhoA and RhoGDI by H_2O_2
Cell lysates of H_2O_2-treated THP-1 cells (0 – 5 mM, 30 min, 37°C) were used for immunoblotting (WCL) or further incubated with immobilised RhoGDI and c-myc (negative control) antibodies (2 h, RT). Samples were immunoblotted with antibodies against RhoA and RhoGDI. **A**: Representative blot for RhoA immunoprecipitation with RhoGDI. **B**: Densitometric quantification: RhoA level were normalised to RhoGDI level and untreated control. Means of two experiments are displayed.

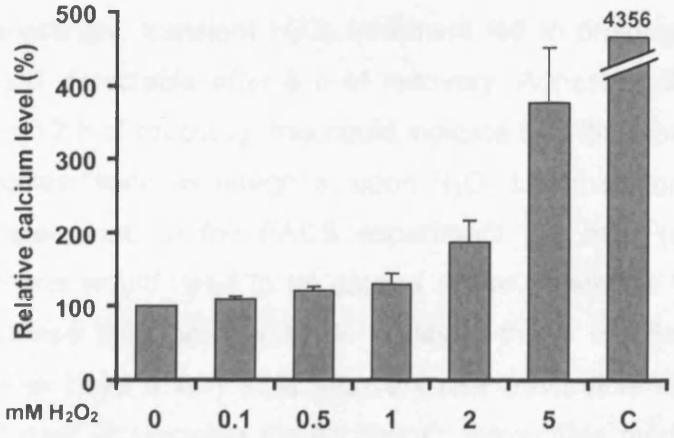

Figure 4.16: H_2O_2 induces Ca^{2+}-influx into THP-1 cells
Fluo-4 NW Ca^{2+} assay kit (Molecular Probes) was used according to the manufacturer's instructions with THP-1 cells treated with 0 – 5 mM H_2O_2 (30 min, 37°C) or 10 µM Ca^{2+} ionophore A23187 (C). Results are normalised to untreated control. Bars represent SEM. n = 3. Number above C indicates value of discontinued bar.

4.11 Discussion

In this chapter the signalling pathways responsible for the H_2O_2-induced decrease in TEM in THP-1 cells were investigated, including tyrosine phosphorylation, intracellular ROS, NO and Rho GTPases.

Endothelial barrier function can be influenced not only by binding of leukocytes but also by leukocyte secretion of pro- and anti-inflammatory mediators, e.g. TNF-α or nucleotides such as ATP (Eltzschig et al., 2003; Kofler et al., 2005). It was therefore important to determine if H_2O_2-induced release of mediators by THP-1 cells could contribute to the observed TEM defect. Conditioned medium from H_2O_2-treated THP-1 cells did not reduce transmigration of untreated cells. Instead, conditioned medium from cells treated with 5 mM H_2O_2 increased TEM significantly. Inadvertent carryover of small amounts of H_2O_2 could be responsible for this result, as it has been shown that low concentrations of H_2O_2 can induce signalling events, such as upregulation of MMPs, in ECs thereby promoting TEM (Deem and Cook-Mills, 2004). However, adhesion of THP-1 cells to HUVECs was not influenced by conditioned medium, arguing against carryover of H_2O_2. Taken together, this experiment demonstrates that H_2O_2-treated THP-1 cells do not secrete any anti-inflammatory mediators that could be responsible for the observed TEM defect in culture. However, it has to be taken into account that the concentrations of a potentially secreted mediator could be higher in the close proximity between THP-1 cell and endothelium. Although THP-1 cells seem to have a pro-inflammatory effect on HUVECs at high H_2O_2 concentrations, the H_2O_2-induced defects in the THP-1 cells do not allow efficient TEM.

Interestingly, transient H_2O_2 treatment led to prolonged decrease in TEM, which was still detectable after 6 h of recovery. Adhesion did not return to control levels within 12 h of recovery; this could indicate that long-term upregulation of adhesion molecules, such as integrins, upon H_2O_2 treatment occurred at later timepoints than determined in the FACS experiment (30 min) (see Fig. 3.11). Further FACS analysis would need to be carried out to determine the integrin cell surface levels at these later timepoints. In addition, these results indicated that targets of H_2O_2 either have a very slow recovery rate (reversible modifications) or need to be turned over (irreversible modifications). Reversible modifications could include oxidation of proteins, most likely of cysteine residues (Salmeen and Barford, 2005{Rhee, 2000 #361)Redox-sensitive proteins include PTPs, whose inactivation leads to a general increase in protein phosphorylation. It was therefore interesting to determine the phosphorylation status in H_2O_2-treated THP-1 cells. Preliminary and

non-quantitative data suggest that pTyr levels are elevated in H_2O_2-treated THP-1 cells when bound to VCAM-1 or HUVECs in response to H_2O_2, particularly in adhesive and motile structures such as podosomes and lamellipodia. To further investigate the role of Tyr phosphorylation in H_2O_2-treated THP-1 cells, the immunofluorescence images should be quantified to determine the increase in pTyr in different areas of the cell. Additionally, pTyr immunoblotting should be carried out to verify the total increase of tyrosine phosphorylation. To determine target proteins of H_2O_2-induced Tyr phosphorylation, co-immunoprecipitations with pTyr antibodies could be carried out and proteins with altered pTyr level identified by mass spectrometry. The role of individual phosphorylated proteins could be investigated by knocking them down using siRNA and possibly reintroducing the protein (e.g. the mouse homolog to prevent k-d) with point mutations that prevent phosphorylation. The role of Tyr phosphorylation in the H_2O_2-mediated decrease of THP-1 cell TEM could also be more generally investigated by preventing Tyr phosphorylation using specific inhibitors against kinases that are likely to play a role in the H_2O_2-mediated response, e.g. the redox-sensitive kinases Src and Pyk2 (Frank et al., 2000; Griendling et al., 2000).

Oxidation of cysteine residues can be reversed by reducing agents or by neutralising oxidants with antioxidants. Antioxidants can be broadly classified into hydrophilic and hydrophobic antioxidants; examples include ascorbic acid (vitamin C) and GSH or carotenes and α-tocopherol (vitamin E). An antioxidant commonly used in medical studies as well as cellular systems is NAC. NAC is a precursor of GSH, which provides the reducing equivalent for the reduction of H_2O_2 to H_2O (Veal et al., 2007). In THP-1 cells, NAC caused only marginal, statistically insignificant changes in TEM and adhesion. This could indicate that either NAC is not the right antioxidant to use or under resting conditions the cellular redox state inhibits TEM slightly, which can be reversed by antioxidants. For future experiments it would be interesting to use other antioxidants, e.g. the above mentioned vitamins or the recently developed cell-permeable peptide antioxidant SS-31 (Cho et al., 2007). However, if the redox state is relatively balanced with only a small excess in oxidants, adding antioxidants would only have a marginal effect. It was not possible to rescue the H_2O_2-induced TEM defect with subsequent NAC treatment, but the increase in adhesion at low H_2O_2 concentration was not observed in NAC-treated cells. Also, the use of PMA and AT, both substances that should increase the intracellular ROS level, led to more drastic inhibition of TEM than exogenous H_2O_2, while adhesion was unchanged. However, the intracellular ROS level in response to

PMA and AT were not measured, and it is therefore not possible to draw any conclusions about the involvement of intracellular ROS at this point. The intracellular ROS level in response to the various substances used (PMA, AT, fMLP, VEGF, ang II, thrombin, TNF-α and the solvent DMSO) should be measured to determine effective substances and concentrations. If intracellular ROS levels are indeed increased in response to PMA and AT, the results could suggest that production of intracellular ROS is more effective in reducing TEM, probably due to the increased proximity to its targets, as ROS concentration will be rapidly diminished with increasing diffusion distance.

This and the NAC data indicate that TEM and adhesion could be differently regulated by H_2O_2, e.g. by targeting different molecules. H_2O_2 could induce signalling cascades leading to the TEM defect that cannot be reversed by addition of antioxidants, whereas adhesion could be influenced by direct oxidative modification of adhesion proteins, which are reversible by antioxidants. To test the latter, specific dyes could be used; these label cysteine thiols (Cys-SH), but are unable to bind oxidised cysteine residues. Two-dimensional difference gel electrophoresis (2-D DIGE)-based redox proteomics and mass spectrometry can be used to determine targets of H_2O_2 treatment (Chan et al., 2005). However, 2-D DIGE of cell surface proteins has proven to be difficult due to the hydrophobic transmembrane domain of these proteins, making the use of specific detergents and procedures necessary.

Treatment of THP-1 cells with H_2O_2 led to a dose-dependent rise in NO. The NO increase was more prominent than ROS increase, suggesting that NO might play a crucial role in mediating H_2O_2 effects. However, limitations of the approach used might have prevented the detection of an early increase in intracellular ROS. Ryu et al. have reported an approximately 3-fold increase in intracellular ROS production when THP-1 cells were stimulated with 10 µM H_2O_2 for 1 h. In contrast to the approach taken in this study, Ryu et al. labelled with 5 µM H_2DCFDA prior to the stimulation with H_2O_2. This allows the detection of all the H_2O_2-induced ROS even at early time points, whereas in the case of this study the early increase in ROS during the H_2O_2 treatment phase might already have disappeared when the cells are subsequently labelled with H_2DCFDA. This approach was taken to define the intracellular redox state at the same time point when THP-1 cells are usually used in TEM and adhesion assays. However, to understand the dynamics of intracellular ROS levels in response to H_2O_2 treatment it would be advisable to label the cells

first with H_2DCFDA and then carry out a time-course of H_2O_2 treatment to determine intracellular ROS levels.

NO can be produced by NOS, which oxidise L-arginine to L-citrullin (Alderton et al., 2001). The major NOS present in leukocytes is iNOS. In THP-1 cells, preliminary data suggest that iNOS expression is rapidly upregulated upon H_2O_2 treatment. This dose-dependent upregulation was still detectable 6 h after H_2O_2 treatment, but was reversed within 12 h. In chondrocytes, O_2^- has been shown to mediate IL-1-induced IκB-α degradation and consequent NFκB activation and iNOS expression (Mendes et al., 2003). Additionally, iNOS is positively regulated by tyrosine phosphorylation (Pan et al., 1996), which is dependent on Src kinase (Hausel et al., 2006). The phosphorylation status of iNOS was not determined in this study, but it is tempting to speculate that iNOS is also activated via this pathway, as general tyrosine phosphorylation was increased after H_2O_2 treatment.

The involvement of NO in THP-1 TEM and adhesion was demonstrated by using a NO donor, which induced a similar TEM defect and increase in adhesion to H_2O_2. It was not possible to prevent the H_2O_2-induced decrease in TEM or increase in adhesion by pre-treating the cells with a NOS inhibitor. Although there is not enough evidence to conclude that NO mediates the observed H_2O_2 effects, the NO donor result is a strong indicator. Findings by others have also suggested a negative role of NO in TEM. Oka et al. have shown that NO derived from HUVECs accumulates in neutrophils and inhibits TEM, at least in part by activating soluble GC (Oka et al., 2005). NO has also been reported to reduce adhesion and TEM in spleen T cells by downregulating β1 integrin and matrix metalloprotease-9 (MMP9) expression (Sun et al., 2006). In a hepatic cell line, NO has been reported to inhibit PDGF-induced and Rac1-driven migration by preventing formation of filopodia (Lee et al., 2005). Application of the NO donor SNAP resulted in a comparable decrease in cellular protrusions as H_2O_2, suggesting that NO is mediating this event. Cellular protrusions are dependent on actin polymerisation, a process regulated by a large number of proteins. Key regulators of this process are Ena/VASP family members (Small et al., 2002). Application of NO donors led to rapid retraction of lamellipodia together with cell rounding in epithelial cells (Lindsay et al., 2007). This process was dependent on GC and type II cGMP-dependent protein kinase (PKG II)-mediated VASP phosphorylation at Ser239 (Lindsay et al., 2007), which has been shown to reduce its actin anti-capping and filament bundling activity (Barzik et al., 2005). NO is known to stimulate the production of cGMP (Katsuki et al., 1977). It is tempting to speculate that a similar pathway is activated in H_2O_2-treated THP-1 cells, leading to

the observed decrease in cellular protrusions. To demonstrate convincingly that NO mediates the H_2O_2-induced decrease in protrusions, it would be necessary to show that inhibition of NO production prevents this event. As L-NAME gave highly variable results, it is advisable to test different NOS inhibitors or NO scavengers to set up a rescue experiment.

These data suggest, that NO could be a mediator of the H_2O_2 effects in THP-1 cells. It is feasible to assume that the defect in TEM is at least partly due to the reduction in cellular protrusions. Cellular protrusions are important during TEM, by acting as exploratory extensions of the cell to probe the endothelium for suitable sites for diapedesis (Carman et al., 2007; Millan et al., 2006). Loss of these extensions is likely to reduce TEM, as was shown with H_2O_2 treatment.

Cellular protrusions are also regulated by Rho GTPases (Chapter 1.3.2.1). The regulation of Rho GTPase after H_2O_2 treatment was investigated. Preliminary data suggest that total levels of Rac1 were unaltered upon H_2O_2 treatment, whereas RhoA levels appeared to be increased. The high increase of RhoA levels at 5 mM was abrogated when cells were pre-treated with a proteasome inhibitor. ROS have been reported to cause modifications of proteins that may lead to changes in their susceptibility to proteolytic attack (Davies, 1987; Dean et al., 1986; Grune et al., 1997). Additionally, proteolysis can be inhibited by millimolar concentrations of H_2O_2 (Grune et al., 1997). These results could tentatively indicate a redox regulation of proteasomal degradation for RhoA. To address the question of proteasomal degradation further, the above described experiment should be repeated to confirm the results, other proteasome inhibitors (e.g. lactacystin) should be used and approaches should be taken to prevent polyubiquitination, e.g. by knocking-down components of the ubiquitination system, such as a RhoA-specific E3 ligase.

Rho GTPase activity in THP-1 cells after H_2O_2 treatment was investigated in adherent and suspension cells. RhoA, Rac1 and Cdc42 displayed similar, activation patterns in suspension cells with activation peaks at intermediate concentrations, whereas Rac1 and Cdc42 showed very different activation patterns in adherent THP-1 cells, while RhoA activation pattern remained similar. Rac1 activity was only marginally changed in suspension cells, but displayed a high activation peak at intermediate concentrations for adherent cells. Cdc42 activity was strongly decreased in a dose-dependent manner when cells were adherent, which was not observed in suspension cells. Rac1 and Cdc42 are known to be activated upon integrin binding (Ridley, 2001), which could explain the observed differences between suspension and adherent THP-1 cells.

Heo and Campbell have shown that in an *in vitro* system RhoA, Rac1 and Cdc42 are redox-sensitive, due to a unique motif containing the redox-sensitive Cys^{18} (Rac1 numbering) (Heo and Campbell, 2005). Oxidation of this site leads to GDP dissociation, but GTP association occurs only when the oxidative reagent is removed. RhoA has been shown to be subsequently inactivated through formation of an intramolecular disulphide bond thereby preventing activation by GTP binding (Fig. 4.17) (Heo et al., 2006). Rac1 has been shown to be activated in response to H_2O_2 in rat fibroblasts, leading to increased cell motility (Alexandrova et al., 2006). Rac1 is also activated in response to Ca^{2+}-elevating reagents, however, this activation is abrogated at high levels of Ca^{2+} (Jin et al., 2005; Price et al., 2003). Rac1 activity can also be regulated in a Ras- and Tiam1-dependent manner (Yamauchi et al., 2005). Ras has been shown to be S-nitrosylated at Cys118 by NO, leading to activation and downstream signalling (Lander et al., 1997). The observed increase in NO in this study could therefore induce Ras-dependent Rac1 activation. The pattern of Rac1 activation in adherent THP-1 cells reflected the changes in cell motility (see Fig. 3.13), in agreement with the well-characterised role of Rac1 as a regulator of cell migration (Ridley, 2001). Cdc42 has been shown to be involved in formation of cellular protrusions. For example, neutrophils from cdc42GAP-deficient mice display increased cdc42 activity and an increase in cellular protrusions and motility (Szczur et al., 2006). Cdc42 has also been shown to be important in chemokine-induced monocyte TEM, where expression of mutant Cdc42 led to a decrease in filopodia and subsequent TEM (Weber et al., 1998). The increased Ca^{2+} level could additionally contribute to the decrease in cellular protrusions by increasing contractility in a MLCK-dependent manner (Pfitzer, 2001). The observed decrease in Cdc42 activity in H_2O_2-treated THP-1 cells would therefore explain the reduction in cellular protrusions and consequential defect in TEM. The decrease in Cdc42 activity could be due to the oxidation of the redox-sensitive Cys^{18}, which would lead to dissociation of GDP but due to the presence of the oxidant no GTP binding, i.e. no activation occurs.

RhoA has been shown to be important during monocyte TEM. Inhibition of RhoA in monocytes with C3 transferase results in a TEM defect, while adhesion is not affected (Worthylake et al., 2001). RhoA inhibition leads to formation of long tails, which can not be retracted by migrating cells. Formation of long tails was not observed in H_2O_2-treated THP-1 cells, even at levels where RhoA activation was lowest. This indicates that H_2O_2-regulated RhoA activity is not likely to be important for the decrease in TEM. Nimnual et al. reported a redox regulation of RhoA activity

via ROS-dependent inactivation of LMW-PTP, leading to increased phosphorylation of p190RhoGAP and consequential downregulation of RhoA activity (Nimnual et al., 2003). RhoA has been shown to be phosphorylated at Ser188 by PKA or PKG (Ellerbroek et al., 2003). Serine phosphorylation leads to increased binding of RhoGDI, independent of nucleotide binding. RhoA is not only extracted from the plasma membrane and localises to the cytoplasm, but it has also been shown to be protected from ubiqutin/proteasome-mediated degradation by binding to RhoGDI (Rolli-Derkinderen et al., 2005). It could be speculated that H_2O_2-induced increase in NO could lead to PKG activation and subsequent RhoA phosphorylation, which could induce increased binding to RhoGDI. Preliminary data from RhoGDI co-immunoprecipitiation experiments did not confirm this; in fact, RhoA/RhoGDI interaction was decreased in H_2O_2-treated THP-1 cells in a dose-dependent manner. However, this decrease only became apparent when RhoA levels were normalised to RhoGDI levels. Further experiments are needed to confirm these observations. The pattern of potentially decreased interaction between RhoGDI and RhoA did not mirror the pattern of RhoA activity. While the increase in activity for 0.1 – 2 mM could be caused by decreased RhoGDI binding, inactivation at high levels must occur via different mechanisms. The downregulation by increased p190RhoGAP activity and inactivation of RhoA by formation of disulphide bonds might play a role at high H_2O_2 concentrations. RhoA activity has also been shown to be downregulated by cytoplasmic Ca^{2+} (Jin et al., 2005), which could explain the decrease in RhoA activity at high H_2O_2 levels, where a 4-fold increase in Ca^{2+} was observed.

RhoGDIs maintain Rho GTPases as soluble cytosolic proteins by forming complexes that shield the geranylgeranyl group, which normally targets the protein to the membrane (DerMardirossian and Bokoch, 2005). Prenylation of Rho GTPases is necessary to bind the respective RhoGDI (Nomanbhoy and Cerione, 1996) and has been shown to be negatively regulated by ROS in other proteins (Clark et al., 2004). It is tempting to speculate that RhoA binding to RhoGDI is decreased due to redox-induced changes in the prenylation status in H_2O_2-treated THP-1 cells. Additionally, RhoGDI has been shown to be phosphorylated at Tyr156 by Src, which causes a decrease in the ability to bind RhoA, Rac1 and Cdc42 (DerMardirossian et al., 2006). H_2O_2-induced Src activation could therefore lead to RhoGDI phosphorylation and a consequential decrease in RhoGDI/RhoA binding. It would be interesting to investigate the binding of Rac1 and Cdc42 to their respective GDIs in response to H_2O_2.

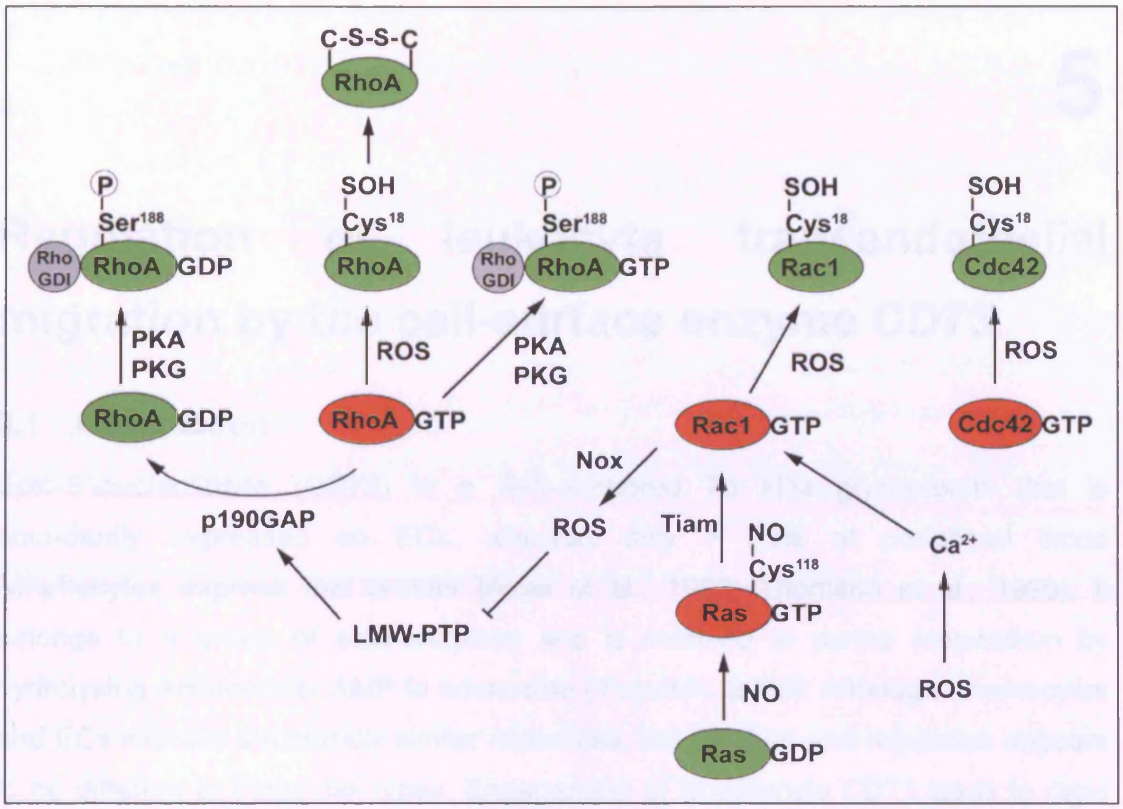

Figure 4.17: Regulation of Rho GTPases by H_2O_2 and NO
See text for details. Red: active Rho GTPase; green: inactive Rho GTPase.

In conclusion, H_2O_2 has multiple effects on THP-1 cells that lead to a dose-dependent decrease in TEM. The increase in intracellular NO is likely to play a crucial role by reducing formation of cellular protrusions, possibly through PKG-mediated phosphorylation of VASP. Additionally, downregulation of Cdc42 activity and a potential Ca^{2+}-induced contractility are likely to participate in the reduction of cellular protrusions. Rac1 activation at intermediate H_2O_2 concentrations, possibly Ca^{2+}-induced, probably accounts for the observed increase in motility, which might contribute to the decrease in TEM. On the other hand high Ca^{2+} levels at 5 mM H_2O_2 might be responsible for the decrease in Rho GTPase activity, particularly Rac1, which would have negative effects on TEM. Taken together, H_2O_2 has concentration-dependent effects on Rho GTPase activity in THP-1 cells, which could mediate the defects in motility and TEM.

5

Regulation of leukocyte transendothelial migration by the cell-surface enzyme CD73

5.1 Introduction

Ecto-5'-nucleotidase (CD73) is a GPI-anchored 70 kDa glycoprotein that is abundantly expressed on ECs, whereas only ~ 20% of peripheral blood lymphocytes express this protein (Airas et al., 1993; Thomson et al., 1990). It belongs to a group of ecto-enzymes and is involved in purine metabolism by hydrolysing extracellular AMP to adenosine (Yegutkin, 2008). Although lymphocytes and ECs express structurally similar molecules, the function and regulation appears to be different in these cell types. Engagement of lymphocyte CD73 leads to rapid surface shedding and induces LFA-1 clustering, thereby promoting lymphocyte binding to the endothelium (Airas et al., 2000; Airas et al., 1997). These events have not been observed in ECs and are thought to be independent of the enzymatic activity of CD73 (Jalkanen and Salmi, 2008). The enzymatic activity of CD73 produces adenosine, a highly anti-inflammatory purine, which exerts its effects via P1 type of purino-receptors (Hasko and Cronstein, 2004). Four types of adenosine receptors exist: A_1, A_{2A}, A_{2B} and A_3. Activation of endothelial adenosine receptor A_{2B} leads to cAMP-dependent activation of ERK1/2 and MLC phosphorylation (Lennon et al., 1998; Srinivas et al., 2004). However, elevated cAMP levels also activate pathways involving the inactivation of MLCK and/or ROCK leading to MLC dephosphorylation. This pathway seems to be dominant, since the net result of elevated cAMP levels is MLC dephosphorylation, which leads to relaxation of the endothelium, thereby increasing endothelial barrier function. Adenosine-induced cAMP also increases barrier function by PKA-mediated phosphorylation of VASP, which thereupon is localised to junctions and co-localises with ZO-1 (Comerford et al., 2002). In addition to increasing endothelial barrier function, adenosine inhibits NF-κB-mediated upregulation of adhesion molecules including P-selectin, E-selectin and VCAM-1 (De Martin et al., 2000; McPherson et al., 2001; Minguet et al., 2005; Walker et al., 1999). The regulation of ICAM-1 by adenosine is unclear; while Bouma et al. did not see an adenosine-mediated decrease in ICAM-1 levels (Bouma

et al., 1996), others have demonstrated inhibition of ICAM-1 expression in response to adenosine analogues/A_{2A} receptor antagonists (McPherson et al., 2001; Walker et al., 1999).

Endothelial CD73 activity has been shown to be inhibited upon leukocyte binding (Henttinen et al., 2003). The residual adenosine is rapidly degraded to inosine by ADA, a soluble enzyme that is bound to the lymphocyte surface via CD26 (Gorrell et al., 2001; Martin et al., 1995). This leukocyte-mediated CD73 inhibition is cell number-dependent and is likely to occur by selective masking and inhibition of the catalytic site, presumably via a temporal and non-competitive mechanism and might be a requisite for subsequent leukocyte TEM into the tissue. The exact mechanism of inhibition is currently unknown, but the structure of CD73 has given some hints as to how it might be achieved. A sequence comparison between *E. coli* and vertebrate 5'-nucleotidase has revealed a sequence identity of only > 20%, but several clusters of highly conserved residues were found (Knofel and Strater, 1999). X-ray crystallography has shown that *E. coli* 5'-nucleotidase consists of two domains: the N-terminal domain coordinates two catalytic divalent metal ions, whereas the C-terminal domain provides the substrate specificity pocket for the nucleotide. These domains are conserved in mammalian CD73 and a homology model predicted a similar domain structure (Strater, 2006). *E. coli* 5'-nucleotidase has been shown to undergo a hinge-bending domain rotation of 96° in order to hydrolyse AMP to adenosine, presumably to allow substrate binding and product release (Schultz-Heienbrok et al., 2005). From the predicted homology model it seems likely that mammalian CD73 undergoes a similar rotation and regulation of the enzymatic activity (Strater, 2006).

CD73 is highly expressed in many tumour cells, but its specific function in tumourigenesis is unclear. Sadej et al. showed that among different melanoma cells, upregulated CD73 expression is associated with a highly invasive phenotype (Sadej et al., 2006). It correlates with a number of metastasis-related markers and might therefore have a role in this process. Overexpression of CD73 in two breast cancer cell lines (T-47D and MB-MDA-231) leads to increased invasion, migration and adhesion to ECM, which can be blocked by a specific CD73 inhibitor (Wang et al., 2008). RNA interference (RNAi) of CD73 in a breast cancer cell line (MB-MDA-231) has been shown to inhibit cell growth, invasion and migration (Zhi et al., 2007). This confirms a role for CD73 in tumourigenesis. RNAi has rapidly become the predominant means of assessing loss of gene function (Sen and Blau, 2006). It allows quick and selective knock-down (k-d) of the gene of interest by transiently

introducing short interfering RNA (siRNA), a class of 20-25 nucleotide-long double-stranded RNA molecules, or by transiently or stably transfecting cells with vector-based short hairpin RNAs (shRNA) (Leung and Whittaker, 2005).

The aim of this chapter is to investigate the role of endothelial CD73 in inflammation. I aim to further the understanding of the protein's enzymatic and non-enzymatic functions during the binding and transendothelial migration of leukocytes.

5.2 CD73 is localised in lipid rafts

There are multiple 5'-nucleotidases: five cytoplasmic 5'-nucleotidases, one mitochondrial and one extracellular ecto-5'-nucloetidase, which is bound to the plasma membrane via a GPI anchor. This study will focus on the function of ecto-5'-nucleotidase and the term 'CD73' will be used to refer to this protein only.

The localisation of CD73 in HUVECs was determined by immunofluorescence. In a confluent monolayer, where cells were not permeabilised, the staining pattern was evenly distributed and dot-like with accumulations at the cell periphery (Fig. 5.1A). This could indicate that CD73 is localised in cell-cell junctions. To determine if this was the case, HUVECs were seeded at a lower density and stained with antibodies against CD73 and the junctional marker β-catenin. CD73 was accumulated around the cell edges even if there was no contact to neighbouring HUVECs (Fig. 5.1B, arrow). Additionally, no co-localisation with β-catenin or similar distribution pattern could be detected. This indicates, that CD73 is not localised in endothelial junctions. The seeming localisation to cell junctions could be due to the membrane curvature at the cell edges, which could lead to the impression of an accumulation.

CD73 has been reported to be localised in microdomains such as caveolae and lipid rafts in other cell types (Ludwig et al., 1999; Monastyrskaya et al., 2003; Sadej et al., 2006; Strohmeier et al., 1997). To address if endothelial CD73 was localised in such microdomains, HUVECs were labelled with antibodies against CD73 and the caveolar marker Cav-1 or the lipid raft marker CD59 (Fig. 5.2A, B). While no co-localisation with Cav-1 could be detected, CD73 partially co-localised with CD59 indicating that some CD73 is localised in CD59-containing rafts. This result was verified by raft fractionation using OG-selective solubility. CD73 was mainly localised in the soluble fraction, but a small portion could be detected in the raft fraction (Fig. 5.2C). Catalase was used as a marker for cytosolic proteins in the raft fractionation and was only detected in the soluble fraction, indicating a clean

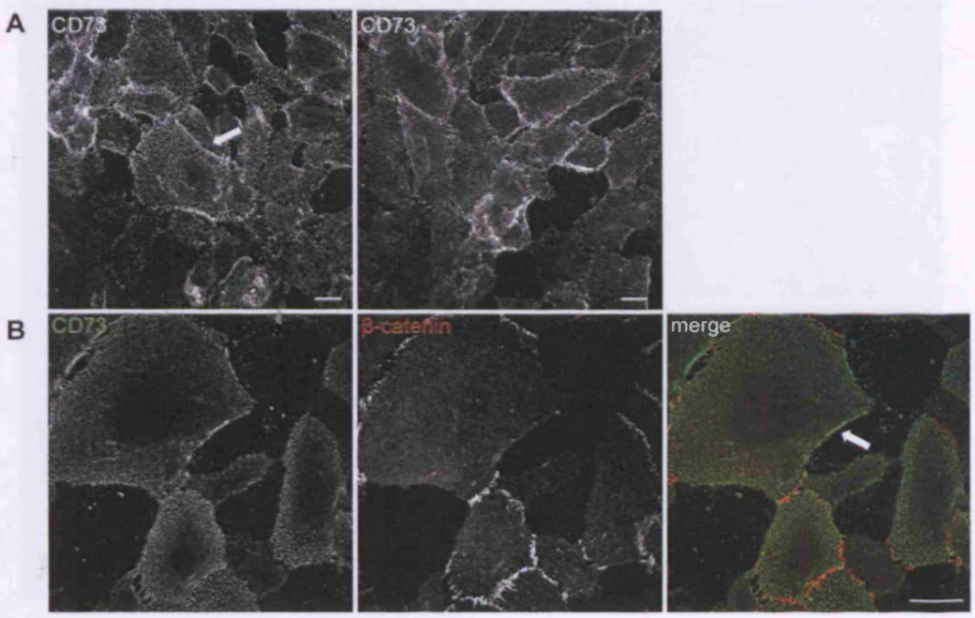

Figure 5.1: CD73 is not localised in endothelial junctions
HUVECs were sequentially labelled with an antibody for CD73 (4°C, 30 min) and AlexaFluor488-conjugated secondary antibody (4°C, 20 min), before being fixed and either mounted onto microscopy slides (**A**) or further labelled with antibodies against β-Catenin (**B**). Arrows indicate sites of CD73 accumulation. Bar = 20 µm.

fractionation. CD59 was mainly found in the raft fraction with some localisation in the soluble as well as the nuclear fraction. The nuclear localisation could be artefactual since CD59 is not known to localise in the nucleus.

5.3 CD73 appears to be localised around transmigrating leukocytes

In order to determine the role of CD73 in TEM, CellTracker™-labelled THP-1 cells or unlabelled T lymphoblasts were allowed to transmigrate across TNF-α-stimulated HUVECs. Co-cultures of HUVECs and T lymphocytes were labelled with antibodies against CD73 and Cav-1, which has been shown to localise around transmigrating T lymphocytes (Millan et al., 2006), and z-stacks were acquired using a confocal microscope. Cav-1 and CD73 both appeared to accumulate around adherent T lymphocytes, but no co-localisation could be detected confirming that CD73 is not localised in caveolae (Fig. 5.3). Co-cultures of HUVECs and THP-1 cells were labelled with antibodies against CD73 and z-stacks were acquired. CD73 appeared to accumulate around transmigrating THP-1 cells, in particular at the area of interaction between the apical surface of the leukocyte protrusion and the basal

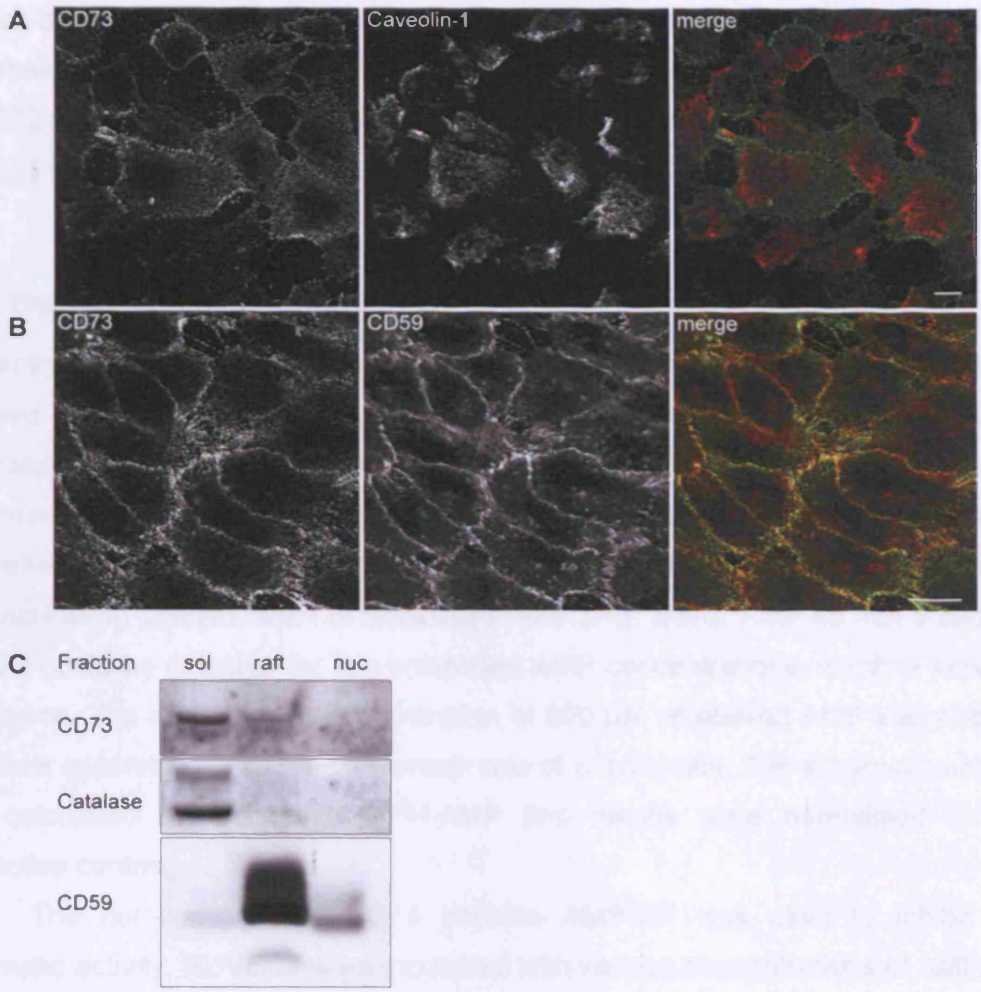

Figure 5.2: CD73 is partially localised in lipid rafts
HUVECs were sequentially labelled with an antibody for CD73 (4°C, 30 min) and AlexaFluor488-conjugated secondary antibody (4°C, 20 min), before being fixed and further labelled with antibodies against Cav-1 (**A**) or CD59 (**B**). Bar = 20 µm. **C**: For raft fractionation by OG-selective solubility, HUVECs were lysed in OG-free buffer, lysates were centrifuged at 18 500 g and supernatants were retained as soluble fraction (sol), while the pellet was further lysed with a buffer containing OG. Lysates were centrifuged at 18 500 g and supernatants were retained as raft fraction (raft), while the pellet was further lysed and represented the nuclear fraction (nuc). Samples were immunoblotted with antibodies against CD73, catalase (soluble marker) and CD59 (raft marker).

surface of HUVECs (Fig. 5.4 arrow). This could be indicative for a role of CD73 as an adhesion protein or in guidance during TEM. To determine the exact localisation of CD73 during leukocyte TEM, transmission electron microscopy and immunogold labelling would need to be carried out.

5.4 Detection of CD73 activity by radio-thin layer chromatography

The enzymatic activity of CD73 converts AMP to adenosine. The activity can be assayed by radio-TLC using tritium-labelled AMP (^{3}H-AMP) and unlabelled AMP, separation of the nucleotides by TLC and detection by tritium-sensitive film. To determine optimal conversion of ^{3}H-AMP, different timepoints and concentrations of unlabelled AMP were tested. As expected, the conversion of ^{3}H-AMP was slower with increasing concentration of unlabelled AMP (Fig. 5.5A). After 45 min a second product could be detected for low unlabelled AMP concentrations, which is likely to be inosine. The intermediate concentration of 200 µM unlabelled AMP was chosen for future experiments, as the conversion was at a good rate. The enzymatic activity was calculated as ^{3}H-adenosine/^{3}H-AMP and results were normalised to the respective control.

The non-hydrolysable CD73 inhibitor AMP-CP was used to inhibit the enzymatic activity. HUVECs were incubated with various concentrations of AMP-CP before the enzymatic activity was determined by radio-TLC. A concentration of 50 µM AMP-CP gave the best inhibitory effect, with 57% inhibition (Fig. 5.5B). This concentration was used in future experiments. The less efficient inhibition at high AMP-CP concentrations could be due to decreased specificity, where other pathways could be activated/inhibited.

The binding of leukocytes to the endothelium has been shown to inhibit endothelial CD73 in a cell number-dependent manner (Henttinen et al., 2003). To determine the optimal number of THP-1 cells for future experiments, different cell numbers were allowed to adhere to TNF-α-activated (10 ng/ml, 15 - 18 h) HUVECs before the enzymatic activity was determined. THP-1 cells have no detectable CD73 activity under these conditions (data not shown). As expected, endothelial CD73 activity was decreased in a cell number-dependent manner, with a maximal decrease of 63%. For future experiments, 3 x 10^5 THP-1 cells per 24-well were chosen since this cell number had a leukocyte/HUVEC ratio of roughly 1.5:1. This number of THP-1 cells inhibited the enzymatic activity by ~ 20%. Under conditions where higher inhibition was needed, 1 x 10^6 THP-1 cells were used, resulting in a leukocyte/HUVEC ratio of roughly 5:1 and ~ 50% inhibition.

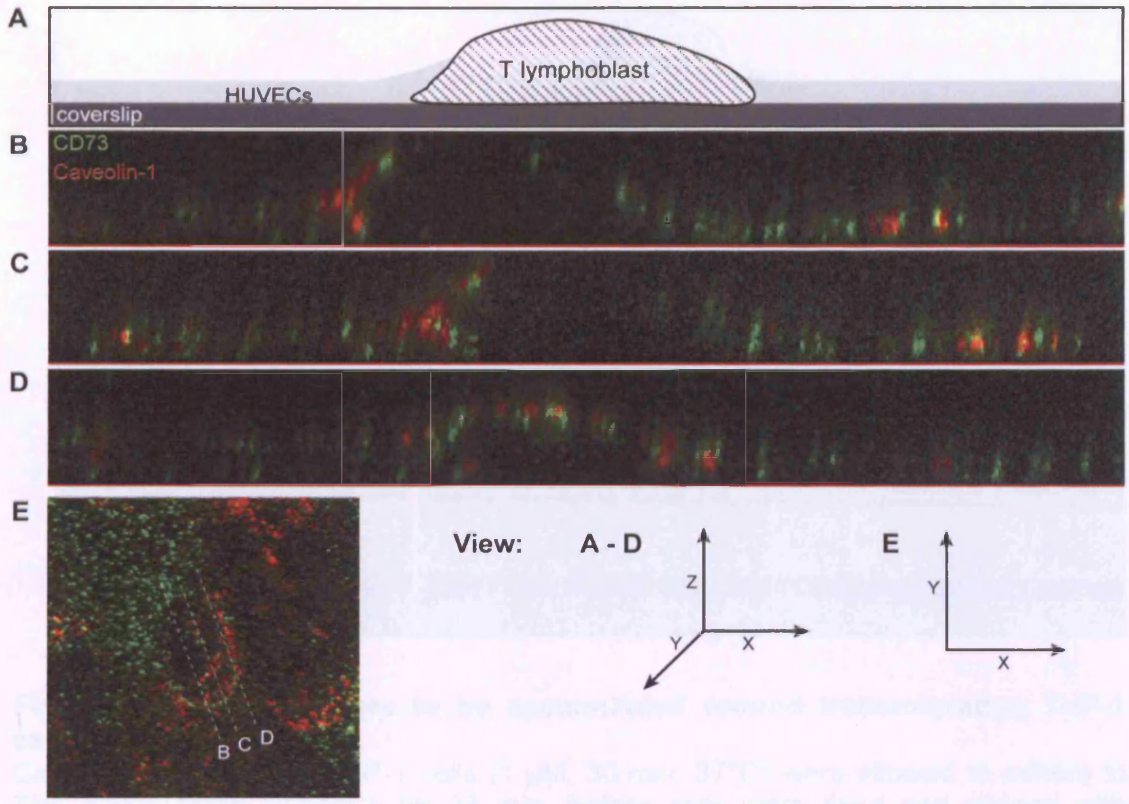

Figure 5.3: CD73 appears to be accumulated around adherent T lymphoblasts
T lymphoblasts were added to TNF-α-stimulated HUVECs for 12 min, before cells were fixed and stained with antibodies against CD73 and Cav-1. Z-stack confocal sections were taken using a Zeiss LSM510. **A**: Schematic of adherent T lymphoblast and HUVEC monolayer. **B - D**: Z-stacks of the same cell are displayed for different values of Y. **E**: Projection of Z-stack. Dotted lines indicate the approximate localisation of sections B – D.

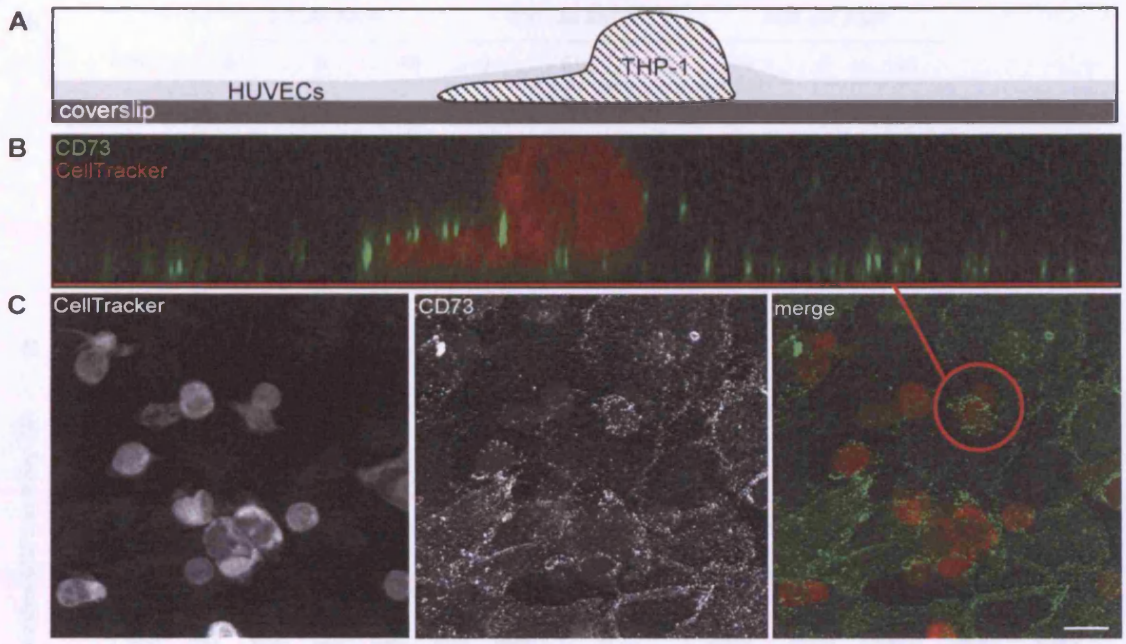

Figure 5.4: CD73 appears to be accumulated around transmigrating THP-1 cells
CellTracker™-labelled THP-1 cells (1 µM, 30 min, 37°C) were allowed to adhere to TNF-α-stimulated HUVECs for 25 min, before cells were fixed and stained with antibodies against CD73. Z-stack confocal sections were taken using a Zeiss LSM 510. **A**: Schematic of transmigrating THP-1 cell and HUVEC monolayer. **B**: Z-stack of THP-1 cell in zy-plane. **C**: Projection of Z-stack. Bar = 20 µm.

5.5 Cross-linking of ICAM-1 and VCAM-1 does not induce inhibition of CD73

Since one of the first steps of leukocyte binding is the interaction of leukocyte integrins with endothelial adhesion molecules such as ICAM-1 and VCAM-1, the effect of engagement of ICAM-1 or VCAM-1 on CD73 inhibition was tested. To this end, ICAM-1, VCAM-1 and CD73 were clustered with antibodies and CD73 enzymatic activity was determined. Cross-linking of adhesion molecules has been shown to induce intracellular signalling, by mimicking leukocyte binding (van Wetering et al., 2003). Clustering of ICAM-1 and VCAM-1 with antibodies did not induce CD73 inhibition when compared to IgG_1 control (Fig. 5.6A). Only cross-linking with CD73 antibodies induced inhibition of the enzymatic activity by 65.1 ± 2.9% of IgG_1 control, or 55.8 ± 2.9% of untreated control. Binding of CD73 antibody without cross-linking induced a similar inhibition. These results indicate that ICAM-1

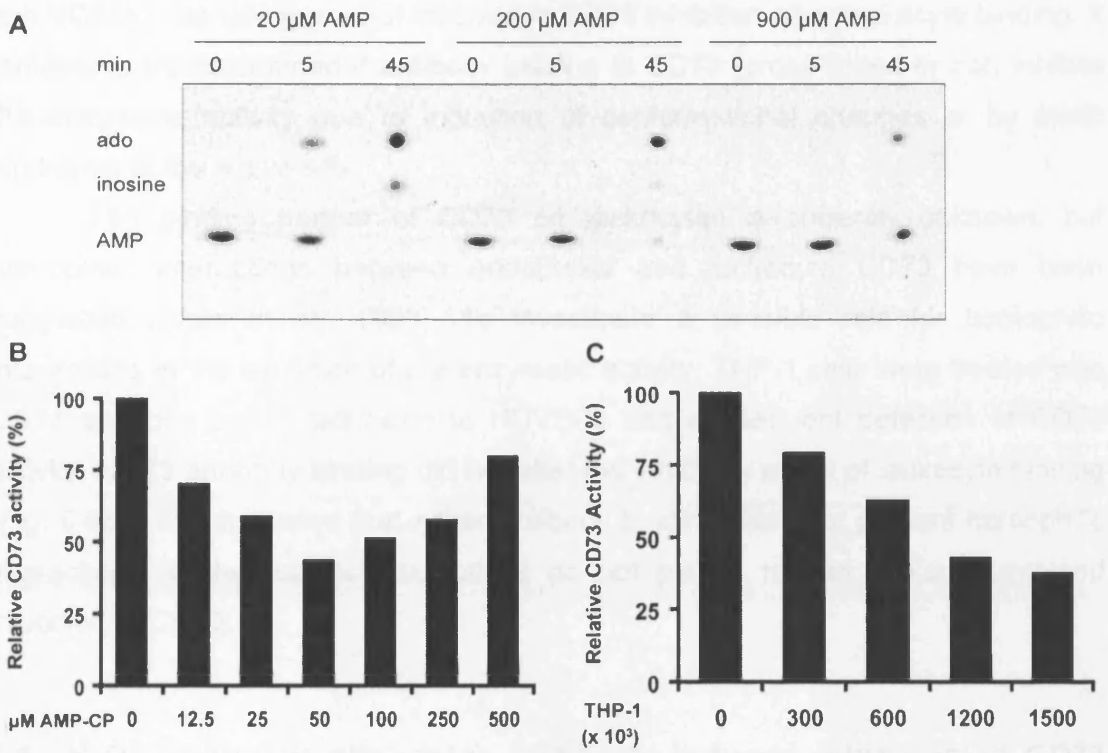

Figure 5.5: Endothelial CD73 enzymatic activity is inhibited by THP-1 cell binding

CD73 activity was determined by radio-TLC procedures. HUVECs were incubated with ^{3}H-AMP (180 µM) and unlabelled AMP. Aliquots of the supernatant were applied to TLC plates and nucleotides were separated using isobutyl alcohol/isoamyl alcohol/2-ethoxyethanol/ammonia/H_2O (ratio 9:6:18:9:15) as a solvent. ^{3}H-nucleotides were visualised using ^{3}H-sensitive film. CD73 activity was calculated as ^{3}H-adenosine/^{3}H-AMP and results were normalised to untreated control. **A**: HUVECs were incubated for 0 – 45 min with ^{3}H-AMP and 20 – 900 µM unlabelled AMP. A representative autoradiograph is shown. **B**: HUVECs were treated with CD73 inhibitor AMP-CP (0 – 500 µM, 60 min, 37°C) before incubation with ^{3}H-AMP/AMP (180/200 µM, 10 min, 37°C) and subsequent detection of CD73 activity by TLC. Mean of two experiments is shown. **C**: Indicated numbers of THP-1 cells were added to TNF-α-stimulated HUVECs for 25 min, before incubation with ^{3}H-AMP/AMP (180/200 µM, 10 min, 37°C) and subsequent detection of CD73 activity by TLC.

and VCAM-1 signalling are not involved in CD73 inhibition after leukocyte binding. It remains to be determined if antibody binding to CD73 (cross-linked or not) inhibits the enzymatic activity due to induction of conformational changes or by steric hindrance of the active site.

The binding partner of CD73 on leukocytes is currently unknown, but homophilic interactions between endothelial and leukocyte CD73 have been suggested (Airas et al., 1993). To investigate a possible role for homophilic interactions in the inhibition of the enzymatic activity, THP-1 cells were treated with CD73 antibody before adhesion to HUVECs and subsequent detection of CD73 activity. CD73 antibody binding did not alter the inhibitory effect of leukocyte binding (Fig. 5.6B). This indicates that either antibody binding does not prevent homophilic interactions, or homophilic interactions do not play a role in leukocyte-induced inhibition of CD73.

5.6 H_2O_2 treatment attenuates leukocyte-induced inhibition of CD73 activity

In rat hepatocytes, CD73 has been shown to be susceptible to oxidative modification (Kocic et al., 2001) and ROS-scavenging substances decreased the elevated CD73 activity in patients with obese type 2 diabetes (Stefanovic et al., 2005). To investigate if endothelial CD73 was regulated by H_2O_2, CD73 enzymatic activity was determined in HUVECs that had previously been treated with or without H_2O_2 or been incubated with H_2O_2-treated THP-1 cells. HUVECs were treated with 10 µM H_2O_2, this concentration was chosen since ECs have been shown to produce ROS in the low µM range (Deem and Cook-Mills, 2004). HUVEC treatment with H_2O_2 had no effect on the enzymatic activity at the tested concentration (Fig. 5.6C). Treatment of THP-1 cells with increasing concentrations of H_2O_2 though had a significant effect on their ability to inhibit endothelial CD73 compared to untreated THP-1 cells. Untreated THP-1 cells induced 52.5 ± 5.6% inhibition; whereas THP-1 cells treated with 5 mM H_2O_2 induced only 30 ± 9.9% inhibition, resulting in a 22.5% difference between untreated and H_2O_2-treated cells.

This result indicates that CD73 inhibition could be mediated by direct interaction with a cell surface molecule on the leukocyte surface. This binding partner could be modified by H_2O_2 treatment, which would lead to less effective inhibition after binding to the endothelium.

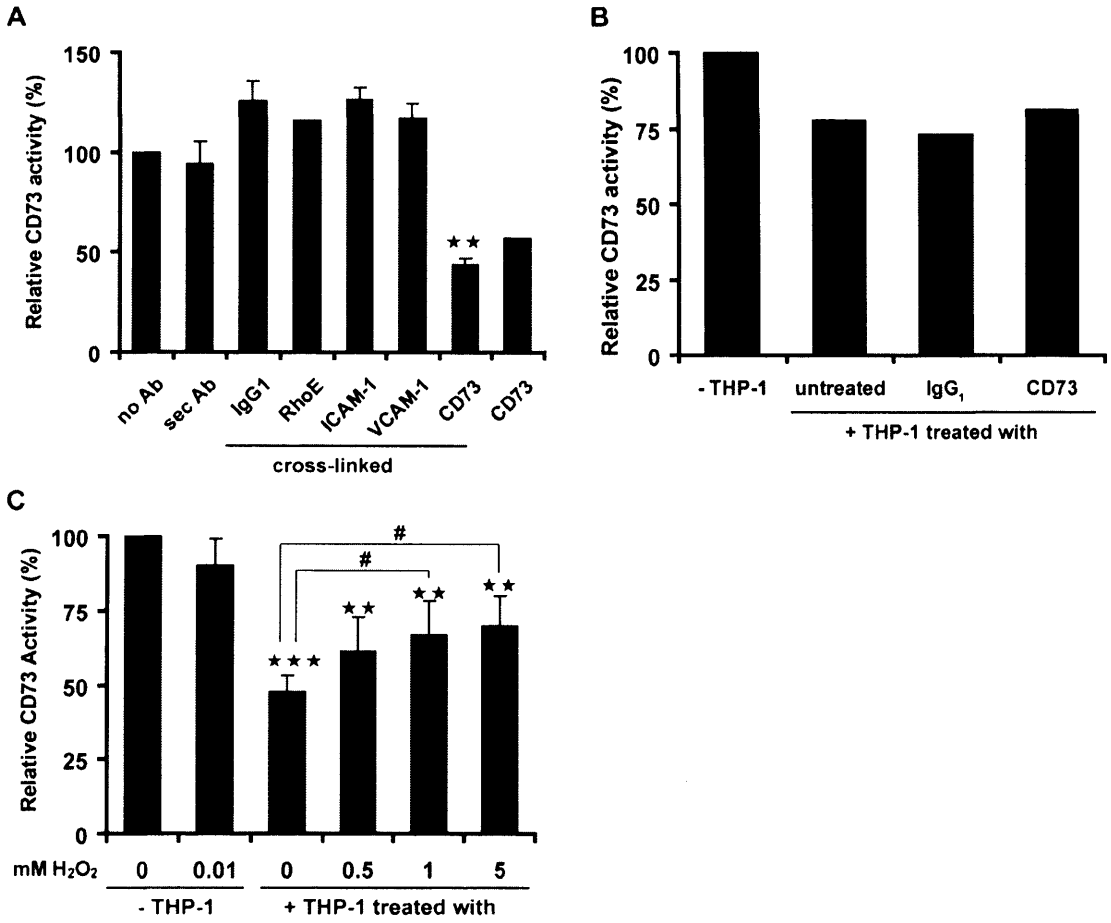

Figure 5.6: Regulation of CD73 activity in ECs
A: TNF-α-stimulated HUVECs were washed and cross-linking was carried out with antibodies against ICAM-1 (1/100), VCAM-1 (1/100), RhoE (undiluted) or CD73 (undiluted) (30 min, 4°C). Monolayers were washed and either incubated with FITC-conjugated anti-mouse antibody (1/100) or PBS only (20 min, 37°C). Controls included HUVECs incubated with no antibody, only secondary antibody or IgG_1 negative control (30 min, 4°C). CD73 activity was detected by radio-TLC. $n \geq 3$, except for RhoE and CD73 without cross-linking, where mean of two experiments is shown. **B**: THP-1 cells (3×10^5) were either incubated with IgG_1 or CD73 antibodies (30 min, 4°C) or left untreated before cells were washed and added to TNF-α-stimulated HUVECs for 25 min. Unbound THP-1 cells were washed off and CD73 activity determined by radio-TLC. Means of two experiments are shown. **C**: 1×10^6 THP-1 cells were treated with H_2O_2 (0 – 5 mM, 30 min, 37°C) before being added to TNF-α-stimulated HUVECs for 25 min. HUVECs were treated with or without 0.01 mM H_2O_2 (30 min, 37°C). CD73 activity in all samples was measured using radio-TLC. n = 6. Results are normalised to 'no Ab' (A), '-THP-1' (B) or '-THP-1 0 H_2O_2' (C). Bars represent SEM. ★★★ $p < 0.001$, ★★ $p < 0.01$, ★ $p < 0.05$ determined by Student's t-test and Bonferroni post-test, compared to 'no Ab' (A), or '-THP-1 0 H_2O_2' (C); # $p < 0.05$ determined by two-way ANOVA.

5.7 Localisation does not influence enzymatic activity and *vice versa*

The cell surface enzyme CD39 has been shown to be partially localised in lipid rafts and cholesterol-depletion with MβCD results in a strong inhibition of the enzymatic activity (Papanikolaou et al., 2005). To test if CD73 activity is dependent on the raft localisation, ECs were subjected to cholesterol-depletion before CD73 activity was determined. To demonstrate effective cholesterol depletion, HUVECs were labelled with filipin, a highly fluorescent cholesterol marker. After 15 min of incubation with MβCD, a large proportion of membrane cholesterol was depleted (Fig. 5.7A). The proportion increased with longer incubation times, but since these can also lead to cell damage the 15 min incubation time was used in all future experiments. The enzymatic activity of CD73 was determined in cholesterol-depleted HUVECs either in the absence (- s) or presence (+ s) of serum. Serum is a source of cholesterol and can therefore interfere with the depletion, but at the same time contributes to the viability of the cells. Cholesterol-depletion had no effect on CD73 activity (Fig. 5.7B), indicating that unlike CD39, CD73 activity is not dependent on raft localisation.

To determine if inhibition of CD73 leads to relocalisation of the protein, immunofluorescence staining with AMP-CP-treated HUVECs was carried out. Confluent HUVEC monolayers were incubated with different concentrations of AMP-CP and cells were stained for CD73 and F-actin (Fig. 5.8A - C). CD73 localisation was not detectably altered by the inhibitor, but HUVECs appeared more elongated when treated with AMP-CP. To determine if CD73 inhibition influenced the localisation during TEM, HUVECs were incubated with different concentrations of AMP-CP before THP-1 cells were allowed to transmigrate. Cells were fixed and stained for CD73, the junctional marker ZO-1 and F-actin. CD73 localisation was not changed upon incubation of the inhibitor: it was still localised around transmigrating leukocytes (Fig. 5.8D - F). Therefore, CD73 enzymatic activity does not influence localisation of the protein.

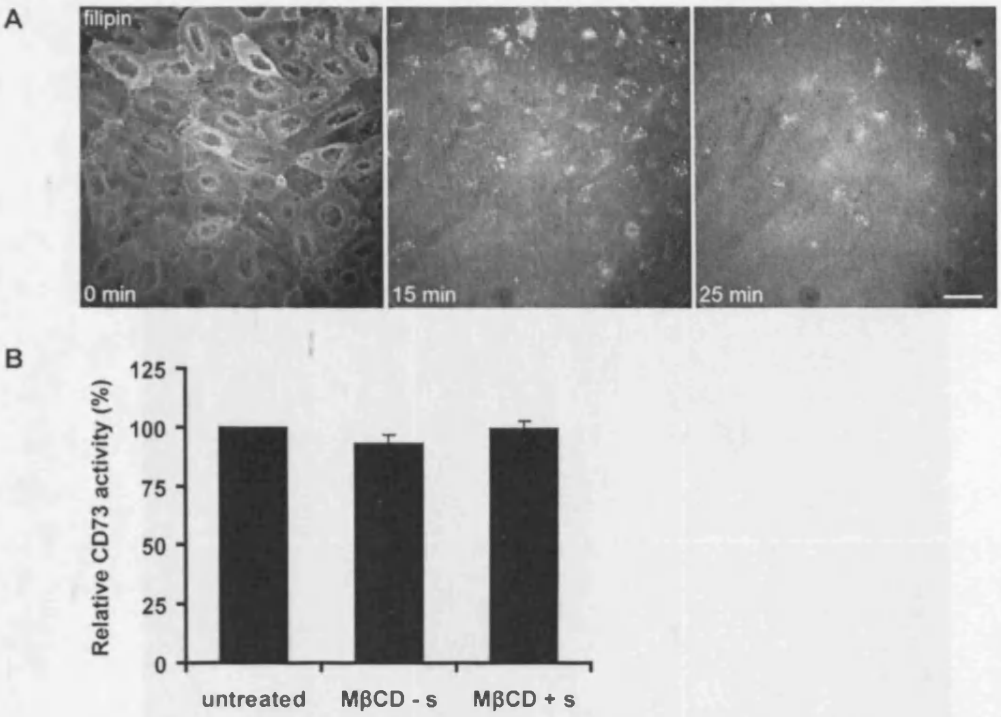

Figure 5.7: Raft localisation is not obligatory for CD73 activity
HUVECs were cholesterol-depleted by treatment with 4 mg/ml MβCD. **A**: Efficiency of cholesterol depletion (0 – 25 min, 37°C) was visualised by filipin staining and fluorescent microscopy. Bar = 50 µm. **B**: CD73 activity was determined in cholesterol-depleted HUVECs (15 min, 37°C) by radio-TLC either in the presence (MβCD + s) or absence (MβCD - s) of serum.

5.8 CD73 inhibitor reduces transendothelial migration

Having characterised CD73 in HUVECs, it was interesting to investigate the role of CD73 enzymatic function in leukocyte TEM by studying the effects of AMP-CP. To this end, TNF-α-activated (10 ng/ml, 15 - 18 h) HUVECs were incubated with different concentrations of AMP-CP before addition of THP-1 cells or T lymphoblasts. TEM was monitored by TLM and results were normalised to the respective untreated control. Preliminary data suggest that THP-1 TEM is decreased for 50 – 250 µM AMP-CP and increased for high concentrations (Fig. 5.9A). For T lymphocytes, TEM was not altered significantly (Fig. 5.9B). The discrepancy between the two cell types could be due to two factors: firstly, different expression levels of leukocyte CD73; and secondly, differences in the expression level of ADA leading to different concentrations of remaining adenosine.

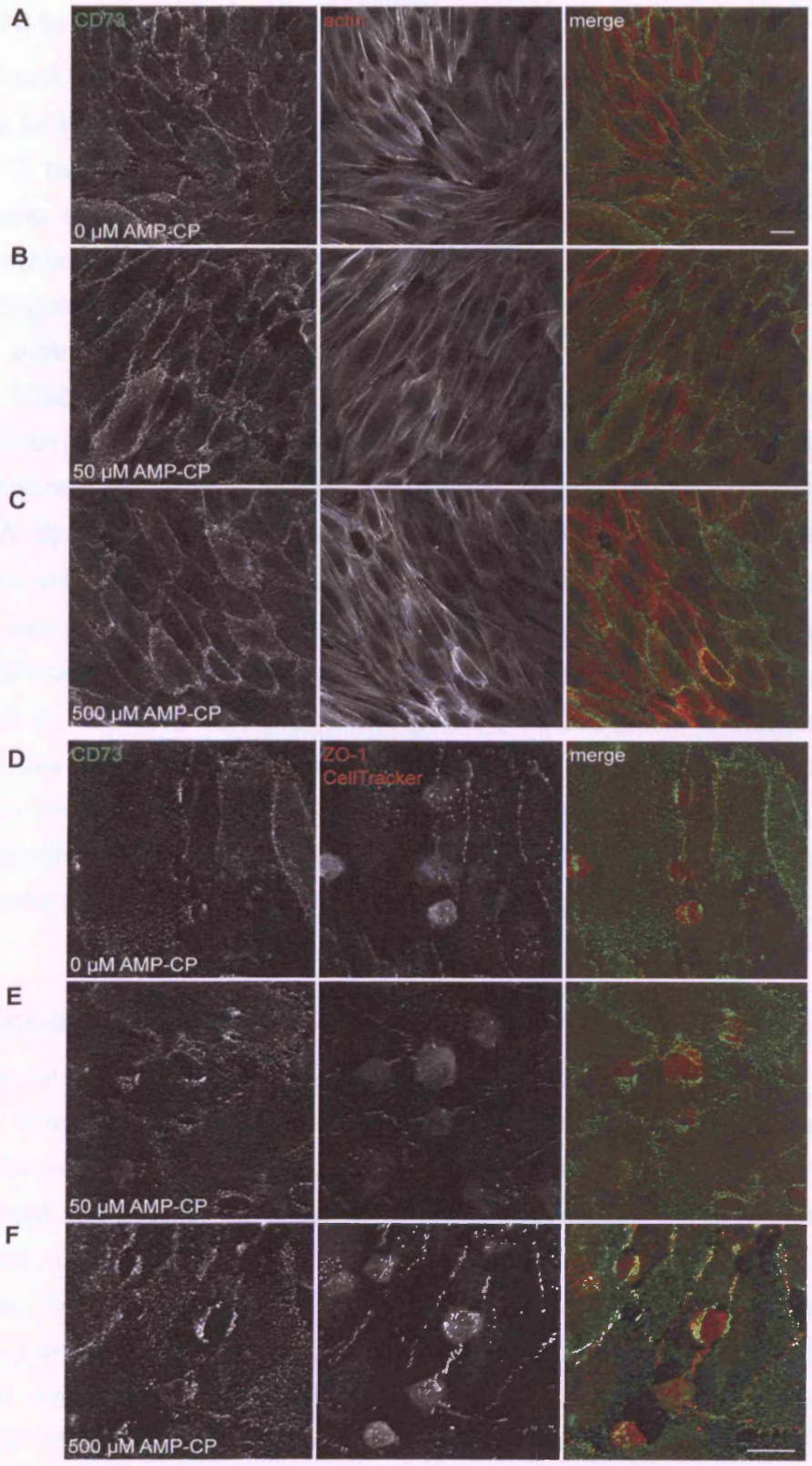

Figure 5.8: CD73 localisation is independent of enzymatic activity
HUVECs were treated with TNF-α for 15 – 18 h and subsequently with AMP-CP (0 – 500 µM, 60 min, 37°C). **A – C**: HUVECs were labelled with specific antibodies against CD73 and phalloidin to visualise F-actin. **D - F**: CellTracker™-labelled THP-1 cells were added to TNF-α-stimulated HUVECs for 25 min before cells were fixed and stained for CD73, ZO-1 and F-actin. Bar = 20 µm.

5.9 CD73 is only partially cleaved by PI-PLC

Having shown that inhibition of CD73 enzymatic activity influences TEM, it was interesting to investigate how removal of CD73 from the surface would influence TEM. CD73 has been proposed to have functions independent of its enzymatic activity (Airas et al., 1995; Airas et al., 2000; Airas et al., 1993). To address the question of whether these functions could play a role in leukocyte TEM, PI-PLC was used to cleave CD73 from the surface. PI-PLC has been shown to cleave GPI-anchored proteins and lead to their shedding from the surface (Ferguson and Williams, 1988; Low and Saltiel, 1988). PI-PLC efficiency in HUVECs was determined by immunofluorescence staining, FACS analysis and immunoblotting. PI-PLC treatment did not alter HUVEC morphology, as revealed by F-actin staining (Fig. 5.10A, B). CD73 on the surface was reduced, but FACS analysis showed that levels were only decreased by 54.2 ± 6.8% (Fig. 5.10C). To examine if PI-PLC-treatment was efficient, lysates from treated HUVECs were immunoblotted against CD59, a GPI-anchored marker of lipid rafts. CD59 was almost completely shed from the surface at 0.05 U/ml PI-PLC, indicating that the treatment was efficient (Fig. 5.10D). It has been shown that some GPI-anchored proteins are resistant to cleavage by PI-PLC due to an inositol acylation of the GPI anchor at an early stage in their biosynthesis (Englund, 1993; Wong and Low, 1992). The results from the PI-PLC treatment suggest that CD73 could contain this modification.

5.10 Knock-down of CD73 in HUVECs by RNAi

Since removal of CD73 from the surface with PI-PLC was not efficient, a k-d approach using siRNA was carried out. Multiple siRNA oligonucleotides from different companies (Dharmacon oligos #1 - #4, Ambion oligo (A), Qiagen oligos #1 - #5) were used (separately) per gene. Since the majority of the experiments were carried out with the oligos from Dharmacon, the term 'oligo xy' refers to the Dharmacon oligo numbering only. The use of multiple oligos allows distinction between k-d and off-target effects. As controls, HUVECs were mock-transfected or transfected with a non-targeting siRNA control oligo (siControl; siC). In all experiments HUVECs were used 72 h after transfection and results were normalised to siControl sample, unless otherwise stated.

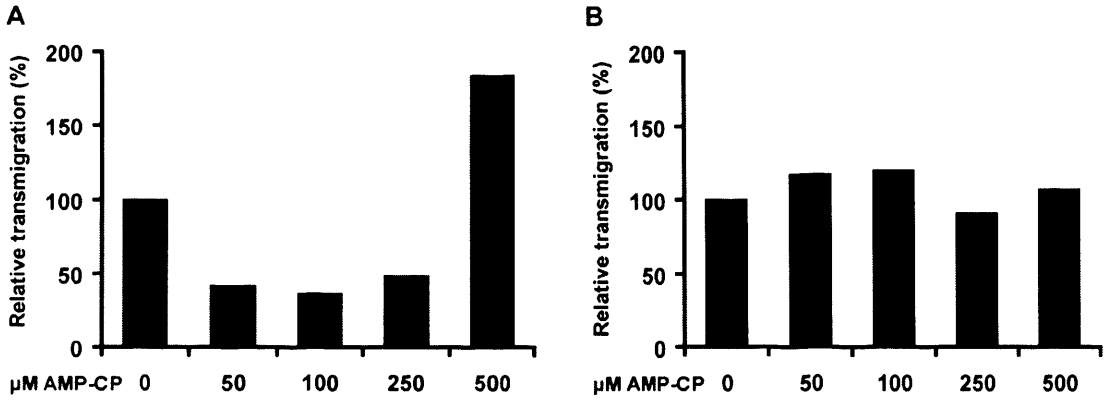

Figure 5.9: Inhibition of CD73 enzymatic activity reduces THP-1 cell TEM
TNF-α-stimulated HUVECs were incubated with AMP-CP (50 µM, 60 min, 37°C). THP-1 cells (A) or T lymphoblasts (B) were allowed to transmigrate for 2 h in a TLM-based TEM assay. Transmigration rate was determined from the time-lapse movies and results were normalised to untreated control. Means of two experiments are shown.

5.10.1 Expression level of cell adhesion proteins

CD73-deficient ($CD73^{-/-}$) mice have been shown to exhibit increased VCAM-1 levels in carotid arteries and cultured aortic ECs (Zernecke et al., 2006). To investigate the cell surface levels of adhesion molecules in CD73 k-d ECs and to determine the k-d efficiency, HUVECs were labelled with specific antibodies for CD73, ICAM-1, VCAM-1, E- and P-selectin and analysed by FACS analysis. Representative FACS traces show that CD73 RNAi induced a clear reduction of CD73 levels for all oligos (Fig. 5.11A). To be able to determine the k-d efficiency for CD73 from the total protein content rather than just the cell surface levels, HUVECs were fixed and permeabilised before staining with CD73 antibodies. Background staining with IgG_1 negative control was very high under these conditions. Again, CD73 siRNA induced a shift of the whole population for all oligos (Fig. 5.11B). Representative FACS traces for ICAM-1 showed a relatively broad curve for siC HUVECs, indicating varying expression levels under control conditions (Fig. 5.11C). CD73 siRNA induced an upwards shift of the ICAM-1-positive cell population, while the broad curve was maintained. In agreement with the literature, VCAM-1 was not expressed above IgG_1 negative control level in samples that were not TNF-α-stimulated (Fig. 5.11D). CD73 siRNA induced a slight shift in the VCAM-1-positive population for most oligos. One oligo (#2, brown trace) displayed a shift and a second

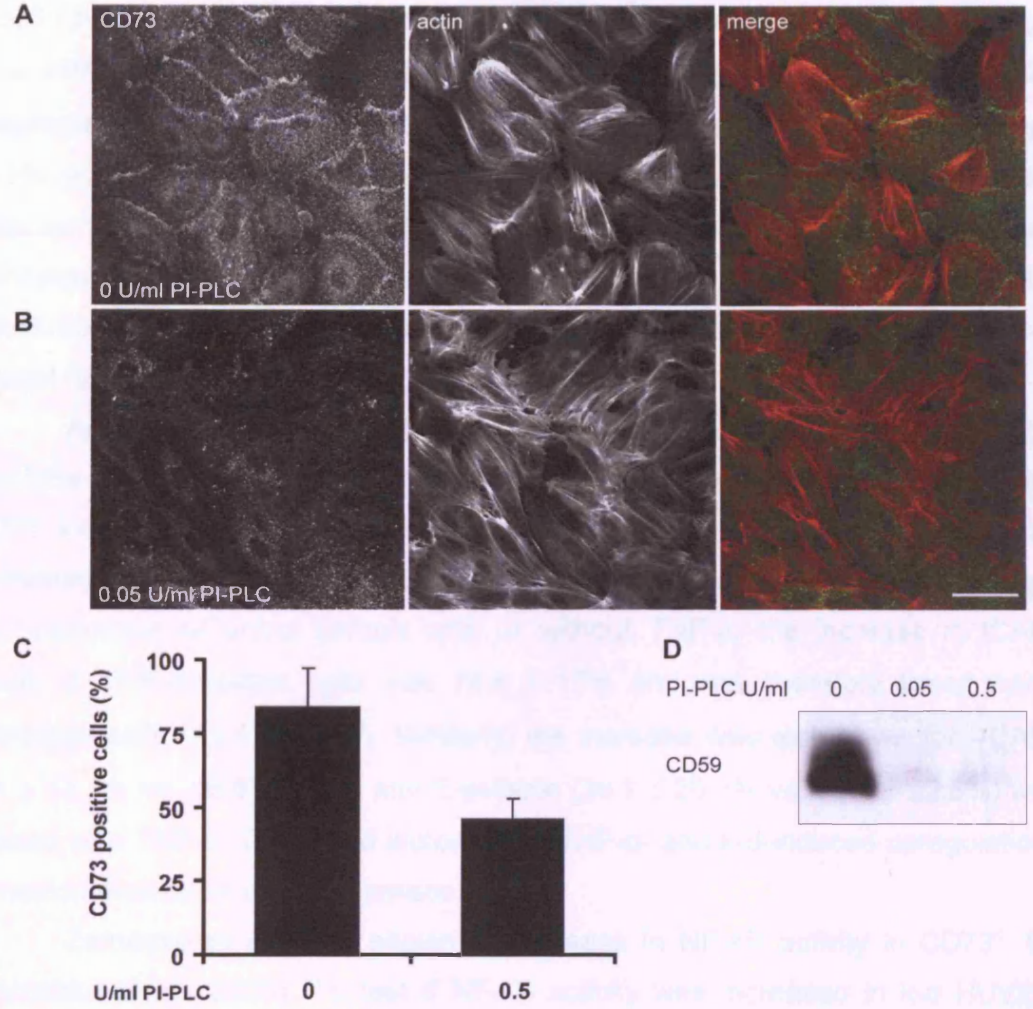

Figure 5.10: CD73 is partially resistant to PI-PLC-mediated shedding
HUVECs were incubated with 0 – 0.5 U/ml PI-PLC (15 min, 37°C). **A, B**: Cells were fixed and stained for CD73 and F-actin. Bar = 50 µm. **C**: Cells were labelled with antibodies against CD73 and CD73-positive cells were determined by FACS analysis. n = 3. **D**: Lysates of PI-PLC-treated HUVECs were used for immunoblotting using antibodies against CD59.

population with higher VCAM-1 expression. E- and P-selectin, similar to VCAM-1, are not expressed under non-inflammatory conditions. CD73 siRNA induced a slight shift in the E- and P-selectin-positive population for most oligos (Fig. 5.11E). For E-selectin, one oligo (#2, brown trace) displayed a shift and a second population with higher E-selectin expression.

The k-d level and the changes in expression level were calculated from the FACS data by normalising the mean fluorescence of the total population of individual samples to the mean fluorescence of the total population of the siControl sample. CD73 was knocked-down maximally by 78.5 ± 2.7% (#3) (Fig. 5.12A), while

CD73 RNAi induced upregulation of cell surface expression of ICAM-1 maximally by 66 ± 15% (#1) (Fig. 5.12B), VCAM-1 maximally by 62.8 ± 15.3% (#4) (Fig. 5.12C), E-selectin maximally by 144 ± 35.8% (#2) (Fig. 5.12D) and P-selectin maximally by 122% (#2) (Fig. 5.12E). It is interesting to note that even though all siRNAs used effectively knock-down CD73, the effect on the expression level of endothelial adhesion molecules is variable. In particular oligo 3, which has the best CD73 knock-down, induces the least increase in expression level of adhesion molecule, except for P-selectin, where oligo 1 shows no expression upregulation.

As TNF-α up-regulates the same adhesion molecules, it was interesting to see how TNF-α treatment influenced the expression level of adhesion molecules in CD73 k-d cells. The actual differences in expression level for TNF-α-treated and untreated HUVECs are displayed in Table 5.1. For relative protein levels referring to the respective siControl sample with or without TNF-α, the increase in ICAM-1 levels in TNF-α-treated cells was 19.6 ± 17% and was therefore lower than in untreated cells (41.4 ± 9.5%). Similarly, the increase was also lower for VCAM-1 (41 ± 12.3% vs. 56.8 ± 2.9%) and E-selectin (36.7 ± 20.3% vs. 70.3 ± 22.6%) when treated with TNF-α. This could indicate that TNF-α- and k-d-induced upregulation of adhesion molecules are antagonistic.

Zernecke et al. have shown an increase in NF-κB activity in $CD73^{-/-}$ ECs (Zernecke et al., 2006). To test if NF-κB activity was increased in k-d HUVECs, immunoblotting against the NF-κB inhibitor IκB-α was carried out. The analysis of very preliminary results suggests that IκB-α level decreased in most of the k-d samples when compared to the loading control, although other oligos (Qiagen #2 and #4) induced an increase in IκB-α level (Fig. 5.13). These results might tentatively suggest a role for NFκB activation in mediating effects of CD73 k-d, but much further work is required to establish this and to correlate activation of NFκB with the observed changes in adhesion molecule expression. Again, the knock-down level of CD73 for the different oligos used do not seem to be directly related to the expression level of IκB-α, since oligo 3 (Dharmacon), which has the best knock-down efficiency does not induce a decrese in IκB-α level.

These results suggest that CD73 k-d induces a pro-inflammatory phenotype in HUVECs, as indicated by the up-regulation of adhesion molecules.

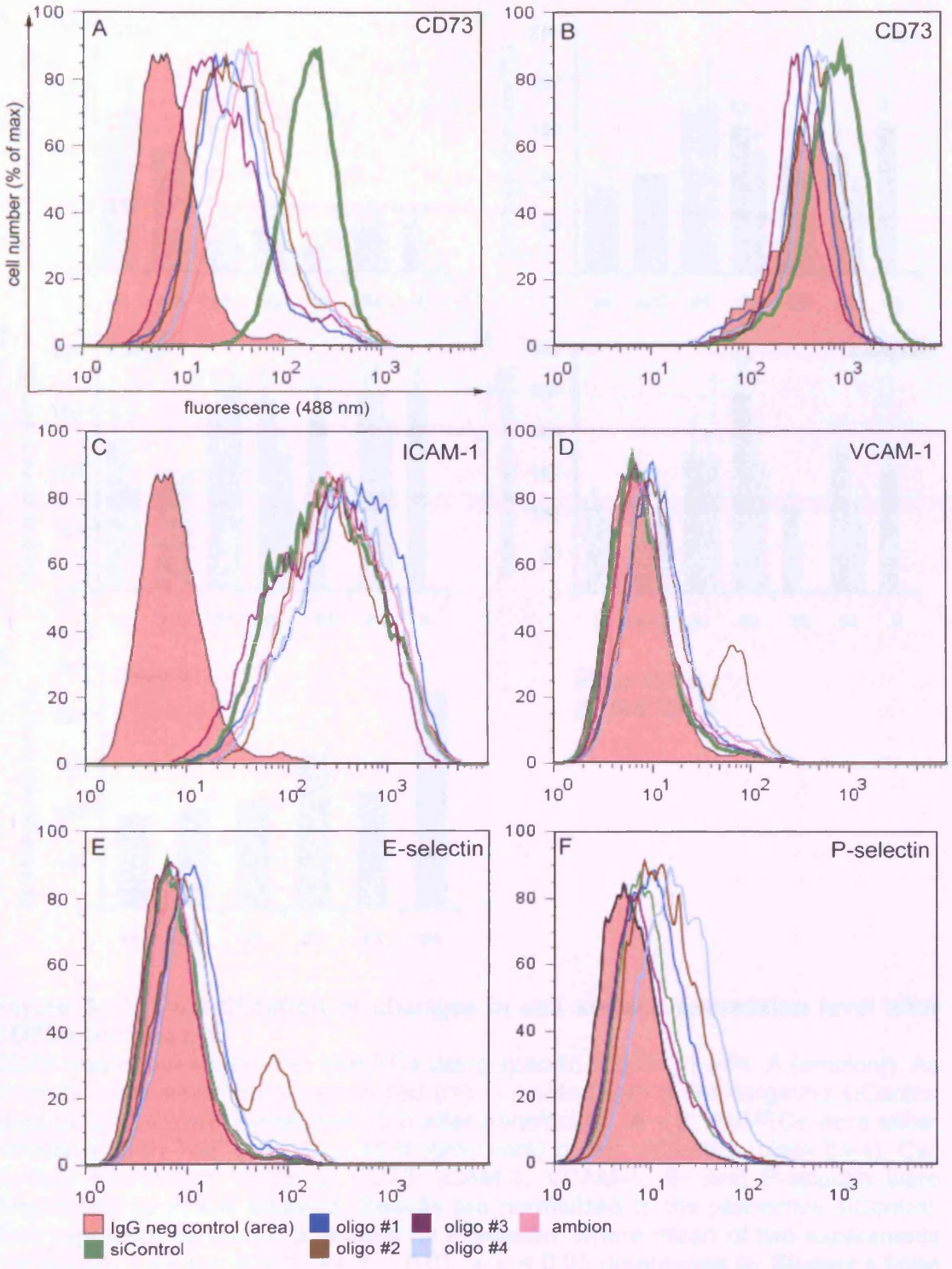

Figure 5.11: Expression of adhesion molecules is upregulated after CD73 k-d
CD73 was knocked-down in HUVECs using specific oligonucleotides (oligos #1 - #4, ambion). As controls, cells were treated with a non-targeting siControl oligo (siControl). Cells were analysed 72 h after transfection; representative FACS traces are shown. Live HUVECs were stained for CD73, ICAM-1, VCAM-1 and E- and P-selectin, except for (B), where cells were fixed and permeabilised prior to staining.

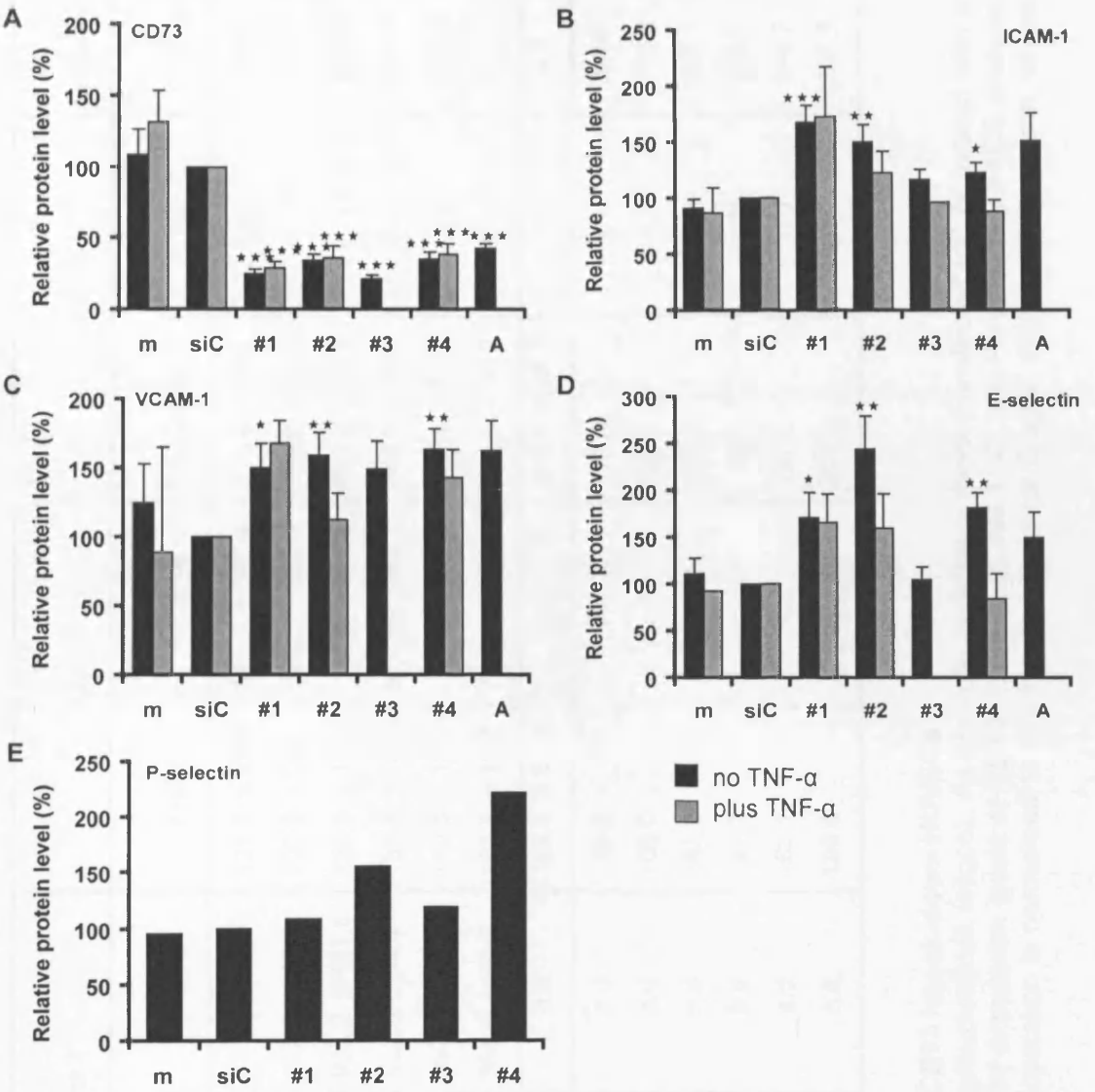

Figure 5.12: Quantification of changes in cell surface expression level after CD73 knock-down

CD73 was knocked down in HUVECs using specific oligos (#1 - #4, A (ambion)). As controls, cells were mock-transfected (m) or treated with a non-targeting siControl oligo (siC). Cells were analysed 72 h after transfection. **A – E**: HUVECs were either stimulated with TNF-α for 15 – 18 h (grey bars) or left untreated (black bars). Cell surface expression levels of CD73, ICAM-1, VCAM-1, E- and P-selectin were determined by FACS analysis. Results are normalised to the respective siControl. Bars represent SEM. n ≥ 3, except for P-selectin, where mean of two experiments are shown. ⋆⋆⋆ $p < 0.001$, ⋆⋆ $p < 0.01$, ⋆ $p < 0.05$ determined by Student's t-test and Bonferroni post-test, compared to siC.

oligos		Relative adhesion molecule expression (% of siControl)								
		CD73		ICAM-1		VCAM-1		E-selectin		P-selectin
		- TNF-α	+ TNF-α	- TNF-α	+ TNF-α	- TNF-α	+ TNF-α	- TNF-α	+ TNF-α	- TNF-α
Dharmacon	m	108.0 ± 18.3	132.0 ± 47.6	91.2 ± 7.3	411.8 ± 121.3	124.7 ± 27.6	611.7 ± 507.4	111.4 ± 16.1	772.8	95.0
	siC	100.0 ± 0.0	91.3 ± 8.6	100.0 ± 0.0	432.9 ± 46.4	100.0 ± 0.0	622.2 ± 226.8	100.0 ± 0.0	551.4 ± 211.6	100.0
	#1	24.7 ± 3.2	27.0 ± 5.8	167.6 ± 14.7	923.2 ± 167.5	150.3 ± 17.0	1180 ± 484.8	171.0 ± 27.1	734.2 ± 310.3	108.6
	#2	33.7 ± 4.6	36.7 ± 9.4	150.0 ± 15.8	522.8 ± 89.0	158.8 ± 16.7	557.5 ± 169.3	244.0 ± 35.9	731.9 ± 240.9	156.2
	#3	21.5 ± 2.7	n.d.	116.0 ± 9.4	397.9 ± 152.3	149.5 ± 19.8	n.d.	105.4 ± 13.0	n.d.	119.0
	#4	35.3 ± 4.3	38.8 ± 9.8	122.9 ± 9.0	368.9 ± 44.7	162.8 ± 15.3	718.5 ± 220.8	181.5 ± 16.2	292.9 ± 34.3	222.1
Ambion (A)		42.4 ± 4.0	n.d.	150.6 ± 25.3	n.d.	162.6 ± 21.8	n.d.	149.7 ± 26.7	n.d.	n.d.
Qiagen	m	103.5	n.d.	85.1	n.d.	88.6	n.d.	179.6	n.d.	94.0
	siC	100.0	n.d.	100.0	n.d.	100.0	n.d.	100.0	n.d.	100.0
	#1	46.6	n.d.	149.3	n.d.	182.9	n.d.	159.8	n.d.	207.1
	#2	21.2	n.d.	96.0	n.d.	97.7	n.d.	99.2	n.d.	84.4
	#4	31.6	n.d.	194.7	n.d.	163.1	n.d.	132.7	n.d.	146.2
	#5	35.1	n.d.	89.4	n.d.	190.5	n.d.	201.7	n.d.	185.5

Table 5.1: Relative adhesion molecule expression in CD73 knock-down HUVECs
CD73 was knocked down in HUVECs using specific oligonucleotides (oligos). As controls, cells were mock-transfected (m) or treated with a non-targeting siControl oligo (siC). Cells were analysed for expression levels of CD73, ICAM-1, VCAM-1, E- and P-selectin by FACS analysis 72 h after transfection. Mean fluorescence of total cell population is normalised to siC. n ≥ 3, except for Qiagen oligos and P-selectin, where means of two experiments are shown.

5.10.2 CD73 enzymatic activity is reduced in k-d cells

The enzymatic activity of CD73 in CD73 k-d cells was determined by radio-TLC. As expected the enzymatic activity was significantly reduced maximally by 92.2 ± 6.48% (#4; Fig. 5.14).

5.10.3 Morphological changes in CD73 k-d HUVECs

There was an obvious change in the morphology of HUVECs following CD73 k-d. Cells knocked down with oligos #1, #2 and #4 exhibited an elongated morphology not unlike morphological changes occurring after TNF-α treatment, while oligo #3, which so far has given the weakest results, displayed a phenotype more similar to the siControl sample (Fig. 5.15). This could indicate that oligo 3 induces off-target effects which prevent the development of the CD73 phenotype, despite the high knock-down efficiency. This further strengthens the previous observation that CD73 k-d induces a pro-inflammatory phenotype.

To follow up on this result, confluent monolayers of CD73 siRNA-, siControl- and mock-transfected cells were fixed and stained for tubulin and F-actin to visualise morphological changes (Fig. 5.16). The tubulin network appeared less prominent in all transfected samples, including siControl, indicating that this might be a transfection artefact. The elongated phenotype previously observed by phase-contrast microscopy on tissue culture plastic was less obvious under conditions on glass coverslips, but an increase in stress fibres was detected, similar to, but less than TNF-α-treated samples (see Fig. 3.2).

5.10.4 Leukocyte adhesion and TEM to and across CD73 k-d HUVECs is increased

The pro-inflammatory phenotype of CD73 k-d cells suggests that leukocyte adhesion and TEM could be affected by the knock-down. Adhesion and TEM of untreated THP-1 and CCRF-CEM cells was determined in adhesion and Transwell™-based TEM assays with TNF-α-stimulated and unstimulated CD73 k-d HUVECs. THP-1 TEM was increased for most of the oligos tested, by a maximum of 21.9 ± 6.6% (#2), while others induced a decrease in TEM, by a maximum of 42.3 ± 5.3% (#1) (Fig. 5.17A). TNF-α-treated samples displayed higher transmigration rates throughout. CCRF-CEM cell TEM was only slightly changed by CD73 k-d with a maximal increase of 8.7 ± 5.3% (#1), while oligo A induced a decrease of

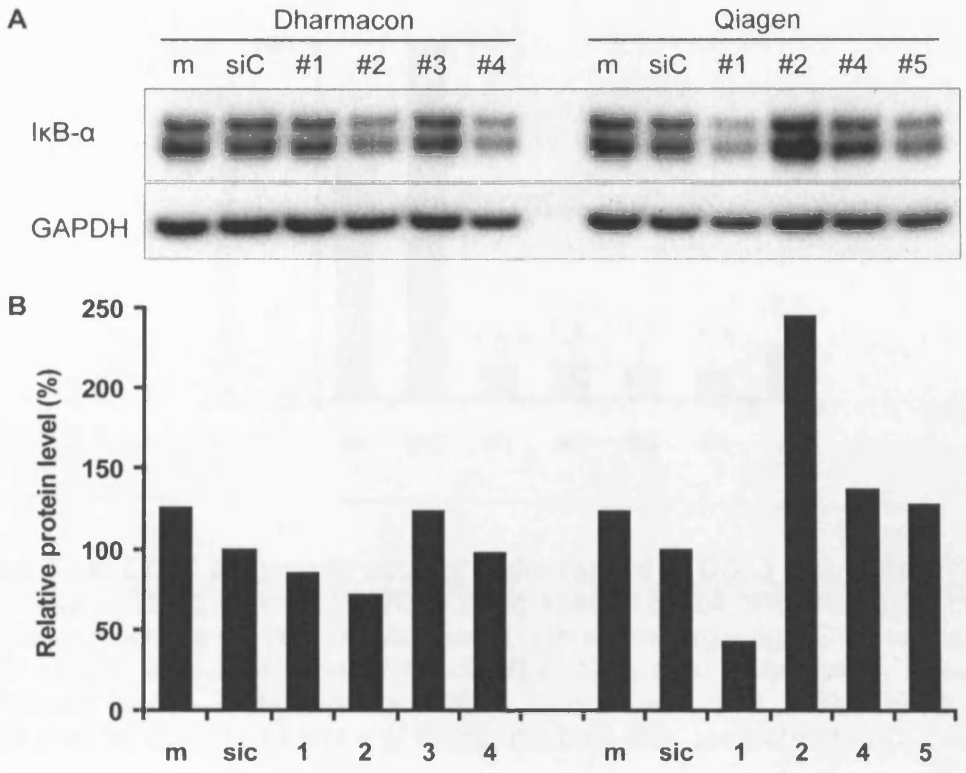

Figure 5.13: CD73 knock-down decreases IκB-α level
CD73 was knocked down in HUVECs using specific oligos. As controls, cells were mock-transfected (m) or treated with a non-targeting siControl oligo (siC). Cells were lysed 72 h after transfection and cell lysates were used for immunoblotting with specific antibodies against IκB-α and GAPDH as loading control (**A**). Densitometric quantification: IκB-α levels were normalised to GAPDH (**B**). Results from one experiment are shown.

28.4 ± 2.9% (Fig. 5.17C). Adhesion was increased for THP-1 and CCRF-CEM cells under non-inflammatory conditions by a maximum of 26.5 ± 10.8% (#2) and 241 ± 153% (#3), respectively, but no increase could be observed with TNF-α-treated HUVECs (Fig. 5.17B, D). Again, not all oligos displayed the same trend. The actual changes between TNF-α and unstimulated HUVECs are shown in Table 5.2. These results indicate that TNF-α treatment overrides the CD73 k-d effects for adhesion, hence no differences in adhesion can be observed, while TEM seems to require additional regulatory mechanisms. In conclusion, no consistent differences in leukocyte TEM following CD73 k-d could be detected. Interestingly, not only did the different oligos used display a variability in the extent of the effect seen, but in the case of TEM displayed opposing results. It would be interesting to determine how these are achieved and what role possible and different off-target effects induced by the oligos play.

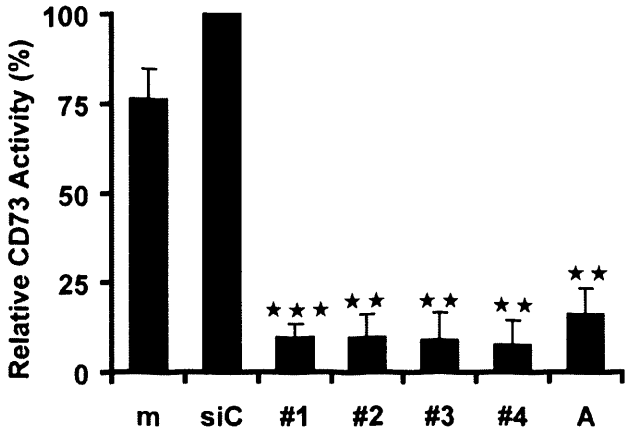

Figure 5.14: CD73 enzymatic activity is decreased in CD73 knock-down cells
CD73 was knocked down in HUVECs using specific oligos (#1 - #4, A). As controls, cells were mock-transfected (m) or treated with a non-targeting siControl oligo (siC). CD73 activity was determined by radio-TLC 72 h after transfection. Results are normalised to siC. Bars represent SEM. n = 3. ★★★ $p < 0.001$, ★★ $p < 0.01$ determined by Student's t-test and Bonferroni post-test, compared to siC.

5.10.5 H_2O_2-induced TEM defect is not dependent on CD73

As previously demonstrated, the ability to induce inhibition of CD73 was compromised in H_2O_2-treated THP-1 cells, and thus it was tempting to speculate that CD73 activity plays a role in the TEM defect of H_2O_2-treated THP-1 cells discussed in the previous chapters. Thus, the H_2O_2-induced TEM defect should not be as pronounced with CD73 k-d HUVECs as seen in control conditions. To test this hypothesis, H_2O_2-treated THP-1 cells were allowed to transmigrate across CD73 siRNA (#2)- or siControl-transfected HUVECs. The results were normalised to the respective untreated control (Fig. 5.18). The decrease in TEM was similar for control cells and CD73 k-d, although the overall TEM rate was higher for k-d HUVECs. This indicates that the reduced ability of H_2O_2-treated cells to inhibit CD73 does not influence TEM. Thus, endothelial CD73 does not seem to play a role in the H_2O_2-mediated decrease in leukocyte TEM.

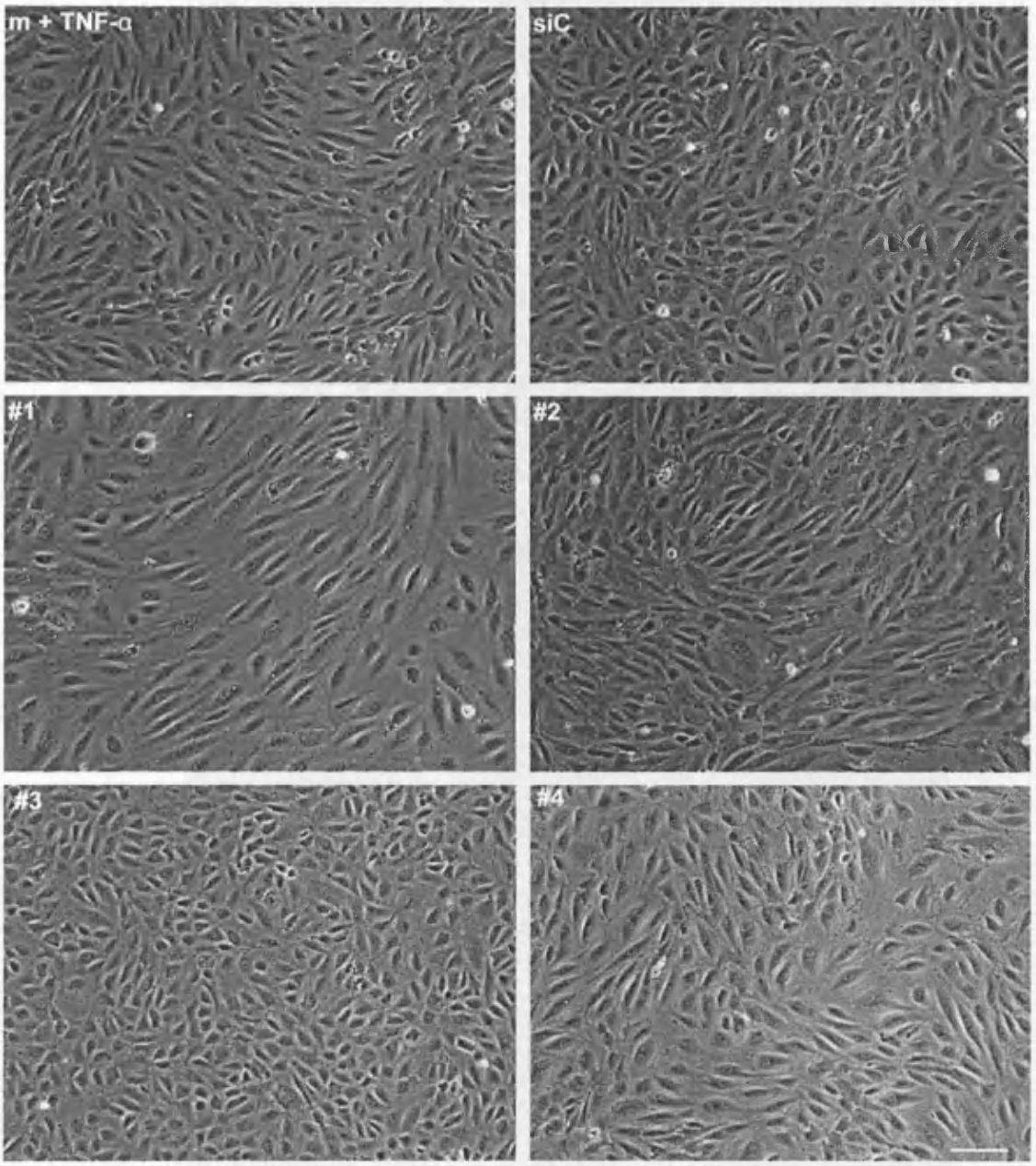

Figure 5.15: CD73 knock-down induces pro-inflammatory phenotype
CD73 was knocked-down in HUVECs using specific oligos (#1 - #4). As controls, cells were mock-transfected (m) or treated with a non-targeting siControl oligo (siC). Cells were either treated with or without TNF-α for 15 – 18 h and were analysed 72 h after transfection. Representative phase-contrast images of at least five experiments are shown. Bar = 50 µm.

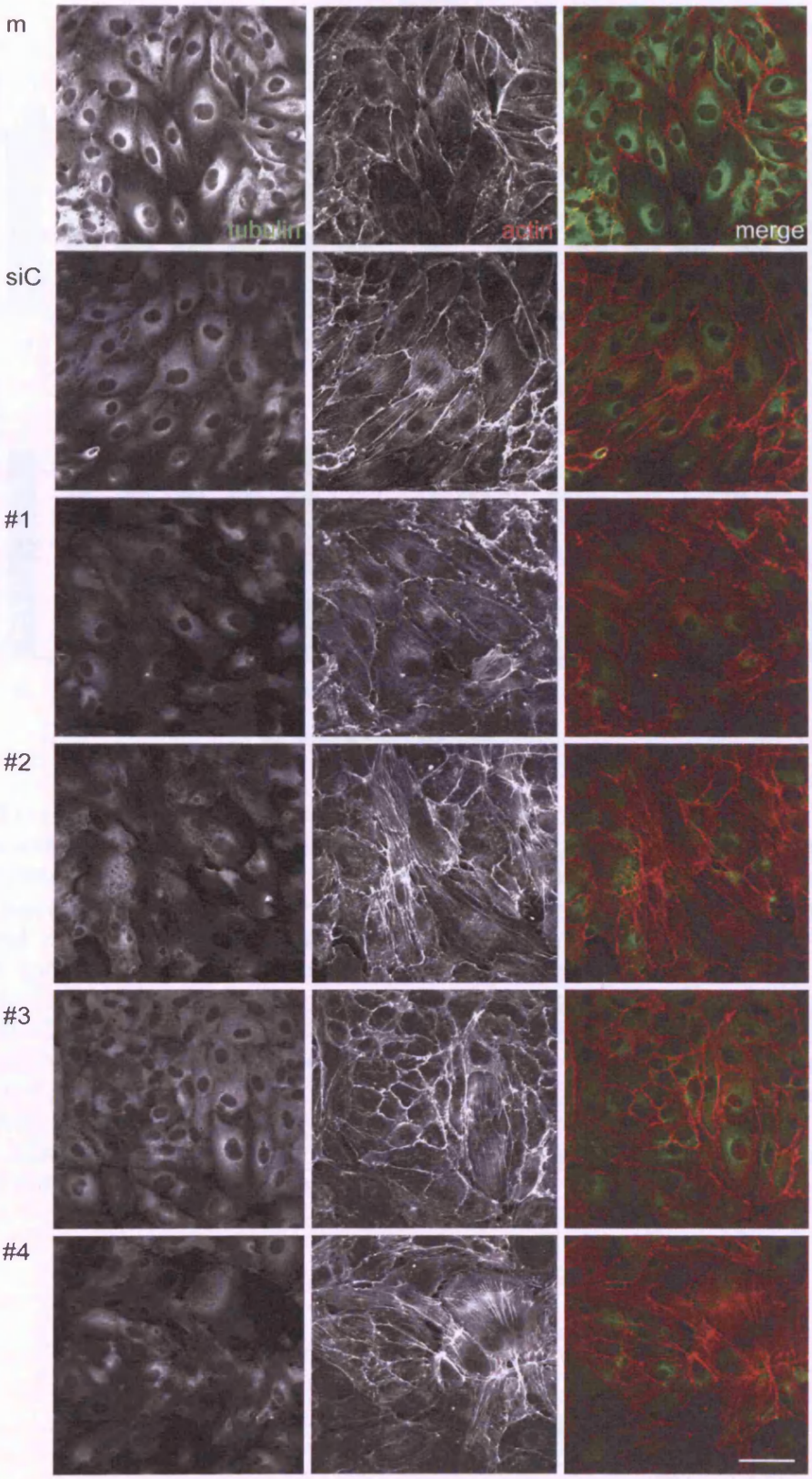

Figure 5.16: HUVECs display more stress fibres after CD73 knock-down
CD73 was knocked-down in HUVECs using specific oligos (#1 - #4). As controls, cells were mock-transfected (m) or treated with a non-targeting siControl oligo (siC). Cells were fixed 72 h after transfection and stained for tubulin and F-actin. Representative images of three experiments are shown. Bar = 50 µm.

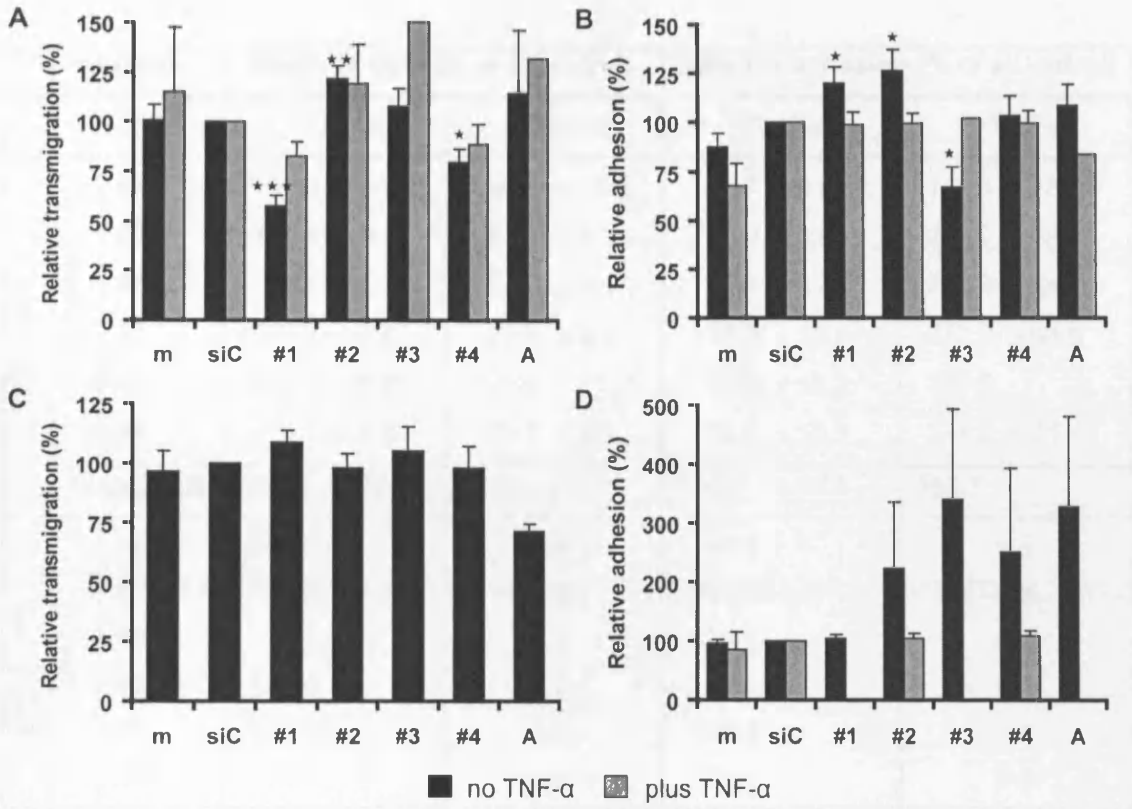

Figure 5.17: Leukocyte TEM and adhesion are affected by CD73 k-d
CD73 was knocked-down in HUVECs using specific oligos (#1 - #4, A). As controls, cells were mock-transfected (m) or treated with a non-targeting siControl oligo (siC). HUVECs were used in Transwell™-based TEM assays or adhesion assays using THP-1 and CCRF-CEM cells. **A**: THP-1 transmigration rate across TNF-α-stimulated (grey bars) or unstimulated (black bars) HUVECs. $n \geq 5$. **B**: THP-1 adhesion to TNF-α-stimulated (grey bars) or unstimulated (black bars) HUVECs. $n \geq 4$. **C**: CCRF-CEM cell transmigration rate across HUVECs. $n = 3$. **D**: CCRF-CEM cell adhesion to TNF-α-stimulated (grey bars) or unstimulated (black bars) HUVECs. $n = 3$.
Results are normalised to the respective siControl. Bars represent SEM. ⋆⋆⋆ $p < 0.001$, ⋆⋆ $p < 0.01$, ⋆ $p < 0.05$ determined by Student's t-test and Bonferroni post-test, compared to siC.

	oligos		Relative TEM (% of siControl)		Relative adhesion (% of siControl)	
			- TNF-α	+ TNF-α	- TNF-α	+ TNF-α
THP-1 cells	Dharmacon	m	100.8 ± 8.0	92.6 ± 15.9	87.7 ± 6.8	145.8 ± 28
		siC	100.0 ± 0.0	87.8 ± 8.3	100.0 ± 0.0	218.0 ± 39.3
		#1	57.7 ± 5.3	70.3 ± 8.7	119.7 ± 8.4	216.9 ± 54.1
		#2	121.9 ± 6.6	98.4 ± 8.4	126.5 ± 10.8	272.2 ± 64.8
		#3	108.2 ± 8.8	121.6	66.8 ± 10.2	187.5
		#4	79.7 ± 6.8	75.7 ± 7.9	103.1 ± 10.3	274.5 ± 71.7
	Ambion (A)		114.4 ± 32.2	106.5	108.7 ± 10.5	153.7
THP-1 cells	Qiagen	m	100.0	n.d.	96.7	n.d.
		siC	87.6	n.d.	100.0	n.d.
		#1	81.1	n.d.	102.4	n.d.
		#2	105.6	n.d.	110.0	n.d.
		#4	86.9	n.d.	107.1	n.d.
		#5	86.3	n.d.	88.1	n.d.
CCRF-CEM cells	Dharmacon	mock	96.7 ± 8.2	n.d.	95.4 ± 6.6	187.5 ± 35.1
		siC	100.0 ± 0.0	n.d.	100.0 ± 0.0	232.9 ± 38.3
		#1	108.7 ± 5.3	n.d.	105.2 ± 6.3	n.d.
		#2	97.8 ± 6.2	n.d.	223.3 ± 112.3	238.3 ± 17.5
		#4	104.9 ± 10.3	n.d.	340.7 ± 152.6	n.d.
		#5	98.2 ± 9.1	n.d.	251.4 ± 142.7	250.5 ± 23.7
		A	71.6 ± 2.9	n.d.	327.4 ± 152.7	n.d.

Table 5.2: Relative leukocyte TEM and adhesion to and across CD73 knock-down HUVECs
CD73 was knocked-down in HUVECs using specific oligonucleotides (oligos). As controls, cells were mock-transfected (m) or treated with a non-targeting siControl oligo (siC). HUVECs were used in Transwell™-based TEM assays or adhesion assays using THP-1 and CCRF-CEM cells. n ≥ 3, except for Qiagen oligos and samples #3 and A plus TNF-α, where means of two experiments are shown.

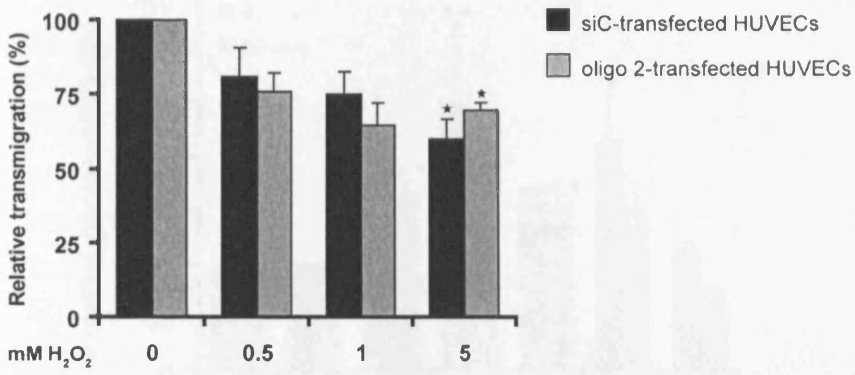

Figure 5.18: H_2O_2 treatment of THP-1 cells decreases TEM across CD73 knock-down HUVECs
CD73 was knocked-down in HUVECs using oligo #2 (grey bars); control cells were transfected with non-targeting siRNA (siC; black bars). Cells were used 72 h after transfection in Transwell™-based TEM assays with H_2O_2-treated THP-1 cells (0 – 5 mM, 30 min, 37°C), which were allowed to transmigrate for 2 h before cells were collected from the lower chamber and the TEM rate was calculated. Results from each group are normalised to the respective control without H_2O_2. Bars represent SEM. n = 3. ⋆ $p < 0.05$ determined by Student's t-test and Bonferroni post-test.

5.10.6 Endothelial permeability is increased in CD73 k-d cells

Adenosine, the product of CD73 enzymatic activity, has been shown to increase endothelial barrier function (Comerford et al., 2002; Lennon et al., 1998; Srinivas et al., 2004). The lack of adenosine due to CD73 k-d should therefore lead to a decrease in endothelial barrier function, i.e. an increase in permeability. This was tested with a FITC-dextran-based permeability assay using mock-, siControl and CD73 siRNA-transfected HUVECs. The permeability was increased by a maximum of 94.7 ± 24.1% (#2) 40 min after FITC-dextran addition and 45.6 ± 19.6% (#2) after 80 min (Fig. 5.19). These results indicate that the lack of adenosine is likely to induce increased permeability in HUVECs.

5.10.7 Junctional organisation is changed following CD73 k-d

To further investigate the pro-inflammatory phenotype induced by CD73 k-d, the junctional organisation was investigated. To this end, mock-, siControl- and CD73 siRNA-transfected HUVECs were fixed and stained for junctional markers: ZO-1,

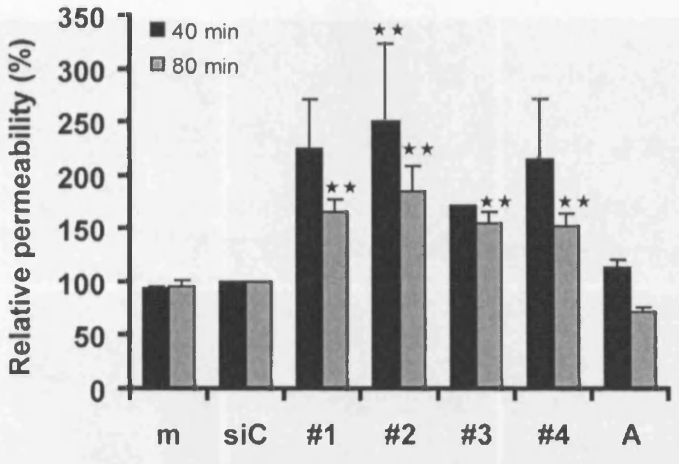

Figure 5.19: Permeability is increased in CD73 k-d HUVECs
HUVECs were transfected with oligos targeting CD73 (#1 - #4, A), non-targeting siRNA (siC) or mock-transfected (m). HUVECs were grown on Transwell™ filters (0.4 µm pore size) until confluency (72 h after transfection). FITC-dextran (100 µg/ml) was added to the upper chamber and samples were taken from the lower chamber at 40 and 80 min. Fluorescence was measured using a Fusion™ α-FP plate reader and results were normalised to the respective control. Bars represent SEM. n = 5. ★★ $p < 0.01$ determined by Student's t-test and Bonferroni post-test.

β-catenin, VE-cadherin, JAM-A and PECAM-1 with tubulin and F-actin staining as cytoskeletal markers. In control cells, ZO-1 staining was localised in the junctions in a rather continuous line, whereas junctional ZO-1 staining in k-d cells was discontinuous (Fig. 5.20). All samples, including the controls showed a punctate nuclear staining, which is likely to be non-specific binding, since it is not abolished by ZO-1 k-d (Jaime Millan, unpublished data). Staining with antibodies against β-catenin showed a slight general decrease of β-catenin in the junctions of k-d cells, while the distribution remained similar to control samples (Fig. 5.21). All k-d samples, except oligo #3, displayed an increase in actin stress fibres, as described previously (Fig. 5.16). The junctional protein VE-cadherin has previously been shown to be localised in 'reticular junctions' as well as non-reticular junctions (Mamdouh et al., 2003). The proportion and breadth of VE-cadherin-containing 'reticular junctions' seemed to be increased in CD73 k-d cells, in particular with oligo #2 and #4 (Fig. 5.22). JAM-A staining on the other hand appeared decreased for most oligos, when compared to the siControl. Preliminary results with PECAM-1 staining did not show a clear phenotype, while some oligos appeared to have

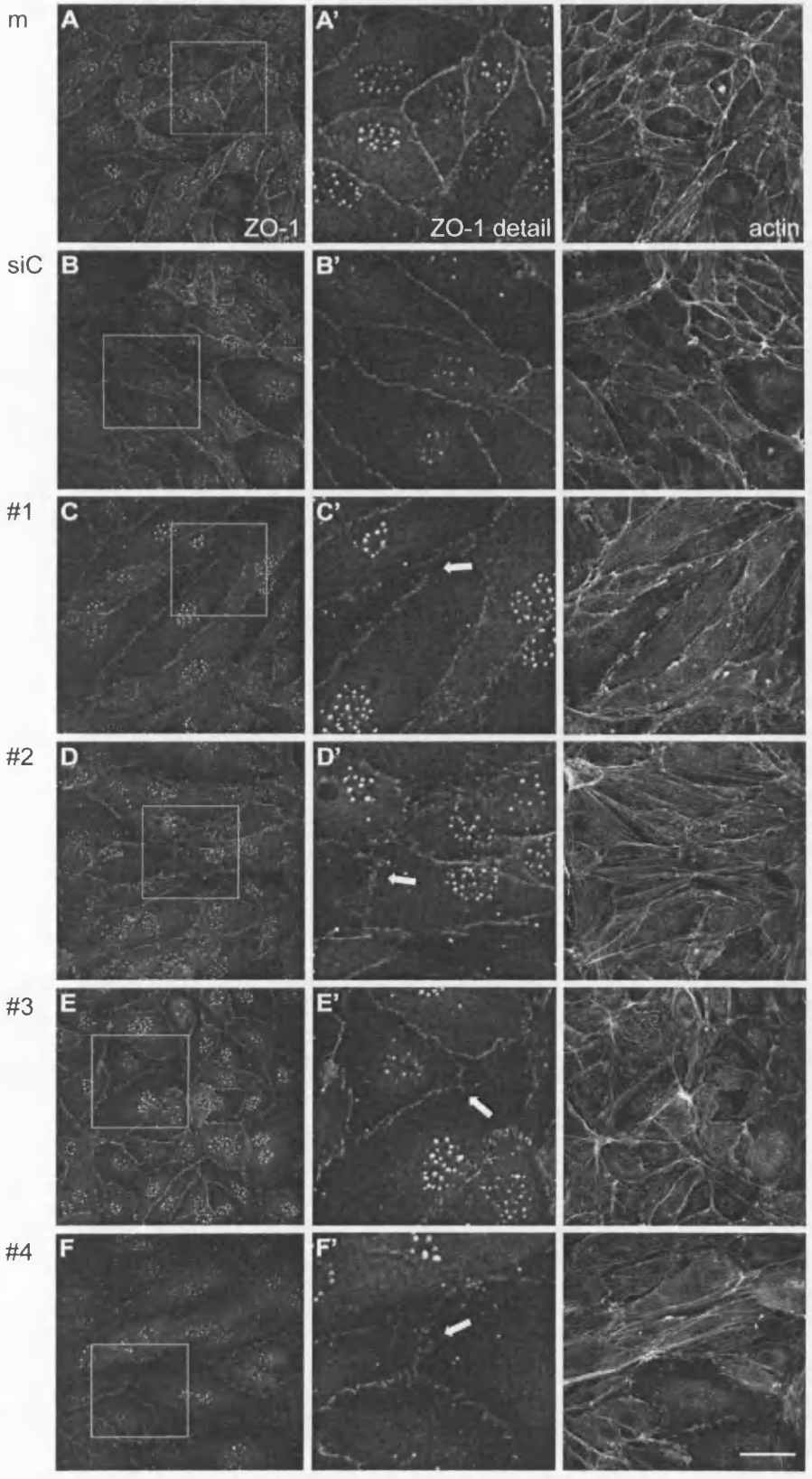

Figure 5.20: ZO-1 staining is discontinuous in CD73 k-d cells
HUVECs were transfected with oligos targeting CD73 (#1 - #4), non-targeting siRNA (siC) or mock-transfected (m) and stained for ZO-1 and F-actin. Arrows indicate discontinuous junctional staining. Representative images of three experiments are shown. Bar = 50 µm. **A' – F'**: Details of images A – F, as indicated by white box.

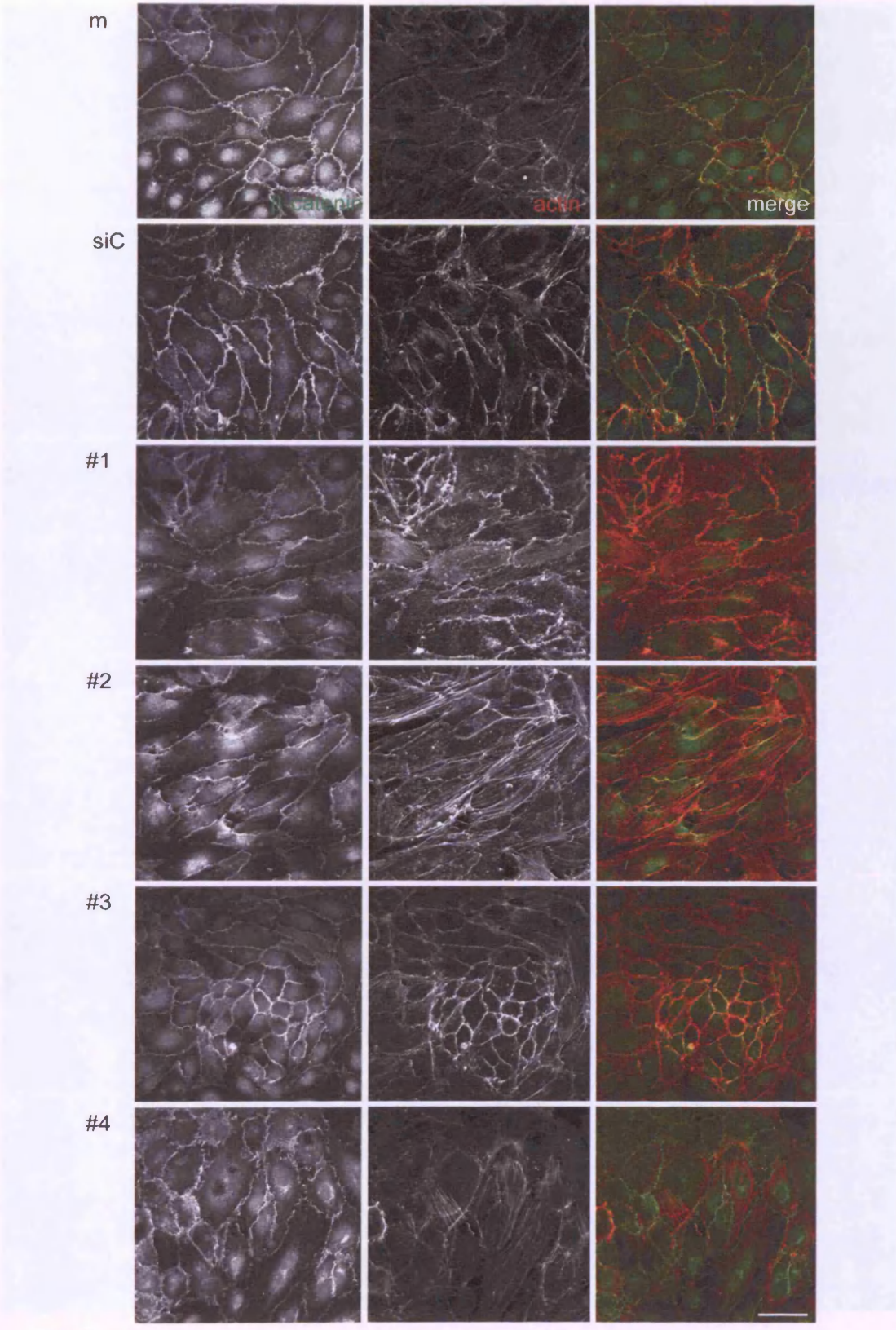

Figure 5.21: β-catenin levels appear to be reduced in CD73 k-d cells
HUVECs were transfected with oligos targeting CD73 (#1 - #4), non-targeting siRNA (siC) or mock-transfected (m). HUVEC monolayers were stained for β-catenin and F-actin. Representative images of two experiments are shown. Bar = 50 µm.

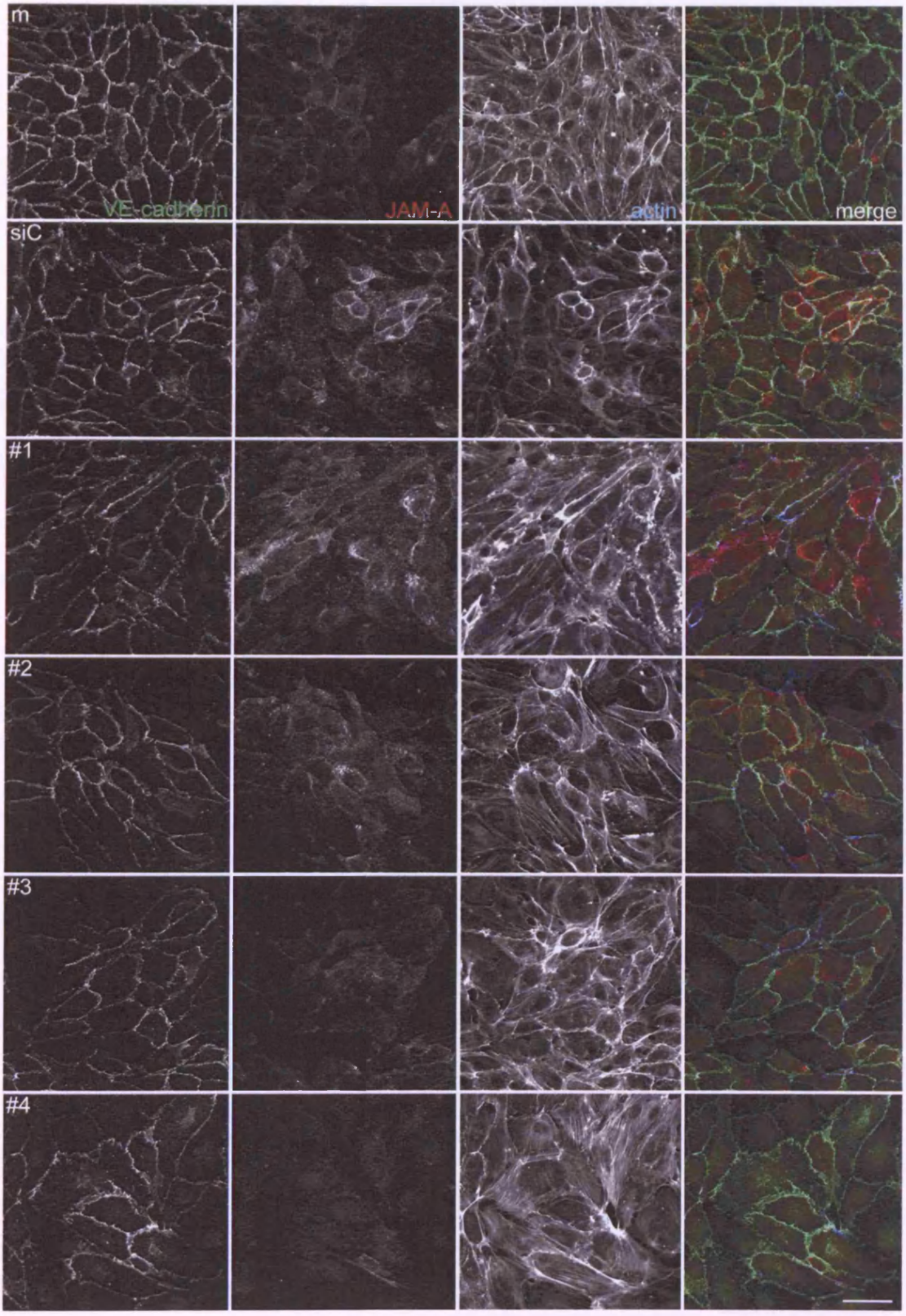

Figure 5.22: VE-containing 'reticular junctions' appear to be increased
HUVECs were transfected with oligos targeting CD73 (#1 - #4), non-targeting siRNA (siC) or mock-transfected (m) and stained for VE-cadherin, JAM-A and F-actin. Representative images of two experiments are shown. Bar = 50 µm.

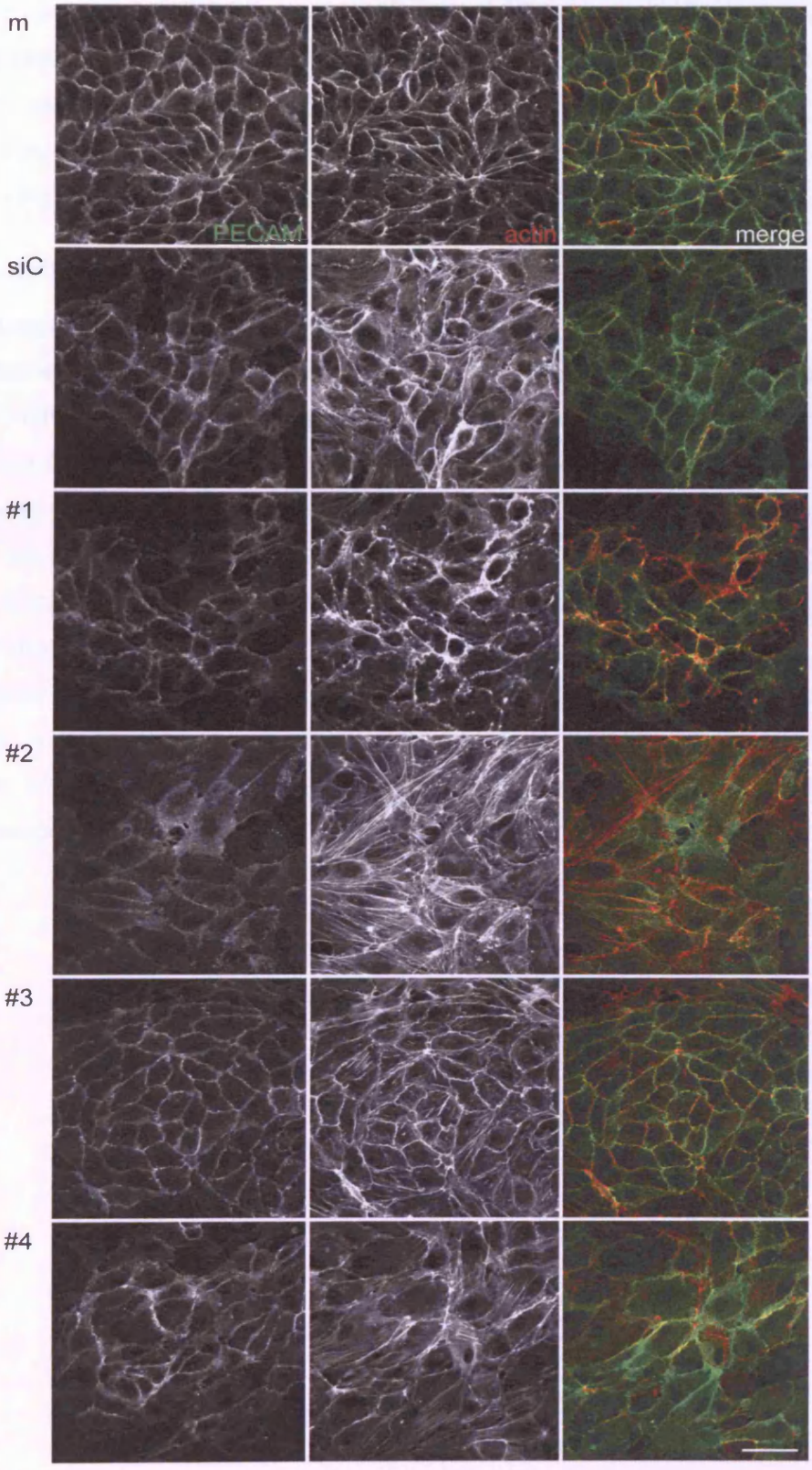

Figure 5.23: PECAM-1 staining in CD73 k-d cells
HUVECs were transfected with oligos targeting CD73 (#1 - #4), non-targeting siRNA (siC) or mock-transfected (m). HUVEC monolayers were stained for PECAM-1 and F-actin. Bar = 50 µm.

decreased junctional PECAM-1 expression (#1 and #2), others showed a stronger junctional staining, with decreased cell surface staining (#3) or no change compared to siControl samples (#4) (Fig. 5.23).

These results indicate that CD73 k-d influences the junctional make-up, which is likely to play a role in the observed increase in permeability.

5.10.8 Summary of siRNA results

To understand the relationship between protein levels of CD73, enzymatic activity, levels of adhesion molecules, adhesion, TEM and permeability in TNF-α-treated and untreated HUVECs, a correlation analysis was carried out (Table 5.3). Significantly negative correlation was found for CD73 k-d and ICAM-1, VCAM-1 and E-selectin level, as well as permeability in untreated HUVECs. CD73 activity was significant positively correlated with CD73 k-d. P-selectin levels were not included in the analysis, since the experiment was carried out only twice. However, no significant correlation between CD73 k-d and adhesion and TEM could be detected.

Taken together the siRNA experiments indicate that CD73 activity retains ECs in a non-inflammatory state. CD73 k-d ECs exhibit a pro-inflammatory phenotype with elongated cells and increased stress fibres and expression of adhesion molecules.

	no TNF-α						with TNF-α					
oligonucleotide	all	#1	#2	#3	#4	A	all	#1	#2	#3	#4	A
CD73 (kd)	70%	76%	67%	79%	65%	58%	66%	72%	64%	n.d.	62%	n.d.
ICAM-1	- 0.4	- 0.6	- 0.5	- 0.2	- 0.3	- 0.4	- 0.4	- 0.6	- 0.6	n.d.	- 0.2	n.d.
VCAM-1	- 0.3	- 0.5	- 0.6	- 0.7	- 0.5	- 0.7	- 0.2	- 0.6	0.1	n.d.	- 0.4	n.d.
E-selectin	-0.4	- 0.5	- 0.8	- 0.1	- 0.6	- 0.7	- 0.3	- 0.8	- 0.7	n.d.	0.3	n.d.
transmigration	0.1	0.7	0.5	0.2	0.4	- 0.1	- 0.1	0.5	- 0.4	n.d.	0.5	n.d.
adhesion	- 0.2	- 0.2	- 0.1	0.8	0.1	0.4	- 0.4	- 0.1	- 0.4	n.d.	- 0.1	n.d.
permeability	- 0.4	- 0.9	- 0.6	- 1	- 0.7	1	n.d.	n.d.	n.d.	n.d.	n.d.	n.d.
CD73 activity	0.9	1	1	1	0.9	1	n.d.	n.d.	n.d.	n.d.	n.d.	n.d.

Table 5.3: Correlation analysis for Dharmacon CD73 oligonucleotides
CD73 was knocked-down in HUVECs using specific oligonucleotides (#1 - #4, A (Ambion)). As controls, cells were mock-transfected or treated with a non-targeting siControl oligo. HUVECs were used 72 h after transfection treated with or without TNF-α for 15 – 18h in several assays to determine expression level of CD73, ICAM-1, VCAM-1 and P-selectin. Additionally, k-d HUVECs were used in transmigration, adhesion, permeability and CD73 activity assays. Results were normalised to siControl and a correlation analysis was carried out. Values represent Pearson's coefficient (r) unless otherwise labelled. Orange background indicates significant negative correlation ($p < 0.05$); green background indicated significant positive correlation ($p < 0.05$), while grey background indicates no statistical significance. $n \geq 3$.

5.11 Discussion

In this chapter the role of CD73 in leukocyte TEM was investigated. The effects of adhesion molecule cross-linking and leukocyte binding on CD73 subcellular distribution and enzymatic activity in HUVECs were explored. Specific inhibitors and k-d using RNAi was utilised to dissect the role of CD73 in adhesion of leukocytes and their subsequent TEM.

Immunofluorescence of HUVECs revealed a discrete punctate staining of CD73, which could indicate localisation in microvilli, which are one of the first points of contact with leukocytes (Carman et al., 2003). The endothelium has been shown to generate ICAM-1- and VCAM-1-enriched microvillus-like structures in response to leukocyte binding (Barreiro et al., 2002; Carman et al., 2003). CD73 localisation in microvilli could therefore indicate a role in adhesion and TEM. In HUVECs, CD73 was primarily localised on the apical surface, but CD73 has been reported to be present on the apical and basolateral membrane in cultured ECs from capillaries isolated from rat epididymal fat (Roberts and Sandra, 1993). CD73 has been shown to be localised to caveolae in 165 glioblastoma cells (Ludwig et al., 1999) and in polarised intestinal epithelial monolayers (T84) (Strohmeier et al., 1997). In the present study, localisation to caveolae could not be detected in HUVECs, instead endothelial CD73 partially co-localised with the raft marker CD59. Raft fractionation confirmed that a proportion of CD73 was localised in rafts. To determine the raft-localised CD73 as a portion of the surface CD73 only, a plasma membrane preparation with subsequent raft fractionation would need to be carried out. Raft localisation of CD73 has been reported by other groups for other ECs (Monastyrskaya et al., 2003) and various melanoma cell lines (Sadej et al., 2006).

The enzymatic activity of the ecto-nucleotidase CD39, which converts ATP to AMP, has been shown to be dependent on the localisation of this protein in lipid rafts in MDCK cells (Papanikolaou et al., 2005). CD73 activity was not influenced by cholesterol-depletion, indicating that endothelial CD73 enzymatic activity is not dependent on the raft localisation.

The enzymatic activity of endothelial CD73 has been shown to be inhibited by binding of leukocytes (Henttinen et al., 2003). The inhibitory effect is cell number-dependent and is likely to occur by masking the catalytic site. The exact mechanism is currently unknown. These results were confirmed in the present study, where binding of THP-1 cells induced a decrease in adenosine production in a cell number-dependent manner. Adenosine promotes endothelial barrier function by autocrine stimulation of A_{2b} receptors, leading to relaxation of the actin cytoskeleton

(Srinivas et al., 2004) and strengthening of the junctions (Comerford et al., 2002). The decline in adenosine production after leukocyte binding has been shown to decrease endothelial barrier function, which was hypothesised to facilitate leukocyte TEM (Henttinen et al., 2003). Leukocytes bind to the endothelium via ICAM-1 and VCAM-1 on the ECs (Ley et al., 2007). It was therefore interesting to see if engagement of these adhesion molecules could contribute to the inhibition of CD73. Neither ICAM-1 nor VCAM-1 cross-linking decreased adenosine production, only antibody binding or cross-linking of CD73 did. Antibody-induced inhibition of CD73 has also been shown for peripheral blood lymphocytes, where antibody binding reduced the enzymatic activity by 22 ± 1.5% (Airas et al., 1995). The possible involvement of homophilic interactions between CD73 on leukocytes and endothelium was investigated by pre-treating THP-1 cells with CD73 antibody. Pre-treated THP-1 cells induced a similar inhibition of endothelial CD73 as untreated cells, indicating that either antibody binding does not prevent homophilic interactions or leukocyte CD73 does not play a role in the leukocyte-induced inhibition of endothelial CD73. Taken together, these findings suggest that mechanisms other than ICAM-1 or VCAM-1 signalling are involved in CD73 inhibition after leukocyte binding. Signalling by other adhesion molecules such as selectins could play a role. CD73 inhibition could also be mediated by direct binding of an unknown ligand on the leukocyte surface. *E. coli* 5'-nucleotidase has been shown to undergo a hinge-bending domain rotation of 96° in order to hydrolyse AMP to adenosine, presumably to allow substrate binding and product release (Schultz-Heienbrok et al., 2005). It is tempting to speculate that binding of CD73 ligand on the leukocytes or antibody binding/cross-linking prevents this domain rotation due to steric hindrance, thereby inhibiting adenosine production.

CD73 activity has also been shown to be regulated by oxidative modifications (Kocic et al., 2001). In rat liver, 5'-nucleotidase is susceptible to Fe^{2+} ion catalysed oxidative modification. In patients with obese type 2 diabetes, increased CD73 activity was found to be reduced by treatment with ROS-scavengers (Stefanovic et al., 2005). Regulation of endothelial CD73 through oxidative modification could not be detected in the present study following H_2O_2 addition. However, only one H_2O_2 concentration was tested. Liu and Sok have reported only a marginal inhibition of CD73 with H_2O_2 alone, while H_2O_2 plus Fe^{2+} induced 21.5 ± 2.8% inhibition (Liu and Sok, 2000). This was verified by Kocic et al., who have also shown a Fe^{2+}-mediated oxidative inhibition of CD73 activity (Kocic et al., 2001). Surprisingly, pre-treatment of THP-1 cells with increasing H_2O_2

concentration led to a dose-dependent decrease in their ability to inhibit endothelial CD73 after binding. This suggests an oxidative modification of the CD73 ligand on the leukocyte surface, which possibly prevents binding or at least inhibition of the enzymatic activity. Taken together, these results suggest that endothelial CD73 is inhibited via direct interaction with a ligand on the leukocyte surface that undergoes oxidative modification and is likely to be different from leukocyte CD73. The identity of this ligand remains to be determined.

CD73 is thought to have non-enzymatic functions, such as promoting leukocyte binding to the endothelium (Airas et al., 1995; Airas et al., 2000; Airas et al., 1993). Engagement of lymphocyte CD73 has been shown to induce LFA-1 clustering and lead to increased adhesion to ECs. Non-quantitative data from immunofluorescence stainings of CD73 in the present study has suggested a possible role in leukocyte TEM. Endothelial CD73 appears to be accumulated around adherent and transmigrating leukocytes. This could indicate a direct involvement of CD73 in diapedesis, possibly as an adhesion molecule. Pre-treatment of ECs with CD73 antibody has been shown to decrease lymphocyte binding by 20% (Airas et al., 1993). Thus, CD73 could have opposing roles in TEM: while the enzymatic activity reduces TEM, the enzyme-independent functions promote adhesion and diapedesis.

To further investigate the role of CD73 in leukocyte TEM, CD73 enzymatic activity was inhibited using a specific, non-hydrolysable inhibitor. The subcellular distribution of CD73 was not altered upon inhibitor treatment, confirming that CD73 activity and localisation are not interdependent. Preliminary data suggest that inhibition of CD73 enzymatic activity reduces leukocyte TEM for most concentrations of AMP-CP, while TEM is increased for 500 µM AMP-CP.

To remove CD73 from the endothelial surface a k-d approach employing specific siRNAs was used. CD73 k-d induced a pro-inflammatory phenotype in HUVECs with elongated cells and an increase in actin stress fibres for most oligos used. The pro-inflammatory phenotype was confirmed by FACS analysis, where increased ICAM-1, VCAM-1 and E- and P-selectin level could be detected. However, even though all oligos knocked-down CD73 efficiently, the extent of the increase in expression was highly variable between oligos. This variability could be observed for most experiments, in particular the adhesion and TEM assays. Even though adhesion and TEM was increased for some oligos, no clear overall effect could be detected, strongly suggesting that off-target effects play an important role for these events. This indicates that a pro-inflammatory phenotype is not sufficient

to increase adhesion and TEM and other regulatory mechanisms are needed, e.g. presentation of chemokines. Data from this study compare well with findings from $CD73^{-/-}$ mice (Koszalka et al., 2004), where ECs displayed increased VCAM-1 level (Zernecke et al., 2006). Monocyte arrest was increased in $CD73^{-/-}$ ECs and predominantly mediated by VLA-4/VCAM-1. ICAM-1 levels were not increased in $CD73^{-/-}$ ECs, in contrast to findings in the present study, where ICAM-1 levels were upregulated following CD73 k-d.

The exact molecular mechanism by which CD73 RNAi induces a pro-inflammatory phenotype remains to be solved, but the NF-κB pathway seems to be a likely candidate. Minguet et al. have shown that stimuli known to enhance intracellular cAMP, such as adenosine, are potent inhibitors of the NF-κB pathway (Minguet et al., 2005). NF-κB is one of the main transcriptional regulators in ECs activated by inflammatory stimuli such as LPS, IL-1 or TNF-α (De Martin et al., 2000). Zernecke et al. reported an increase in NF-κB activity in $CD73^{-/-}$ ECs (Zernecke et al., 2006). Preliminary results indicated lower levels of IκB-α after transfection with some of the oligos used to knock-down CD73 in HUVECs in the present study. This might tentatively suggest NF-κB activation. In future experiments, the activation of NF-κB could be demonstrated by ChIP (chromatin cross-linking immunoprecipitation), EMSA (electrophoretic mobility shift assay) or by investigating nuclear translocation of NF-κB by immunofluorescence. The proposed NF-κB activation following CD73 k-d would imply that the decrease of adenosine receptor activation in CD73 RNAi or $CD73^{-/-}$ ECs leads to a constitutive activation of NF-κB and transcriptional upregulation of downstream targets. These include cell adhesion receptors such as ICAM-1 (Balyasnikova et al., 2000; Collins et al., 1995), VCAM-1 (Collins et al., 1995), E-selectin (Collins et al., 1995; Hallahan et al., 1995) and MAdCAM (De Martin et al., 2000). To determine whether the observed increase in cell surface level of ICAM-1, VCAM-1 and E- and P-selectin in CD73 RNAi HUVECs in the present study are achieved by NF-κB activation, NF-κB inhibitors should be used in CD73 k-d HUVECs to prevent the development of the observed phenotype. Also, to establish the link between adenosine and NF-κB activation, adenosine should be added to CD73 k-d HUVECs and the inflammatory phenotype as well as NF-κB activity assessed.

It is interesting to note that Zernecke et al. observed decreased ICAM-1 levels in $CD73^{-/-}$ arteries, but unaltered mRNA expression (Zernecke et al., 2006). The relationship between adenosine/A_{2A} receptor activation and expression of adhesion molecules such as ICAM-1, VCAM-1, E-selectin and P-selectin is

controversial. Bouma and colleagues showed that in activated HUVECs, adenosine decreased E-selectin and VCAM-1, but not ICAM-1 expression (Bouma et al., 1996). However, they could only demonstrate these differences in submaximally activated HUVECs (0.01 ng/ml TNF-α for 20 h). Surprisingly, ICAM-1 expression was not markedly increased at this concentration, whereas E-selectin and VCAM-1 expression was. This is contradictory to results from other groups, where ICAM-1 level shows a stronger increase even at low TNF-α concentrations, and a dose-dependent decrease in expression level after adenosine or adenosine-analogue addition was observed for ICAM-1 (Zhou et al., 2007). By contrast, Walker et al. reported that treatment of mice with the adenosine analogue 3-deazaadenosine led to inhibition of ICAM-1 and VCAM-1 expression as well as monocyte adhesion and infiltration (Walker et al., 1999). In concordance with these results, McPherson et al. showed decreased expression level of ICAM-1, VCAM-1 and P-selectin in mice treated with the A_{2A} antagonist ATL-146e (McPherson et al., 2001). Taken together, these results and results from the present study suggest that VCAM-1, E-selectin and P-selectin expression are negatively regulated by adenosine, whereas regulation of ICAM-1 remains controversial.

Interestingly, the pro-inflammatory phenotype was not mirrored in increased adhesion and TEM. The oligos used exhibited different, sometimes opposite effects on adhesion and TEM, even though they all induced a pro-inflammatory phenotype to some degree. This indicates that the oligos induce additional off-target effects in the ECs that could interfere with the on-target effect, leading to different outcomes.

In the case where adhesion and TEM were higher, the effects were likely to be due to the elevated levels in adhesion molecules on the surface. TEM could additionally benefit from the increase in endothelial permeability, although higher permeability does not induce TEM *per se*, as has been shown for H_2O_2-treated THP-1 cells (see Chapter 3). The increase in permeability is thought to result from the reduction in adenosine, which has been shown to strengthen endothelial barrier function (Srinivas et al., 2004). Interestingly, changes in leukocyte adhesion were only apparent under non-inflammatory conditions. TNF-α treatment activates the NF-κB pathway, inducing upregulation of cell adhesion receptors involved in adhesion and TEM (De Martin et al., 2000; MacEwan, 2002). NF-κB activation is likely to be a great deal higher in TNF-α-treated HUVECs than in CD73 k-d cells, as can be assumed from the changes in expression level of adhesion molecules (Table 5.2). Thus, TNF-α treatment seems to override the effects of CD73 RNAi, inducing similar levels of adhesion. TNF-α induces upregulation of chemokines (Alom-Ruiz et

al., 2008; De Martin et al., 2000), which induce integrin activation and leukocyte adhesion (Bos, 2005). Chemokine production in CD73 k-d cells has not been determined and it is therefore possible that insufficient leukocyte integrin activation accounts for the differences in adhesion. However, TNF-α-stimulated CD73 k-d cells do have higher expression level of ICAM-1, VCAM-1 and E-selectin, indicating that increasing adhesion molecule levels above a certain threshold does not necessarily increase adhesion further. Transmigration, which is dependent on more than adhesion molecules, seems to be less influenced by CD73 k-d, indicating that CD73 plays a role in the first step of TEM, adhesion, but not necessarily in diapedesis as well. Interestingly, the adhesion of CCRF-CEM cells was increased more than for THP-1 cells, indicating differential usage of adhesion molecules between the different cell types. The potential changes in the junctional composition in CD73 k-d cells could support the general pro-inflammatory phenotype. However, further investigations including quantifications of junctional proteins and the ratio of reticular to non-reticular junctions are necessary to confirm the preliminary results and to understand the implications of these changes.

In conclusion, this study of CD73 has shown that the ecto-enzyme is involved in leukocyte TEM. CD73 is likely to have a non-enzymatic function in TEM as it appears to be accumulated around adherent and transmigrating leukocytes. The k-d of CD73 by RNAi has shown that this ecto-enzyme normally maintains a non-inflammatory phenotype in HUVECs. Knocking-down CD73 leads to a pro-inflammatory phenotype with upregulation of adhesion molecules such as ICAM-1, VCAM-1, E- and P-selectin, and increased leukocyte adhesion. These events are possibly mediated by NF-κB, which could be activated in CD73 k-d cells due to the absence of the inhibitory effect of adenosine (Minguet et al., 2005). However, no direct link between the pro-inflammatory phenotype and leukocyte TEM could be detected.

These data and work by others indicate that CD73 is crucially involved in the regulation of pro- and anti-inflammatory mechanisms in the endothelium. Mimicking or increasing CD73 activity could provide protection against atherosclerosis and inflammation. Taken together, findings from the present study complement data from $CD73^{-/-}$ mice and may help to provide a molecular basis for the therapeutic modulation of CD73, in order to prevent or attenuate vascular inflammation.

6

Concluding remarks

Oxidative stress has been shown to be involved in the development of a range of diseases and has also been implicated in aging. In addition, oxidative stress can occur in pathological conditions such as cancer. Oxidative stress can also be induced by several other factors, including environmental pollution and personal lifestyle choices such as poor diet, smoking and alcohol consumption (Das and Vasudevan, 2007; El-Zayadi, 2006; Stone et al., 2007).

Results from this study have demonstrated that H_2O_2 reduce leukocyte TEM, while increasing adhesion to TNF-α-stimulated endothelial cells. It has been previously reported in the literature that different concentrations of ROS can have different and sometimes even opposing effects (Droge et al., 1994). Similar observations were found in this study and are depicted in Figures 6.1a and 6.1b. This study has investigated the concentration-dependent effects of H_2O_2 on leukocyte TEM and relevant signalling pathways. I have shown for the first time that H_2O_2 induces two patterns of response in THP-1 cells: 1) a progressive increase/decrease with increasing H_2O_2 concentrations; 2) a response to increasing H_2O_2 concentrations that displays a peak at intermediate concentrations around 0.5 to 1 mM. A concentration-dependent decrease was observed for TEM, number of cellular protrusions and Cdc42 activity, while an increase occurred for intracellular ROS, NO and Ca^{2+} levels. Responses with a peak at intermediate concentrations included adhesion to the endothelium, migration velocity, Rac1 activity (in adherent cells) and tyrosine phosphorylation. It is tempting to speculate that adhesion and TEM, which fall into different pattern categories, are regulated by signalling molecules from their respective category.

6.1 Responses with a progressive increase or decrease to H_2O_2

The TEM defect was most likely mediated by a decrease in cellular protrusions. Exploratory protrusions play an important role in TEM, where they probe the endothelium for suitable sites of diapedesis (Barreiro et al., 2007). Loss of these protrusions could therefore reduce TEM significantly. The decrease in TEM and cellular protrusions was accompanied by increased NO levels. Treatment of THP-1

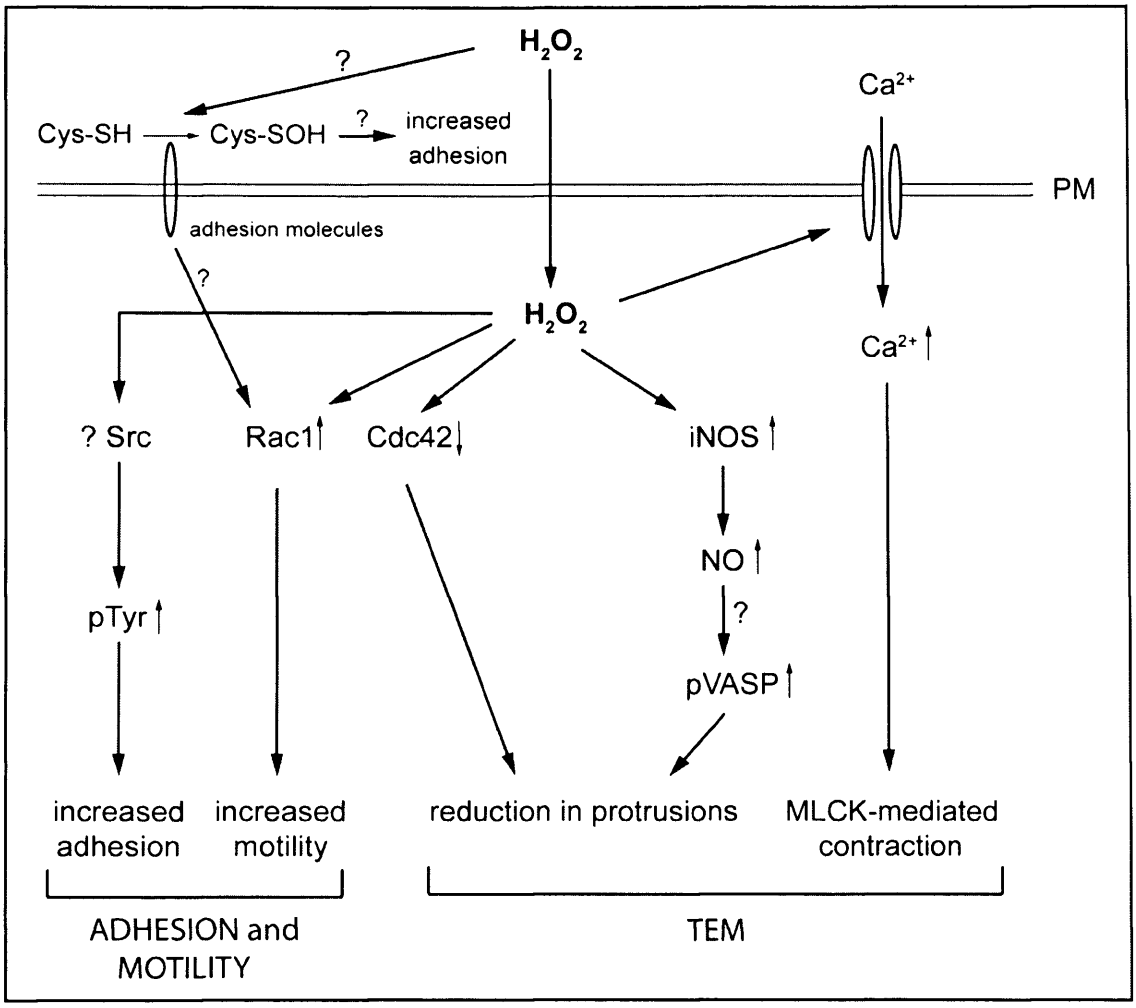

Figure 6.1a: Proposed signal transduction in THP-1 cells at intermediate H_2O_2 concentrations
Incubation of THP-1 cells with intermediate concentrations of H_2O_2 (0.5 – 1 mM, 30 min, 37°C) increases adhesion and migration speed, while TEM is decreased. These events are likely to be mediated by intracellular signalling mechanisms as a consequence of direct oxidative modifications. Increased adhesion and motility could be mediated by higher Rac1 activity, leading to actin polymerisation, and increased tyrosine phosphorylation of adhesion proteins, e.g. paxillin and Src, leading to increased adhesion. Direct oxidative modification of adhesion receptors could additionally increase adhesion and signal to Rac1. The decrease in TEM could be mediated by decreased Cdc42 activity leading to reduction in protrusions. Increases in NO levels via up-regulation of iNOS could also contribute to this pathway, possibly via increased VASP phosphorylation. Additionally, the H_2O_2-induced increase of intracellular Ca^{2+} levels could induce contraction of protrusions.

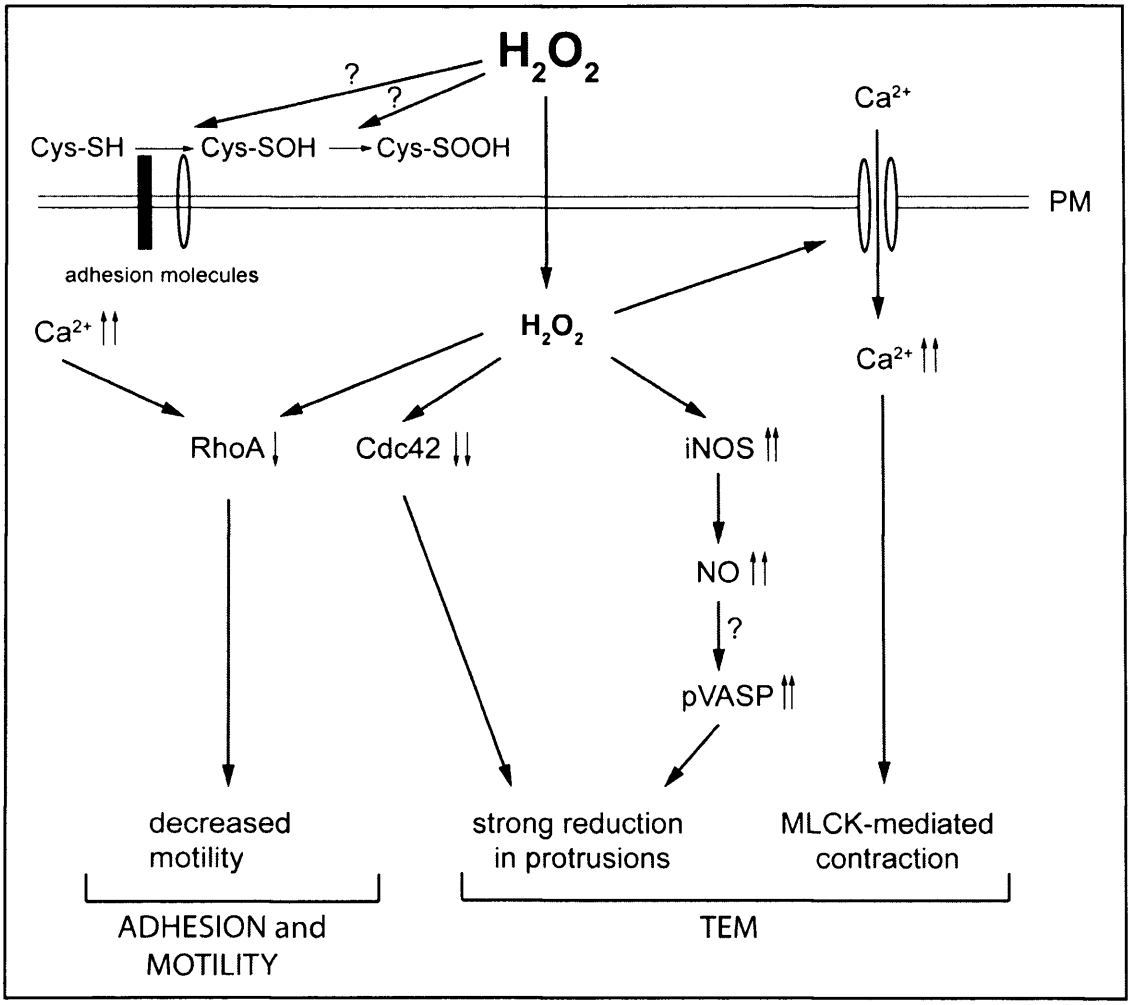

Figure 6.1b: Proposed signal transduction in THP-1 cells at high H_2O_2 concentrations
Incubation of THP-1 cells with high concentrations of H_2O_2 (2 – 5 mM, 30 min, 37°C) decreases TEM, while adhesion and motility are unchanged. Adhesion receptors at the surface could be oxidised (S-OH) as well as hyperoxidised (S-OOH) in the presence of high H_2O_2 levels, which might reduce adhesion to control levels. Decreased RhoA activity could counterbalance the Ca^{2+}-induced increase in actomyosin contraction, since no change in motility can be observed under these conditions. The decrease in TEM is probably mediated by the same pathways as for intermediate H_2O_2 concentrations, although responses are stronger. These pathways include reduction in protrusions due to decreased Cdc42 activity and increased NO level via up-regulation of iNOS, possibly leading to increased VASP phosphorylation and thus VASP inhibition. Additionally, high levels of intracellular Ca^{2+} could induce contraction of the protrusions.

cells with a NO donor induced similar effects as H_2O_2 on adhesion and TEM, leading to the assumption that NO plays a role in mediating H_2O_2 responses. To demonstrate a link between H_2O_2-induced NO and the defect in TEM, L-NAME was used to prevent H_2O_2-induced NO production. L-NAME is a widely used inhibitor of NOS. Pre-treatment with L-NAME did not prevent the H_2O_2-induced decrease in TEM, although a small increase in TEM could be observed when compared to cells without L-NAME. Since the effectiveness of the inhibitor in reducing NO levels was not determined, it is possible that the inhibition of NO production achieved was insufficient to prevent NO-mediated effects. To clarify the role of NO in this process, the effectiveness of L-NAME should be determined and/or different inhibitors of NOS used. Also, when interpreting data from this study, it has to be taken into account that H_2O_2 influences a range of biological responses and the observed phenotype is therefore likely to be mediated by several H_2O_2-induced effects, and inhibition of one pathway might therefore not be sufficient to prevent the TEM defect. The increased NO level could play a role in the decrease of cellular protrusions, since the NO donor SNAP induced a reduction in protrusions similar to H_2O_2, and NO has been shown to induce retraction of cellular protrusions, by stimulating PKG phosphorylation of VASP at Ser239 (Lindsay et al., 2007). This phosphorylation inhibits the anti-capping and filament bundling activity of VASP, which are crucial for protrusion formation (Barzik et al., 2005). It would therefore be interesting to investigate the phosphorylation status of VASP in H_2O_2-treated THP-1 cells. High Ca^{2+} levels could additionally contribute to the reduction in cellular protrusions by increasing contractility via activation of MLCK, leading to increased MLC phosphorylation (Hansen et al., 2000). This hypothesis could be tested by carrying out the experiments under conditions without Ca^{2+} present in the medium, since H_2O_2 has been shown to increase influx of extracellular Ca^{2+} as well as release from intracellular stores (Yan et al., 2006). To prevent release of Ca^{2+} from intracellular stores, thapsigargin, which depletes intracellular Ca^{2+} stores, or xestospongin C, which prevents Ca^{2+} release by inhibiting the inositol 1,4,5-trisphosphate (InsP3) receptor, could be used (Zhao et al., 2008). Cellular protrusions are also regulated by the Rho GTPases Rac1 and Cdc42, with Rac1 being the main driver of lamellipodium protrusion via WAVE and Arp2/3, while Cdc42 induces filopodium formation via mDia/Drf (Ladwein and Rottner, 2008; Ridley, 2001). However, Cdc42 has also been shown to feed into the Arp2/3 pathway via IRSp53. It is therefore possible that the decrease in Cdc42 activity observed in H_2O_2-treated cells is responsible for the reduction of cellular

protrusions. This hypothesis could be tested by over-expressing a 'fast-cycling' mutant of Cdc42 (F28) (Fidyk et al., 2006) in THP-1 cells and investigating whether it rescues cellular protrusions and TEM rate following H_2O_2 treatment. The F28 mutant has proven effective at mediating Cdc42-induced effects, since Cdc42 needs to cycle between the GTP- and GDP-bound state in order to function.

6.2 Responses to H_2O_2 with a peak at intermediate concentrations

Rac1 activity is directly involved in promoting actin polymerisation and migration (Ridley, 2001). At intermediate H_2O_2 concentrations (0.5 to 1 mM) Rac1 activity was high, which was mirrored in increased adhesion and migration. Additionally, tyrosine phosphorylation was increased at these concentrations. Tyrosine phosphorylation of proteins at adhesion sites, e.g. paxillin, is important in increasing migration and adhesion turnover (Nayal et al., 2006). However, leukocytes do not form focal adhesions and due to the faster migration velocity adhesion sites are less stable (Sanchez-Madrid and del Pozo, 1999). Adhesion strength and migration velocity have been shown to be dependent on each other (DiMilla et al., 1993; Huttenlocher et al., 1996; Palecek et al., 1997), and optimised adhesive conditions at intermediate H_2O_2 concentrations could therefore promote migration.

At high H_2O_2 concentrations (2 to 5 mM), adhesion and migration are at control levels and Rac1 activity is decreased. The decrease in Rac1 activity could be due to the high NO levels. NO can decrease Rac1 activity by activating PTP-PEST (protein tyrosine phosphatase-proline, glutamate, serine, and threonine-rich domain), which induces de-phosphorylation of $p130^{CAS}$ and thereby decreases formation of the CrkII-$p130^{CAS}$-Dock180 complex and subsequent Rac1 activation (Ceacareanu et al., 2006; Cote and Vuori, 2007). Since PTP-PEST is also sensitive to redox-inactivation (Salmeen and Barford, 2005), it remains to be determined whether PTP-PEST is active or inactive under conditions where H_2O_2 and NO are present. The decrease in pTyr at high H_2O_2 concentrations could contribute to the reduced migration and adhesion observed under these conditions. How pTyr levels are decreased are unclear, but hyperoxidation (formation of sulphinic acid) of Cys residues of tyrosine kinases or phosphatases could play a role. Additionally, high levels of Ca^{2+} could decrease RhoA activity (Jin et al., 2005), thereby reducing motility.

6.3 Does H_2O_2 modulate TEM and motility by different mechanisms?

These observations indicate that TEM and motility, including adhesion and migration speed, are regulated by separate H_2O_2-induced events. This hypothesis

was further strengthened by the observation that the antioxidant NAC prevented the increase in adhesion of H_2O_2-treated leukocytes, but could not rescue the TEM defect. Additionally, intracellular ROS production via inhibition of catalase or stimulation of NADPH oxidase reduced only TEM, while adhesion was unchanged. These results indicate different mechanisms of regulation for adhesion and TEM. The different mechanisms can be divided into outside and/or outside-in and intracellular signalling. Outside and outside-in signalling could include direct oxidative modifications of adhesion molecules, leading to increased or decreased adhesion. For example, VLA-4 activation is regulated by oxidation of a thiol group in the α4 chain (Liu et al., 2008). Redox-modified integrins could then induce outside-in signalling, e.g. to Rac1, which has been shown to be activated upon integrin binding (del Pozo et al., 2000). Intracellular signalling includes all signalling pathways that are activated or inhibited as a consequence of increased intracellular ROS or NO levels. Events possibly mediated by outside signalling, e.g. adhesion, were reversible by application of antioxidants, while intracellular signalling, leading to decreased TEM, was not. However, since adhesion is also influenced by factors such as protein phosphorylation and Rac1 activity, which could require outside-in and/or intracellular signalling, it is unlikely that the observed phenotypes are dependent on only one route of signal transduction. It is much more likely that adhesion and TEM are regulated predominantly, but not exclusively, by one or the other mechanism.

6.4 Physiological relevance of H_2O_2-regulated leukocyte TEM

Under physiological conditions, the H_2O_2-induced effects on TEM and adhesion could play a role when an acute increase in ROS occurs in the tissue, for example induced by chemotherapeutics (Schumacker, 2006) or alcohol (Das and Vasudevan, 2007), in particular in the liver (Wu et al., 2006), or cigarette smoke-induced ROS in the lung (Yao et al., 2007). Under these circumstances, circulating leukocytes could be exposed to high levels of ROS, leading to adhesion and TEM defects. Although decreased TEM can be beneficial under conditions of chronic inflammation, it also reduces the organism's capacity for immune surveillance, thereby increasing the risk of uncleared infections. A compromised immune surveillance is particularly problematic in the lung, where an enormous surface is in constant contact with inhaled air, which potentially contains a whole range of pathogens. To understand the consequences of the H_2O_2-induced TEM defect, it would be interesting to investigate the effect of H_2O_2 on other leukocytes that play an important role in innate immunity, e.g. neutrophils. Neutrophils are the first

leukocytes to respond to an infection and transmigrate rapidly into the infected site. A H_2O_2-induced TEM defect in neutrophils would therefore severely compromise the innate immune response, which would be relevant for lung infections.

For future studies, it would be intriguing to investigate the effects of long-term treatment with low doses of ROS. This would simulate conditions where leukocytes encounter mild to intermediate levels of oxidative stress during their circulation in the blood before they enter the tissues. Previous studies have shown that long-term treatment with sub-lethal doses of H_2O_2 can protect against cytotoxicity induced by lethal doses of H_2O_2 (Chen et al., 2005). This protection is mediated by increased levels of catalase and Gpx activity. It could be speculated that mild to intermediate levels of oxidative stress could protect cells against high ROS levels in tissues/organs such as in the lung and liver and thus prevent the TEM defect and increase in adhesion at these sites. It would therefore be interesting to compare the TEM of THP-1 cells pre-treated with low levels of H_2O_2 to untreated cells under conditions when they are pulsed with high concentration of ROS.

The lung is, due to its enormous surface and toxic components in inhaled air, susceptible to oxidative stress, in particular the lung of smokers. Inhaled toxic agents stimulate the production of ROS and RNS and provoke inflammatory responses leading to the release of pro-inflammatory cytokines and chemokines (Azad et al., 2008). Inflammation is an important response to lung injury and is vital as a protective mechanism. However, an inflammatory response that is inefficiently resolved can lead to chronic inflammation, which is characterised by the continued infiltration of leukocytes into tissue by leukocytes, tissue destruction, angiogenesis and fibrosis (Kindt et al., 2006). Under these conditions a H_2O_2-induced decrease in TEM would prevent excessive extravasation into the tissue and could therefore be beneficial for the pathogenesis of the condition.

6.5 Role of CD73 as a suppressor of inflammation

The inflammatory reaction in the endothelium is not only regulated by pro- and anti-inflammatory cytokines, but also by purine signalling (Yegutkin, 2008). One modulator of purine signalling is the ecto-enzyme CD73, which has also been implicated in leukocyte TEM (Salmi and Jalkanen, 2005). Results from the present study have demonstrated the role of CD73 in maintaining endothelial cells in a non-inflammatory state. RNAi knock-down of CD73 in HUVECs induced a pro-inflammatory phenotype similar to the response with pro-inflammatory cytokines such as TNF-α, with elongated cells exhibiting increased stress fibres and increased cell surface levels of adhesion molecules such as ICAM-1, VCAM-1, E- and

P-selectin. The increase in adhesion molecules was likely to be mediated by NF-κB, since a reduction of IKK-α levels was observed in CD73 k-d cells. These results are in concordance with findings from $CD73^{-/-}$ mice, where Zernecke et al. demonstrated NF-κB activation and increased VCAM-1 surface expression in aortic endothelial cells and monocyte adhesion (Zernecke et al., 2006). Adenosine and other cAMP-inducing agents are potent inhibitors of the NF-κB pathway (Minguet et al., 2005). Decreased adenosine levels in k-d and $CD73^{-/-}$ ECs therefore allow NF-κB activation, e.g. by GFs present in the tissue or cell culture medium.

Adhesion and TEM of THP-1 cells to and across CD73 k-d HUVECs in this study was not directly dependent on the pro-inflammatory phenotype. While it could be expected that adhesion and TEM are increased under conditions with a CD73 k-d-induced pro-inflammatory phenotype, the different oligos used to knock-down CD73 did not give consistent results. Even though all oligos induced a pro-inflammatory phenotype to some extent, adhesion and TEM was only increased for some oligos, while decreased for others. The results demonstrate that a pro-inflammatory phenotype in HUVECs is not sufficient to induce an increase in leukocyte adhesion and TEM *per se*; leukocytes seemingly need additional signals to bind and transmigrate efficiently. These signals could include chemokines that are presented on the endothelium under inflammatory conditions and are necessary to activate integrins. Chemokine production and presentation was not investigated in CD73 k-d HUVECs, and could be carried out in future studies.

6.6 Oxidative stress in pathological conditions

Oxidative stress has been implicated in the generation of neurodegenerative diseases and the activity of CD73 has been shown to be reduced in the brain of Alzheimer's patients (Kanfer et al., 1986). In an *in vitro* system, Liu and Sok have demonstrated the oxidative inactivation of brain CD73 by Fe^{2+} (Liu and Sok, 2000), which has also been shown for rat liver cytosolic 5'-nucleotidase (Kocic et al., 2001). Liu and Sok demonstrated that H_2O_2 alone is not sufficient to induce oxidative inactivation of CD73, which was confirmed in the present study. Patients with alcoholic liver disease frequently exhibit high levels of iron, and even mild to moderate alcohol consumption has been shown to induce increases in iron (Harrison-Findik, 2007). Oxidative stress in the liver or lung could therefore not only directly induce inflammatory reactions by ROS, but also indirectly by inactivating CD73 and thereby inducing a pro-inflammatory phenotype in the endothelium. It could be speculated that under these conditions, ROS-exposed leukocytes bind to the endothelium, but their TEM is inhibited thereby possibly leading to accumulation

of leukocytes attached to the vessel wall. It would be interesting to investigate if H_2O_2-treated leukocytes display the same behaviour under shear flow or if the increased adhesion is abolished under these conditions. Additionally, different conditions involving H_2O_2-treated THP-1 cells (short/high or long/low H_2O_2) and CD73 k-d endothelial cells could be tested to determine the adhesion and TEM rate.

Interestingly different types of leukocytes displayed big differences in the susceptibility to the toxic effects of H_2O_2; the leukaemia cell lines THP-1 and CCRF-CEM were much more resistant than primary monocytes and T lymphoblasts. For future studies it would be interesting to investigate whether these differences are due to the cancerous nature of the leukaemia cell lines. ROS have been proposed to be involved in tumour metastasis (Wu, 2006) and cancer cells have been shown to have increased ROS levels (Schumacker, 2006). Indeed, increased ROS production in cancer cells can be exploited to selectively kill oncogenically transformed cells (Trachootham et al., 2006). Disabling the GSH system with β-phenylethyl isothiocyanate (PEITC) causes severe ROS accumulation and cell death due to oxidative damage to mitochondria preferentially in transformed cells. It would be interesting to test PEITC or other inhibitors of the antioxidant defence system to determine whether they regulate adhesion and TEM differently in leukaemic *versus* non-leukaemic leukocytes.

Even though the mechanisms of leukocyte TEM and cancer cell extravasation are different in some respects, they do share enough common features to speculate that H_2O_2 might reduce cancer cell extravasation and therefore inhibit metastasis formation. Leukocytes as well as cancer cells bind to E- and P-selectin on the endothelium using sialyl LewisX and sialyl LewisA glycoproteins (Miles et al., 2008). Additionally, both cell types use VLA-4 to bind to immunoglobulin superfamily receptors, although ICAM-1 is used rather than VCAM-1 for cancer cells. When discussing cancer cell extravasation it has to be considered that the exact mechanism may be unique for different cancer cell types. Increasing intracellular ROS levels in cancer cells by inhibiting the antioxidant defence system could have two beneficial effects: reduction of extravasation and induction of apoptosis.

In conclusion, this study has identified H_2O_2 as a novel regulator of leukocyte adhesion and TEM. Additionally, the role of the redox-regulated ecto-enzyme CD73 in maintaining endothelial cells in a non-inflammatory state was shown. The H_2O_2-induced inhibition could have different and opposite effects on the organism

depending on the health condition: while a decrease in TEM could be beneficial in chronic inflammation, it could be harmful under conditions where infections need to be cleared.

Although this study has revealed new insights into the regulation of leukocyte TEM, it also raises many questions about the nature of this regulation and its physiological relevance. This study stresses the importance of preventing and treating oxidative stress as part of a healthy lifestyle and as a therapeutic application for several pathological conditions.

7

References

Adamson, P., Etienne, S., Couraud, P.O., Calder, V., and Greenwood, J. (1999). Lymphocyte migration through brain endothelial cell monolayers involves signaling through endothelial ICAM-1 via a rho-dependent pathway. J Immunol *162*, 2964-2973.

Airas, L., Hellman, J., Salmi, M., Bono, P., Puurunen, T., Smith, D.J., and Jalkanen, S. (1995). CD73 is involved in lymphocyte binding to the endothelium: characterization of lymphocyte-vascular adhesion protein 2 identifies it as CD73. J Exp Med *182*, 1603-1608.

Airas, L., Niemela, J., and Jalkanen, S. (2000). CD73 engagement promotes lymphocyte binding to endothelial cells via a lymphocyte function-associated antigen-1-dependent mechanism. J Immunol *165*, 5411-5417.

Airas, L., Niemela, J., Salmi, M., Puurunen, T., Smith, D.J., and Jalkanen, S. (1997). Differential regulation and function of CD73, a glycosyl-phosphatidylinositol-linked 70-kD adhesion molecule, on lymphocytes and endothelial cells. J Cell Biol *136*, 421-431.

Airas, L., Salmi, M., and Jalkanen, S. (1993). Lymphocyte-vascular adhesion protein-2 is a novel 70-kDa molecule involved in lymphocyte adhesion to vascular endothelium. J Immunol *151*, 4228-4238.

Alderton, W.K., Cooper, C.E., and Knowles, R.G. (2001). Nitric oxide synthases: structure, function and inhibition. Biochem J *357*, 593-615.

Alexandrova, A.Y., Kopnin, P.B., Vasiliev, J.M., and Kopnin, B.P. (2006). ROS up-regulation mediates Ras-induced changes of cell morphology and motility. Experimental cell research *312*, 2066-2073.

Allen, W.E., Jones, G.E., Pollard, J.W., and Ridley, A.J. (1997). Rho, Rac and Cdc42 regulate actin organization and cell adhesion in macrophages. J Cell Sci *110 (Pt 6)*, 707-720.

Allen, W.E., Zicha, D., Ridley, A.J., and Jones, G.E. (1998). A role for Cdc42 in macrophage chemotaxis. J Cell Biol *141*, 1147-1157.

Allingham, M.J., van Buul, J.D., and Burridge, K. (2007). ICAM-1-mediated, Src- and Pyk2-dependent vascular endothelial cadherin tyrosine phosphorylation is required for leukocyte transendothelial migration. J Immunol *179*, 4053-4064.

Alom-Ruiz, S.P., Anilkumar, N., and Shah, A.M. (2008). Reactive oxygen species and endothelial activation. Antioxidants & redox signaling *10*, 1089-1100.

Alon, R., and Dustin, M.L. (2007). Force as a facilitator of integrin conformational changes during leukocyte arrest on blood vessels and antigen-presenting cells. Immunity *26*, 17-27.

Altman, A., and Villalba, M. (2003). Protein kinase C-theta (PKCtheta): it's all about location, location, location. Immunol Rev *192*, 53-63.

An, J.H., and Blackwell, T.K. (2003). SKN-1 links C. elegans mesendodermal specification to a conserved oxidative stress response. Genes Dev *17*, 1882-1893.

Antunes, F., Cadenas, E., and Brunk, U.T. (2001). Apoptosis induced by exposure to a low steady-state concentration of H2O2 is a consequence of lysosomal rupture. Biochem J *356*, 549-555.

Arbiser, J.L., Petros, J., Klafter, R., Govindajaran, B., McLaughlin, E.R., Brown, L.F., Cohen, C., Moses, M., Kilroy, S., Arnold, R.S., and Lambeth, J.D. (2002). Reactive oxygen generated by Nox1 triggers the angiogenic switch. Proc Natl Acad Sci U S A *99*, 715-720.

Azad, N., Rojanasakul, Y., and Vallyathan, V. (2008). Inflammation and lung cancer: roles of reactive oxygen/nitrogen species. Journal of toxicology and environmental health *11*, 1-15.

Ballestrem, C., Hinz, B., Imhof, B.A., and Wehrle-Haller, B. (2001). Marching at the front and dragging behind: differential alphaVbeta3-integrin turnover regulates focal adhesion behavior. J Cell Biol *155*, 1319-1332.

Balyasnikova, I.V., Pelligrino, D.A., Greenwood, J., Adamson, P., Dragon, S., Raza, H., and Galea, E. (2000). Cyclic adenosine monophosphate regulates the expression of the intercellular adhesion molecule and the inducible nitric oxide synthase in brain endothelial cells. J Cereb Blood Flow Metab *20*, 688-699.

Banfi, B., Molnar, G., Maturana, A., Steger, K., Hegedus, B., Demaurex, N., and Krause, K.H. (2001). A Ca(2+)-activated NADPH oxidase in testis, spleen, and lymph nodes. J Biol Chem *276*, 37594-37601.

Barreiro, O., de la Fuente, H., Mittelbrunn, M., and Sanchez-Madrid, F. (2007). Functional insights on the polarized redistribution of leukocyte integrins and their ligands during leukocyte migration and immune interactions. Immunol Rev *218*, 147-164.

Barreiro, O., Yanez-Mo, M., Serrador, J.M., Montoya, M.C., Vicente-Manzanares, M., Tejedor, R., Furthmayr, H., and Sanchez-Madrid, F. (2002). Dynamic interaction of VCAM-1 and ICAM-1 with moesin and ezrin in a novel endothelial docking structure for adherent leukocytes. J Cell Biol *157*, 1233-1245.

Barzik, M., Kotova, T.I., Higgs, H.N., Hazelwood, L., Hanein, D., Gertler, F.B., and Schafer, D.A. (2005). Ena/VASP proteins enhance actin polymerization in the presence of barbed end capping proteins. J Biol Chem *280*, 28653-28662.

Begonja, A.J., Gambaryan, S., Geiger, J., Aktas, B., Pozgajova, M., Nieswandt, B., and Walter, U. (2005). Platelet NAD(P)H-oxidase-generated ROS production regulates alphaIIbbeta3-integrin activation independent of the NO/cGMP pathway. Blood *106*, 2757-2760.

Beinke, S., and Ley, S.C. (2004). Functions of NF-kappaB1 and NF-kappaB2 in immune cell biology. Biochem J *382*, 393-409.

Beny, J.L., and von der Weid, P.Y. (1991). Hydrogen peroxide: an endogenous smooth muscle cell hyperpolarizing factor. Biochem Biophys Res Commun *176*, 378-384.

Bernards, A., and Settleman, J. (2005). GAPs in growth factor signalling. Growth factors (Chur, Switzerland) *23*, 143-149.

Bertram, C., and Hass, R. (2008). Cellular responses to reactive oxygen species-induced DNA damage and aging. Biological chemistry *389*, 211-220.

Bianchi, V., and Spychala, J. (2003). Mammalian 5'-nucleotidases. J Biol Chem *278*, 46195-46198.

Bishop, A.L., and Hall, A. (2000). Rho GTPases and their effector proteins. Biochem J *348 Pt 2*, 241-255.

Blaser, H., Reichman-Fried, M., Castanon, I., Dumstrei, K., Marlow, F.L., Kawakami, K., Solnica-Krezel, L., Heisenberg, C.P., and Raz, E. (2006). Migration of zebrafish primordial germ cells: a role for myosin contraction and cytoplasmic flow. Developmental cell *11*, 613-627.

Bodin, P., and Burnstock, G. (2001). Evidence that release of adenosine triphosphate from endothelial cells during increased shear stress is vesicular. Journal of cardiovascular pharmacology *38*, 900-908.

Boonacker, E., and Van Noorden, C.J. (2003). The multifunctional or moonlighting protein CD26/DPPIV. Eur J Cell Biol *82*, 53-73.

Borek, C. (2004). Dietary antioxidants and human cancer. Integrative cancer therapies *3*, 333-341.

Bos, J.L. (2005). Linking Rap to cell adhesion. Curr Opin Cell Biol *17*, 123-128.

Boulden, B.M., Widder, J.D., Allen, J.C., Smith, D.A., Al-Baldawi, R.N., Harrison, D.G., Dikalov, S.I., Jo, H., and Dudley, S.C., Jr. (2006). Early determinants of H2O2-induced endothelial dysfunction. Free Radic Biol Med *41*, 810-817.

Bouma, M.G., van den Wildenberg, F.A., and Buurman, W.A. (1996). Adenosine inhibits cytokine release and expression of adhesion molecules by activated human endothelial cells. Am J Physiol *270*, C522-529.

Bourmeyster, N., and Vignais, P.V. (1996). Phosphorylation of Rho GDI stabilizes the Rho A-Rho GDI complex in neutrophil cytosol. Biochem Biophys Res Commun *218*, 54-60.

Bours, M.J., Swennen, E.L., Di Virgilio, F., Cronstein, B.N., and Dagnelie, P.C. (2006). Adenosine 5'-triphosphate and adenosine as endogenous signaling molecules in immunity and inflammation. Pharmacol Ther *112*, 358-404.

Boveris, A., and Chance, B. (1973). The mitochondrial generation of hydrogen peroxide. General properties and effect of hyperbaric oxygen. Biochem J *134*, 707-716.

Braganhol, E., Tamajusuku, A.S., Bernardi, A., Wink, M.R., and Battastini, A.M. (2007). Ecto-5'-nucleotidase/CD73 inhibition by quercetin in the human U138MG glioma cell line. Biochim Biophys Acta *1770*, 1352-1359.

Brakebusch, C., Fillatreau, S., Potocnik, A.J., Bungartz, G., Wilhelm, P., Svensson, M., Kearney, P., Korner, H., Gray, D., and Fassler, R. (2002). Beta1 integrin is not essential for hematopoiesis but is necessary for the T cell-dependent IgM antibody response. Immunity *16*, 465-477.

Bretscher, A., Edwards, K., and Fehon, R.G. (2002). ERM proteins and merlin: integrators at the cell cortex. Nature reviews *3*, 586-599.

Burnstock, G. (2007). Physiology and pathophysiology of purinergic neurotransmission. Physiol Rev *87*, 659-797.

Cabrero, J.R., Serrador, J.M., Barreiro, O., Mittelbrunn, M., Naranjo-Suarez, S., Martin-Cofreces, N., Vicente-Manzanares, M., Mazitschek, R., Bradner, J.E., Avila, J., Valenzuela-Fernandez, A., and Sanchez-Madrid, F. (2006). Lymphocyte chemotaxis is regulated by histone deacetylase 6, independently of its deacetylase activity. Mol Biol Cell *17*, 3435-3445.

Campbell, J.J., Hedrick, J., Zlotnik, A., Siani, M.A., Thompson, D.A., and Butcher, E.C. (1998). Chemokines and the arrest of lymphocytes rolling under flow conditions. Science *279*, 381-384.

Carlier, M.F., and Pantaloni, D. (2007). Control of actin assembly dynamics in cell motility. J Biol Chem *282*, 23005-23009.

Carman, C.V., Jun, C.D., Salas, A., and Springer, T.A. (2003). Endothelial cells proactively form microvilli-like membrane projections upon intercellular adhesion molecule 1 engagement of leukocyte LFA-1. J Immunol *171*, 6135-6144.

Carman, C.V., Sage, P.T., Sciuto, T.E., de la Fuente, M.A., Geha, R.S., Ochs, H.D., Dvorak, H.F., Dvorak, A.M., and Springer, T.A. (2007). Transcellular diapedesis is initiated by invasive podosomes. Immunity *26*, 784-797.

Carman, C.V., and Springer, T.A. (2003). Integrin avidity regulation: are changes in affinity and conformation underemphasized? Curr Opin Cell Biol *15*, 547-556.

Carman, C.V., and Springer, T.A. (2004). A transmigratory cup in leukocyte diapedesis both through individual vascular endothelial cells and between them. J Cell Biol *167*, 377-388.

Carpenter, C.L., Tolias, K.F., Van Vugt, A., and Hartwig, J. (1999). Lipid kinases are novel effectors of the GTPase Rac1. Advances in enzyme regulation *39*, 299-312.

Castrop, H., Huang, Y., Hashimoto, S., Mizel, D., Hansen, P., Theilig, F., Bachmann, S., Deng, C., Briggs, J., and Schnermann, J. (2004). Impairment of tubuloglomerular feedback regulation of GFR in ecto-5'-nucleotidase/CD73-deficient mice. J Clin Invest *114*, 634-642.

Ceacareanu, A.C., Ceacareanu, B., Zhuang, D., Chang, Y., Ray, R.M., Desai, L., Chapman, K.E., Waters, C.M., and Hassid, A. (2006). Nitric oxide attenuates IGF-I-induced aortic smooth muscle cell motility by decreasing Rac1 activity: essential role of PTP-PEST and p130cas. Am J Physiol Cell Physiol *290*, C1263-1270.

Chan, H.L., Gharbi, S., Gaffney, P.R., Cramer, R., Waterfield, M.D., and Timms, J.F. (2005). Proteomic analysis of redox- and ErbB2-dependent changes in mammary luminal epithelial cells using cysteine- and lysine-labelling two-dimensional difference gel electrophoresis. Proteomics *5*, 2908-2926.

Chan, J.R., Hyduk, S.J., and Cybulsky, M.I. (2001). Chemoattractants induce a rapid and transient upregulation of monocyte alpha4 integrin affinity for vascular cell adhesion molecule 1 which mediates arrest: an early step in the process of emigration. J Exp Med *193*, 1149-1158.

Chandrasekharan, U.M., Siemionow, M., Unsal, M., Yang, L., Poptic, E., Bohn, J., Ozer, K., Zhou, Z., Howe, P.H., Penn, M., and DiCorleto, P.E. (2007). Tumor necrosis factor alpha (TNF-alpha) receptor-II is required for TNF-alpha-induced leukocyte-endothelial interaction in vivo. Blood *109*, 1938-1944.

Chatzizacharias, N.A., Kouraklis, G.P., and Theocharis, S.E. (2008). Disruption of FAK signaling: a side mechanism in cytotoxicity. Toxicology *245*, 1-10.

Chavakis, T., Bierhaus, A., Al-Fakhri, N., Schneider, D., Witte, S., Linn, T., Nagashima, M., Morser, J., Arnold, B., Preissner, K.T., and Nawroth, P.P. (2003). The pattern recognition receptor (RAGE) is a counterreceptor for leukocyte integrins: a novel pathway for inflammatory cell recruitment. J Exp Med *198*, 1507-1515.

Chen, X.L., Zhang, Q., Zhao, R., Ding, X., Tummala, P.E., and Medford, R.M. (2003). Rac1 and superoxide are required for the expression of cell adhesion molecules induced by tumor necrosis factor-alpha in endothelial cells. J Pharmacol Exp Ther *305*, 573-580.

Chen, Z.H., Yoshida, Y., Saito, Y., and Niki, E. (2005). Adaptation to hydrogen peroxide enhances PC12 cell tolerance against oxidative damage. Neuroscience letters *383*, 256-259.

Cheng, G., Cao, Z., Xu, X., van Meir, E.G., and Lambeth, J.D. (2001). Homologs of gp91phox: cloning and tissue expression of Nox3, Nox4, and Nox5. Gene *269*, 131-140.

Chesnutt, B.C., Smith, D.F., Raffler, N.A., Smith, M.L., White, E.J., and Ley, K. (2006). Induction of LFA-1-dependent neutrophil rolling on ICAM-1 by engagement of E-selectin. Microcirculation *13*, 99-109.

Chiarugi, P., and Fiaschi, T. (2007). Redox signalling in anchorage-dependent cell growth. Cell Signal *19*, 672-682.

Cho, S., Szeto, H.H., Kim, E., Kim, H., Tolhurst, A.T., and Pinto, J.T. (2007). A novel cell-permeable antioxidant peptide, SS31, attenuates ischemic brain injury by down-regulating CD36. J Biol Chem *282*, 4634-4642.

Choi, M.H., Lee, I.K., Kim, G.W., Kim, B.U., Han, Y.H., Yu, D.Y., Park, H.S., Kim, K.Y., Lee, J.S., Choi, C., Bae, Y.S., Lee, B.I., Rhee, S.G., and Kang, S.W. (2005a). Regulation of PDGF signalling and vascular remodelling by peroxiredoxin II. Nature *435*, 347-353.

Choi, S.E., Min, S.H., Shin, H.C., Kim, H.E., Jung, M.W., and Kang, Y. (2006). Involvement of calcium-mediated apoptotic signals in H2O2-induced MIN6N8a cell death. Eur J Pharmacol *547*, 1-9.

Choi, S.H., Lee, D.Y., Kim, S.U., and Jin, B.K. (2005b). Thrombin-induced oxidative stress contributes to the death of hippocampal neurons in vivo: role of microglial NADPH oxidase. J Neurosci *25*, 4082-4090.

Chowdhury, S.K., Raha, S., Tarnopolsky, M.A., and Singh, G. (2007). Increased expression of mitochondrial glycerophosphate dehydrogenase and antioxidant enzymes in prostate cancer cell lines/cancer. Free Radic Res *41*, 1116-1124.

Chuang, T.H., Bohl, B.P., and Bokoch, G.M. (1993). Biologically active lipids are regulators of Rac.GDI complexation. J Biol Chem *268*, 26206-26211.

Clair, T., Aoki, J., Koh, E., Bandle, R.W., Nam, S.W., Ptaszynska, M.M., Mills, G.B., Schiffmann, E., Liotta, L.A., and Stracke, M.L. (2003). Autotaxin hydrolyzes sphingosylphosphorylcholine to produce the regulator of migration, sphingosine-1-phosphate. Cancer research *63*, 5446-5453.

Clark, K.L., Oelke, A., Johnson, M.E., Eilert, K.D., Simpson, P.C., and Todd, S.C. (2004). CD81 associates with 14-3-3 in a redox-regulated palmitoylation-dependent manner. J Biol Chem *279*, 19401-19406.

Collins, T., Read, M.A., Neish, A.S., Whitley, M.Z., Thanos, D., and Maniatis, T. (1995). Transcriptional regulation of endothelial cell adhesion molecules: NF-kappa B and cytokine-inducible enhancers. Faseb J *9*, 899-909.

Comerford, K.M., Lawrence, D.W., Synnestvedt, K., Levi, B.P., and Colgan, S.P. (2002). Role of vasodilator-stimulated phosphoprotein in PKA-induced changes in endothelial junctional permeability. Faseb J *16*, 583-585.

Cook-Mills, J.M. (2002). VCAM-1 signals during lymphocyte migration: role of reactive oxygen species. Mol Immunol *39*, 499-508.

Cook-Mills, J.M., Johnson, J.D., Deem, T.L., Ochi, A., Wang, L., and Zheng, Y. (2004). Calcium mobilization and Rac1 activation are required for VCAM-1 (vascular cell adhesion molecule-1) stimulation of NADPH oxidase activity. Biochem J *378*, 539-547.

Cook, S.A., Sugden, P.H., and Clerk, A. (1999). Regulation of bcl-2 family proteins during development and in response to oxidative stress in cardiac myocytes: association with changes in mitochondrial membrane potential. Circ Res *85*, 940-949.

Cote, J.F., and Vuori, K. (2007). GEF what? Dock180 and related proteins help Rac to polarize cells in new ways. Trends Cell Biol *17*, 383-393.

Cox, E.A., and Huttenlocher, A. (1998). Regulation of integrin-mediated adhesion during cell migration. Microscopy research and technique *43*, 412-419.

Cronstein, B.N. (1994). Adenosine, an endogenous anti-inflammatory agent. J Appl Physiol *76*, 5-13.

Cunningham, S.A., Rodriguez, J.M., Arrate, M.P., Tran, T.M., and Brock, T.A. (2002). JAM2 interacts with alpha4beta1. Facilitation by JAM3. J Biol Chem *277*, 27589-27592.

Daniels, R.H., and Bokoch, G.M. (1999). p21-activated protein kinase: a crucial component of morphological signaling? Trends in biochemical sciences *24*, 350-355.

Das, S.K., and Vasudevan, D.M. (2007). Alcohol-induced oxidative stress. Life sciences *81*, 177-187.

Davies, K.J. (1987). Protein damage and degradation by oxygen radicals. I. general aspects. J Biol Chem *262*, 9895-9901.

De Martin, R., Hoeth, M., Hofer-Warbinek, R., and Schmid, J.A. (2000). The transcription factor NF-kappa B and the regulation of vascular cell function. Arterioscler Thromb Vasc Biol *20*, E83-88.

De Meester, I., Korom, S., Van Damme, J., and Scharpe, S. (1999). CD26, let it cut or cut it down. Immunol Today *20*, 367-375.

de Oliveira-Marques, V., Cyrne, L., Marinho, H.S., and Antunes, F. (2007). A quantitative study of NF-kappaB activation by H2O2: relevance in inflammation and synergy with TNF-alpha. J Immunol *178*, 3893-3902.

Dean, R.T., Thomas, S.M., Vince, G., and Wolff, S.P. (1986). Oxidation induced proteolysis and its possible restriction by some secondary protein modifications. Biomedica biochimica acta *45*, 1563-1573.

Deem, T.L., and Cook-Mills, J.M. (2004). Vascular cell adhesion molecule 1 (VCAM-1) activation of endothelial cell matrix metalloproteinases: role of reactive oxygen species. Blood *104*, 2385-2393.

Defer, N., Azroyan, A., Pecker, F., and Pavoine, C. (2007). TNFR1 and TNFR2 signaling interplay in cardiac myocytes. J Biol Chem *282*, 35564-35573.

Dejana, E. (2004). Endothelial cell-cell junctions: happy together. Nature reviews *5*, 261-270.

del Pozo, M.A., Price, L.S., Alderson, N.B., Ren, X.D., and Schwartz, M.A. (2000). Adhesion to the extracellular matrix regulates the coupling of the small GTPase Rac to its effector PAK. Embo J *19*, 2008-2014.

del Pozo, M.A., Schwartz, M.A., Hu, J., Kiosses, W.B., Altman, A., and Villalba, M. (2003). Guanine exchange-dependent and -independent effects of Vav1 on integrin-induced T cell spreading. J Immunol *170*, 41-47.

DeLeo, F.R., Renee, J., McCormick, S., Nakamura, M., Apicella, M., Weiss, J.P., and Nauseef, W.M. (1998). Neutrophils exposed to bacterial lipopolysaccharide upregulate NADPH oxidase assembly. J Clin Invest *101*, 455-463.

DerMardirossian, C., and Bokoch, G.M. (2005). GDIs: central regulatory molecules in Rho GTPase activation. Trends Cell Biol *15*, 356-363.

DerMardirossian, C., Rocklin, G., Seo, J.Y., and Bokoch, G.M. (2006). Phosphorylation of RhoGDI by Src regulates Rho GTPase binding and cytosol-membrane cycling. Mol Biol Cell *17*, 4760-4768.

DerMardirossian, C., Schnelzer, A., and Bokoch, G.M. (2004). Phosphorylation of RhoGDI by Pak1 mediates dissociation of Rac GTPase. Mol Cell *15*, 117-127.

Di Virgilio, F., Chiozzi, P., Ferrari, D., Falzoni, S., Sanz, J.M., Morelli, A., Torboli, M., Bolognesi, G., and Baricordi, O.R. (2001). Nucleotide receptors: an emerging family of regulatory molecules in blood cells. Blood *97*, 587-600.

DiMilla, P.A., Barbee, K., and Lauffenburger, D.A. (1991). Mathematical model for the effects of adhesion and mechanics on cell migration speed. Biophysical journal *60*, 15-37.

DiMilla, P.A., Stone, J.A., Quinn, J.A., Albelda, S.M., and Lauffenburger, D.A. (1993). Maximal migration of human smooth muscle cells on fibronectin and type IV collagen occurs at an intermediate attachment strength. J Cell Biol *122*, 729-737.

Dimmeler, S., Fleming, I., Fisslthaler, B., Hermann, C., Busse, R., and Zeiher, A.M. (1999). Activation of nitric oxide synthase in endothelial cells by Akt-dependent phosphorylation. Nature *399*, 601-605.

Dombrowski, K.E., Ke, Y., Brewer, K.A., and Kapp, J.A. (1998). Ecto-ATPase: an activation marker necessary for effector cell function. Immunol Rev *161*, 111-118.

Dransfield, I., Cabanas, C., Craig, A., and Hogg, N. (1992). Divalent cation regulation of the function of the leukocyte integrin LFA-1. J Cell Biol *116*, 219-226.

Drees, F., Pokutta, S., Yamada, S., Nelson, W.J., and Weis, W.I. (2005). Alpha-catenin is a molecular switch that binds E-cadherin-beta-catenin and regulates actin-filament assembly. Cell *123*, 903-915.

Droge, W. (2002). Free radicals in the physiological control of cell function. Physiol Rev *82*, 47-95.

Droge, W., Schulze-Osthoff, K., Mihm, S., Galter, D., Schenk, H., Eck, H.P., Roth, S., and Gmunder, H. (1994). Functions of glutathione and glutathione disulfide in immunology and immunopathology. Faseb J *8*, 1131-1138.

Drouin, A., Thorin-Trescases, N., Hamel, E., Falck, J.R., and Thorin, E. (2007). Endothelial nitric oxide synthase activation leads to dilatory H2O2 production in mouse cerebral arteries. Cardiovascular research *73*, 73-81.

Dupuy, C., Ohayon, R., Valent, A., Noel-Hudson, M.S., Deme, D., and Virion, A. (1999). Purification of a novel flavoprotein involved in the thyroid NADPH oxidase. Cloning of the porcine and human cdnas. J Biol Chem *274*, 37265-37269.

Dustin, M.L., Bivona, T.G., and Philips, M.R. (2004). Membranes as messengers in T cell adhesion signaling. Nat Immunol *5*, 363-372.

Dusting, G.J., Moncada, S., and Vane, J.R. (1977). Prostacyclin (PGX) is the endogenous metabolite responsible for relaxation of coronary arteries induced by arachindonic acid. Prostaglandins *13*, 3-15.

Echtay, K.S. (2007). Mitochondrial uncoupling proteins--what is their physiological role? Free Radic Biol Med *43*, 1351-1371.

Eckle, T., Fullbier, L., Wehrmann, M., Khoury, J., Mittelbronn, M., Ibla, J., Rosenberger, P., and Eltzschig, H.K. (2007a). Identification of ectonucleotidases CD39 and CD73 in innate protection during acute lung injury. J Immunol *178*, 8127-8137.

Eckle, T., Krahn, T., Grenz, A., Kohler, D., Mittelbronn, M., Ledent, C., Jacobson, M.A., Osswald, H., Thompson, L.F., Unertl, K., and Eltzschig, H.K. (2007b). Cardioprotection by ecto-5'-nucleotidase (CD73) and A2B adenosine receptors. Circulation *115*, 1581-1590.

Edens, W.A., Sharling, L., Cheng, G., Shapira, R., Kinkade, J.M., Lee, T., Edens, H.A., Tang, X., Sullards, C., Flaherty, D.B., Benian, G.M., and Lambeth, J.D. (2001). Tyrosine cross-linking of extracellular matrix is catalyzed by Duox, a multidomain oxidase/peroxidase with homology to the phagocyte oxidase subunit gp91phox. J Cell Biol *154*, 879-891.

Eguchi, H., Ikeda, Y., Ookawara, T., Koyota, S., Fujiwara, N., Honke, K., Wang, P.G., Taniguchi, N., and Suzuki, K. (2005). Modification of oligosaccharides by reactive oxygen species decreases sialyl lewis x-mediated cell adhesion. Glycobiology *15*, 1094-1101.

El-Zayadi, A.R. (2006). Heavy smoking and liver. World J Gastroenterol *12*, 6098-6101.

Elices, M.J., Osborn, L., Takada, Y., Crouse, C., Luhowskyj, S., Hemler, M.E., and Lobb, R.R. (1990). VCAM-1 on activated endothelium interacts with the leukocyte integrin VLA-4 at a site distinct from the VLA-4/fibronectin binding site. Cell *60*, 577-584.

Ellerbroek, S.M., Wennerberg, K., and Burridge, K. (2003). Serine phosphorylation negatively regulates RhoA in vivo. J Biol Chem *278*, 19023-19031.

Ellis, A., Pannirselvam, M., Anderson, T.J., and Triggle, C.R. (2003). Catalase has negligible inhibitory effects on endothelium-dependent relaxations in mouse isolated aorta and small mesenteric artery. British journal of pharmacology *140*, 1193-1200.

Eltzschig, H.K., Eckle, T., Mager, A., Kuper, N., Karcher, C., Weissmuller, T., Boengler, K., Schulz, R., Robson, S.C., and Colgan, S.P. (2006). ATP release from activated neutrophils occurs via connexin 43 and modulates adenosine-dependent endothelial cell function. Circ Res *99*, 1100-1108.

Eltzschig, H.K., Ibla, J.C., Furuta, G.T., Leonard, M.O., Jacobson, K.A., Enjyoji, K., Robson, S.C., and Colgan, S.P. (2003). Coordinated adenine nucleotide phosphohydrolysis and nucleoside signaling in posthypoxic endothelium: role of ectonucleotidases and adenosine A2B receptors. J Exp Med *198*, 783-796.

Eltzschig, H.K., Thompson, L.F., Karhausen, J., Cotta, R.J., Ibla, J.C., Robson, S.C., and Colgan, S.P. (2004). Endogenous adenosine produced during hypoxia attenuates neutrophil accumulation: coordination by extracellular nucleotide metabolism. Blood *104*, 3986-3992.

England, K., and Cotter, T.G. (2005). Direct oxidative modifications of signalling proteins in mammalian cells and their effects on apoptosis. Redox Rep *10*, 237-245.

Englund, P.T. (1993). The structure and biosynthesis of glycosyl phosphatidylinositol protein anchors. Annu Rev Biochem *62*, 121-138.

Enjyoji, K., Sevigny, J., Lin, Y., Frenette, P.S., Christie, P.D., Esch, J.S., 2nd, Imai, M., Edelberg, J.M., Rayburn, H., Lech, M., Beeler, D.L., Csizmadia, E., Wagner, D.D., Robson, S.C., and Rosenberg, R.D. (1999). Targeted disruption of cd39/ATP diphosphohydrolase results in disordered hemostasis and thromboregulation. Nat Med *5*, 1010-1017.

Eriksson, E.E., Xie, X., Werr, J., Thoren, P., and Lindbom, L. (2001). Importance of primary capture and L-selectin-dependent secondary capture in leukocyte accumulation in inflammation and atherosclerosis in vivo. J Exp Med *194*, 205-218.

Ermak, G., and Davies, K.J. (2002). Calcium and oxidative stress: from cell signaling to cell death. Mol Immunol *38*, 713-721.

Fais, S., and Malorni, W. (2003). Leukocyte uropod formation and membrane/cytoskeleton linkage in immune interactions. J Leukoc Biol *73*, 556-563.

Faix, J., and Rottner, K. (2006). The making of filopodia. Curr Opin Cell Biol *18*, 18-25.

Feletou, M., and Vanhoutte, P.M. (1988). Endothelium-dependent hyperpolarization of canine coronary smooth muscle. British journal of pharmacology *93*, 515-524.

Feletou, M., and Vanhoutte, P.M. (2007). Endothelium-dependent hyperpolarizations: past beliefs and present facts. Annals of medicine *39*, 495-516.

Feng, D., Nagy, J.A., Pyne, K., Dvorak, H.F., and Dvorak, A.M. (1998). Neutrophils emigrate from venules by a transendothelial cell pathway in response to FMLP. J Exp Med *187*, 903-915.

Ferguson, M.A., and Williams, A.F. (1988). Cell-surface anchoring of proteins via glycosyl-phosphatidylinositol structures. Annu Rev Biochem *57*, 285-320.

Fiaschi, T., Cozzi, G., Raugei, G., Formigli, L., Ramponi, G., and Chiarugi, P. (2006). Redox regulation of beta-actin during integrin-mediated cell adhesion. J Biol Chem *281*, 22983-22991.

Fidyk, N., Wang, J.B., and Cerione, R.A. (2006). Influencing cellular transformation by modulating the rates of GTP hydrolysis by Cdc42. Biochemistry *45*, 7750-7762.

Finkel, T., and Holbrook, N.J. (2000). Oxidants, oxidative stress and the biology of ageing. Nature *408*, 239-247.

Forget, M.A., Desrosiers, R.R., Gingras, D., and Beliveau, R. (2002). Phosphorylation states of Cdc42 and RhoA regulate their interactions with Rho GDP dissociation inhibitor and their extraction from biological membranes. Biochem J *361*, 243-254.

Frame, M.C., Fincham, V.J., Carragher, N.O., and Wyke, J.A. (2002). v-Src's hold over actin and cell adhesions. Nature reviews *3*, 233-245.

Francis, K., Palsson, B., Donahue, J., Fong, S., and Carrier, E. (2002). Murine Sca-1(+)/Lin(-) cells and human KG1a cells exhibit multiple pseudopod morphologies during migration. Experimental hematology *30*, 460-463.

Frank, G.D., Motley, E.D., Inagami, T., and Eguchi, S. (2000). PYK2/CAKbeta represents a redox-sensitive tyrosine kinase in vascular smooth muscle cells. Biochem Biophys Res Commun *270*, 761-765.

Fraticelli, A., Serrano, C.V., Jr., Bochner, B.S., Capogrossi, M.C., and Zweier, J.L. (1996). Hydrogen peroxide and superoxide modulate leukocyte adhesion molecule expression and leukocyte endothelial adhesion. Biochim Biophys Acta *1310*, 251-259.

Friedl, J., Puhlmann, M., Bartlett, D.L., Libutti, S.K., Turner, E.N., Gnant, M.F., and Alexander, H.R. (2002). Induction of permeability across endothelial cell monolayers by tumor necrosis factor (TNF) occurs via a tissue factor-dependent mechanism: relationship between the procoagulant and permeability effects of TNF. Blood *100*, 1334-1339.

Friedl, P. (2004). Prespecification and plasticity: shifting mechanisms of cell migration. Curr Opin Cell Biol *16*, 14-23.

Friedl, P., Borgmann, S., and Brocker, E.B. (2001). Amoeboid leukocyte crawling through extracellular matrix: lessons from the Dictyostelium paradigm of cell movement. J Leukoc Biol *70*, 491-509.

Friedl, P., Entschladen, F., Conrad, C., Niggemann, B., and Zanker, K.S. (1998). CD4+ T lymphocytes migrating in three-dimensional collagen lattices lack focal adhesions and utilize beta1 integrin-independent strategies for polarization, interaction with collagen fibers and locomotion. Eur J Immunol *28*, 2331-2343.

Fulton, D., Gratton, J.P., McCabe, T.J., Fontana, J., Fujio, Y., Walsh, K., Franke, T.F., Papapetropoulos, A., and Sessa, W.C. (1999). Regulation of endothelium-derived nitric oxide production by the protein kinase Akt. Nature *399*, 597-601.

Furchgott, R.F., and Vanhoutte, P.M. (1989). Endothelium-derived relaxing and contracting factors. Faseb J *3*, 2007-2018.

Gavazzi, G., Banfi, B., Deffert, C., Fiette, L., Schappi, M., Herrmann, F., and Krause, K.H. (2006). Decreased blood pressure in NOX1-deficient mice. FEBS Lett *580*, 497-504.

Geiger, B., Bershadsky, A., Pankov, R., and Yamada, K.M. (2001). Transmembrane crosstalk between the extracellular matrix--cytoskeleton crosstalk. Nature reviews *2*, 793-805.

Geiszt, M., Kopp, J.B., Varnai, P., and Leto, T.L. (2000). Identification of renox, an NAD(P)H oxidase in kidney. Proc Natl Acad Sci U S A *97*, 8010-8014.

Geiszt, M., and Leto, T.L. (2004). The Nox family of NAD(P)H oxidases: host defense and beyond. J Biol Chem *279*, 51715-51718.

Geiszt, M., Witta, J., Baffi, J., Lekstrom, K., and Leto, T.L. (2003). Dual oxidases represent novel hydrogen peroxide sources supporting mucosal surface host defense. Faseb J *17*, 1502-1504.

Gerasimovskaya, E.V., Ahmad, S., White, C.W., Jones, P.L., Carpenter, T.C., and Stenmark, K.R. (2002). Extracellular ATP is an autocrine/paracrine regulator of hypoxia-induced adventitial fibroblast growth. Signaling through extracellular signal-regulated kinase-1/2 and the Egr-1 transcription factor. J Biol Chem *277*, 44638-44650.

Ginnan, R., Guikema, B.J., Halligan, K.E., Singer, H.A., and Jourd'heuil, D. (2008). Regulation of smooth muscle by inducible nitric oxide synthase and NADPH oxidase in vascular proliferative diseases. Free Radic Biol Med *44*, 1232-1245.

Gismondi, A., Jacobelli, J., Strippoli, R., Mainiero, F., Soriani, A., Cifaldi, L., Piccoli, M., Frati, L., and Santoni, A. (2003). Proline-rich tyrosine kinase 2 and Rac activation by chemokine and integrin receptors controls NK cell transendothelial migration. J Immunol *170*, 3065-3073.

Glading, A., Chang, P., Lauffenburger, D.A., and Wells, A. (2000). Epidermal growth factor receptor activation of calpain is required for fibroblast motility and occurs via an ERK/MAP kinase signaling pathway. J Biol Chem *275*, 2390-2398.

Goding, J.W. (2000). Ecto-enzymes: physiology meets pathology. J Leukoc Biol *67*, 285-311.

Goding, J.W., Grobben, B., and Slegers, H. (2003). Physiological and pathophysiological functions of the ecto-nucleotide pyrophosphatase/phosphodiesterase family. Biochim Biophys Acta *1638*, 1-19.

Goepfert, C., Sundberg, C., Sevigny, J., Enjyoji, K., Hoshi, T., Csizmadia, E., and Robson, S. (2001). Disordered cellular migration and angiogenesis in cd39-null mice. Circulation *104*, 3109-3115.

Goldfinger, L.E., Han, J., Kiosses, W.B., Howe, A.K., and Ginsberg, M.H. (2003). Spatial restriction of alpha4 integrin phosphorylation regulates lamellipodial stability and alpha4beta1-dependent cell migration. J Cell Biol *162*, 731-741.

Gonzalez-Gronow, M., Misra, U.K., Gawdi, G., and Pizzo, S.V. (2005). Association of plasminogen with dipeptidyl peptidase IV and Na+/H+ exchanger isoform NHE3 regulates invasion of human 1-LN prostate tumor cells. J Biol Chem *280*, 27173-27178.

Gopalakrishna, R., and Anderson, W.B. (1989). Ca2+- and phospholipid-independent activation of protein kinase C by selective oxidative modification of the regulatory domain. Proc Natl Acad Sci U S A *86*, 6758-6762.

Gordon-Weeks, P.R. (2004). Microtubules and growth cone function. Journal of neurobiology *58*, 70-83.

Gorrell, M.D., Gysbers, V., and McCaughan, G.W. (2001). CD26: a multifunctional integral membrane and secreted protein of activated lymphocytes. Scandinavian journal of immunology *54*, 249-264.

Graf, T. (2008). Immunology: blood lines redrawn. Nature *452*, 702-703.

Griendling, K.K., Sorescu, D., Lassegue, B., and Ushio-Fukai, M. (2000). Modulation of protein kinase activity and gene expression by reactive oxygen species and their role in vascular physiology and pathophysiology. Arterioscler Thromb Vasc Biol *20*, 2175-2183.

Grinnell, F. (1994). Fibroblasts, myofibroblasts, and wound contraction. J Cell Biol *124*, 401-404.

Grune, T., Reinheckel, T., and Davies, K.J. (1997). Degradation of oxidized proteins in mammalian cells. Faseb J *11*, 526-534.

Gu, Y., Filippi, M.D., Cancelas, J.A., Siefring, J.E., Williams, E.P., Jasti, A.C., Harris, C.E., Lee, A.W., Prabhakar, R., Atkinson, S.J., Kwiatkowski, D.J., and Williams, D.A. (2003). Hematopoietic cell regulation by Rac1 and Rac2 guanosine triphosphatases. Science *302*, 445-449.

Guzik, T.J., Korbut, R., and Adamek-Guzik, T. (2003). Nitric oxide and superoxide in inflammation and immune regulation. J Physiol Pharmacol *54*, 469-487.

Guzik, T.J., West, N.E., Pillai, R., Taggart, D.P., and Channon, K.M. (2002). Nitric oxide modulates superoxide release and peroxynitrite formation in human blood vessels. Hypertension *39*, 1088-1094.

Hallahan, D., Clark, E.T., Kuchibhotla, J., Gewertz, B.L., and Collins, T. (1995). E-selectin gene induction by ionizing radiation is independent of cytokine induction. Biochem Biophys Res Commun *217*, 784-795.

Halleen, J.M., Raisanen, S., Salo, J.J., Reddy, S.V., Roodman, G.D., Hentunen, T.A., Lehenkari, P.P., Kaija, H., Vihko, P., and Vaananen, H.K. (1999). Intracellular fragmentation of bone resorption products by reactive oxygen species generated by osteoclastic tartrate-resistant acid phosphatase. J Biol Chem *274*, 22907-22910.

Hampton, M.B., Kettle, A.J., and Winterbourn, C.C. (1998). Inside the neutrophil phagosome: oxidants, myeloperoxidase, and bacterial killing. Blood *92*, 3007-3017.

Han, J., Lim, C.J., Watanabe, N., Soriani, A., Ratnikov, B., Calderwood, D.A., Puzon-McLaughlin, W., Lafuente, E.M., Boussiotis, V.A., Shattil, S.J., and Ginsberg, M.H. (2006). Reconstructing and deconstructing agonist-induced activation of integrin alphaIIbbeta3. Curr Biol *16*, 1796-1806.

Hansen, S.H., Zegers, M.M., Woodrow, M., Rodriguez-Viciana, P., Chardin, P., Mostov, K.E., and McMahon, M. (2000). Induced expression of Rnd3 is associated with transformation of polarized epithelial cells by the Raf-MEK-extracellular signal-regulated kinase pathway. Mol Cell Biol *20*, 9364-9375.

Harris, A.L. (2002). Hypoxia--a key regulatory factor in tumour growth. Nat Rev Cancer *2*, 38-47.

Harrison-Findik, D.D. (2007). Role of alcohol in the regulation of iron metabolism. World J Gastroenterol *13*, 4925-4930.

Hashimoto, S., Gon, Y., Matsumoto, K., Takeshita, I., and Horie, T. (2001). N-acetylcysteine attenuates TNF-alpha-induced p38 MAP kinase activation and p38 MAP kinase-mediated IL-8 production by human pulmonary vascular endothelial cells. British journal of pharmacology *132*, 270-276.

Hasko, G., and Cronstein, B.N. (2004). Adenosine: an endogenous regulator of innate immunity. Trends Immunol *25*, 33-39.

Hausel, P., Latado, H., Courjault-Gautier, F., and Felley-Bosco, E. (2006). Src-mediated phosphorylation regulates subcellular distribution and activity of human inducible nitric oxide synthase. Oncogene *25*, 198-206.

Hayes, J.D., and McLellan, L.I. (1999). Glutathione and glutathione-dependent enzymes represent a co-ordinately regulated defence against oxidative stress. Free Radic Res *31*, 273-300.

Hayflick, J.S., Kilgannon, P., and Gallatin, W.M. (1998). The intercellular adhesion molecule (ICAM) family of proteins. New members and novel functions. Immunologic research *17*, 313-327.

Henttinen, T., Jalkanen, S., and Yegutkin, G.G. (2003). Adherent leukocytes prevent adenosine formation and impair endothelial barrier function by Ecto-5'-nucleotidase/CD73-dependent mechanism. J Biol Chem *278*, 24888-24895.

Heo, J., and Campbell, S.L. (2005). Mechanism of redox-mediated guanine nucleotide exchange on redox-active Rho GTPases. J Biol Chem *280*, 31003-31010.

Heo, J., Raines, K.W., Mocanu, V., and Campbell, S.L. (2006). Redox regulation of RhoA. Biochemistry *45*, 14481-14489.

Hess, D.T., Matsumoto, A., Kim, S.O., Marshall, H.E., and Stamler, J.S. (2005). Protein S-nitrosylation: purview and parameters. Nature reviews *6*, 150-166.

Hidalgo, A., Peired, A.J., Wild, M.K., Vestweber, D., and Frenette, P.S. (2007). Complete identification of E-selectin ligands on neutrophils reveals distinct functions of PSGL-1, ESL-1, and CD44. Immunity *26*, 477-489.

Hill, C.E., Rummery, N., Hickey, H., and Sandow, S.L. (2002). Heterogeneity in the distribution of vascular gap junctions and connexins: implications for function. Clinical and experimental pharmacology & physiology *29*, 620-625.

Hixenbaugh, E.A., Goeckeler, Z.M., Papaiya, N.N., Wysolmerski, R.B., Silverstein, S.C., and Huang, A.J. (1997). Stimulated neutrophils induce myosin light chain phosphorylation and isometric tension in endothelial cells. Am J Physiol *273*, H981-988.

Hofmann, F., Ammendola, A., and Schlossmann, J. (2000). Rising behind NO: cGMP-dependent protein kinases. J Cell Sci *113 (Pt 10)*, 1671-1676.

Hogg, N., and Landis, R.C. (1993). Adhesion molecules in cell interactions. Curr Opin Immunol *5*, 383-390.

Huang, A.J., Manning, J.E., Bandak, T.M., Ratau, M.C., Hanser, K.R., and Silverstein, S.C. (1993). Endothelial cell cytosolic free calcium regulates neutrophil migration across monolayers of endothelial cells. J Cell Biol *120*, 1371-1380.

Huang, D.Y., Vallon, V., Zimmermann, H., Koszalka, P., Schrader, J., and Osswald, H. (2006a). Ecto-5'-nucleotidase (cd73)-dependent and -independent generation of adenosine participates in the mediation of tubuloglomerular feedback in vivo. Am J Physiol Renal Physiol *291*, F282-288.

Huang, J., Upadhyay, U.M., and Tamargo, R.J. (2006b). Inflammation in stroke and focal cerebral ischemia. Surgical neurology *66*, 232-245.

Hunsucker, S.A., Mitchell, B.S., and Spychala, J. (2005). The 5'-nucleotidases as regulators of nucleotide and drug metabolism. Pharmacol Ther *107*, 1-30.

Huo, Y., Schober, A., Forlow, S.B., Smith, D.F., Hyman, M.C., Jung, S., Littman, D.R., Weber, C., and Ley, K. (2003). Circulating activated platelets exacerbate atherosclerosis in mice deficient in apolipoprotein E. Nat Med *9*, 61-67.

Huot, J., Houle, F., Rousseau, S., Deschesnes, R.G., Shah, G.M., and Landry, J. (1998). SAPK2/p38-dependent F-actin reorganization regulates early membrane blebbing during stress-induced apoptosis. J Cell Biol *143*, 1361-1373.

Huttenlocher, A., Ginsberg, M.H., and Horwitz, A.F. (1996). Modulation of cell migration by integrin-mediated cytoskeletal linkages and ligand-binding affinity. J Cell Biol *134*, 1551-1562.

Hyduk, S.J., Chan, J.R., Duffy, S.T., Chen, M., Peterson, M.D., Waddell, T.K., Digby, G.C., Szaszi, K., Kapus, A., and Cybulsky, M.I. (2007). Phospholipase C, calcium, and calmodulin are critical for alpha4beta1 integrin affinity up-regulation and monocyte arrest triggered by chemoattractants. Blood *109*, 176-184.

Idzko, M., Dichmann, S., Ferrari, D., Di Virgilio, F., la Sala, A., Girolomoni, G., Panther, E., and Norgauer, J. (2002). Nucleotides induce chemotaxis and actin polymerization in immature but not mature human dendritic cells via activation of pertussis toxin-sensitive P2y receptors. Blood *100*, 925-932.

Ignarro, L.J. (2002). Nitric oxide as a unique signaling molecule in the vascular system: a historical overview. J Physiol Pharmacol *53*, 503-514.

Ivetic, A., Florey, O., Deka, J., Haskard, D.O., Ager, A., and Ridley, A.J. (2004). Mutagenesis of the ezrin-radixin-moesin binding domain of L-selectin tail affects shedding, microvillar positioning, and leukocyte tethering. J Biol Chem *279*, 33263-33272.

Jackson, S.H., Gallin, J.I., and Holland, S.M. (1995). The p47phox mouse knock-out model of chronic granulomatous disease. J Exp Med *182*, 751-758.

Jaffe, A.B., and Hall, A. (2005). Rho GTPases: biochemistry and biology. Annual review of cell and developmental biology *21*, 247-269.

Jagnandan, D., Church, J.E., Banfi, B., Stuehr, D.J., Marrero, M.B., and Fulton, D.J. (2007). Novel mechanism of activation of NADPH oxidase 5. calcium sensitization via phosphorylation. J Biol Chem *282*, 6494-6507.

Jalkanen, S., and Salmi, M. (2008). VAP-1 and CD73, endothelial cell surface enzymes in leukocyte extravasation. Arterioscler Thromb Vasc Biol *28*, 18-26.

Jin, M., Guan, C.B., Jiang, Y.A., Chen, G., Zhao, C.T., Cui, K., Song, Y.Q., Wu, C.P., Poo, M.M., and Yuan, X.B. (2005). Ca2+-dependent regulation of rho GTPases triggers turning of nerve growth cones. J Neurosci *25*, 2338-2347.

Jones, D.P. (2006). Redefining oxidative stress. Antioxidants & redox signaling *8*, 1865-1879.

Jones, R.J., Brunton, V.G., and Frame, M.C. (2000). Adhesion-linked kinases in cancer; emphasis on src, focal adhesion kinase and PI 3-kinase. Eur J Cancer *36*, 1595-1606.

Kaibuchi, K., Kuroda, S., and Amano, M. (1999). Regulation of the cytoskeleton and cell adhesion by the Rho family GTPases in mammalian cells. Annu Rev Biochem *68*, 459-486.

Kalsi, K., Lawson, C., Dominguez, M., Taylor, P., Yacoub, M.H., and Smolenski, R.T. (2002). Regulation of ecto-5'-nucleotidase by TNF-alpha in human endothelial cells. Molecular and cellular biochemistry *232*, 113-119.

Kameoka, J., Tanaka, T., Nojima, Y., Schlossman, S.F., and Morimoto, C. (1993). Direct association of adenosine deaminase with a T cell activation antigen, CD26. Science *261*, 466-469.

Kanfer, J.N., Hattori, H., and Orihel, D. (1986). Reduced phospholipase D activity in brain tissue samples from Alzheimer's disease patients. Annals of neurology *20*, 265-267.

Karin, M., and Greten, F.R. (2005). NF-kappaB: linking inflammation and immunity to cancer development and progression. Nat Rev Immunol *5*, 749-759.

Karlsson, A., Markfjall, M., Stromberg, N., and Dahlgren, C. (1995). Escherichia coli-induced activation of neutrophil NADPH-oxidase: lipopolysaccharide and formylated peptides act synergistically to induce release of reactive oxygen metabolites. Infect Immun *63*, 4606-4612.

Katagiri, K., Maeda, A., Shimonaka, M., and Kinashi, T. (2003). RAPL, a Rap1-binding molecule that mediates Rap1-induced adhesion through spatial regulation of LFA-1. Nat Immunol *4*, 741-748.

Katagiri, K., Ohnishi, N., Kabashima, K., Iyoda, T., Takeda, N., Shinkai, Y., Inaba, K., and Kinashi, T. (2004). Crucial functions of the Rap1 effector molecule RAPL in lymphocyte and dendritic cell trafficking. Nat Immunol *5*, 1045-1051.

Kato, M., Iwashita, T., Takeda, K., Akhand, A.A., Liu, W., Yoshihara, M., Asai, N., Suzuki, H., Takahashi, M., and Nakashima, I. (2000). Ultraviolet light induces redox reaction-mediated dimerization and superactivation of oncogenic Ret tyrosine kinases. Mol Biol Cell *11*, 93-101.

Katsuki, S., Arnold, W., Mittal, C., and Murad, F. (1977). Stimulation of guanylate cyclase by sodium nitroprusside, nitroglycerin and nitric oxide in various tissue preparations and comparison to the effects of sodium azide and hydroxylamine. Journal of cyclic nucleotide research *3*, 23-35.

Kattan, Z., Minig, V., Leroy, P., Dauca, M., and Becuwe, P. (2008). Role of manganese superoxide dismutase on growth and invasive properties of human estrogen-independent breast cancer cells. Breast cancer research and treatment *108*, 203-215.

Kaushansky, K. (2006). Lineage-specific hematopoietic growth factors. The New England journal of medicine *354*, 2034-2045.

Kazzaz, J.A., Xu, J., Palaia, T.A., Mantell, L., Fein, A.M., and Horowitz, S. (1996). Cellular oxygen toxicity. Oxidant injury without apoptosis. J Biol Chem *271*, 15182-15186.

Kelly, K.J., Sandoval, R.M., Dunn, K.W., Molitoris, B.A., and Dagher, P.C. (2003). A novel method to determine specificity and sensitivity of the TUNEL reaction in the quantitation of apoptosis. Am J Physiol Cell Physiol *284*, C1309-1318.

Keshavan, P., Deem, T.L., Schwemberger, S.J., Babcock, G.F., Cook-Mills, J.M., and Zucker, S.D. (2005). Unconjugated bilirubin inhibits VCAM-1-mediated transendothelial leukocyte migration. J Immunol *174*, 3709-3718.

Kikuchi, H., Hikage, M., Miyashita, H., and Fukumoto, M. (2000). NADPH oxidase subunit, gp91(phox) homologue, preferentially expressed in human colon epithelial cells. Gene *254*, 237-243.

Kim, M., Carman, C.V., and Springer, T.A. (2003). Bidirectional transmembrane signaling by cytoplasmic domain separation in integrins. Science *301*, 1720-1725.

Kindt, T.J., Goldsby, R.A., and Osborne, B.A. (2006). Kuby Immunology, 6th edn (New York, W. H. Feeman and Company).

Kinnula, V.L., and Crapo, J.D. (2004). Superoxide dismutases in malignant cells and human tumors. Free Radic Biol Med *36*, 718-744.

Kiss, J., Yegutkin, G.G., Koskinen, K., Savunen, T., Jalkanen, S., and Salmi, M. (2007). IFN-beta protects from vascular leakage via up-regulation of CD73. Eur J Immunol *37*, 3334-3338.

Knofel, T., and Strater, N. (1999). X-ray structure of the Escherichia coli periplasmic 5'-nucleotidase containing a dimetal catalytic site. Nature structural biology *6*, 448-453.

Kocic, G., Pavlovic, D., Jevtovic, T., Kocic, R., Bojic, A., Vlahovic, P., Djordjevic, V., Sokolovic, D., and Djindjic, B. (2001). Oxidative modification of rat liver 5'-nucleotidase: the mechanisms for protection and re-activation. Archives of physiology and biochemistry *109*, 323-330.

Kofler, S., Nickel, T., and Weis, M. (2005). Role of cytokines in cardiovascular diseases: a focus on endothelial responses to inflammation. Clin Sci (Lond) *108*, 205-213.

Komori, K., Lorenz, R.R., and Vanhoutte, P.M. (1988). Nitric oxide, ACh, and electrical and mechanical properties of canine arterial smooth muscle. Am J Physiol *255*, H207-212.

Konishi, H., Tanaka, M., Takemura, Y., Matsuzaki, H., Ono, Y., Kikkawa, U., and Nishizuka, Y. (1997). Activation of protein kinase C by tyrosine phosphorylation in response to H2O2. Proc Natl Acad Sci U S A *94*, 11233-11237.

Konstantinopoulos, P.A., Karamouzis, M.V., and Papavassiliou, A.G. (2007). Post-translational modifications and regulation of the RAS superfamily of GTPases as anticancer targets. Nat Rev Drug Discov *6*, 541-555.

Koopman, G., Reutelingsperger, C.P., Kuijten, G.A., Keehnen, R.M., Pals, S.T., and van Oers, M.H. (1994). Annexin V for flow cytometric detection of phosphatidylserine expression on B cells undergoing apoptosis. Blood *84*, 1415-1420.

Koszalka, P., Ozuyaman, B., Huo, Y., Zernecke, A., Flogel, U., Braun, N., Buchheiser, A., Decking, U.K., Smith, M.L., Sevigny, J., Gear, A., Weber, A.A., Molojavyi, A., Ding, Z., Weber, C., Ley, K., Zimmermann, H., Godecke, A., and Schrader, J. (2004). Targeted disruption of cd73/ecto-5'-nucleotidase alters thromboregulation and augments vascular inflammatory response. Circ Res *95*, 814-821.

Ladwein, M., and Rottner, K. (2008). On the Rho'd: The regulation of membrane protrusions by Rho-GTPases. FEBS Lett.

Lafuente, E.M., van Puijenbroek, A.A., Krause, M., Carman, C.V., Freeman, G.J., Berezovskaya, A., Constantine, E., Springer, T.A., Gertler, F.B., and Boussiotis, V.A. (2004). RIAM, an Ena/VASP and Profilin ligand, interacts with Rap1-GTP and mediates Rap1-induced adhesion. Developmental cell *7*, 585-595.

Lamagna, C., Meda, P., Mandicourt, G., Brown, J., Gilbert, R.J., Jones, E.Y., Kiefer, F., Ruga, P., Imhof, B.A., and Aurrand-Lions, M. (2005). Dual interaction of JAM-C with JAM-B and alpha(M)beta2 integrin: function in junctional complexes and leukocyte adhesion. Mol Biol Cell *16*, 4992-5003.

Lambeir, A.M., Proost, P., Durinx, C., Bal, G., Senten, K., Augustyns, K., Scharpe, S., Van Damme, J., and De Meester, I. (2001). Kinetic investigation of chemokine truncation by CD26/dipeptidyl peptidase IV reveals a striking selectivity within the chemokine family. J Biol Chem *276*, 29839-29845.

Lander, H.M., Hajjar, D.P., Hempstead, B.L., Mirza, U.A., Chait, B.T., Campbell, S., and Quilliam, L.A. (1997). A molecular redox switch on p21(ras). Structural basis for the nitric oxide-p21(ras) interaction. J Biol Chem *272*, 4323-4326.

Landino, L.M., Hasan, R., McGaw, A., Cooley, S., Smith, A.W., Masselam, K., and Kim, G. (2002). Peroxynitrite oxidation of tubulin sulfhydryls inhibits microtubule polymerization. Archives of biochemistry and biophysics *398*, 213-220.

Landino, L.M., Skreslet, T.E., and Alston, J.A. (2004). Cysteine oxidation of tau and microtubule-associated protein-2 by peroxynitrite: modulation of microtubule assembly kinetics by the thioredoxin reductase system. J Biol Chem *279*, 35101-35105.

Lassegue, B., Sorescu, D., Szocs, K., Yin, Q., Akers, M., Zhang, Y., Grant, S.L., Lambeth, J.D., and Griendling, K.K. (2001). Novel gp91(phox) homologues in vascular smooth muscle cells : nox1 mediates angiotensin II-induced superoxide formation and redox-sensitive signaling pathways. Circ Res *88*, 888-894.

Lauffenburger, D.A., and Horwitz, A.F. (1996). Cell migration: a physically integrated molecular process. Cell *84*, 359-369.

Lee, J.S., Kang Decker, N., Chatterjee, S., Yao, J., Friedman, S., and Shah, V. (2005). Mechanisms of nitric oxide interplay with Rho GTPase family members in modulation of actin membrane dynamics in pericytes and fibroblasts. The American journal of pathology *166*, 1861-1870.

Lee, S.R., Yang, K.S., Kwon, J., Lee, C., Jeong, W., and Rhee, S.G. (2002). Reversible inactivation of the tumor suppressor PTEN by H2O2. J Biol Chem *277*, 20336-20342.

Lefer, D.J., Jones, S.P., Girod, W.G., Baines, A., Grisham, M.B., Cockrell, A.S., Huang, P.L., and Scalia, R. (1999). Leukocyte-endothelial cell interactions in nitric oxide synthase-deficient mice. Am J Physiol *276*, H1943-1950.

Lennon, P.F., Taylor, C.T., Stahl, G.L., and Colgan, S.P. (1998). Neutrophil-derived 5'-adenosine monophosphate promotes endothelial barrier function via CD73-mediated conversion to adenosine and endothelial A2B receptor activation. J Exp Med *188*, 1433-1443.

Leonberg, A.K., and Chai, Y.C. (2007). The functional role of cysteine residues for c-Abl kinase activity. Molecular and cellular biochemistry *304*, 207-212.

Leung, R.K., and Whittaker, P.A. (2005). RNA interference: from gene silencing to gene-specific therapeutics. Pharmacol Ther *107*, 222-239.

Ley, K., Laudanna, C., Cybulsky, M.I., and Nourshargh, S. (2007). Getting to the site of inflammation: the leukocyte adhesion cascade updated. Nat Rev Immunol *7*, 678-689.

Li, X., Zhou, T., Zhi, X., Zhao, F., Yin, L., and Zhou, P. (2006). Effect of hypoxia/reoxygenation on CD73 (ecto-5'-nucleotidase) in mouse microvessel endothelial cell lines. Microvascular research *72*, 48-53.

Lin, W.W., and Karin, M. (2007). A cytokine-mediated link between innate immunity, inflammation, and cancer. J Clin Invest *117*, 1175-1183.

Lindsay, S.L., Ramsey, S., Aitchison, M., Renne, T., and Evans, T.J. (2007). Modulation of lamellipodial structure and dynamics by NO-dependent phosphorylation of VASP Ser239. J Cell Sci *120*, 3011-3021.

Liu, H., Nishitoh, H., Ichijo, H., and Kyriakis, J.M. (2000). Activation of apoptosis signal-regulating kinase 1 (ASK1) by tumor necrosis factor receptor-associated factor 2 requires prior dissociation of the ASK1 inhibitor thioredoxin. Mol Cell Biol *20*, 2198-2208.

Liu, S., Thomas, S.M., Woodside, D.G., Rose, D.M., Kiosses, W.B., Pfaff, M., and Ginsberg, M.H. (1999). Binding of paxillin to alpha4 integrins modifies integrin-dependent biological responses. Nature *402*, 676-681.

Liu, S.Y., Tsai, M.Y., Chuang, K.P., Huang, Y.F., and Shieh, C.C. (2008). Ligand binding of leukocyte integrin very late antigen-4 involves exposure of sulfhydryl groups and is subject to redox modulation. Eur J Immunol *38*, 410-423.

Liu, W.S., and Heckman, C.A. (1998). The sevenfold way of PKC regulation. Cell Signal *10*, 529-542.

Liu, X.W., and Sok, D.E. (2000). Oxidative inactivation of brain ecto-5'-nucleotidase by thiols/Fe2+ system. Neurochemical research *25*, 1475-1484.

Low, M.G., and Saltiel, A.R. (1988). Structural and functional roles of glycosyl-phosphatidylinositol in membranes. Science *239*, 268-275.

Lu, Y., and Wahl, L.M. (2005). Oxidative stress augments the production of matrix metalloproteinase-1, cyclooxygenase-2, and prostaglandin E2 through enhancement of NF-kappa B activity in lipopolysaccharide-activated human primary monocytes. J Immunol *175*, 5423-5429.

Lucas, R., Juillard, P., Decoster, E., Redard, M., Burger, D., Donati, Y., Giroud, C., Monso-Hinard, C., De Kesel, T., Buurman, W.A., Moore, M.W., Dayer, J.M., Fiers, W., Bluethmann, H., and Grau, G.E. (1997). Crucial role of tumor necrosis factor (TNF) receptor 2 and membrane-bound TNF in experimental cerebral malaria. Eur J Immunol *27*, 1719-1725.

Ludwig, H.C., Rausch, S., Schallock, K., and Markakis, E. (1999). Expression of CD 73 (ecto-5'-nucleotidase) in 165 glioblastomas by immunohistochemistry and electronmicroscopic histochemistry. Anticancer Res *19*, 1747-1752.

Lushchak, V.I. (2006). Budding yeast Saccharomyces cerevisiae as a model to study oxidative modification of proteins in eukaryotes. Acta Biochim Pol *53*, 679-684.

Maaser, K., Wolf, K., Klein, C.E., Niggemann, B., Zanker, K.S., Brocker, E.B., and Friedl, P. (1999). Functional hierarchy of simultaneously expressed adhesion receptors: integrin alpha2beta1 but not CD44 mediates MV3 melanoma cell migration and matrix reorganization within three-dimensional hyaluronan-containing collagen matrices. Mol Biol Cell *10*, 3067-3079.

MacEwan, D.J. (2002). TNF receptor subtype signalling: differences and cellular consequences. Cell Signal *14*, 477-492.

Male, D., Brostoff, J., Roth, D.B., and Roitt, I. (2006). Immunology, 7th edn (Canada, Elsevier Limited).

Mallavarapu, A., and Mitchison, T. (1999). Regulated actin cytoskeleton assembly at filopodium tips controls their extension and retraction. J Cell Biol *146*, 1097-1106.

Mamdouh, Z., Chen, X., Pierini, L.M., Maxfield, F.R., and Muller, W.A. (2003). Targeted recycling of PECAM from endothelial surface-connected compartments during diapedesis. Nature *421*, 748-753.

Mamdouh, Z., Kreitzer, G.E., and Muller, W.A. (2008). Leukocyte transmigration requires kinesin-mediated microtubule-dependent membrane trafficking from the lateral border recycling compartment. J Exp Med *205*, 951-966.

Mandel, S., Weinreb, O., Amit, T., and Youdim, M.B. (2004). Cell signaling pathways in the neuroprotective actions of the green tea polyphenol (-)-epigallocatechin-3-gallate: implications for neurodegenerative diseases. Journal of neurochemistry *88*, 1555-1569.

Mansat-de Mas, V., Bezombes, C., Quillet-Mary, A., Bettaieb, A., D'Orgeix A, D., Laurent, G., and Jaffrezou, J.P. (1999). Implication of radical oxygen species in ceramide generation, c-Jun N-terminal kinase activation and apoptosis induced by daunorubicin. Molecular pharmacology *56*, 867-874.

Marshall, B.T., Long, M., Piper, J.W., Yago, T., McEver, R.P., and Zhu, C. (2003). Direct observation of catch bonds involving cell-adhesion molecules. Nature *423*, 190-193.

Martin, M., Huguet, J., Centelles, J.J., and Franco, R. (1995). Expression of ecto-adenosine deaminase and CD26 in human T cells triggered by the TCR-CD3 complex. Possible role of adenosine deaminase as costimulatory molecule. J Immunol *155*, 4630-4643.

Martinez-Martinez, A., Munoz-Delgado, E., Campoy, F.J., Flores-Flores, C., Rodriguez-Lopez, J.N., Fini, C., and Vidal, C.J. (2000). The ecto-5'-nucleotidase subunits in dimers are not linked by disulfide bridges but by non-covalent bonds. Biochim Biophys Acta *1478*, 300-308.

Matheny, H.E., Deem, T.L., and Cook-Mills, J.M. (2000). Lymphocyte migration through monolayers of endothelial cell lines involves VCAM-1 signaling via endothelial cell NADPH oxidase. J Immunol *164*, 6550-6559.

Matoba, T., Shimokawa, H., Kubota, H., Morikawa, K., Fujiki, T., Kunihiro, I., Mukai, Y., Hirakawa, Y., and Takeshita, A. (2002). Hydrogen peroxide is an endothelium-derived hyperpolarizing factor in human mesenteric arteries. Biochem Biophys Res Commun *290*, 909-913.

Matoba, T., Shimokawa, H., Nakashima, M., Hirakawa, Y., Mukai, Y., Hirano, K., Kanaide, H., and Takeshita, A. (2000). Hydrogen peroxide is an endothelium-derived hyperpolarizing factor in mice. J Clin Invest *106*, 1521-1530.

Matsukawa, J., Matsuzawa, A., Takeda, K., and Ichijo, H. (2004). The ASK1-MAP kinase cascades in mammalian stress response. Journal of biochemistry *136*, 261-265.

Matter, K., and Balda, M.S. (2003). Signalling to and from tight junctions. Nature reviews *4*, 225-236.

McEver, R.P. (2002). Selectins: lectins that initiate cell adhesion under flow. Curr Opin Cell Biol *14*, 581-586.

McPherson, J.A., Barringhaus, K.G., Bishop, G.G., Sanders, J.M., Rieger, J.M., Hesselbacher, S.E., Gimple, L.W., Powers, E.R., Macdonald, T., Sullivan, G., Linden, J., and Sarembock, I.J. (2001). Adenosine A(2A) receptor stimulation reduces inflammation and neointimal growth in a murine carotid ligation model. Arterioscler Thromb Vasc Biol *21*, 791-796.

Mendes, A.F., Caramona, M.M., Carvalho, A.P., and Lopes, M.C. (2003). Differential roles of hydrogen peroxide and superoxide in mediating IL-1-induced NF-kappa B activation and iNOS expression in bovine articular chondrocytes. Journal of cellular biochemistry *88*, 783-793.

Michelson, A.D. (2003). How platelets work: platelet function and dysfunction. Journal of thrombosis and thrombolysis *16*, 7-12.

Miki, H., Yamaguchi, H., Suetsugu, S., and Takenawa, T. (2000). IRSp53 is an essential intermediate between Rac and WAVE in the regulation of membrane ruffling. Nature *408*, 732-735.

Miles, F.L., Pruitt, F.L., van Golen, K.L., and Cooper, C.R. (2008). Stepping out of the flow: capillary extravasation in cancer metastasis. Clinical & experimental metastasis *25*, 305-324.

Millan, J., Hewlett, L., Glyn, M., Toomre, D., Clark, P., and Ridley, A.J. (2006). Lymphocyte transcellular migration occurs through recruitment of endothelial ICAM-1 to caveola- and F-actin-rich domains. Nat Cell Biol *8*, 113-123.

Millan, J., and Ridley, A.J. (2004). Rho GTPases and leukocyte-induced endothelial remodelling. Biochem J.

Mills, G.B., and Moolenaar, W.H. (2003). The emerging role of lysophosphatidic acid in cancer. Nat Rev Cancer *3*, 582-591.

Minguet, S., Huber, M., Rosenkranz, L., Schamel, W.W., Reth, M., and Brummer, T. (2005). Adenosine and cAMP are potent inhibitors of the NF-kappa B pathway downstream of immunoreceptors. Eur J Immunol *35*, 31-41.

Mitchison, T.J., and Cramer, L.P. (1996). Actin-based cell motility and cell locomotion. Cell *84*, 371-379.

Mittal, C.K., and Murad, F. (1977). Activation of guanylate cyclase by superoxide dismutase and hydroxyl radical: a physiological regulator of guanosine 3',5'-monophosphate formation. Proc Natl Acad Sci U S A *74*, 4360-4364.

Mizumoto, N., Kumamoto, T., Robson, S.C., Sevigny, J., Matsue, H., Enjyoji, K., and Takashima, A. (2002). CD39 is the dominant Langerhans cell-associated ecto-NTPDase: modulatory roles in inflammation and immune responsiveness. Nat Med *8*, 358-365.

Moldovan, L., Moldovan, N.I., Sohn, R.H., Parikh, S.A., and Goldschmidt-Clermont, P.J. (2000). Redox changes of cultured endothelial cells and actin dynamics. Circ Res *86*, 549-557.

Monastyrskaya, K., Babiychuk, E.B., Schittny, J.C., Rescher, U., Gerke, V., Mannherz, H.G., and Draeger, A. (2003). The expression levels of three raft-associated molecules in cultivated vascular cells are dependent on culture conditions. Cell Mol Life Sci *60*, 2702-2709.

Moon, S.Y., and Zheng, Y. (2003). Rho GTPase-activating proteins in cell regulation. Trends Cell Biol *13*, 13-22.

Moores, S.L., Selfors, L.M., Fredericks, J., Breit, T., Fujikawa, K., Alt, F.W., Brugge, J.S., and Swat, W. (2000). Vav family proteins couple to diverse cell surface receptors. Mol Cell Biol *20*, 6364-6373.

Mordelet, E., Davies, H.A., Hillyer, P., Romero, I.A., and Male, D. (2007). Chemokine transport across human vascular endothelial cells. Endothelium *14*, 7-15.

Moser, T.L., Kenan, D.J., Ashley, T.A., Roy, J.A., Goodman, M.D., Misra, U.K., Cheek, D.J., and Pizzo, S.V. (2001). Endothelial cell surface F1-F0 ATP synthase is active in ATP synthesis and is inhibited by angiostatin. Proc Natl Acad Sci U S A *98*, 6656-6661.

Muller, G., and Lipp, M. (2003). Shaping up adaptive immunity: the impact of CCR7 and CXCR5 on lymphocyte trafficking. Microcirculation *10*, 325-334.

Muller, W.A. (2003). Leukocyte-endothelial-cell interactions in leukocyte transmigration and the inflammatory response. Trends Immunol *24*, 327-334.

Murphy, K., Travers, P., and Walport, M. (2008). Janeway's Immunobiology, 7th edn (New York, Garland Science, Taylor & Francis Group, LLC).

Napoli, C., and Palinski, W. (2005). Neurodegenerative diseases: insights into pathogenic mechanisms from atherosclerosis. Neurobiology of aging *26*, 293-302.

Narravula, S., Lennon, P.F., Mueller, B.U., and Colgan, S.P. (2000). Regulation of endothelial CD73 by adenosine: paracrine pathway for enhanced endothelial barrier function. J Immunol *165*, 5262-5268.

Nathan, C. (2003). Specificity of a third kind: reactive oxygen and nitrogen intermediates in cell signaling. J Clin Invest *111*, 769-778.

Nathan, C.F., and Root, R.K. (1977). Hydrogen peroxide release from mouse peritoneal macrophages: dependence on sequential activation and triggering. J Exp Med *146*, 1648-1662.

Nayal, A., Webb, D.J., Brown, C.M., Schaefer, E.M., Vicente-Manzanares, M., and Horwitz, A.R. (2006). Paxillin phosphorylation at Ser273 localizes a GIT1-PIX-PAK complex and regulates adhesion and protrusion dynamics. J Cell Biol *173*, 587-589.

Nicoletti, I., Migliorati, G., Pagliacci, M.C., Grignani, F., and Riccardi, C. (1991). A rapid and simple method for measuring thymocyte apoptosis by propidium iodide staining and flow cytometry. Journal of immunological methods *139*, 271-279.

Nicotera, P., Leist, M., and Ferrando-May, E. (1999). Apoptosis and necrosis: different execution of the same death. Biochem Soc Symp *66*, 69-73.

Niemela, J., Henttinen, T., Yegutkin, G.G., Airas, L., Kujari, A.M., Rajala, P., and Jalkanen, S. (2004). IFN-alpha induced adenosine production on the endothelium: a mechanism mediated by CD73 (ecto-5'-nucleotidase) up-regulation. J Immunol *172*, 1646-1653.

Nimnual, A.S., Taylor, L.J., and Bar-Sagi, D. (2003). Redox-dependent downregulation of Rho by Rac. Nat Cell Biol *5*, 236-241.

Nishiya, N., Kiosses, W.B., Han, J., and Ginsberg, M.H. (2005). An alpha4 integrin-paxillin-Arf-GAP complex restricts Rac activation to the leading edge of migrating cells. Nat Cell Biol *7*, 343-352.

Nobes, C.D., and Hall, A. (1995). Rho, rac, and cdc42 GTPases regulate the assembly of multimolecular focal complexes associated with actin stress fibers, lamellipodia, and filopodia. Cell *81*, 53-62.

Nomanbhoy, T.K., and Cerione, R. (1996). Characterization of the interaction between RhoGDI and Cdc42Hs using fluorescence spectroscopy. J Biol Chem *271*, 10004-10009.

Oess, S., Icking, A., Fulton, D., Govers, R., and Muller-Esterl, W. (2006). Subcellular targeting and trafficking of nitric oxide synthases. Biochem J *396*, 401-409.

Ohta, A., Gorelik, E., Prasad, S.J., Ronchese, F., Lukashev, D., Wong, M.K., Huang, X., Caldwell, S., Liu, K., Smith, P., Chen, J.F., Jackson, E.K., Apasov, S., Abrams, S., and Sitkovsky, M. (2006). A2A adenosine receptor protects tumors from antitumor T cells. Proc Natl Acad Sci U S A *103*, 13132-13137.

Oka, S., Sasada, M., Yamamoto, K., Nohgawa, M., Takahashi, A., Yamashita, K., Yamada, H., and Uchiyama, T. (2005). Nitric oxide derived from human umbilical vein endothelial cells inhibits transendothelial migration of neutrophils. International journal of hematology *81*, 220-227.

Ostermann, G., Weber, K.S., Zernecke, A., Schroder, A., and Weber, C. (2002). JAM-1 is a ligand of the beta(2) integrin LFA-1 involved in transendothelial migration of leukocytes. Nat Immunol *3*, 151-158.

Palecek, S.P., Huttenlocher, A., Horwitz, A.F., and Lauffenburger, D.A. (1998). Physical and biochemical regulation of integrin release during rear detachment of migrating cells. J Cell Sci *111 (Pt 7)*, 929-940.

Palecek, S.P., Loftus, J.C., Ginsberg, M.H., Lauffenburger, D.A., and Horwitz, A.F. (1997). Integrin-ligand binding properties govern cell migration speed through cell-substratum adhesiveness. Nature *385*, 537-540.

Paleolog, E.M., Delasalle, S.A., Buurman, W.A., and Feldmann, M. (1994). Functional activities of receptors for tumor necrosis factor-alpha on human vascular endothelial cells. Blood *84*, 2578-2590.

Palmer, R.M., Ferrige, A.G., and Moncada, S. (1987). Nitric oxide release accounts for the biological activity of endothelium-derived relaxing factor. Nature *327*, 524-526.

Pan, J., Burgher, K.L., Szczepanik, A.M., and Ringheim, G.E. (1996). Tyrosine phosphorylation of inducible nitric oxide synthase: implications for potential post-translational regulation. Biochem J *314 (Pt 3)*, 889-894.

Pantano, C., Shrivastava, P., McElhinney, B., and Janssen-Heininger, Y. (2003). Hydrogen peroxide signaling through tumor necrosis factor receptor 1 leads to selective activation of c-Jun N-terminal kinase. J Biol Chem *278*, 44091-44096.

Papanikolaou, A., Papafotika, A., Murphy, C., Papamarcaki, T., Tsolas, O., Drab, M., Kurzchalia, T.V., Kasper, M., and Christoforidis, S. (2005). Cholesterol-dependent lipid assemblies regulate the activity of the ecto-nucleotidase CD39. J Biol Chem *280*, 26406-26414.

Paravicini, T.M., and Touyz, R.M. (2008). NADPH oxidases, reactive oxygen species, and hypertension: clinical implications and therapeutic possibilities. Diabetes care *31 Suppl 2*, S170-180.

Park, S.W., Huq, M.D., Hu, X., and Wei, L.N. (2005). Tyrosine nitration on p65: a novel mechanism to rapidly inactivate nuclear factor-kappaB. Mol Cell Proteomics *4*, 300-309.

Pasvolsky, R., Grabovsky, V., Giagulli, C., Shulman, Z., Shamri, R., Feigelson, S.W., Laudanna, C., and Alon, R. (2008). RhoA Is Involved in LFA-1 Extension Triggered by CXCL12 but Not in a Novel Outside-In LFA-1 Activation Facilitated by CXCL9. J Immunol *180*, 2815-2823.

Paul, A., Wilson, S., Belham, C.M., Robinson, C.J., Scott, P.H., Gould, G.W., and Plevin, R. (1997). Stress-activated protein kinases: activation, regulation and function. Cell Signal *9*, 403-410.

Pellegrin, S., and Mellor, H. (2005). The Rho family GTPase Rif induces filopodia through mDia2. Curr Biol *15*, 129-133.

Perez, L.M., Milkiewicz, P., Ahmed-Choudhury, J., Elias, E., Ochoa, J.E., Sanchez Pozzi, E.J., Coleman, R., and Roma, M.G. (2006). Oxidative stress induces actin-cytoskeletal and tight-junctional alterations in hepatocytes by a Ca2+ -dependent, PKC-mediated mechanism: protective effect of PKA. Free Radic Biol Med *40*, 2005-2017.

Perlstein, T.S., and Lee, R.T. (2006). Smoking, metalloproteinases, and vascular disease. Arterioscler Thromb Vasc Biol *26*, 250-256.

Pfitzer, G. (2001). Invited review: regulation of myosin phosphorylation in smooth muscle. J Appl Physiol *91*, 497-503.

Phillipson, M., Heit, B., Colarusso, P., Liu, L., Ballantyne, C.M., and Kubes, P. (2006). Intraluminal crawling of neutrophils to emigration sites: a molecularly distinct process from adhesion in the recruitment cascade. J Exp Med *203*, 2569-2575.

Phillipson, M., Kaur, J., Colarusso, P., Ballantyne, C.M., and Kubes, P. (2008). Endothelial domes encapsulate adherent neutrophils and minimize increases in vascular permeability in paracellular and transcellular emigration. PLoS ONE *3*, e1649.

Pieters, R., and Veerman, A.J. (1988). The role of 5'nucleotidase in therapy-resistance of childhood leukemia. Medical hypotheses *27*, 77-80.

Pollard, T.D., and Borisy, G.G. (2003). Cellular motility driven by assembly and disassembly of actin filaments. Cell *112*, 453-465.

Pollock, J.D., Williams, D.A., Gifford, M.A., Li, L.L., Du, X., Fisherman, J., Orkin, S.H., Doerschuk, C.M., and Dinauer, M.C. (1995). Mouse model of X-linked chronic granulomatous disease, an inherited defect in phagocyte superoxide production. Nature genetics *9*, 202-209.

Postea, O., Krotz, F., Henger, A., Keller, C., and Weiss, N. (2006). Stereospecific and redox-sensitive increase in monocyte adhesion to endothelial cells by homocysteine. Arterioscler Thromb Vasc Biol *26*, 508-513.

Price, L.S., Langeslag, M., ten Klooster, J.P., Hordijk, P.L., Jalink, K., and Collard, J.G. (2003). Calcium signaling regulates translocation and activation of Rac. J Biol Chem *278*, 39413-39421.

Purdom, S., and Chen, Q.M. (2005). Epidermal growth factor receptor-dependent and -independent pathways in hydrogen peroxide-induced mitogen-activated protein kinase activation in cardiomyocytes and heart fibroblasts. J Pharmacol Exp Ther *312*, 1179-1186.

Quinn, M.T., Ammons, M.C., and Deleo, F.R. (2006). The expanding role of NADPH oxidases in health and disease: no longer just agents of death and destruction. Clin Sci (Lond) *111*, 1-20.

Radmark, O., Werz, O., Steinhilber, D., and Samuelsson, B. (2007). 5-Lipoxygenase: regulation of expression and enzyme activity. Trends in biochemical sciences *32*, 332-341.

Ralevic, V., and Burnstock, G. (1998). Receptors for purines and pyrimidines. Pharmacol Rev *50*, 413-492.

Ratner, S., Sherrod, W.S., and Lichlyter, D. (1997). Microtubule retraction into the uropod and its role in T cell polarization and motility. J Immunol *159*, 1063-1067.

Rattan, V., Sultana, C., Shen, Y., and Kalra, V.K. (1997). Oxidant stress-induced transendothelial migration of monocytes is linked to phosphorylation of PECAM-1. Am J Physiol *273*, E453-461.

Rhee, S.G., Bae, Y.S., Lee, S.R., and Kwon, J. (2000). Hydrogen peroxide: a key messenger that modulates protein phosphorylation through cysteine oxidation. Sci STKE *2000*, PE1.

Rickert, P., Weiner, O.D., Wang, F., Bourne, H.R., and Servant, G. (2000). Leukocytes navigate by compass: roles of PI3Kgamma and its lipid products. Trends Cell Biol *10*, 466-473.

Ridley, A.J. (2001). Rho GTPases and cell migration. J Cell Sci *114*, 2713-2722.

Riento, K., Guasch, R.M., Garg, R., Jin, B., and Ridley, A.J. (2003). RhoE binds to ROCK I and inhibits downstream signaling. Mol Cell Biol *23*, 4219-4229.

Robb, L. (2007). Cytokine receptors and hematopoietic differentiation. Oncogene *26*, 6715-6723.

Robbesyn, F., Garcia, V., Auge, N., Vieira, O., Frisach, M.F., Salvayre, R., and Negre-Salvayre, A. (2003). HDL counterbalance the proinflammatory effect of oxidized LDL by inhibiting intracellular reactive oxygen species rise, proteasome activation, and subsequent NF-kappaB activation in smooth muscle cells. Faseb J *17*, 743-745.

Roberts, R.L., and Sandra, A. (1993). Apical-basal membrane polarity of membrane phosphatases in isolated capillary endothelium: alteration in ultrastructural localisation under culture conditions. Journal of anatomy *182 (Pt 3)*, 339-347.

Rodrigues, E.B., Maia, M., Meyer, C.H., Penha, F.M., Dib, E., and Farah, M.E. (2007). Vital dyes for chromovitrectomy. Current opinion in ophthalmology *18*, 179-187.

Rolli-Derkinderen, M., Sauzeau, V., Boyer, L., Lemichez, E., Baron, C., Henrion, D., Loirand, G., and Pacaud, P. (2005). Phosphorylation of serine 188 protects RhoA from ubiquitin/proteasome-mediated degradation in vascular smooth muscle cells. Circ Res *96*, 1152-1160.

Rose, D.M., Alon, R., and Ginsberg, M.H. (2007). Integrin modulation and signaling in leukocyte adhesion and migration. Immunol Rev *218*, 126-134.

Rosen, H., and Goetzl, E.J. (2005). Sphingosine 1-phosphate and its receptors: an autocrine and paracrine network. Nat Rev Immunol *5*, 560-570.

Rossman, K.L., Der, C.J., and Sondek, J. (2005). GEF means go: turning on RHO GTPases with guanine nucleotide-exchange factors. Nature reviews *6*, 167-180.

Rottner, K., Hall, A., and Small, J.V. (1999). Interplay between Rac and Rho in the control of substrate contact dynamics. Curr Biol *9*, 640-648.

Ryu, J.W., Hong, K.H., Maeng, J.H., Kim, J.B., Ko, J., Park, J.Y., Lee, K.U., Hong, M.K., Park, S.W., Kim, Y.H., and Han, K.H. (2004). Overexpression of uncoupling protein 2 in THP1 monocytes inhibits beta2 integrin-mediated firm adhesion and transendothelial migration. Arterioscler Thromb Vasc Biol *24*, 864-870.

Sablina, A.A., Budanov, A.V., Ilyinskaya, G.V., Agapova, L.S., Kravchenko, J.E., and Chumakov, P.M. (2005). The antioxidant function of the p53 tumor suppressor. Nat Med *11*, 1306-1313.

Sadej, R., Spychala, J., and Skladanowski, A.C. (2006). Expression of ecto-5'-nucleotidase (eN, CD73) in cell lines from various stages of human melanoma. Melanoma research *16*, 213-222.

Sahai, E., and Marshall, C.J. (2003). Differing modes of tumour cell invasion have distinct requirements for Rho/ROCK signalling and extracellular proteolysis. Nat Cell Biol *5*, 711-719.

Saitoh, M., Nishitoh, H., Fujii, M., Takeda, K., Tobiume, K., Sawada, Y., Kawabata, M., Miyazono, K., and Ichijo, H. (1998). Mammalian thioredoxin is a direct inhibitor of apoptosis signal-regulating kinase (ASK) 1. Embo J *17*, 2596-2606.

Salmeen, A., and Barford, D. (2005). Functions and mechanisms of redox regulation of cysteine-based phosphatases. Antioxidants & redox signaling *7*, 560-577.

Salmi, M., and Jalkanen, S. (2005). Cell-surface enzymes in control of leukocyte trafficking. Nat Rev Immunol *5*, 760-771.

Sanchez-Madrid, F., and del Pozo, M.A. (1999). Leukocyte polarization in cell migration and immune interactions. Embo J *18*, 501-511.

Sander, E.E., van Delft, S., ten Klooster, J.P., Reid, T., van der Kammen, R.A., Michiels, F., and Collard, J.G. (1998). Matrix-dependent Tiam1/Rac signaling in epithelial cells promotes either cell-cell adhesion or cell migration and is regulated by phosphatidylinositol 3-kinase. J Cell Biol *143*, 1385-1398.

Sandow, S.L. (2004). Factors, fiction and endothelium-derived hyperpolarizing factor. Clinical and experimental pharmacology & physiology *31*, 563-570.

Sato, E., Mokudai, T., Niwano, Y., Kamibayashi, M., and Kohno, M. (2008). Existence of a new reactive intermediate oxygen species in hypoxanthine and xanthine oxidase reaction. Chemical & pharmaceutical bulletin *56*, 1194-1197.

Scandalios, J.G. (2005). Oxidative stress: molecular perception and transduction of signals triggering antioxidant gene defenses. Brazilian journal of medical and biological research = Revista brasileira de pesquisas medicas e biologicas / Sociedade Brasileira de Biofisica [et al *38*, 995-1014.

Schenkel, A.R., Mamdouh, Z., and Muller, W.A. (2004). Locomotion of monocytes on endothelium is a critical step during extravasation. Nat Immunol *5*, 393-400.

Schreibelt, G., Kooij, G., Reijerkerk, A., van Doorn, R., Gringhuis, S.I., van der Pol, S., Weksler, B.B., Romero, I.A., Couraud, P.O., Piontek, J., Blasig, I.E., Dijkstra, C.D., Ronken, E., and de Vries, H.E. (2007). Reactive oxygen species alter brain endothelial tight junction dynamics via RhoA, PI3 kinase, and PKB signaling. Faseb J *21*, 3666-3676.

Schultz-Heienbrok, R., Maier, T., and Strater, N. (2005). A large hinge bending domain rotation is necessary for the catalytic function of Escherichia coli 5'-nucleotidase. Biochemistry *44*, 2244-2252.

Schumacker, P.T. (2006). Reactive oxygen species in cancer cells: live by the sword, die by the sword. Cancer cell *10*, 175-176.

Segal, A.W., Geisow, M., Garcia, R., Harper, A., and Miller, R. (1981). The respiratory burst of phagocytic cells is associated with a rise in vacuolar pH. Nature *290*, 406-409.

Seger, R.A. (2008). Modern management of chronic granulomatous disease. British journal of haematology *140*, 255-266.

Sen, G.L., and Blau, H.M. (2006). A brief history of RNAi: the silence of the genes. Faseb J *20*, 1293-1299.

Shamri, R., Grabovsky, V., Gauguet, J.M., Feigelson, S., Manevich, E., Kolanus, W., Robinson, M.K., Staunton, D.E., von Andrian, U.H., and Alon, R. (2005). Lymphocyte arrest requires instantaneous induction of an extended LFA-1 conformation mediated by endothelium-bound chemokines. Nat Immunol *6*, 497-506.

Shaw, S.K., Bamba, P.S., Perkins, B.N., and Luscinskas, F.W. (2001). Real-time imaging of vascular endothelial-cadherin during leukocyte transmigration across endothelium. J Immunol *167*, 2323-2330.

Shen, H.M., and Liu, Z.G. (2006). JNK signaling pathway is a key modulator in cell death mediated by reactive oxygen and nitrogen species. Free Radic Biol Med *40*, 928-939.

Shiose, A., Kuroda, J., Tsuruya, K., Hirai, M., Hirakata, H., Naito, S., Hattori, M., Sakaki, Y., and Sumimoto, H. (2001). A novel superoxide-producing NAD(P)H oxidase in kidney. J Biol Chem *276*, 1417-1423.

Shryock, J.C., and Belardinelli, L. (1997). Adenosine and adenosine receptors in the cardiovascular system: biochemistry, physiology, and pharmacology. The American journal of cardiology *79*, 2-10.

Sims, J.R., Karp, S., and Ingber, D.E. (1992). Altering the cellular mechanical force balance results in integrated changes in cell, cytoskeletal and nuclear shape. J Cell Sci *103 (Pt 4)*, 1215-1222.

Singbartl, K., Thatte, J., Smith, M.L., Wethmar, K., Day, K., and Ley, K. (2001). A CD2-green fluorescence protein-transgenic mouse reveals very late antigen-4-dependent CD8+ lymphocyte rolling in inflamed venules. J Immunol *166*, 7520-7526.

Skulachev, V.P. (1996). Role of uncoupled and non-coupled oxidations in maintenance of safely low levels of oxygen and its one-electron reductants. Quarterly reviews of biophysics *29*, 169-202.

Slemmer, J.E., Shacka, J.J., Sweeney, M.I., and Weber, J.T. (2008). Antioxidants and free radical scavengers for the treatment of stroke, traumatic brain injury and aging. Current medicinal chemistry *15*, 404-414.

Small, J.V., Stradal, T., Vignal, E., and Rottner, K. (2002). The lamellipodium: where motility begins. Trends Cell Biol *12*, 112-120.

Spychala, J. (2000). Tumor-promoting functions of adenosine. Pharmacol Ther *87*, 161-173.

Srinivas, S.P., Satpathy, M., Gallagher, P., Lariviere, E., and Van Driessche, W. (2004). Adenosine induces dephosphorylation of myosin II regulatory light chain in cultured bovine corneal endothelial cells. Experimental eye research *79*, 543-551.

Stefanovic, V., Djordjevic, V., Ivic, M., Mitic-Zlatkovic, M., and Vlahovic, P. (2005). Lymphocyte PC-1 activity in patients on maintenance haemodialysis treated with human erythropoietin and 1-alpha-D3. Annals of clinical biochemistry *42*, 55-60.

Stone, V., Johnston, H., and Clift, M.J. (2007). Air pollution, ultrafine and nanoparticle toxicology: cellular and molecular interactions. IEEE transactions on nanobioscience *6*, 331-340.

Strater, N. (2006). Ecto-5'-nucleotidase: Structure function relationships. Purinergic Signalling *2*, 343 - 350.

Strohmeier, G.R., Lencer, W.I., Patapoff, T.W., Thompson, L.F., Carlson, S.L., Moe, S.J., Carnes, D.K., Mrsny, R.J., and Madara, J.L. (1997). Surface expression, polarization, and functional significance of CD73 in human intestinal epithelia. J Clin Invest *99*, 2588-2601.

Su, W.H., Chen, H.I., and Jen, C.J. (2002). Differential movements of VE-cadherin and PECAM-1 during transmigration of polymorphonuclear leukocytes through human umbilical vein endothelium. Blood *100*, 3597-3603.

Suh, Y.A., Arnold, R.S., Lassegue, B., Shi, J., Xu, X., Sorescu, D., Chung, A.B., Griendling, K.K., and Lambeth, J.D. (1999). Cell transformation by the superoxide-generating oxidase Mox1. Nature *401*, 79-82.

Sun, Y., Liu, J., Qian, F., and Xu, Q. (2006). Nitric oxide inhibits T cell adhesion and migration by down-regulation of beta1-integrin expression in immunologically liver-injured mice. Int Immunopharmacol *6*, 616-626.

Sundaresan, M., Yu, Z.X., Ferrans, V.J., Irani, K., and Finkel, T. (1995). Requirement for generation of H2O2 for platelet-derived growth factor signal transduction. Science *270*, 296-299.

Svitkina, T.M., Verkhovsky, A.B., McQuade, K.M., and Borisy, G.G. (1997). Analysis of the actin-myosin II system in fish epidermal keratocytes: mechanism of cell body translocation. J Cell Biol *139*, 397-415.

Szatrowski, T.P., and Nathan, C.F. (1991). Production of large amounts of hydrogen peroxide by human tumor cells. Cancer research *51*, 794-798.

Szczur, K., Xu, H., Atkinson, S., Zheng, Y., and Filippi, M.D. (2006). Rho GTPase CDC42 regulates directionality and random movement via distinct MAPK pathways in neutrophils. Blood *108*, 4205-4213.

Tadokoro, S., Shattil, S.J., Eto, K., Tai, V., Liddington, R.C., de Pereda, J.M., Ginsberg, M.H., and Calderwood, D.A. (2003). Talin binding to integrin beta tails: a final common step in integrin activation. Science *302*, 103-106.

Takada, Y., Kamata, T., Irie, A., Puzon-McLaughlin, W., and Zhang, X.P. (1997). Structural basis of integrin-mediated signal transduction. Matrix Biol *16*, 143-151.

Takada, Y., Ye, X., and Simon, S. (2007). The integrins. Genome biology *8*, 215.

Takahashi, K., Nakanishi, H., Miyahara, M., Mandai, K., Satoh, K., Satoh, A., Nishioka, H., Aoki, J., Nomoto, A., Mizoguchi, A., and Takai, Y. (1999). Nectin/PRR: an immunoglobulin-like cell adhesion molecule recruited to cadherin-based adherens junctions through interaction with Afadin, a PDZ domain-containing protein. J Cell Biol *145*, 539-549.

Takano, M., Meneshian, A., Sheikh, E., Yamakawa, Y., Wilkins, K.B., Hopkins, E.A., and Bulkley, G.B. (2002). Rapid upregulation of endothelial P-selectin expression via reactive oxygen species generation. Am J Physiol Heart Circ Physiol *283*, H2054-2061.

Tamariz, E., and Grinnell, F. (2002). Modulation of fibroblast morphology and adhesion during collagen matrix remodeling. Mol Biol Cell *13*, 3915-3929.

Taylor, S.G., and Weston, A.H. (1988). Endothelium-derived hyperpolarizing factor: a new endogenous inhibitor from the vascular endothelium. Trends Pharmacol Sci *9*, 272-274.

Thiel, M., Chambers, J.D., Chouker, A., Fischer, S., Zourelidis, C., Bardenheuer, H.J., Arfors, K.E., and Peter, K. (1996). Effect of adenosine on the expression of beta(2) integrins and L-selectin of human polymorphonuclear leukocytes in vitro. J Leukoc Biol *59*, 671-682.

Thompson, L.F., Eltzschig, H.K., Ibla, J.C., Van De Wiele, C.J., Resta, R., Morote-Garcia, J.C., and Colgan, S.P. (2004). Crucial role for ecto-5'-nucleotidase (CD73) in vascular leakage during hypoxia. J Exp Med *200*, 1395-1405.

Thompson, P.W., Randi, A.M., and Ridley, A.J. (2002). Intercellular adhesion molecule (ICAM)-1, but not ICAM-2, activates RhoA and stimulates c-fos and rhoA transcription in endothelial cells. J Immunol *169*, 1007-1013.

Thomson, L.F., Ruedi, J.M., Glass, A., Moldenhauer, G., Moller, P., Low, M.G., Klemens, M.R., Massaia, M., and Lucas, A.H. (1990). Production and characterization of monoclonal antibodies to the glycosyl phosphatidylinositol-anchored lymphocyte differentiation antigen ecto-5'-nucleotidase (CD73). Tissue Antigens *35*, 9-19.

Tokumura, A., Majima, E., Kariya, Y., Tominaga, K., Kogure, K., Yasuda, K., and Fukuzawa, K. (2002). Identification of human plasma lysophospholipase D, a lysophosphatidic acid-producing enzyme, as autotaxin, a multifunctional phosphodiesterase. J Biol Chem *277*, 39436-39442.

Tolias, K.F., Hartwig, J.H., Ishihara, H., Shibasaki, Y., Cantley, L.C., and Carpenter, C.L. (2000). Type Ialpha phosphatidylinositol-4-phosphate 5-kinase mediates Rac-dependent actin assembly. Curr Biol *10*, 153-156.

Tominaga, T., Sahai, E., Chardin, P., McCormick, F., Courtneidge, S.A., and Alberts, A.S. (2000). Diaphanous-related formins bridge Rho GTPase and Src tyrosine kinase signaling. Mol Cell *5*, 13-25.

Totsukawa, G., Yamakita, Y., Yamashiro, S., Hartshorne, D.J., Sasaki, Y., and Matsumura, F. (2000). Distinct roles of ROCK (Rho-kinase) and MLCK in spatial regulation of MLC phosphorylation for assembly of stress fibers and focal adhesions in 3T3 fibroblasts. J Cell Biol *150*, 797-806.

Touyz, R.M. (2005). Reactive oxygen species as mediators of calcium signaling by angiotensin II: implications in vascular physiology and pathophysiology. Antioxidants & redox signaling *7*, 1302-1314.

Trachootham, D., Zhou, Y., Zhang, H., Demizu, Y., Chen, Z., Pelicano, H., Chiao, P.J., Achanta, G., Arlinghaus, R.B., Liu, J., and Huang, P. (2006). Selective killing of oncogenically transformed cells through a ROS-mediated mechanism by beta-phenylethyl isothiocyanate. Cancer cell *10*, 241-252.

True, A.L., Rahman, A., and Malik, A.B. (2000). Activation of NF-kappaB induced by H(2)O(2) and TNF-alpha and its effects on ICAM-1 expression in endothelial cells. Am J Physiol Lung Cell Mol Physiol *279*, L302-311.

Tsuruta, F., Sunayama, J., Mori, Y., Hattori, S., Shimizu, S., Tsujimoto, Y., Yoshioka, K., Masuyama, N., and Gotoh, Y. (2004). JNK promotes Bax translocation to mitochondria through phosphorylation of 14-3-3 proteins. Embo J *23*, 1889-1899.

Ujhazy, P., Klobusicka, M., Babusikova, O., Strausbauch, P., Mihich, E., and Ehrke, M.J. (1994). Ecto-5'-nucleotidase (CD73) in multidrug-resistant cell lines generated by doxorubicin. International journal of cancer *59*, 83-93.

Umezu-Goto, M., Kishi, Y., Taira, A., Hama, K., Dohmae, N., Takio, K., Yamori, T., Mills, G.B., Inoue, K., Aoki, J., and Arai, H. (2002). Autotaxin has lysophospholipase D activity leading to tumor cell growth and motility by lysophosphatidic acid production. J Cell Biol *158*, 227-233.

Ushio-Fukai, M. (2006). Localizing NADPH oxidase-derived ROS. Sci STKE *2006*, re8.

Ushio-Fukai, M., Tang, Y., Fukai, T., Dikalov, S.I., Ma, Y., Fujimoto, M., Quinn, M.T., Pagano, P.J., Johnson, C., and Alexander, R.W. (2002). Novel role of gp91(phox)-containing NAD(P)H oxidase in vascular endothelial growth factor-induced signaling and angiogenesis. Circ Res *91*, 1160-1167.

Vainio, P.J., Kortekangas-Savolainen, O., Mikkola, J.H., Jaakkola, K., Kalimo, K., Jalkanen, S., and Veromaa, T. (2005). Safety of blocking vascular adhesion protein-1 in patients with contact dermatitis. Basic & clinical pharmacology & toxicology *96*, 429-435.

van Buul, J.D., Anthony, E.C., Fernandez-Borja, M., Burridge, K., and Hordijk, P.L. (2005). Proline-rich tyrosine kinase 2 (Pyk2) mediates vascular endothelial-cadherin-based cell-cell adhesion by regulating beta-catenin tyrosine phosphorylation. J Biol Chem *280*, 21129-21136.

van Buul, J.D., and Hordijk, P.L. (2004). Signaling in leukocyte transendothelial migration. Arterioscler Thromb Vasc Biol *24*, 824-833.

van Buul, J.D., Voermans, C., van den Berg, V., Anthony, E.C., Mul, F.P., van Wetering, S., van der Schoot, C.E., and Hordijk, P.L. (2002). Migration of human hematopoietic progenitor cells across bone marrow endothelium is regulated by vascular endothelial cadherin. J Immunol *168*, 588-596.

van den Bosch, H., Schutgens, R.B., Wanders, R.J., and Tager, J.M. (1992). Biochemistry of peroxisomes. Annu Rev Biochem *61*, 157-197.

van Leeuwen, F.N., van Delft, S., Kain, H.E., van der Kammen, R.A., and Collard, J.G. (1999). Rac regulates phosphorylation of the myosin-II heavy chain, actinomyosin disassembly and cell spreading. Nat Cell Biol *1*, 242-248.

van Wetering, S., van den Berk, N., van Buul, J.D., Mul, F.P., Lommerse, I., Mous, R., ten Klooster, J.P., Zwaginga, J.J., and Hordijk, P.L. (2003). VCAM-1-mediated Rac signaling controls endothelial cell-cell contacts and leukocyte transmigration. Am J Physiol Cell Physiol *285*, C343-352.

Vartiainen, M.K., and Machesky, L.M. (2004). The WASP-Arp2/3 pathway: genetic insights. Curr Opin Cell Biol *16*, 174-181.

Vaupel, P., Thews, O., and Hoeckel, M. (2001). Treatment resistance of solid tumors: role of hypoxia and anemia. Medical oncology (Northwood, London, England) *18*, 243-259.

Veal, E.A., Day, A.M., and Morgan, B.A. (2007). Hydrogen peroxide sensing and signaling. Mol Cell *26*, 1-14.

Verma, R.P., and Hansch, C. (2007). Matrix metalloproteinases (MMPs): chemical-biological functions and (Q)SARs. Bioorganic & medicinal chemistry *15*, 2223-2268.

Vestweber, D. (2002). Regulation of endothelial cell contacts during leukocyte extravasation. Curr Opin Cell Biol *14*, 587-593.

Vestweber, D. (2008). VE-cadherin: the major endothelial adhesion molecule controlling cellular junctions and blood vessel formation. Arterioscler Thromb Vasc Biol *28*, 223-232.

Vidali, L., Chen, F., Cicchetti, G., Ohta, Y., and Kwiatkowski, D.J. (2006). Rac1-null mouse embryonic fibroblasts are motile and respond to platelet-derived growth factor. Mol Biol Cell *17*, 2377-2390.

Vielkind, S., Gallagher-Gambarelli, M., Gomez, M., Hinton, H.J., and Cantrell, D.A. (2005). Integrin regulation by RhoA in thymocytes. J Immunol *175*, 350-357.

Viola, A., and Luster, A.D. (2008). Chemokines and their receptors: drug targets in immunity and inflammation. Annual review of pharmacology and toxicology *48*, 171-197.

Vitale, N., Patton, W.A., Moss, J., Vaughan, M., Lefkowitz, R.J., and Premont, R.T. (2000). GIT proteins, A novel family of phosphatidylinositol 3,4, 5-trisphosphate-stimulated GTPase-activating proteins for ARF6. J Biol Chem *275*, 13901-13906.

Volmer, J.B., Thompson, L.F., and Blackburn, M.R. (2006). Ecto-5'-nucleotidase (CD73)-mediated adenosine production is tissue protective in a model of bleomycin-induced lung injury. J Immunol *176*, 4449-4458.

von Hundelshausen, P., Weber, K.S., Huo, Y., Proudfoot, A.E., Nelson, P.J., Ley, K., and Weber, C. (2001). RANTES deposition by platelets triggers monocyte arrest on inflamed and atherosclerotic endothelium. Circulation *103*, 1772-1777.

Walker, G., Langheinrich, A.C., Dennhauser, E., Bohle, R.M., Dreyer, T., Kreuzer, J., Tillmanns, H., Braun-Dullaeus, R.C., and Haberbosch, W. (1999). 3-deazaadenosine prevents adhesion molecule expression and atherosclerotic lesion formation in the aortas of C57BL/6J mice. Arterioscler Thromb Vasc Biol *19*, 2673-2679.

Wang, L., Zhou, X., Zhou, T., Ma, D., Chen, S., Zhi, X., Yin, L., Shao, Z., Ou, Z., and Zhou, P. (2008). Ecto-5'-nucleotidase promotes invasion, migration and adhesion of human breast cancer cells. Journal of cancer research and clinical oncology *134*, 365-372.

Wang, W., Wyckoff, J.B., Frohlich, V.C., Oleynikov, Y., Huttelmaier, S., Zavadil, J., Cermak, L., Bottinger, E.P., Singer, R.H., White, J.G., Segall, J.E., and Condeelis, J.S. (2002). Single cell behavior in metastatic primary mammary tumors correlated with gene expression patterns revealed by molecular profiling. Cancer research *62*, 6278-6288.

Wang, X., Martindale, J.L., Liu, Y., and Holbrook, N.J. (1998). The cellular response to oxidative stress: influences of mitogen-activated protein kinase signalling pathways on cell survival. Biochem J *333 (Pt 2)*, 291-300.

Wang, X.T., McCullough, K.D., Wang, X.J., Carpenter, G., and Holbrook, N.J. (2001). Oxidative stress-induced phospholipase C-gamma 1 activation enhances cell survival. J Biol Chem *276*, 28364-28371.

Watanabe, T., Noritake, J., and Kaibuchi, K. (2005). Regulation of microtubules in cell migration. Trends Cell Biol *15*, 76-83.

Weber, K.S., Klickstein, L.B., Weber, P.C., and Weber, C. (1998). Chemokine-induced monocyte transmigration requires cdc42-mediated cytoskeletal changes. Eur J Immunol *28*, 2245-2251.

Wedmore, C.V., and Williams, T.J. (1981). Control of vascular permeability by polymorphonuclear leukocytes in inflammation. Nature *289*, 646-650.

Werr, J., Xie, X., Hedqvist, P., Ruoslahti, E., and Lindbom, L. (1998). beta1 integrins are critically involved in neutrophil locomotion in extravascular tissue In vivo. J Exp Med *187*, 2091-2096.

Wheeler, A.P., Wells, C.M., Smith, S.D., Vega, F.M., Henderson, R.B., Tybulewicz, V.L., and Ridley, A.J. (2006). Rac1 and Rac2 regulate macrophage morphology but are not essential for migration. J Cell Sci *119*, 2749-2757.

Wheelock, M.J., and Johnson, K.R. (2003). Cadherin-mediated cellular signaling. Curr Opin Cell Biol *15*, 509-514.

Wittchen, E.S., van Buul, J.D., Burridge, K., and Worthylake, R.A. (2005). Trading spaces: Rap, Rac, and Rho as architects of transendothelial migration. Current opinion in hematology *12*, 14-21.

Wojciak-Stothard, B., Williams, L., and Ridley, A.J. (1999). Monocyte adhesion and spreading on human endothelial cells is dependent on Rho-regulated receptor clustering. J Cell Biol *145*, 1293-1307.

Wolf, K., Muller, R., Borgmann, S., Brocker, E.B., and Friedl, P. (2003). Amoeboid shape change and contact guidance: T-lymphocyte crawling through fibrillar collagen is independent of matrix remodeling by MMPs and other proteases. Blood *102*, 3262-3269.

Wong, C.W., Christen, T., Roth, I., Chadjichristos, C.E., Derouette, J.P., Foglia, B.F., Chanson, M., Goodenough, D.A., and Kwak, B.R. (2006). Connexin37 protects against atherosclerosis by regulating monocyte adhesion. Nat Med *12*, 950-954.

Wong, Y.W., and Low, M.G. (1992). Phospholipase resistance of the glycosyl-phosphatidylinositol membrane anchor on human alkaline phosphatase. Clinical chemistry *38*, 2517-2525.

Worthylake, R.A., Lemoine, S., Watson, J.M., and Burridge, K. (2001). RhoA is required for monocyte tail retraction during transendothelial migration. J Cell Biol *154*, 147-160.

Wu, D., Zhai, Q., and Shi, X. (2006). Alcohol-induced oxidative stress and cell responses. Journal of gastroenterology and hepatology *21 Suppl 3*, S26-29.

Wu, W.S. (2006). The signaling mechanism of ROS in tumor progression. Cancer metastasis reviews *25*, 695-705.

Xiao, J., Messinger, Y., Jin, J., Myers, D.E., Bolen, J.B., and Uckun, F.M. (1996). Signal transduction through the beta1 integrin family surface adhesion molecules VLA-4 and VLA-5 of human B-cell precursors activates CD19 receptor-associated protein-tyrosine kinases. J Biol Chem *271*, 7659-7664.

Yamauchi, J., Miyamoto, Y., Tanoue, A., Shooter, E.M., and Chan, J.R. (2005). Ras activation of a Rac1 exchange factor, Tiam1, mediates neurotrophin-3-induced Schwann cell migration. Proc Natl Acad Sci U S A *102*, 14889-14894.

Yan, Y., Wei, C.L., Zhang, W.R., Cheng, H.P., and Liu, J. (2006). Cross-talk between calcium and reactive oxygen species signaling. Acta pharmacologica Sinica *27*, 821-826.

Yang, C., and Kazanietz, M.G. (2003). Divergence and complexities in DAG signaling: looking beyond PKC. Trends Pharmacol Sci *24*, 602-608.

Yao, H., Yang, S.R., Kode, A., Rajendrasozhan, S., Caito, S., Adenuga, D., Henry, R., Edirisinghe, I., and Rahman, I. (2007). Redox regulation of lung inflammation: role of NADPH oxidase and NF-kappaB signalling. Biochemical Society transactions *35*, 1151-1155.

Yegutkin, G.G. (2008). Nucleotide- and nucleoside-converting ectoenzymes: Important modulators of purinergic signalling cascade. Biochim Biophys Acta.

Yegutkin, G.G., Henttinen, T., Samburski, S.S., Spychala, J., and Jalkanen, S. (2002). The evidence for two opposite, ATP-generating and ATP-consuming, extracellular pathways on endothelial and lymphoid cells. Biochem J *367*, 121-128.

Zalcman, G., Closson, V., Camonis, J., Honore, N., Rousseau-Merck, M.F., Tavitian, A., and Olofsson, B. (1996). RhoGDI-3 is a new GDP dissociation inhibitor (GDI). Identification of a non-cytosolic GDI protein interacting with the small GTP-binding proteins RhoB and RhoG. J Biol Chem *271*, 30366-30374.

Zeiffer, U., Schober, A., Lietz, M., Liehn, E.A., Erl, W., Emans, N., Yan, Z.Q., and Weber, C. (2004). Neointimal smooth muscle cells display a proinflammatory phenotype resulting in increased leukocyte recruitment mediated by P-selectin and chemokines. Circ Res *94*, 776-784.

Zernecke, A., Bidzhekov, K., Ozuyaman, B., Fraemohs, L., Liehn, E.A., Luscher-Firzlaff, J.M., Luscher, B., Schrader, J., and Weber, C. (2006). CD73/ecto-5'-nucleotidase protects against vascular inflammation and neointima formation. Circulation *113*, 2120-2127.

Zhao, Z., Walczysko, P., and Zhao, M. (2008). Intracellular Ca2+ stores are essential for injury induced Ca2+ signaling and re-endothelialization. J Cell Physiol *214*, 595-603.

Zhao, Z.S., Manser, E., Loo, T.H., and Lim, L. (2000). Coupling of PAK-interacting exchange factor PIX to GIT1 promotes focal complex disassembly. Mol Cell Biol *20*, 6354-6363.

Zhi, X., Chen, S., Zhou, P., Shao, Z., Wang, L., Ou, Z., and Yin, L. (2007). RNA interference of ecto-5'-nucleotidase (CD73) inhibits human breast cancer cell growth and invasion. Clinical & experimental metastasis *24*, 439-448.

Zhou, Z., Connell, M.C., and MacEwan, D.J. (2007). TNFR1-induced NF-kappaB, but not ERK, p38MAPK or JNK activation, mediates TNF-induced ICAM-1 and VCAM-1 expression on endothelial cells. Cell Signal *19*, 1238-1248.

Zhu, L., Castranova, V., and He, P. (2005). fMLP-stimulated neutrophils increase endothelial [Ca2+]i and microvessel permeability in the absence of adhesion: role of reactive oxygen species. Am J Physiol Heart Circ Physiol *288*, H1331-1338.

Ziegler-Heitbrock, L. (2007). The CD14+ CD16+ blood monocytes: their role in infection and inflammation. J Leukoc Biol *81*, 584-592.

Zimmermann, H. (1992). 5'-Nucleotidase: molecular structure and functional aspects. Biochem J *285 (Pt 2)*, 345-365.

Zuo, L., Christofi, F.L., Wright, V.P., Bao, S., and Clanton, T.L. (2004). Lipoxygenase-dependent superoxide release in skeletal muscle. J Appl Physiol *97*, 661-668.